Title
Nonrelativistic Naturalness in Aristotelian Quantum Field Theories

Permalink
https://escholarship.org/uc/item/4qf2c64b

Author
Yan, Ziqi

Publication Date
2017

Peer reviewed|Thesis/dissertation

Nonrelativistic Naturalness in Aristotelian Quantum Field Theories

by

Ziqi Yan

A dissertation submitted in partial satisfaction of the

requirements for the degree of

Doctor of Philosophy

in

Physics

in the

Graduate Division

of the

University of California, Berkeley

Committee in charge:

Professor Petr Hořava, Chair
Professor Ori J. Ganor
Professor Richard E. Borcherds

Spring 2017

Nonrelativistic Naturalness in Aristotelian Quantum Field Theories

Abstract

Nonrelativistic Naturalness in Aristotelian Quantum Field Theories

by

Ziqi Yan

Doctor of Philosophy in Physics

University of California, Berkeley

Professor Petr Hořava, Chair

Some of the most fundamental questions in theoretical physics can be formulated as puzzles of naturalness, such as the cosmological constant problem and the Higgs mass hierarchy problem. In condensed matter physics, the interpretation of the linear scaling of resistivity with temperature in the strange metal phase of high-temperature superconductors also arises as a naturalness puzzle. In this thesis, we explore the landscape of naturalness in nonrelativistic quantum field theories that exhibit anisotropic scaling in space and time. Such theories are referred to as the "Aristotelian quantum field theories." In the simple case with scalars, we find that the constant shift symmetry is extended to a shift by a polynomial in spatial coordinates, which protects the technical naturalness of modes with a higher order dispersion $\omega \sim k^z$ (z is the dynamical critical exponent). This discovery leads to a generalization of the relativistic Coleman-Hohenberg-Mermin-Wagner (CHMW) theorem to multicritical cases in lower critical dimension. By breaking the polynomial shift symmetries in a hierarchy, we find novel cascading phenomena with large natural hierarchies between the scales at which the values of z change, leading to an evasion of the "no-go" consequences of the relativistic CHMW theorem. Based on these formal developments, we propose potential applications both to the Higgs mass hierarchy problem and to the problem of linear resistivity in strange metals. Finally, encouraged by these nonrelativistic surprises that already arise in simple systems with scalars, we move on to more complicated systems with gauge symmetries. We study the quantization of Hořava gravity in $2 + 1$ dimensions and compute the anomalous dimension of the cosmological constant at one loop. However, nonrelativistic naturalness in gravity is still largely unexplored. Whether or not such nonrelativsitic twists have any implications for important naturalness puzzles, such as the cosmological constant problem, remains as an intriguing question.

To my mother, Lin, and my father, Liulin.

Contents

List of Figures

Acknowledgments

I would like to express my greatest thanks to my research advisor, Petr Hořava, for his breath of experience, depth of knowledge, and his continuous patience and support. It was under his guidance that I was first introduced to the field of high energy theory and I was enlightened to pursue it as a career. My sincere gratitude also goes to other members in my doctoral committee, Ori Ganor and Richard Borcherds. I would also like to thank all my research collaborators, Tom Griffin, Kevin Grosvenor, Charles Melby-Thompson, Christopher Mogni, Shinsei Ryu, Xueda Wen and Laure Berthier, for their enthusiasm, brilliance and hard work; without them the work presented in this thesis would not have been possible. My work was supported by Berkeley Center for Theoretical Physics and jointly by the BCTP Brantley-Tuttle Fellowship, for the latter I would like to thank Lynn Brantley and Doug Tuttle for their generosity. It is also a great pleasure to thank all members of Berkeley Center for Theoretical Physics, from whom I learned so much. I am grateful for hospitality of Niels Bohr Institute; I would like to especially thank Niels Obers and Kevin Grosvenor for organizing this enjoyable and fruitful trip. Thanks for hospitality of Fudan University and Charles Melby-Thompson for hosting me there. I would also like to thank Ming-wen Xiao from Nanjing University, who has always inspired me in many ways since I was a freshman in college. Last but not the least, I wish to thank all my family and friends; I would like to thank my mother for her incessant support and undying love throughout my life.

Chapter 1

Introduction

1.1   Principle of Technical Naturalness

The concept of naturalness has been a guiding principle in modern theoretical physics for the past decades, which not only is behind many successes but also leads to some of the most pressing fundamental questions. Perhaps the most famous naturalness problem is the *cosmological constant problem*, where the value of the observed cosmological constant is many orders much smaller than any known energy scales. In particle physics, the discovery of the Higgs boson in 2012 [1, 2] led in a renewed focus the naturalness at the TeV scale: The observed Higgs mass is again very small compared to any high particle-physics scale, be it the quantum gravity scale, or the scale of grand unification, or some other scale of new physics. This is famously known as the *Higgs mass hierarchy problem*. If one considers slow-roll inflation in cosmology, another naturalness problem emerges as the *eta problem*: The effective inflaton mass is required to be extremely small compared to the Hubble parameter in a successful slow-roll scenario.

Remarkably, all these three fundamental problems, the cosmological constant problem, the Higgs mass hierarchy problem and the eta problem in slow-roll inflation, are intimately related to gravity. In principle, a quantum theory of gravity is responsible for an ultimate answer. In the framework of effective field theory (EFT), however, these naturalness puzzles can be phrased as questions about naturalness of various small parameters in quantum field theories (QFTs) of scalars, insensitive of what the short-distance theories are. In fact, important naturalness puzzles not only arise in particle physics and cosmology, but also exist in condensed matter systems where the microscopic theory is defined on a discrete lattice. For example, in high-T_c superconductors, the resistivity develops a linear dependence in temperature in the strange metallic phase above the critical temperature T_c. This linear dependence persists over a large range of scales by condensed matter standards and is stable over a fairly large range of dopings. This surprisingly robust behavior begs for an explanation in terms of a mechanism naturally protecting the observed hierarchy of scales [3].

The precise notion of naturalness is formulated by 't Hooft in 1979, known as the principle of *technical naturalness* [4]. Following the time-honored physical principle of causality and

the hierarchy of energy scales from the microscopic to macroscopic phenomena, 't Hooft conjectured the following dogma:

> — *at any energy scale μ, a physical parameter or set of physical parameters $\alpha_i(\mu)$ is allowed to be very small only if the replacement $\alpha_i(\mu) = 0$ would increase the symmetry of the system.*

The essence of the naturalness problem of a light scalar with nonderivative self-interactions (such as the Higgs) can be succinctly illustrated by considering a single relativistic scalar $\Phi(x^\mu)$ in $3 + 1$ dimensions with action

$$S = \frac{1}{2} \int d^4x \left(\partial_\mu \Phi \partial^\mu \Phi - m^2 \Phi^2 - \frac{1}{4!} \lambda \Phi^4 \right), \tag{1.1}$$

where m^2 cannot be small independently of the value of λ: Both nonderivative terms in (1.1) break the same, constant shift symmetry $\Phi \to \Phi + \delta\Phi$ with $\delta\Phi = b$, and therefore must be of the same order of smallness (measured by $\varepsilon \ll 1$) relative to the naturalness scale M, *i.e.*,

$$m^2 \sim \varepsilon M^2, \qquad \lambda \sim \varepsilon. \tag{1.2}$$

This gives the following simple but important relation,

$$M \sim \frac{m}{\sqrt{\lambda}}, \tag{1.3}$$

which then implies the naturalness problem: m cannot be made arbitrarily smaller than M without λ being made correspondingly small to assure that the naturalness condition (1.3) hold. At typical values of λ not much smaller than 1, m will be of the order of the naturalness scale M, ruining the hierarchy.

It is conceivable that some puzzles of naturalness may only have environmental explanations, based on the landscape of many vacua in the multiverse. However, before we give up naturalness as our guiding principle, it is important to investigate more systematically the *landscape of naturalness*: To map out the various quantum systems and scenarios in which technical naturalness does hold, identifying possible surprises and new pieces of the puzzle that might help restore the power of naturalness in fundamental physics.

1.2 The Aristotelian Spacetime

One area in which naturalness has not yet been fully explored is nonrelativistic gravity theory [5, 6]. This approach to quantum gravity has attracted a lot of attention in recent years, largely because of its improved quantum behavior at short distances, novel phenomenology at long distances [7], its connection to the nonperturbative Causal Dynamical Triangulations approach to quantum gravity [8, 9, 10], as well as for its applications to holography and the AdS/CFT correspondence of nonrelativistic systems [11, 12, 13]. This area of research in

quantum gravity is still developing rapidly, with new surprises already encountered and other ones presumably still awaiting discovery. Mapping out the quantum structure of nonrelativistic gravity theories, and in particular investigating the role of naturalness, represents an intriguing and largely outstanding challenge.

Before embarking on a systematic study of the quantum properties of nonrelativistic gravity, one can probe some of the new conceptual features of nonrelativistic quantum field theories in simpler systems, without gauge symmetry, dynamical gravity and fluctuating spacetime geometry. We start with one of the ubiquitous themes of modern physics: The phenomenon of spontaneous symmetry breaking, in the simplest case of global, continous internal symmetries. According to Goldstone's theorem, spontaneous breaking of such symmetries implies the existence of a gapless Nambu-Goldstone (NG) mode in the system. For Lorentz invariant systems, the relativistic version of Goldstone's theorem is stronger, and we know more: There is a one-to-one correspondence between broken symmetry generators and the NG modes, whose gaplessness implies that they all share the same dispersion relation $\omega = ck$. On the other hand, nonrelativistic systems are phenomenologically known to exhibit a more complex pattern: Sometimes, the number of NG modes is smaller than the number of broken symmetry generators, and sometimes they disperse quadratically instead of linearly. This rich phenomenology opens up the question of a full classification of possible NG modes. A natural and elegant approach to this problem has been pursued in [14]: In order to classify NG modes, one classifies the low-energy EFTs available to control their dynamics.

For clarity and simplicity, we focus on systems on the flat spacetime with *Aristotelian spacetime*[1] symmetries. The terminology "Aristotelian spacetime" is borrowed from [16]. We define this spacetime to be $\mathcal{M}_{D+1} = \mathbb{R}^{D+1}$ with a preferred foliation $\mathcal{F}$ by fixed spatial slices $\mathbb{R}^D$, and equipped with a flat metric. Such a spacetime with the preferred foliation $\mathcal{F}$ would for example appear as a ground-state solution of nonrelativistic gravity with a zero cosmological constant [6] and gauge symmetry given by the group of foliation-preserving spacetime diffeomorphisms, $\text{Diff}(\mathcal{M}_{D+1}, \mathcal{F})$ (or a nonrelativistic extension thereof [17]). It is useful to parametrize M by coordinates $(t, \mathbf{x} = \{x^i, i = 1, \dots D\})$, such that the leaves of $\mathcal{F}$ are the leaves of constant t, and the metric has the canonical form

$$g_{ij}(t, \mathbf{x}) = \delta_{ij}, \quad N(t, \mathbf{x}) = 1, \quad N_i(t, \mathbf{x}) = 0. \tag{1.4}$$

Here g_{ij} is the spatial metric on the leaves of $\mathcal{F}$, N is the lapse function, and N_i the shift vector.

We shall be interested in the QFTs on $\mathcal{M}_{D+1}$ that respect the group of symmetries of the Aristotelian spacetime. It is natural to define the group of isometries of $\mathcal{M}_{D+1}$ to be that subgroup of the foliation-preserving diffeomorphism group of $\mathcal{M}_{D+1}$ that respects the constant metric on $\mathcal{M}_{D+1}$. This group is a direct product of the spatial Euclidean group

---

[1]It would be natural to refer to M with the flat metric (1.4) as the "Lifshitz spacetime". Unfortunately, this term already has another widely accepted meaning in the holography literature, where it denotes the curved spacetime geometry in one dimension higher, whose isometries realize the Aristotelian symmetries (1.5) plus the Lifshitz scaling symmetry (1.6) for some fixed value of z [15].

parametrized by $(\Theta^i{}_j, \Theta^i)$ and the one-dimensional non-compact group of time translations parametrized by Θ; it acts on $\mathcal{M}_{D+1}$ via

$$\widetilde{x}^i = \Theta^i{}_j x^j + \Theta^i, \qquad \widetilde{t} = t + \Theta. \tag{1.5}$$

The connected component of the group of isometries of our spacetime $\mathcal{M}$ with the flat metric (1.4) is generated by (1.5), and we will refer to it as the "Aristotelian symmetry" group. The full isometry group of this spacetime has four disconnected components, which can be obtained by combining the Aristotelian symmetry group generated by (1.5) with two discrete symmetries: The time-reversal symmetry $\mathcal{T}$, and a discrete symmetry $\mathcal{P}$ that reverses the orientation of space. We shall be interested in systems that are invariant under the Aristotelian symmetry group. Note that this mandatory Aristotelian symmetry does not contain either the discrete symmetries $\mathcal{T}$ and $\mathcal{P}$.

At renormalization group (RG) fixed points, the Aristotelian spacetime symmetries (1.5) are further extended by a one-parameter group of anisotropic scaling transformations

$$\widetilde{x}^i = b x^i, \qquad \widetilde{t} = b^z t, \tag{1.6}$$

with $b \in \mathbb{R}^+$ a real non-zero constant scaling factor. The dynamical critical exponent z is an important characteristic of the fixed point.

1.3 Outline of the Thesis

In Chapter 2 (published in [18, 19]), We investigate spontaneous global symmetry breaking in the Aristotelian spacetime, and study technical naturalness of Nambu-Goldstone modes whose dispersion relation exhibits a hierarchy of multicritical phenomena with Lifshitz scaling and dynamical exponents $z > 1$. The mechanism is protected by an enhanced "polynomial shift" symmetry in the free-field limit. (See [20] for a brief review.)

An immediate potential application of such NG modes of higher-order dispersion relations is found in condensed matter theory. In Chapter 3 (to appear in [21]), we consider the case in which the multicritical NG bosons play the role of acoustic phonons, associated with spontaneous breaking of spatial Euclidean symmetries. We couple the multicritical acoustic phonons to a Fermi liquid of nonrelativistic electrons, and study the physical properes of such "multicritical metals" in the simplest, isotropic case. Both thermodynamic and transport properties depend on the degree of multicriticality of the phonon sector and the dimension of space. We calculate the resistivity of the metal as a function of temperature T, at the leading order in the Bloch-Boltzmann transport theory. In particular, we point out that the system of $z = 3$ phonons in $3 + 1$ dimensions (which is their lower critical dimension), minimally coupled to the Fermi surface, gives resistivity linear in T over a naturally large hierarchy of scales.

Generic interactions break the polynomial shift symmetry explicitly to the constant shift. In the considered examples, both the Φ^4 self-interaction in (1.1) and the interaction between multicritical phonons and electrons in Chapter 3 break the polynomial shift symmetries to no

shift symmetry at all. It is thus natural to ask: Given a Gaussian fixed point with polynomial shift symmetry of degree P, what are the lowest-dimension operators that preserve this symmetry, and deform the theory into a self-interacting scalar field theory with the shift symmetry of degree P? To answer this (essentially cohomological) question, in Chapter 4 (published in [19]), we develop a new graph-theoretical technique, and use it to prove several classification theorems. First, in the special case of $P = 1$ (essentially equivalent to Galileons), we reproduce the known Galileon N-point invariants, and find their novel interpretation in terms of graph theory, as an equal-weight sum over all labeled trees with N vertices. Then we extend the classification to $P > 1$ and find a whole host of new invariants, including those that represent the most relevant (or least irrelevant) deformations of the corresponding Gaussian fixed points, and we study their uniqueness.

In Chapter 5 (published in [22]), we continue the study of the quantum properties of Aristotelian QFTs with polynomial shift symmetries. We investigate the role of infrared divergences and the nonrelativistic generalization of the Coleman-Hohenberg-Mermin-Wagner (CHMW) theorem. We find novel cascading phenomena with large hierarchies between the scales at which the value of n changes, leading to an evasion of the "no-go" consequences of the relativistic CHMW theorem. We present a series of examples to illustrate the cascading phenomena.

In Chapter 6 (to appear in [23]), we focus on the rich quantum properties of a toy model introduced in Chapter 5: A renormalizable nonrelativistic scalar field theory in $3 + 1$ spacetime dimensions with Aristotelian spacetime symmetries, and with linear shift symmetries. We show that its unique self-interaction coupling satisfies a non-renormalization theorem to all loop orders. However, despite this non-renormalization of the coupling, the self-interaction strength does depend on scales, as a result of the nontrivial renormalization of the two-point function. We show that in contrast to the relativistic case, there are several natural perspectives on the Callan-Symanzik equation and the process of the renormalization group flow, associated with the observer's freedom to choose how to relate time to space.

Finally, in Chapter 7 (published in [24]), using the simple toy model studied in Chapter 5 and Chapter 6 as a short-distance completion of the relativisitic EFT defined by (1.1), we argue that this high-energy cross-over to nonrelativistic behavior naturally leads to light scalars, and thus represents a useful ingredient for technically natural resolutions of scalar mass hierarchies, perhaps even the Higgs mass hierarchy puzzle.

In Chapter 8 (to appear in [25]), we use the techniques and intuitions established in the previous chapters about the Aristotelian QFTs to study more complicated systems. We examine the renormalization group behavior in the nonlinear sigma model around a $z = 2$ anisotropic Lifshitz fixed point in $2 + 1$ dimensions, focusing on the simple case of the S^{N-1} target manifold with full $O(N)$ symmetry. We calculate the one-loop beta functions of all coupling constants in this theory, and study its renormalization group structure. In the large N limit, the beta functions to all loops are obtained by summing over cactus diagrams.

Up to now, we only considered Aristotelian QFTs of scalar fields, and intriguing surprises about nonrelativistic naturalness already arise in these simple models. It remains a challenging question to explore the nonrelativistic naturalness in systems with gauge symmetries,

particularly in gravity. In Chapter 9 (published in [26]), we study quantum corrections to projectable Hořava gravity with $z = 2$ scaling in $2 + 1$ dimensions. Using the background field method, we utilize a non-singular gauge to compute the anomalous dimension of the cosmological constant at one loop, in a normalization adapted to the spatial curvature term.

In Chapter 10 we conclude the thesis.

Chapter 2

Multicritical Symmetry Breaking

Gapless Nambu-Goldstone modes [27, 28, 29, 30] appear prominently across an impressive array of physical phenomena, both relativistic and nonrelativistic. (For reviews, see *e.g.* [31, 32, 33, 34, 35].) They are a robust consequence of spontaneous symmetry breaking. Moreover, when further combined with gauge symmetries, they lead to the Higgs phenomenon, responsible for controlling the origin of elementary particle masses.

The NG modes are controlled by Goldstone's theorem: A spontaneously broken generator of a continuous internal rigid symmetry implies the existence of a gapless mode. With Lorentz invariance, the theorem implies a one-to-one correspondence between the generators of broken symmetry and massless NG modes, but in the nonrelativistic setting, it leaves questions [36, 37, 38]: What is the number of independent NG modes? What are their low-energy dispersion relations?

In this chapter, we study the general classification of NG modes, and their naturalness, in nonrelativistic theories with Aristotelian spacetime symmetries. Our study illustrates that in Aristotelian QFTs, not only the short-distance behavior but also the concept of naturalness acquires interesting new features.

2.1 Effective Field Theory and Goldstone's Theorem

In [39, 40], elegant arguments based on effective field theory have been used to clarify the consequences of Goldstone's theorem in the absence of Lorentz invariance. The main idea is to classify possible NG modes by classifying the EFTs available for describing their low-energy dynamics. We start with the NG field components π^A, $A = 1, \ldots, n$, which serve as coordinates on the space of possible vacua $M = \mathcal{G}/H$ in a system with symmetries broken spontaneously from $\mathcal{G}$ to $H \subset \mathcal{G}$. Our spacetime will be the flat $\mathbb{R}^{D+1}$ with coordinates t, x^i, $i = 1, \ldots, D$, and we impose the Aristotelian spacetime symmetry consisting of all Euclidean isometries of the spatial $\mathbb{R}^D$ and the time translations. At the fixed points of the renormalization group, this symmetry is enhanced by anisotropic scaling symmetry $x^i \to bx^i$, $t \to b^z t$, with the dynamical exponent z characterizing the degree of anisotropy at the fixed point.

Arguments of [39, 40] suggest that the generic low-energy EFT action for the NG fields π^A with these symmetries is

$$
S_{\text{eff}} = \frac{1}{2} \int dt\, d^D\mathbf{x}\, \big\{ \Omega_A(\pi)\dot{\pi}^A + g_{AB}(\pi)\dot{\pi}^A\dot{\pi}^B
$$
$$
- h_{AB}(\pi)\partial_i\pi^A\partial_i\pi^B + \ldots \big\}, \tag{2.1}
$$

where Ω_A, g_{AB} and h_{AB} are backgrounds transforming appropriately under $\mathcal{G}$, and "..." stands for higher-order derivative terms. The term linear in $\dot{\pi}^A$ is only possible because of the special role of time. Lorentz invariance would require $\Omega_A = 0$ and $g_{AB} = h_{AB}$, thus reproducing the standard relativistic result: One massless, linearly dispersing NG mode per each broken symmetry generator. In the nonrelativistic case, turning on Ω_A leads to *two* types of NG bosons [39, 40]: First, those field components that get their canonical momentum from Ω_A form canonical pairs; each pair corresponds to a pair of broken generators, and gives one Type-B NG mode with a quadratic dispersion. The remaining, Type-A modes then get their canonical momenta from the second term in (2.1), and behave as in the relativistic case, with $z = 1$. In both cases, higher values of z can arise if h_{AB} becomes accidentally degenerate [39].

We will show that in Aristotelian theories, h_{AB} can be small *naturally, without fine tuning*. When that happens, the low-energy behavior of the NG modes will be determined by the next term, of higher order in ∂_i. The argument can be iterated: When the terms of order ∂^4 are also small, terms with $z = 3$ will step in, etc. This results in a hierarchy of multicritical Type-A and Type-B NG modes with increasing values of z. Compared to the generic NG modes described by (2.1), these multicritical NG modes are anomalously slow at low energies.

2.2   Type A and B Nambu-Goldstone Bosons

We are interested in the patterns of spontaneous symmetry breaking of global continuous internal symmetries in the flat spacetime with the Aristotelian symmetries, as defined in the introduction. Our analysis gives an example of phenomena that are novel to Goldstone's theorem in nonrelativistic settings, and can in principle be generalized to nonrelativistic systems with even less symmetry.

An elegant strategy has been proposed in [14]: In order to classify Nambu-Goldstone modes, we can classify the corresponding EFTs available to describe their low-energy dynamics. In this EFT approach, we organize the terms in the effective action by their increasing dimension. Such dimensions are defined close enough to the infrared (IR) fixed point. However, until we identify the infrared fixed point, we don't a priori know the value of the dynamical critical exponent, and hence the relative dimension of the time and space derivatives – it is then natural to count the time derivatives and spatial derivatives separately. Consider first the "potential terms" in the action, *i.e.*, terms with no time derivatives. The general statement of Goldstone's theorem implies that non-derivative terms will be absent,

and the spatial rotational symmetry further implies that (for $D > 1$) all derivatives will appear in pairs contracted with the flat spatial metric. Hence, we can write the general "potential term" in the action as

$$S_{\text{eff}, V} = \int dt \, d^D \mathbf{x} \left\{ \frac{1}{2} g_{IJ}(\pi) \partial_i \pi^I \partial_i \pi^J + \dots \right\} \tag{2.2}$$

where $g_{IJ}(\pi)$ is the most general metric on the vacuum manifold which is compatible with all the global symmetries, and ... stand for all the terms of higher order in spatial derivatives.

If the system is also invariant under the primitive version $\mathcal{T}$ of time reversal, defined as the transformation that acts trivially on fields,

$$\mathcal{T} : \left\{ \begin{array}{ccc} t & \to & -t, \\ \pi^I & \to & \pi^I, \end{array} \right. \tag{2.3}$$

the time derivatives will similarly have to appear in pairs, and the kinetic term will be given by

$$S_{\text{eff}, K} = \int dt \, d^D \mathbf{x} \left\{ \frac{1}{2} h_{IJ}(\pi) \dot{\pi}^I \dot{\pi}^J + \dots \right\}, \tag{2.4}$$

where again h_{IJ} is a general metric on the vacuum manifold compatible with all symmetries, but not necessarily equal to the g_{IJ} that appeared in (2.2); and ... are higher-derivative terms.

However, invariance under $\mathcal{T}$ is not mandated by the Aristotelian symmetry. If it is absent, the Aristotelian symmetries allow a new, more relevant kinetic term,

$$\widetilde{S}_{\text{eff}, K} = \int dt \, d^D \mathbf{x} \left\{ \Omega_I(\pi) \dot{\pi}^I + \dots \right\}, \tag{2.5}$$

assuming one can define the suitable object $\Omega_I(\pi)$ on the vacuum manifold so that all the symmetry requirements are satisfied, and $\Omega_I(\pi) \dot{\pi}^I$ is not a total derivative. Since $\Omega_I(\pi)$ plays the role of the canonical momentum conjugate to π^I, if such Ω-terms are present in the action, they induce a natural canonical pairing on an even-dimensional subset of the coordinates on the vacuum manifold.

In specific dimensions, new terms in the effective action that are odd under spatial parity $\mathcal{P}$ may exist. For example, in $D = 2$ spatial dimensions, we can add new terms to the "potential" part of the action, of the form

$$\widetilde{S}_{\text{eff}, V} = \int dt \, d^D \mathbf{x} \left\{ \frac{1}{2} \Omega_{IJ}(\pi) \, \varepsilon_{ij} \, \partial_i \pi^I \partial_j \pi^J + \dots \right\}, \tag{2.6}$$

where Ω_{IJ} is any two-form on the vacuum manifold that respects all the symmetries.[1] In the interest of simplicity, we wish to forbid such terms, and will do so by imposing the $\mathcal{P}$

---

[1] For example, if $\Omega_I(\pi)$ suitable for (2.5) exist, one can take $\Omega_{IJ} = \partial_{[I} \Omega_{J]}$.

invariance of the action, focusing on the symmetry breaking patterns that respect spatial parity. This condition can of course be easily relaxed, without changing our conclusions significantly.

This structure of low-energy effective theories suggests the following classification of NG modes, into two general types:

- **Type A**: *One NG mode per broken symmetry generator (not paired by Ω_I). The low-energy dispersion relation is linear, $\omega \propto k$.*

- **Type B**: *One NG mode per each pair of broken symmetry generators (paired by Ω_I). The low-energy dispersion relation is quadratic, $\omega \propto k^2$.*

Based on the intuition developed in the context of relativistic QFT, one might be tempted to conclude that everything else would be fine tuning, as quantum corrections would be likely to generate large terms of the form (2.2) in the effective action if we attempted to tune them to zero.

2.3 The $z = 2$ Linear and Nonlinear $O(N)$ Sigma Models

The naive intuition about fine-tuning summarized in the previous section is, however, incorrect. As we will illustrate in a series of examples by explicit calculations of loop corrections, it turns out that the leading spatial-derivative term in (2.2) can be naturally small (or even zero).

We will demonstrate our results by focusing on a simple but representative example of symmetry breaking, the $O(N)$ nonlinear sigma model (NLSM) with target space S^{N-1}. (For some background on Aristotelian scalar theories, see [5, 41, 42, 43, 44, 45].) Until stated otherwise, we will also impose time reversal invariance, to forbid Ω_A. The action of the $O(N)$-invariant Aristotelian NLSM with a $z = 2$ scaling [43] is then

$$
\begin{aligned}
S_{\text{NLSM}} \;=\; & \frac{1}{2G^2} \int dt d^D \mathbf{x} \left\{ g_{AB} \dot{\pi}^A \dot{\pi}^B - e^2 g_{AB} \Delta \pi^A \Delta \pi^B \right. \\
& - \lambda_1 \left(g_{AB} \partial_i \pi^A \partial_j \pi^B \right) \left(g_{CD} \partial_i \pi^C \partial_j \pi^D \right) \\
& \left. - \lambda_2 \left(g_{AB} \partial_i \pi^A \partial_i \pi^B \right)^2 - c^2 g_{AB} \partial_i \pi^A \partial_i \pi^B \right\}.
\end{aligned}
\tag{2.7}
$$

Here

$$
\Delta \pi^A \equiv \partial_i \partial_i \pi^A + \Gamma^A_{BC} \partial_i \pi^B \partial_i \pi^C,
\tag{2.8}
$$

and g_{AB} is the round metric on the unit S^{N-1}, and Γ^A_{BC} is its connection. Later we will use

$$
g_{AB} = \delta_{AB} + \frac{\pi^A \pi^B}{1 - \delta_{CD} \pi^C \pi^D}.
\tag{2.9}
$$

The Gaussian $z = 2$ RG fixed point is defined by the first two terms in (2.7) as $G \to 0$.

To specify the canonical scaling dimensions at the $z = 2$ Gaussian fixed point, two natural conventions suggest themselves. First, one can measure the scaling dimensions in the units of spatial momentum – this is perhaps more prevalent in the literature, as it leads to simple integer dimensions of most objects of interest. However, we find that in Aristotelian theories, it is more appropriate to specify the scaling dimensions in the units of energy. It eases the comparison when more than one Gaussian fixed points with integer z are involved. We define scaling dimensions throughout in the units of energy,

$$[\partial_t] \equiv 1, \qquad [\partial_i] \equiv \frac{1}{2}. \tag{2.10}$$

Due to its geometric origin, the NG field π^A is dimensionless,

$$[\pi^A] = 0. \tag{2.11}$$

The first four terms in S_{NLSM} are all of the same dimension, so

$$[e^2] = [\lambda_1] = [\lambda_2] = 0. \tag{2.12}$$

We can set $e = 1$ by the rescaling of space and time, and will do so throughout this chapter. All interactions are controlled by the coupling constant G, whose dimension is

$$[G] = \frac{2 - D}{4}. \tag{2.13}$$

Thus, the critical spacetime dimension of the system, at which the first four terms in (2.7) are classically marginal, is equal to $2 + 1$. The remaining term has a coupling of dimension

$$[c^2] = 1, \tag{2.14}$$

and represents a relevant deformation away from $z = 2$, even in the non-interacting limit $G \to 0$. Since c determines the speed of the NG modes in the $\mathbf{k} \to 0$ limit, we refer to this term as the "speed term" for short. Given the symmetries, this relevant deformation is unique.

We are mainly interested in $3 + 1$ dimensions, so we set $D = 3$ from now on. We will defer the discussion on the $3 + 1$ dimensions to Chapter 8. Since this is above the critical dimension of $2 + 1$ and $[G]$ is negative, the theory described by (2.7) must be viewed as an EFT: S_{NLSM} gives the first few (most relevant) terms out of an infinite sequence of operators of growing dimension, compatible with all the symmetries. It is best to think of this EFT as descending from some ultraviolet (UV) completion. For example, we can engineer this effective NLSM by starting with the $z = 2$ linear sigma model (LSM) of the unconstrained $O(N)$ vector ϕ^I, $I = 1, \ldots, N$, and action

$$S_{\text{LSM}} = \frac{1}{2} \int dt d^3\mathbf{x} \left\{ \dot{\phi}^I \dot{\phi}^I - e^2 \partial^2 \phi^I \partial^2 \phi^I - c^2 \partial_i \phi^I \partial_i \phi^I - \left[e_1 \phi^I \phi^I + e_2 (\phi^I \phi^I)^2 \right] \partial_i \phi^J \partial_i \phi^J \right.$$

$$- f_1(\phi^I \partial_i \phi^I)(\phi^J \partial_i \phi^J) - f_2(\phi^I \phi^I)(\phi^J \partial_i \phi^J)(\phi^K \partial_i \phi^K)$$

$$- m^4 \phi^I \phi^I - \frac{\lambda}{2}(\phi^I \phi^I)^2 - \sum_{s=3}^{5} \frac{g_s}{s!}(\phi^I \phi^I)^s \Big\}. \tag{2.15}$$

The first two terms define the Gaussian $z = 2$ fixed point. We again set $e = 1$ by rescaling space and time. At this fixed point, the field is of dimension $[\phi] = 1/4$, and the dimensions of the couplings – in the order from the marginal to the more relevant – are:

$$[e] = [g_5] = [e_2] = [f_2] = 0, \qquad [g_4] = [e_1] = [f_1] = \frac{1}{2}, \qquad [g_3] = [c^2] = 1,$$

$$[\lambda] = \frac{3}{2}, \qquad [m^4] = 2. \tag{2.16}$$

This theory can be studied in the unbroken phase, the broken phase with a spatially uniform condensate (which we take to lie along the N-th component, $\langle \phi^N \rangle = v$), or in a spatially modulated phase which also breaks spontaneously some of the spacetime symmetry. We will focus on the unbroken and the uniformly broken phase. In the latter, we will write $\phi^I = (\Pi^A, v + \sigma)$. Changing variables to

$$\phi^I = (r\pi^A, r\sqrt{1 - \delta_{AB}\pi^A \pi^B}) \tag{2.17}$$

and integrating out perturbatively the gapped radial field $r - v$ gives the NLSM (2.7) of the gapless π^A at leading order, followed by higher-derivative corrections. This is an expansion in the powers of the momenta $|\mathbf{k}|/m_{\text{gap}}$ and frequency ω/m_{gap}^2, where m_{gap} is the gap scale of the radial mode.

The simplest example with a uniform broken phase is given by the special case of LSM, in which we turn off all self-interaction couplings except λ, and also set $c^2 = 0$ classically. This theory is superrenormalizable: Since $[\lambda] = 3$, the theory becomes free at asymptotically high energies, and stays weakly coupled until we reach the scale of strong coupling $m_s = \lambda^{1/3}$. Since the speed term is relevant, our intuition from the relativistic theory may suggest that once interactions are turned on, relevant terms are generated by loop corrections, with a leading power-law dependence on the UV momentum cutoff Λ. In fact, this does not happen here. To show this, consider the broken phase, with the potential minimized by

$$v = \frac{m^2}{\sqrt{\lambda}}, \tag{2.18}$$

and set $c^2 = 0$ at the classical level. The Π^A fields are gapless, and represent our NG modes. The σ has a gapped dispersion relation, $\omega^2 = |\mathbf{k}|^4 + 2m^4$. The Feynman rules in the broken phase are almost identical to those of the relativistic version of this theory [46], except for the nonrelativistic form of the propagators,

$$A \xrightarrow{\quad \omega, \mathbf{k} \quad} B \quad = \quad \frac{i\delta_{AB}}{\omega^2 - |\mathbf{k}|^4 + i\epsilon},$$
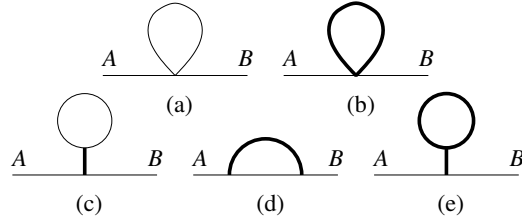
Figure 2.1: One-loop corrections to Γ_{AB} of the NG modes in the broken phase of the super-renormalizable LSM.

$$\xrightarrow{\omega,\,\mathbf{k}} \quad = \quad \frac{i}{\omega^2 - |\mathbf{k}|^4 - 2m^4 + i\epsilon}. \tag{2.19}$$

Because of the $z = 2$ anisotropy, the superficial degree of divergence of a diagram with L loops, E external legs and V_3 cubic vertices is

$$\mathcal{D} = 8 - 2E - 3L - 2V_3. \tag{2.20}$$

Loop corrections to the speed term are actually finite. If we start at the classical level by setting $c^2 = 0$, this relation can be viewed as a "zeroth order natural relation" (in the sense of [46]): True classically and acquiring only finite corrections at all loops. We can even set c^2 at any order to zero by a finite local counterterm, but an infinite counterterm for c^2 is not needed for renormalizability.

How large is this finite correction to c^2? At one loop, five diagrams (shown in Fig.2.1) contribute to the inverse propagator

$$\Gamma_{AB}(\omega, \mathbf{k}) \equiv (\omega^2 - |\mathbf{k}|^4 + \Sigma(\omega, \mathbf{k}))\delta_{AB}. \tag{2.21}$$

We can read off the one-loop correction to $c^2 = 0$ by expanding

$$\Sigma = -\delta m^4 - \delta c^2 \mathbf{k}^2 + \dots. \tag{2.22}$$

Four of these diagrams give a (linearly) divergent contribution to δm^4, but both the divergent and finite contributions to δm^4 sum to zero, as they must by Goldstone's theorem. The next term in Σ is then proportional to $\mathbf{k}^2$ and finite. It gets its only one-loop contribution from diagram (d) in Fig. 2.1, whose explicit evaluation gives

$$\delta c^2 = \frac{2^{7/4} \cdot 5}{63\pi^{5/2}} \left[\Gamma\left(\tfrac{5}{4}\right)\right]^2 \frac{\lambda}{m} \approx 0.0125 \frac{\lambda}{m}. \tag{2.23}$$

Thus, the first quantum correction to c^2 is indeed finite and nonzero. But is it small or large? There are much higher scales in the theory, such as m and Λ, yet in our weak coupling limit the correction to the speed term is found to be $\delta c^2 \propto \lambda/m$ naturally. In this sense, δc^2 is small, and so c^2 can also be small without fine tuning.

We can also calculate δc^2 at one loop in the effective NLSM. The Feynman rules derived from (2.7) for the rescaled field π^A/G involve a propagator independent of G (in which we set $c^2 = 0$), and an infinite sequence of vertices with an arbitrary even number of legs, of which we will only need the lowest one. When the radial direction of ϕ is integrated out in our superrenormalizable LSM, at the leading order we get (2.7) with $G = 1/v$, $\lambda_1 = 0$ and $\lambda_2 = 1$. In this special case, the 4-vertex is

$$
\begin{array}{c}
I_1 \diagdown \qquad \diagup I_2 \\
\omega_1, \mathbf{k}_1 \qquad \omega_2, \mathbf{k}_2 \\
\times \\
\omega_3, \mathbf{k}_3 \qquad \omega_4, \mathbf{k}_4 \\
I_3 \diagup \qquad \diagdown I_4
\end{array}
= -iG^2 \left\{ (\omega_1 + \omega_2)(\omega_3 + \omega_4) + (\mathbf{k}_1 + \mathbf{k}_2)^2 (\mathbf{k}_3 + \mathbf{k}_4)^2 \right\} \delta_{I_1 I_2} \delta_{I_3 I_4}
$$
$$
+ \, 2 \text{ permutations.} \quad (2.24)
$$

The first quantum correction to δc^2 comes at one loop, from

$$(2.25)$$

which is cubically divergent. With the sharp cutoff at $|\mathbf{k}| = \Lambda$, we get

$$
\delta c^2 = \frac{G^2 \Lambda^3}{3\pi^2}. \quad (2.26)
$$

This theory is only an EFT, and its natural cutoff scale Λ is given by m, the gap scale of the σ. With this value of the cutoff, the one-loop result (2.26) gives

$$
\delta c^2 = \mathcal{O}(\lambda/m), \quad (2.27)
$$

which matches our LSM result.

If one wishes to extend the control over the LSM beyond weak coupling in λ, one can take the large-N limit, holding the 't Hooft coupling λN fixed. In this limit, the LSM and the NLSM actually become equivalent, by the same argument as in the relativistic case [47]. An explicit calculation shows that at large N, δc^2 is not just finite but actually zero, to all orders in the 't Hooft coupling.

We will discuss in details about the RG structure of Aristotelian nonlinear sigma models in Chapter 8.

2.4 Naturalness and Slow Nambu-Goldstone Modes

Now, we return to the question of naturalness of small δc^2, in the technical context articulated in [4]. As a warm-up, consider first our superrenormalizable LSM in its unbroken phase. The leading contribution to the speed term in the inverse propagator of ϕ^I is now at two-loop order, from

$$(2.28)$$

This diagram is finite; even the leading constant, independent of ω and $\mathbf{k}$, only yields a finite correction to the gap m^4. The contribution of order $\mathbf{k}^2$ is then also finite, and gives

$$\delta c^2 = \frac{\xi \lambda^2}{m^4},\tag{2.29}$$

with ξ a pure number independent of all couplings. But is this δc^2 small?

Let us first recall a well-known fact from the relativistic $\lambda \phi^4$ theory [4]: λ and m^2 may be simultaneously small, $\sim \varepsilon$, because in the limit of $\varepsilon \to 0$, the system acquires an enhanced symmetry – in this case, the constant shift symmetry,

$$\phi^I \to \phi^I + a^I.\tag{2.30}$$

The same constant shift symmetry works also in our superrenormalizable Aristotelian LSM. Restoring dimensions, we have

$$\lambda = \mathcal{O}(\varepsilon \mu^3), \qquad m^4 = \mathcal{O}(\varepsilon \mu^4).\tag{2.31}$$

Here μ is the scale at which the constant shift symmetry is broken (or other new physics steps in), and represents the *scale of naturalness*: The theory is natural until we reach the scale $\mu = \mathcal{O}(m^4/\lambda)$. This result is sensible – if we wish for the scale of naturalness to be much larger than the gap scale, $\mu \gg m$, we must keep the theory at weak coupling, $\lambda/m^3 \ll 1$. Now, how about the speed term? If we assume that c^2 is also technically small, $c^2 \sim \varepsilon$, this assumption predicts $c^2 = \mathcal{O}(\lambda^2/m^4)$, which is exactly the result we found above in our explicit perturbative calculation. It looks like there must be a symmetry at play, protecting simultaneously the smallness of m^4, λ as well as c^2! We propose that the symmetry in question is the generalized shift symmetry (2.30), with a^I now a quadratic polynomial in the spatial coordinates,

$$a^I = a^I_{ij} x^i x^j + a^I_i x^i + a^I_0.\tag{2.32}$$

The speed term $\partial_i \phi^I \partial_i \phi^I$ is forbidden by this "quadratic shift" symmetry, while $\partial^2 \phi^I \partial^2 \phi^I$ is invariant up to a total derivative.[2] This symmetry holds in the free-field limit, and will be broken by interactions. It can be viewed as a generalization of the Galileon symmetry, much studied in cosmology [48], which acts by shifts linear in the spacetime coordinates.

As long as the coupling is weak, the unbroken phase of the LSM exhibits a natural hierarchy of scales, $c \ll m \ll \mu$, with the speed term much smaller than the gap scale. The effects of the speed term on the value of z would only become significant at low-enough energies, where the system is already gapped. Note that another interesting option is also available, since there is no obligation to keep c small at the classical level. If instead we choose c much above the gap scale m (but below the naturalness scale μ), as we go to lower energies the system will experience a crossover from $z = 2$ to $z = 1$ before reaching the gap,

---

[2]A more minimalistic approach is to apply the linear shift symmetry, $\delta\phi(t, \mathbf{x}) = a + a_i x^i$, instead of the quadratic shift symmetry. The c^2 term is invariant under this symmetry, up to a total derivative, and therefore protected from large quantum corrections.

and the theory will flow to the relativistic $\lambda\phi^4$ in the infrared. The coupling λ can stay small throughout the RG flow from the free $z = 2$ fixed point in the UV to the $z = 1$ theory in the infrared.

Now consider the same LSM in the broken phase. In this case, we are not trying to make m small – this is a fixed scale, setting the nonzero gap of the σ. Moreover, the π's are gapless, by Goldstone's theorem. We claim that c^2 can be naturally small in the regime of small λ,

$$\lambda = \mathcal{O}(\varepsilon\mu^3), \quad c^2 = \mathcal{O}(\varepsilon\mu^2), \tag{2.33}$$

as a consequence of an enhanced symmetry. The symmetry in question is again the "quadratic shift" symmetry, now acting only on the gapless NG modes in their free-field limit:

$$\Pi^A \to \Pi^A + a^A_{ij}x^i x^j + \dots. \tag{2.34}$$

It follows from (2.18) that the radius v of the vacuum manifold S^{N-1} goes to infinity with $\epsilon \to 0$, $v = \mathcal{O}(m^2/\sqrt{\mu^3\varepsilon})$, and $v \to \infty$ corresponds to the free-field limit of the π's. Our enhanced symmetry does not protect m from acquiring large corrections; we can view m in principle as a separate mass scale, but it is natural to take it to be of the order of the naturalness scale, $m = \mathcal{O}(\mu)$. Altogether, this predicts

$$\delta c^2 = \mathcal{O}(\lambda/\mu) = \mathcal{O}(\lambda/m), \tag{2.35}$$

in accord with our explicit loop result (2.23).

The technically natural smallness of the speed term in our examples is not an artifact of the superrenormalizability of our LSM. To see that, consider the full renormalizable LSM (2.15), first in the unbroken phase. As we turn off all self-interactions by sending $\varepsilon \to 0$, the enhanced quadratic shift symmetry will again protect the smallness of $c^2 \sim \varepsilon$. In terms of the naturalness scale μ, this argument predicts that in the action (2.15), all the deviations from the $z = 2$ Gaussian fixed point can be naturally of order ε in the units set by μ:

$$e_2 = \mathcal{O}(\varepsilon), \qquad \dots, \qquad c^2 = \mathcal{O}(\varepsilon\mu^2), \qquad \lambda = \mathcal{O}(\varepsilon\mu^3), \qquad m^4 = \mathcal{O}(\varepsilon\mu^4). \tag{2.36}$$

If we want the naturalness scale to be much larger than the gap scale, $\mu \gg m$, all couplings must be small; for example,

$$e_2 = \mathcal{O}(m^4/\mu^4) \ll 1, \tag{2.37}$$

etc. We then get an estimate

$$\delta c^2 = \mathcal{O}(e_2\mu^2) = \mathcal{O}(\sqrt{e_2}m^2) \ll m^2. \tag{2.38}$$

As in the superrenormalizable case, the speed term can be naturally much smaller than the gap scale. This prediction can be verified by a direct loop calculation. The leading contribution to δc^2 comes from several two-loop diagrams, including

$$\tag{2.39}$$

with one e_2 vertex. Each loop in this diagram is separately linearly divergent, giving

$$\delta c^2 \sim e_2 \Lambda^2 = \mathcal{O}(\sqrt{e_2} m^2), \qquad (2.40)$$

in accord with our scaling argument.

The story extends naturally to the broken phase of the renormalizable LSM, although this theory is technically rather complicated: The $\langle \phi \rangle$ itself is no longer given by (2.18) but it is at the minimum of a generic fifth-order polynomial in $\phi^I \phi^I$. It is thus more practical to run our argument directly in the low-energy NLSM. The advantage is that even for the generic renormalizable LSM (2.15), the leading-order NLSM action is of the general form (2.7). The leading order of matching gives $G = 1/v$, with v the radius of the vacuum manifold S^{N-1}. The NLSM is weakly coupled when this radius is large. The enhanced "quadratic shift" symmetry of the NG modes π^A in their free-field limit implies $G^2 = \mathcal{O}(\varepsilon/\mu)$ and $c^2 = \mathcal{O}(\varepsilon \mu^2)$ with $\lambda_{1,2} = \mathcal{O}(1)$, and predicts

$$c^2 = \mathcal{O}(G^2 \mu^3). \qquad (2.41)$$

The naturalness scale μ is set by the gap of the σ particle, which is generally of order m. Thus, (2.41) implies that in the large-v regime of the weakly-coupled NLSM, the speed term is naturally much smaller than the naturalness scale. This can be again confirmed by a direct loop calculation: The leading contribution to δc^2 comes from the one-loop diagram

$$(2.42)$$

This diagram is cubically divergent and its vertex gives a G^2 factor, leading to $\delta c^2 \sim G^2 \Lambda^3$. Setting $\Lambda \sim \mu$ confirms our scaling prediction (2.41). In the special case of our superrenormalizable LSM, we can go one step further, and use (2.18) and $G = 1/v$ to reproduce again our earlier result, $\delta c^2 = \mathcal{O}(\lambda/m)$.

We have shown that Type-A NG modes can naturally have an anomalously slow speed, characterized by an effective $z = 2$ dispersion relation. This construction can obviously be iterated, leading to Type-A NG modes with higher dispersion of $z = 3, 4, \ldots$. In such higher multicritical cases, the smallness of all the relevant terms is protected by the enhanced "polynomial shift" symmetry in the free-field limit, with a^I now a polynomial in x^i of degree $2z - 2$. Our results also extend easily to Type-B NG modes, which break time reversal invariance. Instead of their generic $z = 2$ dispersion, they can exhibit a $z = 4$ (or higher) behavior over a large range of energy scales.

2.5 Polynomial Shift Symmetries

Since the polynomial shift symmetries act on the fields $\pi^I(t, \mathbf{x})$ separately component by component, from now on we shall focus on just one field component, and rename it $\phi(t, \mathbf{x})$.

The generators of the polynomial shift symmetry of degree P act on ϕ by

$$\delta_P \phi = a_{i_1 \ldots i_P} x^{i_1} \cdots x^{i_P} + \ldots + a_i x^i + a. \qquad (2.43)$$

The multicritical Gaussian fixed point with dynamical exponent $z = n$ is described by

$$S_n = \int dt\, d\mathbf{x} \left\{ \frac{1}{2}\dot{\phi}^2 - \frac{1}{2}\zeta_n^2 \left(\partial_{i_1} \ldots \partial_{i_n} \phi \right) \left(\partial_{i_1} \ldots \partial_{i_n} \phi \right) \right\}. \tag{2.44}$$

In fact, it is a one-parameter family of fixed points, parametrized by the real positive coupling ζ_n^2. (Sometimes it is convenient to absorb ζ_n into the rescaling of space, and we will often do so when there is no competition between different fixed points.)

The action S_n is invariant under polynomial shift symmetries (2.43) of degree $P \leq 2n-1$: It is strictly invariant under the symmetries of degree $P < n$, and invariant up to a total derivative for degrees $n \leq P \leq 2n - 1$.

Morally, this infinite hierarchy of symmetries can be viewed as a natural generalization of the Galileon symmetry, proposed in [49] and much studied since, mostly in the cosmological literature. In the case of the Galileons, the theory is relativistic, and the symmetry is linear in space-*time* coordinates. The requirement of relativistic invariance is presumably the main reason that has precluded the generalization of the Galileon symmetries past the linear shift: The higher polynomial shift symmetries in spacetime coordinates would lead to actions dominated by higher time derivatives, endangering perturbative unitarity.

So far, we considered shifts by generic polynomials of degree P, whose coefficients $a_{i_1 \ldots i_\ell}$ are arbitrary symmetric real tensors of rank ℓ for $\ell = 0, \ldots, P$. We note here in passing that for degrees $P \geq 2$, the polynomial shift symmetries allow an interesting refinement. To illustrate this feature, we use the example of the quadratic shift,

$$\delta_2 \phi = a_{ij} x^i x^j + a_i x^i + a_0. \tag{2.45}$$

The coefficient a_{ij} of the quadratic part is a general symmetric 2-tensor. It can be decomposed into its traceless part $\widetilde{a}_{ij}$ and the trace part a_{ii},

$$a_{ij} = \widetilde{a}_{ij} + \frac{1}{D} a_{kk} \delta_{ij}. \tag{2.46}$$

Since this decomposition is compatible with the spacetime Aristotelian symmetries (1.5), one can restrict the symmetry group to be generated by a strictly smaller invariant subalgebra in the original algebra generated by a_{ij}. For example, setting the traceless part $\widetilde{a}_{ij}$ of the quadratic shift symmetry to zero reduces the number of independent generators from $(D+2)(D+1)/2$ to $D+2$, but it is still sufficient to prevent $\partial_i \phi\, \partial_i \phi$ from being an invariant under the smaller symmetry. This intriguing pattern extends to $P > 2$, leading to intricate hierarchies of polynomial shift symmetries whose coefficients $a_{i_1 \ldots i_\ell}$ have been restricted by various invariant conditions. As another example, invariance under the traceless part has been studied in [50]. In the interest of simplicity, we concentrate in the rest of this chapter on the maximal case of polynomial shift symmetries with arbitrary unrestricted real coefficients $a_{i_1 \ldots i_\ell}$.

The invariance of the action under each polynomial shift leads to a conserved Noether current. Each such current then implies a set of Ward identities on the correlation functions

and the effective action. Take, for example, the case of $n = 2$ in (2.44): The currents for the infinitesimal shift by a general function $a(\mathbf{x})$ of the spatial coordinates x^i are collectively given by

$$\mathcal{J}_t = a(\mathbf{x})\dot{\phi}, \qquad \mathcal{J}_i = a(\mathbf{x})\partial_i\partial^2\phi - \partial_j a(\mathbf{x})\partial_i\partial_j\phi + \partial_i\partial_j a(\mathbf{x})\partial_j\phi - \partial_i\partial^2 a(\mathbf{x})\,\phi, \qquad (2.47)$$

and their conservation requires

$$\dot{\mathcal{J}}_t + \partial_i\mathcal{J}_i \equiv a(\mathbf{x})\left\{\ddot{\phi} + (\partial^2)^2\phi\right\} - (\partial^2)^2 a(\mathbf{x})\,\phi = 0. \qquad (2.48)$$

The term in the curly brackets is zero on shell, and the current conservation thus reduces to the condition $(\partial^2)^2 a(\mathbf{x})\phi = 0$, which is certainly satisfied by a polynomial of degree three,

$$a(\mathbf{x}) = a_{ijk}x^i x^j x^k + a_{ij}x^i x^j + a_i x^i + a. \qquad (2.49)$$

Note that if we start instead with the equivalent form of the classical action

$$\widetilde{S}_2 = \int dt\,d\mathbf{x}\left\{\frac{1}{2}\dot{\phi}^2 - \frac{1}{2}\left(\partial_i\partial_i\phi\right)^2\right\}, \qquad (2.50)$$

the Noether currents will be related, as expected, by

$$\begin{aligned}
\widetilde{\mathcal{J}}_t &= \mathcal{J}_t, \\
\widetilde{\mathcal{J}}_i &= a(\mathbf{x})\partial_i\partial^2\phi - \partial_i a(\mathbf{x})\partial^2\phi + \partial^2 a(\mathbf{x})\partial_i\phi - \partial_i\partial^2 a(\mathbf{x})\phi \\
&= \mathcal{J}_i + \partial_j\left[\partial_i a(\mathbf{x})\partial_j\phi - \partial_j a(\mathbf{x})\partial_i\phi\right].
\end{aligned} \qquad (2.51)$$

From these conserved currents, one can formally define the charges

$$Q[a] = \int_\Sigma d\mathbf{x}\,\mathcal{J}_t. \qquad (2.52)$$

However, for infinite spatial slices $\Sigma = \mathbb{R}^D$, such charges are all zero on the entire Hilbert space of states generated by the normalizable excitations of the fields ϕ. This behavior is quite analogous to the standard case of NG modes invariant under the constant shifts, and it simply indicates that the polynomial shift symmetry is being spontaneously broken by the vacuum.

2.6 Refinement of the Goldstone Theorem

In its original form, Goldstone's theorem guarantees the existence of a gapless mode when a global continuous internal symmetry is spontaneously broken. However, in the absence of Lorentz symmetry, it does not predict the number of such modes, or their low-energy dispersion relation.

The classification of the effective field theories which are available to describe the low-energy limit of the Nambu-Goldstone mode dynamics leads to a natural refinement of the Goldstone theorem in the nonrelativistic regime. In the specific case of spacetimes with Aristotelian symmetry, we get two hierarchies of NG modes:

- **Type A:** *One NG mode per broken symmetry generator (not paired by Ω_I) The low-energy dispersion relation is $\omega \propto k^n$, where $n = 1, 2, 3, \ldots$.*

- **Type B:** *One NG mode per each pair of broken symmetry generators (paired by Ω_I). The low-energy dispersion relation is $\omega \propto k^{2n}$, where $n = 1, 2, 3, \ldots$.*

It is natural to label the members of these two hierarchies by the value of the dynamical critical exponent of their corresponding Gaussian fixed point. From now on, we will refer to these multicritical universality classes of Nambu-Goldstone modes as "Type A_n" and "Type B_{2n}", respectively.

We conclude this chapter with the following comments:

1. While Type B NG modes represent a true infinite hierarchy of consistent fixed points, the Type A NG modes hit against the nonrelativistic analog of the Coleman-Hohenberg-Mermin-Wagner (CHMW) theorem: At the critical value of $n = D$, they develop infrared singularities and cease to exist as well-defined quantum fields. We will discuss this behavior in details in Chapter 5.

2. Type A preserve $\mathcal{T}$ invariance, while Type B break $\mathcal{T}$. (This does not mean that a suitable time reversal invariance cannot be defined on Type B modes, but it would have to extend $\mathcal{T}$ of (2.3) to act nontrivially on the fields.)

3. Our classification shows the existence of A_n and B_{2n} hierarchies of NG modes described by Gaussian fixed points, and therefore represents a refinement of the classifications studied in the literature so far. However, it does not pretend to completeness: We find it plausible that nontrivial fixed points (and fixed points at non-integer values of n) suitable for describing NG modes may also exist. In this sense, the full classification of all possible types of nonrelativistic NG dynamics – even under the assumption of Aristotelian symmetries – still remains a fascinating open question.

4. For simplicity, we worked under the assumption of Aristotelian spacetime symmetry. Obviously, this simplifying restriction can be removed, and the classification of multicritical NG modes in principle extended to cases whereby some of the the spacetime symmetries are further broken by additional features of the system – such as spatial anisotropy, layers, an underlying lattice structure, etc. We also expect that the classification can be naturally extended to Nambu-Goldstone fermions associated with spontaneous breaking of symmetries associated with supergroups. Such generalizations, however, are beyond the scope of this thesis.

Chapter 3

Application: Linear Resistivity in Strange Metals

In the last chapter, we have demonstrated that Nambu-Goldstone modes produced by non-relativistic spontaneous symmetry breaking can exhibit naturally higher-order dispersion relations over a large hierarchy of scales. In flat noncompact space, the naturalness of this behavior is protected by a polynomial shift symmetry. In this chapter, we present an immediate application of these new technically natural Nambu-Goldstone modes. Since the Aristotelian spacetime that we are working with throughout the thesis is fundamentally nonrelativisitic, it is natural for us to first look for potential applications in the field of condensed matter physics.

3.1 T-linear Resistivity in Strange Metals

As preluded in §1.1, the linear temperature dependence of the resistivity in the strange metal phase above the critical temperature in high-T_c superconductors can be formulated as a naturalness puzzle. Qualitatively, the relation between the resistivity $\rho(T)$ and the temperature T is graphed for typical high-T_c superconductors in Figure 3.1. This behavior persists over a large range of scales in temperature and also survives under a changing of doping of $5 \sim 10\%$. This robust behavior seeks for an effective field theoretical explanation: Is there any mechanism which gives rise to the T-linear resistivity in metals in a technically natural way?

In the standard BCS theory, the electron-phonon interactions is responsible for the superconductivity. In the metallic phase above T_c, the resistivity from the electron-phonon interactions is given by the Bloch-Grüneisen formula, which yields $\rho(T) \sim T^5$. This is far off. How about other interactions? The electron-electron scatterings give $\rho(T) \sim T^2$ and the interactions with impurities give $\rho(T) \sim$ const. There is *nothing* that gives $\rho(T) \sim T$. Perhaps the effective field theory that describes the low energy excitations have to be something very different.

Notably, acoustic phonons are NG modes associated with spontaneous breaking of translational invariance. This opens up a curious question: What will happen in the BCS theory if the role of the phonons is played by the Type A$_n$ NG modes with $n > 1$? This is the
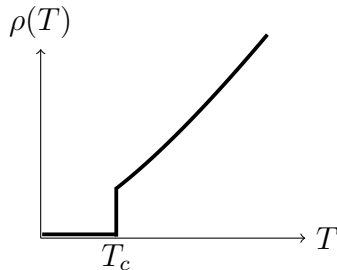
Figure 3.1: Temperature dependence of resistivity $\rho(T)$ in high-T_c superconductors.

question that we will be focusing on in the rest of this chapter: First we show how to generalize the polynomial shift symmetry when some spatial dimensions are compactified on a torus or replaced by a periodic finite lattice. Then we consider the case in which the multicritical NG bosons play the role of acoustic phonons, associated with spontaneous breaking of spatial Euclidean symmetries. We couple the multicritical acoustic phonons to a Fermi liquid of nonrelativistic electrons, and study the physical properties of such "multicritical metals" in the simplest, isotropic case. Both thermodynamic and transport properties depend on the degree of multicriticality of the phonon sector and the dimension of space. We calculate the resistivity of the metal as a function of temperature T, at the leading order in the Bloch-Boltzmann transport theory. In particular, we point out that the system of $z = 3$ multicritical phonons in $3 + 1$ dimensions (which is their lower critical dimension), minimally coupled to the Fermi surface, gives resistivity linear in T over a naturally large hierarchy of scales.

3.2 Polynomial Shift Symmetries and the Lattice

Having established in the previous chapter the possibility of a new symmetry in the continuum theory, one can naturally ask whether there is a discretized version of this symmetry, such that it can be implemented on the lattice and reproduce the continuous polynomial symmetry as the continuum infinite-volume limit is taken.

There are several reasons why to ask this question. First, especially with condensed matter applications in mind, it is useful to know whether lattice systems exist in which the analog of the polynomial shift can be realized as an exact symmetry at the microscopic level, at least in principle. Secondly, even if one is only interested in the continuum limit itself, it is useful to know whether there is a lattice regularization of the theory which maintains the lattice version of the polynomial shift symmetry before the continuum limit is taken. Besides, one might be interested in taking continuum limits other than the infinite volume limit, for example the limit in which the radius of the periodic lattice in one or more dimensions is held fixed as the number of sites goes to infinity. Having a lattice version of the polynomial shift symmetry will then yield automatically a natural continuum symmetry that works on toroidal spatial compactifications.

As an illustration of principle, we consider the theory in one spatial dimension, on a finite, periodic lattice of N sites, labeled by the site index $j = 0, \ldots, N - 1$. We are interested in the dynamics of a single scalar field, represented by the real-valued ϕ_j at each site j of the lattice, with periodic boundary conditions (*i.e.*, we define $\phi_{j+N} \equiv \phi_j$ for all $j \in \mathbb{Z}$). We also introduce the uniform lattice spacing a, which represents a natural microscopic scale in the theory: The lattice sites are located at $X = X_j \equiv aj$. Similarly, N serves as an infrared cutoff, and the radius of the spatial circle is given by $R = Na/(2\pi)$: We have $X = X + 2\pi R$.

The dual momentum lattice also consists of N points, labeled by integers $k = 0 \ldots, N-1$, arranged uniformly on a circle with periodic boundary conditions. Since the momentum K dual to X is naturally quantized in the units of $1/R = 2\pi/(Na)$, the lattice sites of the dual lattice are at $K_k \equiv 2\pi k/(Na)$, implying that $K = K + 2\pi/a$: The radius of the momentum circle is $1/a$. For now, we will set $a = 1$ for simplicity.

The momentum modes $\widetilde{\phi}_k$ associated with the scalar field ϕ_j are given by the discrete Fourier transform,

$$\widetilde{\phi}_k = \sum_{j=0}^{N-1} \phi_j e^{2\pi ijk/N}, \tag{3.1}$$

with the inverse given by

$$\phi_j = \frac{1}{N} \sum_{k=0}^{N-1} \widetilde{\phi}_k e^{-2\pi ijk/N}. \tag{3.2}$$

The constant shift symmetry is easily realized by the lattice degrees of freedom ϕ_j: The simplest textbook example of a nearest-neighbor Hamiltonian describing lattice vibrations,

$$H = \sum_{j=0}^{N-1} (\phi_{j+1} - \phi_j)^2, \tag{3.3}$$

is indeed manifestly invariant under the constant shift, $\phi_j \to \phi_j + \alpha$, with $\alpha \in \mathbb{R}$.

Moving on to polynomial shift symmetries of degree $P > 0$, we are facing our first issue: The polynomial functions of the spatial coordinate X, even when discretized and evaluated at the lattice sites $X_j = aj$, are not well-defined as uni-valued functions on the periodic lattice. To find our way out, let us consider the action of our symmetries as they act in the momentum space. In the continuum theory in $D + 1$ dimensions, the constant shift symmetry $\phi(\mathbf{x}) \to \phi(\mathbf{x}) + \alpha$ acts on the momentum modes via $\phi(\mathbf{k}) \to \phi(\mathbf{k}) + \alpha\delta^{(D)}(\mathbf{k})$. The polynomial shift symmetries of degree P similarly act on the momentum modes as shifts by derivatives of degree P of $\delta^{(D)}(\mathbf{k})$. Thus, the textbook Hamiltonian (3.3), when rewritten in momentum space,

$$H = \sum_{k=0}^{N-1} \sin^2\left(\frac{\pi k}{N}\right) \widetilde{\phi}_k^* \widetilde{\phi}_k, \tag{3.4}$$

is invariant under the shift of $\widetilde{\phi}_k$ by the lattice delta-function δ_k at the origin,

$$\delta_k = \begin{cases} 1, & k = 0; \\ 0, & k \neq 0. \end{cases} \tag{3.5}$$

simply because the coefficient $\sin^2(\pi k/N)$ vanishes at $k = 0$, the only place where the delta function δ_k is non-zero. The idea now is to extend this picture to higher polynomial symmetries, and to simply define our lattice analog of the "polynomial shift symmetry of degree P" in its momentum space representation as a shift of the momentum modes by the properly discretized P-th order derivative of the momentum-space delta function.

As an example, consider the quadratic shift $\phi(\mathbf{x}) \to \phi(\mathbf{x}) + \alpha \mathbf{x}^2$ of the continuum theory, which translates in momentum space into $\phi(\mathbf{k}) \to \phi(\mathbf{k}) + \alpha \Delta \delta^{(D)}(\mathbf{k})$ (Δ here denotes the Laplacian in the $\mathbf{k}$-space). We now *define* our lattice analog of this symmetry (in the one-dimensinal case) via

$$\widetilde{\phi}_k \to \widetilde{\phi}_k + \alpha(\delta_{k+1} + \delta_{k-1} - 2\delta_k), \tag{3.6}$$

a shift by the discretized lattice version of the second derivative of the momentum-space delta function at $k = 0$.

In order to construct a Hamiltonian invariant under (3.6), we just need to make sure that the coefficient of $\widetilde{\phi}_k^* \widetilde{\phi}_k$ vanishes not only at $k = 0$, but also at $k = \pm 1$. One natural way to accomplish this is to write

$$H = \sum_k \sin^2\left(\frac{\pi k}{N}\right) \sin\left(\frac{\pi(k+1)}{N}\right) \sin\left(\frac{\pi(k-1)}{N}\right) \widetilde{\phi}_k^* \widetilde{\phi}_k. \tag{3.7}$$

This is manifestly real, invariant under $k \to -k$, and invariant under the lattice $P = 2$ shift symmetry defined in (3.6).

In the continuum infinite-volume limit $a \to 0$ and $R \to \infty$, we find $\sin^2(2\pi k/N) \to K^2$, as well as $\sin(2\pi(k \pm 1)/N) \to K$. Thus, this limit correctly reproduces the $z = 2$ Hamiltonian of the continuum theory on the decompactified spatial dimension,

$$H = \int dK\, K^4 \phi^*(K)\phi(K), \tag{3.8}$$

known to be invariant under the quadratic shift symmetry $\phi(X) \to \phi(X) + \alpha X^2$ (which acts via $\phi(K) \to \phi(K) + \alpha \delta''(K)$ in the momentum-space picture).

Note that (3.7) is of course not the only lattice Hamiltonian with the exact symmetry (3.6) which gives this continuum limit. For example, the lattice Hamiltonian

$$H' = \sum_k \sin^2\left(\frac{\pi k}{N}\right) \left\{ \sin^2\left(\frac{\pi k}{N}\right) - \sin^2\left(\frac{\pi}{N}\right) \right\} \widetilde{\phi}_k^* \widetilde{\phi}_k \tag{3.9}$$

is also invariant under (3.6). It gives the same continuum infinite-volume limit as (3.7), but differs from (3.7) on the lattice by terms that are technically irrelevant in the limit.

The generalization for arbitrary polynomial shift symmetry of degree $2n-2$, with $n \in \mathbb{N}$, is straightforward. The symmetry is defined as a shift in momentum space by the corresponding $(2n-2)$-th lattice derivative of δ_k at $k = 0$. The important point is that any such $(2n-2)$-th order derivative has its support on sites in the range [1]

$$- n + 1 \leq k \leq n - 1 \tag{3.10}$$

around the origin in momentum space. Our Hamiltonian (3.7) generalizes to

$$H_n = \sum_k \sin^2 \left(\frac{\pi k}{N} \right) \prod_{\ell=1}^{n-1} \left[\sin \left(\frac{\pi(k+\ell)}{N} \right) \sin \left(\frac{\pi(k-\ell)}{N} \right) \right] \widetilde{\phi}_k^* \widetilde{\phi}_k, \tag{3.11}$$

and H' of (3.9) to

$$H'_n = \sum_k \sin^2 \left(\frac{\pi k}{N} \right) \prod_{\ell=1}^{n-1} \left\{ \sin^2 \left(\frac{\pi k}{N} \right) - \sin^2 \left(\frac{\pi \ell}{N} \right) \right\} \widetilde{\phi}_k^* \widetilde{\phi}_k. \tag{3.12}$$

Both H_n and H'_n are invariant under the lattice version of the shift symmetry of degree $2n - 2$, and they both give the same continuum infinite-volume limit

$$H = \int dK \, K^{2n} \phi^*(K) \phi(K). \tag{3.13}$$

This process is easily geneanlized to the square lattice in any spatial dimension D. In the following discussion, we will take the long-wave limit and only work with the continuous effective field theories.

3.3   Multicritical Phonons

For simplicity, we will work with the conventional jellium model of a metal in the Aristotelian spacetime of $3 + 1$ dimensions, in which the ionic lattice is replaced by a uniform mediem and the Fermi surface of the electrons is assumed to be spherically symmetric; all umkalpp processes are neglected, and the transverse components of phonons are omitted so that the phonon field is a true scalar. With the scalar being of Type A_1, this would be the simplest model of a conventional BCS superconductor. In the following we construct theories in which the phonons are replaced with NG modes of Type A_n with $n > 1$ and examine how the standard physical properties of metals change. We will refer to such NG modes in metals the "multicritical phonons."

---

[1] This is more obvious for the more interesting case considered here, with the shift symmetries of even degree, since an even-degree lattice derivative of any function f_k defined on the sites k is again naturally a function on these sites. Odd-degree shift symmetries would be implemented via odd-degree derivatives of δ_k. It is more accurate to think of the odd-degree derivative of any function f_k as a function on the links between neighboring sites k and $k+1$, and label the link by the half-integer $k+1/2$. With this interpretation, Eqn. (3.10) is correct also for shift symmetries represented by the odd-degree derivatives of δ_k.

In the hydrodynamic description [51, 52], we model the phonon system by sound waves in an isotropic Bose liquid without dissipation. Three distribution functions are required to characterize an ideal fluid, namely, the pressure distribution $p(\mathbf{x}, t)$, the density function $f(\mathbf{x}, t)$, and the velocity distribution $v(\mathbf{x}, t)$. We split the total density $f(\mathbf{x}, t)$ into an equilibrium background density $f_0(\mathbf{x}, t)$ plus the deviation from equilibrium which we denote by $Q(\mathbf{x}, t)$,

$$f(\mathbf{x}, t) = f_0(\mathbf{x}, t) + Q(\mathbf{x}, t). \tag{3.14}$$

From now on, we will assume that $\rho_0(\mathbf{x}, t) = \rho_0$ is uniform in space and time, and that $Q(\mathbf{x}, t)$ is small and slowly varied. The flow of the liquid is described by its velocity $\mathbf{v}(\mathbf{x}, t)$. We will assume that the flow is a potential flow,

$$\mathbf{v} = \nabla \phi. \tag{3.15}$$

For isotropic fluids, having $\mathbf{v}$ to be the gradient of a potential function will lead to purely longitudinal phonons – hence, the condition that the flow be a potential flow eliminates the transverse polarizations of the phonons. The system is assumed to satisfy the continuity equation for mass, which in the linearized approximation is[2]

$$\dot{Q} \approx -\rho_0 \nabla \cdot \mathbf{v} = -\rho_0 \Delta \phi. \tag{3.16}$$

The Hamiltonian of the system, in the Gaussian approximation, is expected to be

$$H = \int d^D \mathbf{x} \left(\frac{1}{2} f_0 \mathbf{v}^2 + \mathcal{V}(Q) \right). \tag{3.17}$$

The first term is just the standard kinetic energy of the liquid. The potential part $\mathcal{V}$ is to be determined below; in standard hydrodynamics, one has

$$\mathcal{V} = \frac{c_s^2}{2 f_0} Q^2. \tag{3.18}$$

To quantize the theory, we assume the standard microphysics interpretation of ρ (or $\mathbf{v}$) as the coarse graining of the sum, over all particles, of the spatial delta functions weighted by m (or $\mathbf{k}/m$), one finds that Q and ϕ form a canonical pair, with Q a generalized coordinate and ϕ its canonical momentum,

$$[\phi(\mathbf{x}), Q(\mathbf{x}')] = -i\hbar \delta(\mathbf{x} - \mathbf{x}'). \tag{3.19}$$

Moreover, The Hamiltonian (3.17) can be rewritten in terms of the canonically normalized creation and annihilaton operators

$$[a_{\mathbf{k}}, a_{\mathbf{k}'}^{\dagger}] = \delta_{\mathbf{k}\mathbf{k}'} \tag{3.20}$$

---

[2]Note that we are not proposing to replace the conventional continuity equation with a multicritical version (such as for example $\dot{Q} \sim \nabla \cdot \Delta \mathbf{v}$).

as

$$H = \sum_{\mathbf{k}} \omega_{\mathbf{k}} a_{\mathbf{k}}^{\dagger} a_{\mathbf{k}}. \tag{3.21}$$

Solving for (3.16) together with (3.19) gives

$$\phi = C \sum_{\mathbf{k}} \frac{\sqrt{\omega_{\mathbf{k}}}}{k} \left(a_{\mathbf{k}} e^{i(\mathbf{k} \cdot \mathbf{x} - \omega_{\mathbf{k}} t)} + a_{\mathbf{k}}^{\dagger} e^{-i(\mathbf{k} \cdot \mathbf{x} - \omega_{\mathbf{k}} t)} \right) \tag{3.22}$$

and

$$Q = iC' \sum_{\mathbf{k}} \frac{k}{\sqrt{\omega_{\mathbf{k}}}} \left(a_{\mathbf{k}} e^{i(\mathbf{k} \cdot \mathbf{x} - \omega_{\mathbf{k}} t)} - a_{\mathbf{k}}^{\dagger} e^{-i(\mathbf{k} \cdot \mathbf{x} - \omega_{\mathbf{k}} t)} \right). \tag{3.23}$$

The overall constants C and C' only depend on f_0, the total volume, and $\hbar$ – determine them explicitly. The free propagator for Q will be

$$D(\mathbf{k}, \omega) \sim \frac{k^2}{\omega^2 - \omega_{\mathbf{k}}^2 + i\epsilon}. \tag{3.24}$$

Our intention is to describe multicritical phonons with a higher-order dispersion relation

$$\omega_{\mathbf{k}} = \zeta_n k^n, \tag{3.25}$$

where $k = |\mathbf{k}|$. In order to get the expected phonon dispersion relation, we must choose $\mathcal{V}$ in (3.17) so that the Hamiltonian equations of motion reproduce this relation. Choosing

$$\mathcal{V} = \frac{1}{2} \zeta_n^2 \, \nabla^{n-1} Q \cdot \nabla^{n-1} Q \equiv \frac{1}{2} \zeta_n^2 \left(\partial_{i_1} \dots \partial_{i_{n-1}} Q \right) \left(\partial_{i_1} \dots \partial_{i_{n-1}} Q \right) \tag{3.26}$$

yields the desired dispersion relation. This means that in order to obtain the dispersion relation characterized by the (integer) exponent n, we must impose the polynomial shift symmetry of degree $2n - 4$ on the field Q. In this case, the free propagator (3.24) has a pole at $\omega = \zeta_n k^n$, and hence describes a multicritical phonon mode.

In this linearized approximation, we have expanded our theory around a fixed uniform density f_0, and obtained a description of the multicritical liquid in terms of the fluctuations Q around this equilibrium density. Such a non-interacting limit defines a Gaussian fixed point, with polynomial shift symmetry protecting the scaling with the dynamical exponent z. When interactions are restored, generically they explicitly break the polynomial shift symmetry. Indeed, in the full non-linear theory, we expect self-interaction terms to come from $f_0 \to f$. While f_0 is not acted on by the polynomial shift, f is.

The fixed point scaling is defined as follows:

$$[\partial_i] = 1, \qquad [\partial_t] = z, \qquad [Q] = (D - z)/2, \tag{3.27}$$

holding f_0 fixed (and hence of $[f_0] \equiv 0$). Thus, we scale *towards the state with uniform fixed density* $f = f_0$, and not towards the naive empty state with $f = 0$. This interplay between

the nonlinear structure of the theory versus the RG scaling near one of its fixed points is somewhat reminiscent of a similar split in the theory of gravity, where in order to define the Gaussian fixed point that describes free gravitons, one splits the spacetime metric into the sum of a non-zero background which defines the inertia and the fluctuations describing the propagating gravitons with the appropriate, background-dependent dispersion relation.

In a realistic crystal, there will be a finite number of oscillation modes. In the simplest Debye model description of the crystal, one assumes homogeneity and isotropy as in our discussion of multicritical hydrodynamics, and implements the finiteness of the total number of degrees of freedom by cutting off the spatial momenta at the appropriate value $k = k_D$, so that the total number of states reproduces this finiteness. Since the counting of states inside the sphere of radius k_D is the same as in the standard Debye model of linearly dispersing phonons, k_D is the standard Debye momentum of the crystal.[3] The cutoff on k translates into a natural cutoff $\widetilde{\omega}_D$ on phonon frequencies, and the existence of the characteristic temperature $\widetilde{\Theta}_D$ of the system. Due to the higher-order nature of the dispersion relation,

$$\widetilde{\omega}_D = \omega_{k_D} \equiv \zeta_n k_D^n \tag{3.28}$$

(and $\widetilde{\Theta}_D = \widetilde{\omega}_D$, in the units of $\hbar = 1 = k_B$) are not the standard Debye frequency and Debye temperature, but depend on the order n of the dispersion relation. In our comparison to the standard Debye model with the same Debye momentum k_D, we have

$$\frac{\widetilde{\omega}_D}{\omega_D} = \frac{\zeta_n}{c_s} k_D^{n-1}. \tag{3.29}$$

Similarly, the density of states $\rho(\omega)$, defined via

$$\int_0^{\omega_k} \rho(\omega) d\omega = \int_0^{|\mathbf{k}|=k} \frac{d^D \mathbf{k}}{(2\pi)^D}, \tag{3.30}$$

is not proportional to ω^{D-1} as in the standard Debye model, but given instead by

$$\rho(\omega) \propto \omega^{(D-z)/z}. \tag{3.31}$$

Note that when the phonons with the n-th order dispersion are at their lower critical dimension, $D = n$, then the density of states is a constant across all values of ω. Consequently, there are many more phonon states available near $\omega = 0$ than in the standard Debye model of linearly dispersing phonons.

Finally, we consider the interaction of the multicritical phonon system with a Fermi liquid of nonrelativistic electrons. In order to illustrate the the main robust features caused by the multicriticality of the phonons, we consider the simplest model, with the electrons modelled

---

[3]One can easily relax this condition, and allow $\widetilde{N} \neq N$. Consequently, the value of the Debye momentum would also change, to $\widetilde{k}_D = (\widetilde{N}/N)^{1/D} k_D$. In this chapter, for simplicity, we will focus on $\widetilde{N} = N$ and hence $\widetilde{k}_D = k_D$.
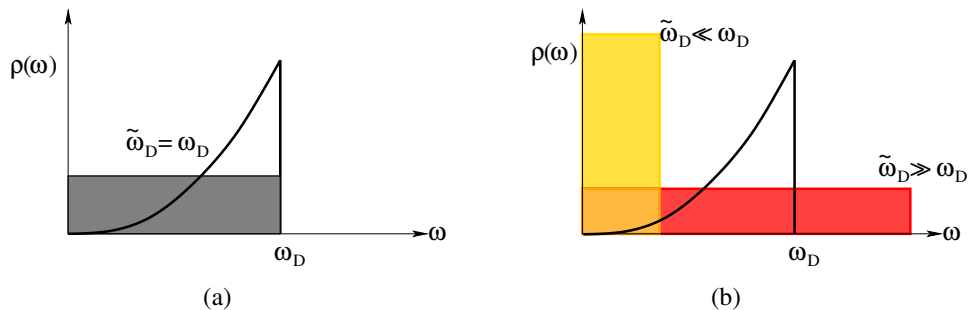
Figure 3.2: The density of states $\rho(\omega)$ as a function of frequency in the multicritical Debye model at the lower critical dimension, compared to the density of states in the standard Debye model. (a) the case of $\widetilde{\omega}_D = \omega_D$; (b) the regimes with $\widetilde{\omega}_D \ll \omega_D$ and $\widetilde{\omega}_D \gg \omega_D$, assuming fixed k_D.

by a Fermi liquid of spinless screened quasiparticles with a spherical Fermi surface, coupled to the multicritical Debye model of phonons characterized by their dispersion exponent n. Thus, we are assuming that the range of length and time scales is such that the phonons are well-approximated by a fixed value of n. Later on we will return to the question of what happens at the lower or higher scales, where this assumption may no longer be valid. The important point is that once such a hierarchy of scales open up, across which the photon dispersion is characterized by fixed $n > 1$, such a hierarchy can be naturally protected by the corresponding polynomial shift symmetry.

The coupling between electrons and our phonon liquid is taken to be minimal,[4]

$$H_{\text{int}} = g \int d^D \mathbf{x} \, Q \Psi^\dagger \Psi. \tag{3.32}$$

In the language of the "lattice displacement field" $\mathbf{Q}$, we are anticipating that $Q = \nabla \cdot \mathbf{Q}$. Thus, the minimal vertex between Q and the electrons will reproduce the calculations that used the momentum-dependent vertex because the photon propagator is different in those two pictures. Such standard coupling breaks the polynomial shift symmetry of the phonon system all the way to the constant shifts of $\mathbf{Q}$, in a way which however does not violate the hierarchy of scales. Moreover, this coupling generates relevant deformations and produces a natural pairing mechanism for the electrons.

To quantize the theory with the Yukawa coupling, we take the mode expansion of Ψ,

$$\Psi = C'' \sum_{\mathbf{k}} c_{\mathbf{k}} \, e^{i(\mathbf{k} \cdot \mathbf{x} - \omega t)}. \tag{3.33}$$

---

[4]As an alternative, we could also consider non-minimal couplings, for example the shift-symmetry-preserving coupling, of the form $\Psi^\dagger \Psi \Delta^\# Q$, with the appropriate power $\#$. What is the appropriate $\#$? If we want an exact invariant, we need $\Psi^\dagger \Psi \Delta^{2z-2} Q$. Intriguingly, if we allow the polynomial shift to act on the chemical potential by a shift, we can have $\Psi^\dagger \Psi \Delta^{2z-4} Q$, whose variation under the shift of degree $2z - 4$ is a constant which can be compensated for by the shift of the chemical potential...

Again, similar to C and C' in (3.22) and (3.23), the overall constant C'' only depends on f_0, the total volume and $\hbar$. Substitute (3.22), (3.23) and (3.33) into (3.32), we obtain the well-known Fröhlich interaction,

$$H_{\mathrm{int}} = -i \sum_{\mathbf{k}, bq} g_{\mathbf{q}} \, a_{\mathbf{q}} \, c^{\dagger}_{\mathbf{k}+\mathbf{q}} \, c_{\mathbf{k}} + \mathrm{h.c.}, \tag{3.34}$$

where the coupling $g_{\mathbf{q}}$ is given by

$$g_{\mathbf{q}} = g \frac{q}{\sqrt{\omega_{\mathbf{q}}}}. \tag{3.35}$$

3.4   Bloch-Grüneisen Formula and Resistivity in Strange Metals

In this section, we use the Bloch-Boltzmann kinetic theory of transport, to calculate the resistivity of the fermions in the multicritical metal, caused by the interactions between the electrons and the multicritical phonons in $3+1$ demensions. In the low-temperature regime, we find a power-law dependence on T. More generally, we obtain a natural generalization of the well-known Bloch-Grüneisen formula (that computes the resistivity in metals) to the multicritical case.

We start with a short review of the derivation of the standard Bloch-Grüneisen formula [53, 54]. In Bloch-Boltzman theory, the Hamiltonian of the electron-phonon interaction in (3.32) induces the transitions of the electrons between different Bloch states $|\mathbf{k}\rangle$. Denote the distribution function for the electrons by n_k, and the distribution function for the phonons by N_q. In the first Brillouin zone[5], the electrons can be scattered via the following two processes and their inverses:

- An electron at state $|\mathbf{k}\rangle$ emits a phonon of momentum $\mathbf{q}$ and thus scatters into the state $|\mathbf{k}'\rangle$. The conservation law of momenta requires $\mathbf{k} = \mathbf{k}' + \mathbf{q}$.

- An electron at state $|\mathbf{k}\rangle$ absorbs a phonon of momentum $\mathbf{q}$ and thus scatters into the state $|\mathbf{k}'\rangle$. The conservation law of momenta requires $\mathbf{k} + \mathbf{q} = \mathbf{k}'$.

Furthermore, due to the Pauli principle, a transition can take place only to an unoccupied state. Therefore, the collision function is

$$
\begin{aligned}
C(n_{\mathbf{k}}) = & \int \frac{d^3\mathbf{q}}{(2\pi)^3} \frac{d^3\mathbf{k}'}{(2\pi)^3} \, |g_q|^2 \, (2\pi) \, \delta \left(\varepsilon_{\mathbf{k}} - \varepsilon_{\mathbf{k}'} - \omega_{\mathbf{q}} \right) (2\pi)^3 \, \delta^{(3)} \left(\mathbf{k} - \mathbf{k}' - \mathbf{q} \right) \\
& \times \left[(1 - n_{\mathbf{k}}) \, n_{\mathbf{k}'} N_{\mathbf{q}} - n_k \, (1 - n_{\mathbf{k}'}) \, (N_{\mathbf{q}} + 1) \right] \\
& + \int \frac{d^3\mathbf{q}}{(2\pi)^3} \frac{d^3\mathbf{k}'}{(2\pi)^3} \, |g_q|^2 \, (2\pi) \, \delta \left(\varepsilon_{\mathbf{k}} + \omega_{\mathbf{q}} - \varepsilon_{\mathbf{k}'} \right) (2\pi)^3 \, \delta^{(3)} \left(\mathbf{k} + \mathbf{q} - \mathbf{k}' \right) \\
& \times \left[(1 - n_{\mathbf{k}}) \, n_{\mathbf{k}'} \, (N_{\mathbf{q}} + 1) - n_k \, (1 - n_{\mathbf{k}'}) \, N_{\mathbf{q}} \right].
\end{aligned}
\tag{3.36}
$$

---

[5]The Umklapp process has a zero contribution in a metal.

Here, $\varepsilon_{\mathbf{k}}$ is the energy of the quasi-particle. We treat the phonon system as if it were in thermal equilibrium, *i.e.*,

$$N_{\mathbf{q}} = N_q^{(0)} = \frac{1}{\exp\left(\omega_q/T\right) - 1}. \tag{3.37}$$

For multicritical phonons of Type A_n, $\omega_q \approx \zeta_n q^n$. We further denote the Fermi-Dirac distribution by

$$n_k^{(0)} = \frac{1}{\exp[(\varepsilon_k - \varepsilon_F)/T] + 1}. \tag{3.38}$$

Denote $\Phi_{\mathbf{k}}$ the average extra energy that the quasi-particles have because of the transport process. For small $\Phi_{\mathbf{k}}$ we can write

$$n_{\mathbf{k}} \approx n_k^{(0)} - \frac{\partial n_k^{(0)}}{\partial \varepsilon_k} \Phi_{\mathbf{k}}. \tag{3.39}$$

At low temperatures, $T \ll \varepsilon_F$, with ε_F the Fermi energy, we have

$$n_{\mathbf{k}} \approx n_k^{(0)} + \delta(\varepsilon_k - \varepsilon_F) \Phi_{\mathbf{k}}, \tag{3.40}$$

Let us expand $C(n_{\mathbf{k}})$ in (3.36) with respect to $\Phi_{\mathbf{k}}$ and $\Phi_{\mathbf{k}'}$ and write

$$C(n_{\mathbf{k}}) = \frac{1}{T} \int \frac{d^3\mathbf{k}'}{(2\pi)^3} \left(\Phi_{\mathbf{k}'} - \Phi_{\mathbf{k}}\right) \mathcal{P}_k^{k'}, \tag{3.41}$$

where

$$\mathcal{P}_k^{k'} = 2\pi \int d^3\mathbf{q} \, |g_q|^2 n_k^{(0)} \left(1 - n_{k'}^{(0)}\right) \left[\left(N_q^{(0)} + 1\right) \delta(\varepsilon_k - \varepsilon_{k'} - \omega_q) \delta^{(3)}\left(\mathbf{k} - \mathbf{k}' - \mathbf{q}\right) \right.$$
$$\left. + N_q^{(0)} \delta(\varepsilon_k - \varepsilon_{k'} + \omega_q) \delta^{(3)}\left(\mathbf{k} - \mathbf{k}' + \mathbf{q}\right)\right] \tag{3.42}$$

is the equilibrium transition rate between states $|\mathbf{k}\rangle$ and $|\mathbf{k}'\rangle$. According to the principle of microscopic reversibility, we have

$$\mathcal{P}_k^{k'} = \mathcal{P}_{k'}^k. \tag{3.43}$$

To compute the resistivity as a linear response, we consider the presence of an external electric field $\mathbf{E}$. We assume that there is no temperature gradient. The Boltzmann transport equation is

$$- e\left(\mathbf{E} \cdot \mathbf{v}_{\mathbf{k}}\right) \frac{\partial n_k^{(0)}}{\partial \varepsilon_k} = -C(n_{\mathbf{k}}) = \frac{1}{T} \int \frac{d^3\mathbf{k}'}{(2\pi)^3} \left(\Phi_{\mathbf{k}} - \Phi_{\mathbf{k}'}\right) \mathcal{P}_k^{k'}, \tag{3.44}$$

where $\mathbf{v}_{\mathbf{k}}$ is the drifting velocity of the electron. The resistivity ρ is defined to be the ratio of the electric field $\mathbf{E}$ to the density of the current $\mathbf{J}$ it creates, namely

$$\mathbf{E} = \rho \, \mathbf{J}, \tag{3.45}$$

where we have assumed isotropy in the material. The electric current is

$$\mathbf{J} = \int \frac{d^3\mathbf{k}}{(2\pi)^3} \, e \, \mathbf{v_k} \big(n_\mathbf{k} - n_\mathbf{k}^{(0)}\big) = - \int \frac{d^3\mathbf{k}}{(2\pi)^3} \, e \, \mathbf{v_k} \frac{\partial n_k^{(0)}}{\partial \varepsilon_k} \Phi_\mathbf{k}. \tag{3.46}$$

Applying the Boltzmann transport equation (3.44), we obtain

$$\rho = \frac{\mathbf{E} \cdot \mathbf{J}}{J^2} = \frac{C_\rho}{T} \int \frac{d^3\mathbf{k}}{(2\pi)^3} \frac{d^3\mathbf{k}'}{(2\pi)^3} \left(\Phi_\mathbf{k} - \Phi_{\mathbf{k}'}\right)^2 \mathcal{P}_k^{k'}, \tag{3.47}$$

where C_ρ is an overall T-independent prefactor.

To proceed, we need an explicit expression for $\Phi_\mathbf{k}$. We have assumed that the Fermi surface is spherical. This assumption requires that the drifting velocity $\mathbf{v_k}$ of electrons be parallel to $\mathbf{k}$. Moreover, we make a further assumption that the scattering probability only depends on the angle between $\mathbf{k}$ and $\mathbf{k}'$, where $\mathbf{k}$ and $\mathbf{k}'$ are respectively associated with the incoming state $|\mathbf{k}\rangle$ and the outgoing state $|\mathbf{k}'\rangle$. Under these additional assumptions, we obtain

$$\Phi_k \propto k \cos\theta \tag{3.48}$$

in $3+1$ dimensions, where θ is the angle between $\mathbf{k}$ and the electric field $\mathbf{E}$. In two spatial dimensions, a similar analysis gives $\Phi_k \propto \sin\theta$.

We would like to introduce a final assumption: The collisions between electrons and multicritical phonons are dominated by the long wave phonon modes, and thus the scattering can be treated as a quasi-elastic process [55, 56], *i.e.*, in (3.42),

$$\delta\left(\varepsilon_k - \varepsilon_{k'} + \omega_q\right) \approx \delta\left(\varepsilon_k - \varepsilon_{k'}\right). \tag{3.49}$$

Under this additional assumption, the resistivity given in (3.47) takes the form

$$\rho = C_\rho' \int_{\mu_{\mathrm{IR}}}^{2k_D} (dq \, q) \, q^2 \, |g_q|^2 \, N_q^{(0)}. \tag{3.50}$$

Here, C_ρ' is a T-independent coefficient, g_q is the vertex given in (3.35), and $N_q^{(0)}$ is the multicritical phonon distribution defined in (3.37). The infrared regulator μ_{IR} can be set to zero in the absence of infrared divergences. Plugging (3.35) and (3.37) into (3.50), we obtain

$$\rho = C_\rho' g^2 \int_{\mu_{\mathrm{IR}}}^{2k_D} dq \, \frac{q^5}{\omega_q} \frac{1}{\exp(\omega_q/T) - 1}, \tag{3.51}$$

where $\omega_q = \zeta_n q^n$ for Type A_n multicritical phonon. In the low temperature limit,

$$\zeta_n \mu_{\mathrm{IR}}^n \ll T \ll \Theta_D = \zeta_n (2k_n)^n, \tag{3.52}$$

with Θ_D the Debye temperature, we obtain the resistivity as a function of T,

$$\rho(T) \sim T^{\frac{6-n}{n}}. \tag{3.53}$$

In the standard case of $n = 1$, this reproduces the standard Bloch-Grüneisen scaling $\rho \sim T^5$. More interestingly, in the case of the multicritical phonons at their lower critical dimension, $n = 3$, we obtain $\rho \sim T$.

Without the elastic approximation (3.49), the resistivity (3.47) takes a slightly more complicated form,

$$\rho(T) \propto \int \frac{d^3\mathbf{k}}{(2\pi)^3} \frac{d^3\mathbf{k}'}{(2\pi)^3} q^2 |g_q|^2 N_q^{(0)} \delta(\varepsilon_k - \varepsilon_F) \delta(\varepsilon_k - \varepsilon_{k'} + \omega_q), \tag{3.54}$$

which reduces to

$$\rho(T) = C_\rho'' g^2 \int_0^{2k_F} dq \, \frac{q^5}{\sinh^2[\omega_q/(2T)]}. \tag{3.55}$$

Here, C_ρ'' is a T-independent coefficient. This modification does not alter the scaling in T in (3.53).

The calculation can be repeated in any number of spatial dimensions D, generalizing (3.53) to

$$\rho(T) \propto T^{\frac{3+D-n}{n}}. \tag{3.56}$$

Type A_n multicritical phonons with $n \leq D$ suggests resistivity going as T^5 or T^2 (which matches the scaling of the electron-electron contribution) or T in $D = 3$, and T^4 or $T^{3/2}$ in $D = 2$.

3.5 Infrared Behavior and Cascading Phenomena

We study the IR behavior of (3.50) in this section. We consider the multicritical phonons at their lower critical dimension, with $n = 3$ and

$$\omega_q = \zeta_3 q^3. \tag{3.57}$$

It is useful to define

$$\omega_\otimes = \zeta_3 \mu_{\text{IR}}^3 \ll \Theta_D. \tag{3.58}$$

The resistivity is evaluated to be

$$\rho(T) = \frac{C_\rho' g^2}{3\zeta_3^2} T \int_{\frac{\omega_\otimes}{T}}^{\frac{\Theta_D}{T}} dx \, \frac{1}{e^x - 1}$$

$$= \frac{C_\rho' g^2}{3\zeta_3^2} T \log\left(\frac{T}{\omega_\otimes}\right) + \mathcal{O}(\omega_\otimes), \tag{3.59}$$

We have taken the low temperature limit $\omega_\otimes \ll T \ll \Theta_D$. This asymptotic expansion contains a log divergence in $\omega_\otimes$, which shows that $\rho(T)$ is sensitive to the IR regulator. This IR regulator has a simple physical interpretation: We can choose $\omega_\otimes$ to be the crossover scale around which the theory flows to a $n = 1$ fixed point. Then, the $n = 3$ dispersion dominates
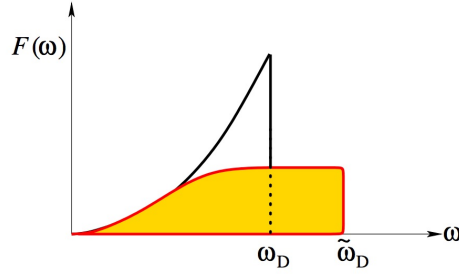
Figure 3.3: The density of states $\rho(\omega)$ as a function of frequency with a crossover to $n = 1$ below $\omega_\otimes$.

in the regime below the Debye frequency Θ_D, and transits to $n = 1$ at the hierarchically much smaller scale $\omega_\otimes$, breaking the polynomial shift symmetries all the way to constant shift. This breaking modifies the dispersion relation to[6]

$$\omega^2 = \zeta_3^2 q^6 + c_s^2 q^2, \tag{3.60}$$

where c_s is the speed of sound for standard phonons with $n = 1$. At the crossover scale $\omega_\otimes$, the k^6 and k^2 terms in (3.60) become comparable. For clarity, we take

$$\omega_\otimes^2 = \frac{c_s^3}{\zeta_3}. \tag{3.61}$$

This modified dispersion relation suggests the behavior of the density of states in Figure 3.3. In low energies, our theory flows to the conventional BSC.

Does this modification in the IR spoil the T-linear dependence? Naïvely, it seems that there is no linear term in T in (3.59) (but only a $T \log T$ term). However, a concrete answer to this question requires explicit evaluation of the resistivity. Without affecting the qualitative behavior, we assume a simple behavior for the dispersion relation:

- In the high energy regime $\omega_\otimes < \omega_q < \Theta_D$: $\omega_q = \zeta_3 q^3$;

- In the low energy regime $\omega_q < \omega_\otimes$: $\omega_q = c_s q$.

The resistivity is evaluated to be

$$\rho = C_\rho' g^2 \left(\int_{0<\omega<\omega_\otimes} dq \, \frac{q^5}{\omega_q} \frac{1}{\exp(\omega_{\mathbf{q}}/T) - 1} \bigg|_{\omega_q = c_s q} + \int_{\omega_\otimes<\omega<\Theta_D} dq \, \frac{q^5}{\omega_q} \frac{1}{\exp(\omega_{\mathbf{q}}/T) - 1} \bigg|_{\omega_q = \zeta_3 q^3} \right)$$

$$= \frac{C_\rho' g^2}{\zeta_3^2} T \left[\frac{1}{4} + \frac{1}{3} \log(T/\omega_\otimes) \right] + \mathcal{O}(\omega_\otimes). \tag{3.62}$$

---

[6]In more general cases, one may also include an intermediate crossover to a $n = 2$ fixed. Including this $z = 2$ fixed point modifies the dispersion relation to $\omega^2 = \zeta_3^2 k^6 + \zeta_2^2 k^4 + c_s^2 k^2$.

The linear dependence on T persists, but now receives a $T \log T$ correction.

The behavior of having the multicritical phonons crossover to lower n's in the IR by explicitly breaking the polynomial shift symmetries and thus protect a large hierarchy between energy scales is called to the *cascading phenomena*. In Chapter 5, we will study this phenomena systematically by examining a series of examples.

Similarly, if we use (3.55) that takes into account the inelastic effects and again let the theory crossover to a $n = 1$ fixed point in the IR, then (3.55) can be split into two parts as in (3.62):

$$
\begin{aligned}
\rho &= \frac{C''_\rho g^2}{T} \left(\int_{0 < \omega < \omega_\otimes} dq \left. \frac{q^5}{\sinh^2[\omega_q/(2T)]} \right|_{\omega_q = c_s q} + \int_{\omega_\otimes < \omega < \Theta_D} dq \left. \frac{q^5}{\sinh^2[\omega_q/(2T)]} \right|_{\omega_q = \zeta_3 q^3} \right) \\
&= C''_\rho g^2 T \left\{ \frac{\omega_\otimes^4}{c^6} + \frac{1}{3\zeta_3^2} \left[1 + \log\left(\frac{T}{\omega_\otimes} \right) \right] \right\} + \mathcal{O}(\omega_\otimes) \\
&= \frac{C''_\rho g^2}{3\zeta_3^2} T \left[4 + \log\left(\frac{T}{\omega_\otimes} \right) \right] + \mathcal{O}(\omega_\otimes).
\end{aligned}
\tag{3.63}
$$

Again, we obtain the T-linear dependence.

In conclusion, by considering the interacting between electron and multicritical phonons protected by polynomial shift symmetries in the framework of the BCS theory, we obtain a refined classification of EFTs that describe the low energy excitations. In particular, by requiring that the high-energy behavior of acoustic phonons be described by multicritical phonons of Type A_3, we provide a technically natural explanation for the T-linear behavior in $3 + 1$ dimensions. What role this new mechanism could play in high-T_c superconductivity remains as an intriguing open question.

Chapter 4

Polynomial Shift Symmetries and Graph Theory

In Chapter 2, we have established a new infinite sequence of symmetries in scalar field theories, and have shown that they can protect the smallness of quantum mechanical corrections to their low-energy dispersion relations near the Gaussian fixed points. The symmetries are exact at the infrared Gaussian fixed point, and turning on interactions typically breaks them explicitly. Yet, the polynomial shift symmetry at the Gaussian fixed point is useful for the interacting theory as well: It controls the interaction terms, allowing them to be naturally small, parametrized by the amount ε of the explicit polynomial symmetry breaking near the fixed point.

Generally, this explicit breaking by interactions breaks the polynomial shift symmetries of NG modes all the way to the constant shift (for example, the electron-phonon interaction in (3.32)), which remains mandated by the original form of the Goldstone theorem (guaranteeing the existence of gapless modes). However, one can now turn the argument around, and ask the following question: Starting at a given Type A_n or B_{2n} fixed point, what are the lowest-dimension scalar composite operators that involve N fields ϕ and respect the polynomial shift symmetry of degree P exactly, up to a total derivative? Such operators can be added to the action, and for $N = 3, 4, \ldots$ they represent self-interactions of the system, invariant under the polynomial shift of degree P. More generally, one can attempt to classify all independent composite operators invariant under the polynomial shift symmetry of degree P, organized in the order of their increasing dimensions.

These are the questions on which we focus in this chapter. In order to provide some answers, we will first translate this classification problem into a more precise mathematical language, and then we will develop techniques – largely based on abstract graph theory – that lead us to systematic answers. For some low values of the degree P of the polynomial symmetry and of the number N of fields involved, we can even find the most relevant invariants and prove their uniqueness. In the following, we will start with the special case of $P = 1$ (essentially equivalently to Galileons); we reproduce the known Galielon N-point invariants, and find their nowvel interpretation in terms of graph theory, as an equal-weight sum over all labeled trees with N vertices. Then we extend the classification to $P > 1$ and find a whole host of new invariants, including those that represent the most relevant

(or least irrelevant) deformations of the corresponding Gaussian fixed points. The rigorous mathematical treatment of the associated theorems is quite technical and involved, for which we will mostly refer the readers to the appendix in our original paper [19]. This chapter is also, however, self-contained, and can be read independently of [19].

4.1 Galileon Invariants

Consider a quantum field theory of a single scalar field $\phi(t, \mathbf{x})$ in D spatial dimensions and one time dimension. Consider the transformation of the field which is linear in spatial coordinates: $\delta\phi = a_i x^i + a_0$, where a_i and a_0 are arbitrary real coefficients. Other than the split between time and space and the exclusion of the time coordinate from the linear shift transformation, this is the same as the theory of the Galileon [49].

The goal is to find Lagrangian terms which are invariant (up to a total derivative) under this linear shift transformation. We will classify the Lagrangian terms by their numbers of fields N and derivatives 2Δ. Imposing spatial rotation invariance requires that spatial derivatives be contracted in pairs by the flat metric δ_{ij}. Thus Δ counts the number of contracted pairs of derivatives. It is easy to find Lagrangian terms which are exactly invariant (*i.e.*, not just up to a total derivative): Let $\Delta \geq N$ and let at least two spatial derivatives act on every ϕ. For the linear shift case, all terms with at least twice as many derivatives as there are fields are equal to exact invariants, up to total derivatives. However, it is possible for a term to have fewer derivatives than this and still be invariant up to a non-vanishing total derivative. For fixed N, the terms with the lowest Δ are more relevant in the sense of the renormalization group. Therefore, we will focus on invariant terms with the lowest number of derivatives, which we refer to as *minimal invariants*.

These minimal invariants have already been classified for the case of the linear shift. There is a unique (up to total derivatives and an overall constant prefactor) N-point minimal invariant, which contains $2(N-1)$ derivatives (*i.e.*, $\Delta = N - 1$). These are listed below up to $N = 5$.

$$L_{\text{1-pt}} = \phi, \tag{4.1a}$$

$$L_{\text{2-pt}} = \partial_i\phi\,\partial_i\phi, \tag{4.1b}$$

$$L_{\text{3-pt}} = 3\,\partial_i\phi\,\partial_j\phi\,\partial_i\partial_j\phi, \tag{4.1c}$$

$$L_{\text{4-pt}} = 12\,\partial_i\phi\,\partial_i\partial_j\phi\partial_j\partial_k\phi\,\partial_k\phi + 4\,\partial_i\phi\,\partial_j\phi\,\partial_k\phi\,\partial_i\partial_j\partial_k\phi, \tag{4.1d}$$

$$\begin{aligned} L_{\text{5-pt}} &= 60\,\partial_i\phi\,\partial_i\partial_j\phi\,\partial_j\partial_k\phi\,\partial_k\partial_\ell\phi\,\partial_\ell\phi + 60\,\partial_i\phi\,\partial_i\partial_j\phi\,\partial_j\partial_k\phi\,\partial_\ell\phi\,\partial_k\phi\,\partial_\ell\phi \\ &\quad + 5\,\partial_i\phi\,\partial_j\phi\,\partial_k\phi\,\partial_\ell\phi\,\partial_i\partial_j\partial_j\partial_k\partial_\ell\phi. \end{aligned} \tag{4.1e}$$

These are not identical to the usual expressions (*e.g.*, in [49]), but one can easily check that they are equivalent.

We can represent the terms in (4.1) as formal linear combinations of graphs. In these graphs, ϕ is represented by a $\bullet$-vertex. An edge joining two vertices represents a pair of contracted derivatives, one derivative acting on each of the ϕ's representing the endpoints of

the edge. The graphical representations of the above terms are given below:

$$L_{1\text{-pt}} = \bullet, \tag{4.2a}$$

$$L_{2\text{-pt}} = \bullet\!\!-\!\!-\!\!\bullet\ , \tag{4.2b}$$

$$L_{3\text{-pt}} = 3\ \diagdown\!\!\!\!\diagup\ , \tag{4.2c}$$

$$L_{4\text{-pt}} = 12\ \square\ + 4\ \diagdown\!\!\!\!\diagup\ , \tag{4.2d}$$

$$L_{5\text{-pt}} = 60\ \diagup\!\!\!\!\diagdown\ + 60\ \diagup\!\!\!\!\diagdown\ + 5\ \diagup\!\!\!\!\diagdown\ . \tag{4.2e}$$

The structure of the graph (*i.e.*, the connectivity of the vertices) is what distinguishes graphs; the placement of the vertices is immaterial. This reflects the fact that the order of the ϕ's in the algebraic expressions is immaterial and the only thing that matters is which contracted pairs of derivatives act on which pairs of ϕ's. Therefore, for example, the graphs below all represent the same algebraic expression.

$$\diagdown\!\!\!\!\diagup \qquad \diagup\!\!\!\!\diagdown \qquad \diagdown\!\!\!\!\diagup \tag{4.3}$$

Similarly, the four graphs below represent the same algebraic expression.

$$\diagup\!\!\!\!\diagdown \qquad \diagdown\!\!\!\!\diagup \qquad \diagup\!\!\!\!\diagdown \qquad \diagdown\!\!\!\!\diagup \tag{4.4}$$

A more nontrivial example is given by the following twelve graphs, which all represent the same algebraic expression.

$$\tag{4.5}$$

The graphs in the second line above appear to have intersecting edges. However, since there is no $\bullet$-vertex at the would-be intersection, these edges do not actually intersect.

There are three times as many graphs in (4.5) as there are in (4.4). It so happens that the coefficient with which the first graph in (4.5) appears in $L_{4\text{-pt}}$ (4.2d) is also three times the coefficient with which the first graph in (4.4) appears in $L_{4\text{-pt}}$. This suggests that

the coefficient with which a graph appears in a minimal term is precisely the number of graphs with the exact same structure (*i.e.*, isomorphic), just with various vertices and edges permuted.

One simple way to state this is to actually label the vertices in the graphs. If the vertices were labeled, and thus distinguished from each other, then all of the graphs in each one of (4.3), (4.4) and (4.5) would actually be distinct graphs. Of course, this means that the corresponding algebraic expressions have ϕ's similarly labeled, but this labeling is fiducial and may be removed afterwards. Note the simplicity that this labeled convention introduces: $L_{4\text{-pt}}$ is the sum of all of the graphs in (4.4) and (4.5) with unit coefficients.

The graphs in (4.4) and (4.5) have an elegant and unified interpretation in graph theory. These graphs are called *trees*. A tree is a graph which is connected (*i.e.*, cannot be split into two or more separate graphs without cutting an edge), and contains no loops (edges joining a vertex to itself) or cycles (edges joining vertices in a closed cyclic manner). One can check that there are exactly 16 trees with four vertices and they are given by (4.4) and (4.5). Cayley's formula, a well-known result in graph theory, says that the number of trees with N vertices is N^{N-2}.

For $N = 3$, the $3^{3-2} = 3$ trees are in (4.3), and we indeed find that $L_{3\text{-pt}}$ is the sum of all three graphs with unit coefficients. The same can be said for $L_{2\text{-pt}}$ and $L_{1\text{-pt}}$. Therefore, the minimal terms for $N = 1, 2, 3$ and 4 are represented graphically as a sum of trees with unit coefficients (an equal-weight sum of trees). If this were to hold for the $N = 5$ case, it would strongly suggest that this may hold for all N.

There are $5^3 = 125$ trees for $N = 5$. They can be divided into three sets such that the trees in each set are isomorphic to one of the three graphs appearing in $L_{5\text{-pt}}$ (4.2e). There are 60 graphs which are isomorphic to the first graph appearing in $L_{5\text{-pt}}$; 12 of these are listed below and the rest are given by the five rotations acting on each of these 12 graphs:

$$(4.6)$$
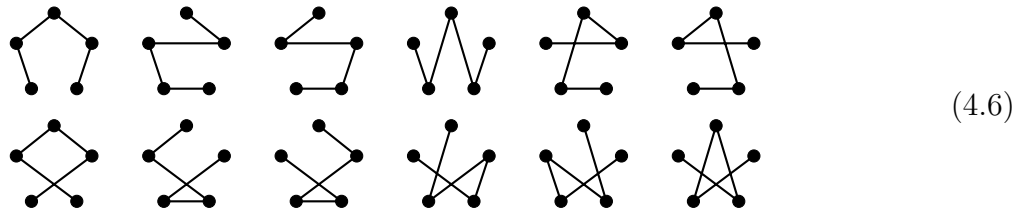
There are 60 graphs which are isomorphic to the second graph appearing in L_5; 12 of these are listed below and the rest are given by their rotations:

$$(4.7)$$
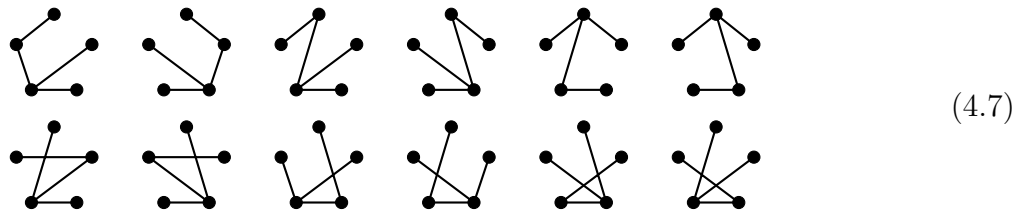
Finally, there are five graphs which are isomorphic to the third graph appearing in $L_{5\text{-pt}}$, which are simply the five rotations acting on that graph. Therefore, $L_{5\text{-pt}}$ is indeed the sum with unit coefficients of all trees with five vertices!

Thus, we arrive at the main result of this section:

— the unique minimal N-point linear shift-invariant Lagrangian term is represented graphically as a sum with unit coefficients of all labeled trees with N vertices.

We refer the reader to [19] for a thorough proof of this theorem.

4.2 Beyond the Galileons

Now, we extend the linear shift transformation to polynomials of higher degree. We will need to develop the graphical approach further in order to tackle this problem and numerous technicalities will arise. However, a rather elegant and beautiful description of these polynomial shift invariants will emerge.

Consider the problem of determining all possible terms in a Lagrangian that are invariant under the polynomial shift symmetry:

$$\phi(t, x^i) \to \phi(t, x^i) + \delta_P \phi, \qquad \delta_P \phi = a_{i_1 \cdots i_P} x^{i_1} \cdots x^{i_P} + \cdots + a_i x^i + a. \qquad (4.8)$$

The a's are arbitrary real coefficients that parametrize the symmetry transformation, and are symmetric in any pair of indices. $P = 0, 1, 2, \ldots$ corresponds to constant shift, linear shift, quadratic shift, and so on. Obviously, if a term is invariant under a polynomial shift of order P, then it is also invariant under a polynomial shift of order P' with $0 \le P' \le P$.

We will call a term with N fields and 2Δ derivatives an (N, Δ) term. We are interested in interaction terms, for which $N \ge 3$. As previously mentioned, terms with the lowest possible value of Δ are of greatest interest. It is straightforward to write down invariant terms with $\Delta \ge \frac{1}{2} N(P + 1)$ since, if each ϕ has more than P derivatives acting on it, then the term is exactly invariant. Are there any invariant terms with lower values of Δ? If so, then these invariant terms will be more relevant than the exact invariants.

To be invariant, a term must transform into a total derivative under the polynomial shift symmetry. In other words, for a specific P and given (N, Δ), we are searching for terms L such that

$$\delta_P L = \partial_i(L_i). \qquad (4.9)$$

Here L is a linear combination of terms with N ϕ's and 2Δ ∂'s, and L_i is a linear combination of terms with $N - 1$ ϕ's. Such L's are called *P-invariants*.

How might we determine such invariant terms in general? For a given (N, Δ), the most brute-force method for determining invariant terms can be described as follows. First, write down all possible terms in the Lagrangian with a given (N, Δ) and ensure that they are independent up to integration by parts. Next, take the variation of all these terms under the polynomial shift. There may exist linear combinations of these variations which are equal to a total derivative, which we call *total derivative relations*. If we use these total derivative relations to maximally reduce the number of variation terms, then the required P-invariants form the kernel of the map from the independent Lagrangian terms to the independent variation terms. Let us consider some examples of this brute-force procedure in action.

Example 1: $(P, N, \Delta) = (1, 3, 2)$. In this case, a general Lagrangian is made up of two independent terms, after integrating by parts, given by

$$L_1 = \partial_i\phi\,\partial_j\phi\,\partial_i\partial_j\phi, \qquad\qquad L_2 = \phi\,\partial_i\partial_j\phi\,\partial_i\partial_j\phi.$$

The variation under the linear shift symmetry (for $P = 1$) of these terms is given by

$$\delta_1(L_1) = 2L_a^\times, \qquad\qquad \delta_1(L_2) = L_b^\times,$$

where $L_a^\times = a_i\,\partial_j\phi\,\partial_i\partial_j\phi$ and $L_b^\times = a_k x^k\,\partial_i\partial_j\phi\,\partial_i\partial_j\phi$. There is only one total derivative that can be formed from these terms, namely

$$\partial_i(a_i\partial_j\phi\,\partial_j\phi) = 2L_a^\times.$$

Therefore, there is a single invariant term for $(P, N, \Delta) = (1, 3, 2)$, given by

$$L_1 = \partial_i\phi\,\partial_j\phi\,\partial_i\partial_j\phi.$$

Example 2: $(P, N, \Delta) = (3, 3, 4)$. In this case, a general Lagrangian is made up of four independent terms, after integrating by parts, given by

$$L_1 = \partial_i\partial_j\phi\,\partial_k\partial_l\phi\,\partial_i\partial_j\partial_k\partial_l\phi, \qquad L_2 = \partial_i\partial_j\phi\,\partial_i\partial_k\partial_l\phi\,\partial_j\partial_k\partial_l\phi,$$
$$L_3 = \partial_i\phi\,\partial_j\partial_k\partial_l\phi\,\partial_i\partial_j\partial_k\partial_l\phi, \qquad L_4 = \phi\,\partial_i\partial_j\partial_k\partial_l\phi\,\partial_i\partial_j\partial_k\partial_l\phi.$$

The variation under the cubic shift symmetry (for $P = 3$) of these terms is given by

$$\delta_3(L_1) = 2L_a^\times, \qquad\qquad \delta_3(L_2) = L_b^\times + 2L_c^\times,$$
$$\delta_3(L_3) = L_d^\times + L_e^\times, \qquad\qquad \delta_3(L_4) = L_f^\times.$$

where

$$
\begin{aligned}
L_a^\times &= (6a_{ijm}x^m + 2a_{ij})\partial_k\partial_l\phi\,\partial_i\partial_j\partial_k\partial_l\phi \\
L_b^\times &= (6a_{ijm}x^m + 2a_{ij})\partial_i\partial_k\partial_l\phi\,\partial_j\partial_k\partial_l\phi \\
L_c^\times &= 6a_{ikl}\partial_i\partial_j\phi\,\partial_j\partial_k\partial_l\phi \\
L_d^\times &= (3a_{imn}x^m x^n + 2a_{im}x^m + a_i)\partial_i\phi\,\partial_j\partial_k\partial_l\phi\,\partial_i\partial_j\partial_k\partial_l\phi \\
L_e^\times &= 6a_{jkl}\partial_i\phi\,\partial_i\partial_j\partial_k\partial_l\phi \\
L_f^\times &= (a_{mnp}x^m x^n x^p + a_{mn}x^m x^n + a_m x^m + a)\partial_i\partial_j\partial_k\partial_l\phi\,\partial_i\partial_j\partial_k\partial_l\phi.
\end{aligned}
$$

There are three independent total derivatives that can be formed out of these:

$$\partial_i[2(6a_{ijm}x^m + 2a_{ij})\partial_k\partial_l\phi\,\partial_j\partial_k\partial_l\phi - 6a_{ijj}\partial_k\partial_l\phi\,\partial_k\partial_l\phi] = 2(L_a^\times + L_b^\times),$$
$$\partial_i[6a_{ijk}\partial_j\partial_l\phi\,\partial_k\partial_l\phi] = 2L_c^\times,$$
$$\partial_i[6a_{ijk}\partial_j\partial_k\partial_\ell\phi\,\partial_\ell\phi] = L_c^\times + L_e^\times.$$

It is a non-trivial exercise to find and verify this, and a more systematic way of finding the total derivative relations will be introduced later.

Applying these relations, one finds a single invariant for $(P, N, \Delta) = (3, 3, 4)$ term:

$$L_1 + 2L_2 = \partial_i \partial_j \phi \, \partial_k \partial_l \phi \, \partial_i \partial_j \partial_k \partial_l \phi + 2\partial_i \partial_j \phi \, \partial_i \partial_k \partial_l \phi \, \partial_j \partial_k \partial_l \phi.$$

Note that $\delta_3(L_1 + 2L_2) = 2(L_a^\times + L_b^\times) + 2(2L_c^\times)$, which is a total derivative.

It is clear that even for these simple examples, the calculations quickly become unwieldy, and it becomes increasingly difficult to classify all of the total derivative relations. In the following we will rewrite these results in a graphical notation which will make it easier to keep track of the contractions of indices in the partial derivatives. In addition to the $\bullet$-vertex and edges we introduced in Section 4.1, we represent $\delta_P \phi$ by a $\otimes$ (a $\times$-vertex). Note that there are at most P edges incident to a $\times$-vertex since $P+1$ derivatives acting on $\delta_P \phi$ yields zero, whereas an arbitrary number of edges can be incident to a $\bullet$-vertex. Moreover, we introduce another vertex, called a $\star$-vertex, which will be used to represent terms that are total derivatives. We require that a $\star$-vertex always be incident to exactly one edge, and that this edge be incident to a $\bullet$-vertex or $\times$-vertex. This edge represents a derivative acting on the entire term as a whole, and the index of that derivative is contracted with the index of another derivative acting on the ϕ or $\delta_P \phi$ of the $\bullet$- or $\times$- vertex, respectively, to which the $\star$-vertex is adjacent. Therefore, directly from the definition, any graph with a $\star$-vertex represents a total derivative term. The expansion of this derivative using the Leibniz rule is graphically represented by the summation of the graphs formed by removing the $\star$-vertex and attaching the edge that was incident to the $\star$-vertex to each remaining vertex. This operation is denoted by the *derivative map* ρ. The symbols $N(\bullet)$, $N(\times)$ and $N(\star)$ represent the numbers of each type of vertex. Note that $N = N(\bullet) + N(\times)$ does not include $N(\star)$ since $\star$-vertices represent neither ϕ nor $\delta_P \phi$.

We define three special types of graphs: A *plain-graph* is a graph in which all vertices are $\bullet$-vertices. A $\times$-*graph* is a plain-graph with one $\bullet$-vertex replaced with a $\times$-vertex. A $\star$-*graph* is a graph with one $\times$-vertex and at least one $\star$-vertex.

Note that the variation δ_P of a plain-graph under the polynomial shift symmetry is given by summing over all graphs that have exactly one $\bullet$-vertex in the original graph replaced with a $\times$-vertex. To illustrate the graphical approach, we rewrite the examples mentioned earlier in the section using this new graphical notation. Since the algebraic expressions have unlabeled ϕ's, the graphs in this section will be unlabeled.

Example 1 revisited: $(P, N, \Delta) = (1, 3, 2)$. The two independent terms are written in the graphical notation as

The variation under the linear shift symmetry (for $P = 1$) is given by

$$\delta_1 \left(\vcenter{\hbox{\includegraphics{}}} \right) = 2 \vcenter{\hbox{\includegraphics{}}} \qquad\qquad \delta_1 \left(\vcenter{\hbox{\includegraphics{}}} \right) = \vcenter{\hbox{\includegraphics{}}}$$

The only independent total derivative that can be formed out of these terms is

$$\rho \left(\vcenter{\hbox{\includegraphics{}}} \right) = 2 \vcenter{\hbox{\includegraphics{}}}$$

As before, there is a single invariant for $(P, N, \Delta) = (1, 3, 2)$ given by L_1. In this case, the graphical version of (4.9) is given by

$$\delta_1 \left(\vcenter{\hbox{\includegraphics{}}} \right) = 2 \vcenter{\hbox{\includegraphics{}}} = \rho \left(\vcenter{\hbox{\includegraphics{}}} \right)$$

Example 2 revisited: $(P, N, \Delta) = (1, 3, 2)$. The four independent terms are written in the graphical notation as

$$L_1 = \vcenter{\hbox{\includegraphics{}}} \qquad L_2 = \vcenter{\hbox{\includegraphics{}}} \qquad L_3 = \vcenter{\hbox{\includegraphics{}}} \qquad L_4 = \vcenter{\hbox{\includegraphics{}}} \qquad (4.10)$$

The variation under the cubic shift symmetry (for $P = 3$) is given by

$$\delta_3 \left(\vcenter{\hbox{\includegraphics{}}} \right) = 2 \vcenter{\hbox{\includegraphics{}}} \qquad\qquad \delta_3 \left(\vcenter{\hbox{\includegraphics{}}} \right) = \vcenter{\hbox{\includegraphics{}}} + 2 \vcenter{\hbox{\includegraphics{}}}$$

$$\delta_3 \left(\vcenter{\hbox{\includegraphics{}}} \right) = \vcenter{\hbox{\includegraphics{}}} + \vcenter{\hbox{\includegraphics{}}} \qquad\qquad \delta_3 \left(\vcenter{\hbox{\includegraphics{}}} \right) = \vcenter{\hbox{\includegraphics{}}}$$

The independent total derivatives that can be formed out of these terms are

$$\rho \left(2 \vcenter{\hbox{\includegraphics{}}} - \vcenter{\hbox{\includegraphics{}}} \right) = 2 \vcenter{\hbox{\includegraphics{}}} + 2 \vcenter{\hbox{\includegraphics{}}}$$

$$\rho \left(\vcenter{\hbox{\includegraphics{}}} \right) = 2 \vcenter{\hbox{\includegraphics{}}}$$

$$\rho \left(\vcenter{\hbox{\includegraphics{}}} \right) = \vcenter{\hbox{\includegraphics{}}} + \vcenter{\hbox{\includegraphics{}}}$$

Once again, there is a single invariant for $(P, N, \Delta) = (3, 4)$ given by $L_1 + 2L_2$. The graphical version of (4.9) is given by

$$
\delta_3 \left(\text{[graph]} + 2 \, \text{[graph]} \right) = 2 \, \text{[graph]} + 2 \, \text{[graph]} + 4 \, \text{[graph]}
$$

$$
= \rho \left(2 \, \text{[graph]} - \text{[graph]} + 2 \, \text{[graph]} \right) \tag{4.11}
$$

So far all we have done is rewrite our results in a new notation. But the graphical notation is more than just a succinct visual way of expressing the invariant terms. The following section illustrates the virtue of this approach.

4.3 New Invariants via the Graphical Approach

As shown in [19], the graphical approach allows us to prove many general theorems. In particular, we have the following useful outcomes:

1. Without loss of generality, we can limit our search for invariants to graphs with very specific properties.

2. There is a simple procedure for obtaining all the independent total derivative relations between the variation terms for each P, N and Δ.

3. The graphical method allows a complete classification of 1-invariants.

4. The graphical method allows many higher P-invariant terms to be constructed from lower P invariants.

We will expound upon the above points by presenting explicit examples. These examples are generalizable and their invariance is proven in [19]. However, the reader can also check by brute force that the terms we present are indeed invariant. We will now summarize points 1 and 2 and will return to point 4 in Section 4.5. Point 3 was discussed in Section 4.1. We will refer the reader to the appendix in [19] for proofs and further details, but we will summarize the main results in the following.

When building invariants, we need only consider loopless plain-graphs, since a loop represents $\partial_i \partial_i$ acting on a single ϕ and one can always integrate by parts to move one of the ∂_i's to act on the remaining ϕ's. Furthermore, a careful analysis shows that we can also restrict to plain-graphs with vertices of degree no less that $\frac{1}{2}(P + 1)$. This represents a significant simplification from the procedure used in 4.2. For instance, in (4.10), the graphs L_3 and L_4 are immediately discarded.

Taking the variation of these terms yields $\times$-graphs and we need to determine the total derivative relations between them. Since all plain-graphs we are considering are loopless, any $\times$-graphs involved in these total derivative relations are also loopless. The total derivative

relations that we need to consider can be obtained with the use of graphs called *Medusas*. A Medusa is a loopless $\star$-graph with all of its $\star$-vertices adjacent to the $\times$-vertex and such that the degree of the $\times$-vertex is given by:

$$\deg(\times) = P + 1 - N(\star), \tag{4.12}$$

where, again, $N(\star)$ is the number of $\star$-vertices. Note that because $\deg(\times) \geq N(\star)$ for a Medusa, (4.12) implies that $N(\star) \leq \frac{1}{2}(P+1) \leq \deg(\times)$ for any Medusa. Furthermore, we need only consider Medusas with $\times$-vertex and $\bullet$-vertices of degree no less than $\frac{1}{2}(P+1)$. From each of these Medusas, we obtain a total derivative relation, containing only loopless $\times$-graphs, by applying the map ρ and then omitting all looped graphs. We will denote this map as $\rho^{(0)}$. In Section 4.4, we will give an introduction to the construction of such total derivative relations from Medusas. Importantly, this procedure captures all relevant total derivative relations.

In general, for given N and P, we call an invariant consisting of graphs containing the lowest possible value of Δ a *minimal* invariant. Minimal invariants are of particular interest in a QFT, since they are the most relevant N-point interactions. In the following, as some illustrative examples, we apply the graphical approach to classify all minimal invariants for $N = 4$ and $P = 2, 3$.

The Minimal Invariant: $(P, N, \Delta) = (2, 4, 5)$.

As our first example, let us find the minimal 2-invariant for $N = 4$. For $P = 2$, any Medusa must have $N(\star) \leq \frac{1}{2}(P+1) = \frac{3}{2}$, and thus there is exactly one $\star$-vertex in a $P = 2$ Medusa. Furthermore, we need only consider Medusas in which each vertex has degree at least 2, since $\frac{1}{2}(P+1) = \frac{3}{2}$. Therefore, the counting implies that we need only consider $P = 2$ Medusas with $\Delta \geq N + 1$. In particular, when $N = 4$, the minimal Δ is 5 (representing terms with 10 derivatives). In the following we show that there is exactly one 2-invariant with $\Delta = 5$. The relevant Medusas are:

$$M_1 = \qquad\qquad M_2 =$$

The resulting loopless total derivative relations are:

$$\rho^{(0)}(M_1) = 2 \quad + \quad \equiv 2L_a^\times + L_e^\times$$
$$\rho^{(0)}(M_2) = \quad + \quad + \quad \equiv L_b^\times + L_c^\times + L_d^\times \tag{4.13}$$

Note that, when acting on these $P = 2$ Medusas, ρ and $\rho^{(0)}$ are in fact the same.

On the other hand, the invariants must be constructed out of plain-graphs containing vertices of degree no less than $\frac{1}{2}(P+1) = \frac{3}{2}$. The only possibilities are:

$$L_1 = \quad\quad L_2 = \quad\quad L_3 = \quad\quad L_4 = \quad\quad L_5 =$$
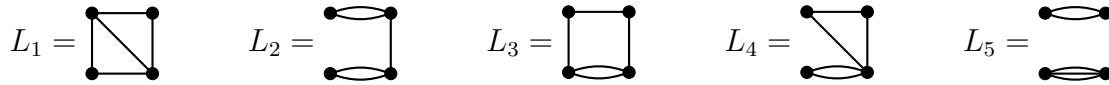
The invariant cannot be constructed out of L_5 since $\delta_2(L_5)$ is absent from the total derivative relations (4.13). Hence, we need only consider the variations of L_1, L_2, L_3 and L_4.

We can now determine the 2-invariants. The total derivative relations allow us to identify $L_d^{\times} \sim -L_b^{\times} - L_c^{\times}$ and $L_e^{\times} \sim -2L_a^{\times}$. Up to total derivatives,

$$\delta_2 \begin{pmatrix} L_1 \\ L_2 \\ L_3 \\ L_4 \end{pmatrix} = \begin{pmatrix} 2 & 0 & 0 & 0 & 0 \\ 0 & 2 & 0 & 0 & 0 \\ 0 & 0 & 2 & 0 & 0 \\ 0 & 0 & 0 & 2 & 1 \end{pmatrix} \begin{pmatrix} L_a^{\times} \\ L_b^{\times} \\ L_c^{\times} \\ L_d^{\times} \\ L_e^{\times} \end{pmatrix} \sim \begin{pmatrix} 2 & 0 & 0 \\ 0 & 2 & 0 \\ 0 & 0 & 2 \\ -2 & -1 & -1 \end{pmatrix} \begin{pmatrix} L_a^{\times} \\ L_b^{\times} \\ L_c^{\times} \end{pmatrix} \quad\quad (4.14)$$

The invariants form the nullspace of the transpose of the final 4×3 matrix in (4.14). The nullspace is spanned by $(1, 1, 1, 1)$. Therefore, there is one 2-invariant given by the linear combination $L_1 + L_2 + L_3 + L_4$, i.e.,

$$\quad + \quad + \quad + \quad \quad\quad (4.15)$$
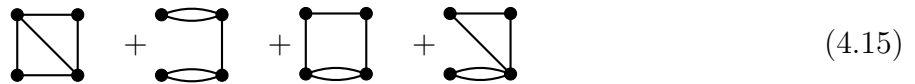
Therefore, (4.15) gives the only independent minimal 2-invariant for $N = 4$.

The Minimal Invariant: $(P, N, \Delta) = (3, 4, 6)$.

Next, let us consider $P = 3$, $N = 4$, for which each vertex degree must be at least $\frac{1}{2}(P+1) = 2$. Again we would like to find the minimal invariant in this case. By counting alone, it is possible to write down Medusas with $\Delta = 5$. In fact, a 3-invariant with $N = 4$ and $\Delta = 5$ would also be 2-invariant. The only possible 2-invariant with $(N, \Delta) = (4, 5)$ is (4.15). However, this is not a 3-invariant because it is impossible for some graphs contained in it to appear in a 3-invariant. For example, by replacing a degree-2 vertex in L_2 in (4.15) with a $\times$-vertex, a $\times$-graph $\Gamma^{\times}$ is produced; $\Gamma^{\times}$ and the only $P = 3$ Medusa M that generates $\Gamma^{\times}$ are given below:

$$\Gamma^{\times} = \quad\quad\quad\quad M =$$

But M contains a $\bullet$-vertex of degree lower than 2, and therefore (4.15) cannot be 3-invariant. This sets a lower bound for Δ: $\Delta \geq 6$. For $\Delta = 6$, the Medusas are:

$$M_1 = \quad\quad M_2 = \quad\quad M_3 = \quad\quad M_4 =$$
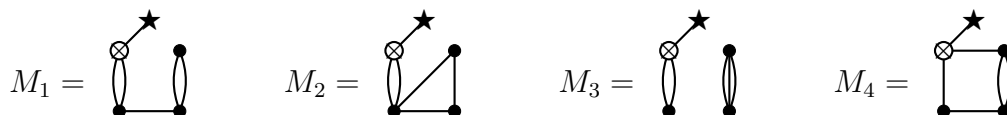
$$M_5 = \quad M_6 = \quad M_7 = \quad M_8 = \qquad (4.16)$$

These give the following total derivative relations:

$$\rho^{(0)}(M_1) = \qquad + \qquad + \qquad \equiv L_a^\times + L_b^\times + L_c^\times$$

$$\rho^{(0)}(M_2) = \qquad + 2 \qquad \equiv L_d^\times + 2L_e^\times$$

$$\rho^{(0)}(M_3) = \qquad + 2 \qquad \equiv L_f^\times + 2L_g^\times$$

$$\rho^{(0)}(M_4) = \qquad + \qquad + \qquad \equiv L_a^\times + L_h^\times + L_i^\times$$

$$\rho^{(0)}(M_5) = 2 \qquad + \qquad \equiv 2L_e^\times + L_j^\times$$

$$\rho^{(0)}(M_6) = \qquad + \qquad + \qquad \equiv L_b^\times + L_k^\times + L_h^\times$$

$$\rho^{(0)}(M_7) = 2 \qquad + \qquad + 4 \qquad + 2 \qquad \equiv 2L_\ell^\times + L_m^\times + 4L_n^\times + 2L_o^\times$$

$$\rho^{(0)}(M_8) = 2 \qquad + \qquad + 2 \qquad + 4 \qquad \equiv 2L_p^\times + L_q^\times + 2L_r^\times + 4L_s^\times$$

Then the invariants must be made up of plain-graphs whose variations are contained in the total derivative relations above. In other words, the invariants are made from:

$$L_1 = \qquad L_2 = \qquad L_3 = \qquad L_4 = \qquad L_5 =$$

$$L_6 = \qquad L_7 = \qquad L_8 = \qquad L_9 = \qquad L_{10} =$$

We can now determine the 3-invaraints:

$$
\delta_3
\begin{pmatrix}
L_1 \\ L_2 \\ L_3 \\ L_4 \\ L_5 \\ L_6 \\ L_7 \\ L_8 \\ L_9 \\ L_{10}
\end{pmatrix}
=
\begin{pmatrix}
4 & 0 & 0 & 0 & 0 & 0 & 0 & 0 & 0 & 0 & 0 & 0 & 0 & 0 & 0 & 0 & 0 & 0 & 0 \\
0 & 2 & 0 & 0 & 0 & 0 & 0 & 0 & 0 & 0 & 0 & 0 & 1 & 0 & 0 & 0 & 0 & 0 & 0 \\
0 & 0 & 0 & 0 & 1 & 0 & 0 & 1 & 0 & 0 & 0 & 0 & 0 & 1 & 0 & 0 & 0 & 0 & 0 \\
0 & 0 & 0 & 0 & 0 & 4 & 0 & 0 & 0 & 0 & 0 & 0 & 0 & 0 & 0 & 0 & 0 & 0 & 0 \\
0 & 0 & 0 & 0 & 0 & 0 & 0 & 0 & 2 & 0 & 0 & 0 & 0 & 0 & 0 & 0 & 0 & 1 & 0 \\
0 & 0 & 0 & 0 & 0 & 0 & 0 & 0 & 0 & 0 & 4 & 0 & 0 & 0 & 0 & 0 & 0 & 0 & 0 \\
0 & 0 & 0 & 0 & 0 & 0 & 0 & 0 & 0 & 0 & 1 & 1 & 0 & 0 & 0 & 0 & 0 & 0 & 1 \\
0 & 0 & 0 & 0 & 0 & 0 & 0 & 0 & 0 & 0 & 0 & 0 & 0 & 0 & 0 & 2 & 0 & 0 & 0 \\
0 & 0 & 0 & 0 & 0 & 0 & 0 & 0 & 0 & 0 & 0 & 0 & 0 & 0 & 0 & 0 & 2 & 0 & 0 \\
0 & 0 & 0 & 0 & 0 & 0 & 0 & 0 & 0 & 0 & 0 & 0 & 0 & 0 & 0 & 0 & 3 & 0 & 0
\end{pmatrix}
\begin{pmatrix}
L_a^\times \\ L_b^\times \\ L_c^\times \\ L_d^\times \\ L_e^\times \\ L_f^\times \\ L_g^\times \\ L_h^\times \\ L_i^\times \\ L_j^\times \\ L_k^\times \\ L_\ell^\times \\ L_m^\times \\ L_n^\times \\ L_o^\times \\ L_p^\times \\ L_q^\times \\ L_r^\times \\ L_s^\times
\end{pmatrix}
$$

$$
\sim
\begin{pmatrix}
4 & 0 & 0 & 0 & 0 & 0 & 0 & 0 & 0 & 0 & 0 \\
0 & 2 & 0 & 0 & 0 & -2 & -4 & -2 & 0 & 0 & 0 \\
0 & 0 & 1 & 0 & 1 & 0 & 1 & 0 & 0 & 0 & 0 \\
0 & 0 & 0 & 4 & 0 & 0 & 0 & 0 & 0 & 0 & 0 \\
-2 & 0 & 0 & 0 & -2 & 0 & 0 & 0 & 0 & 1 & 0 \\
0 & 0 & -8 & 0 & 0 & 0 & 0 & 0 & 0 & 0 & 0 \\
0 & -1 & 0 & 0 & -1 & 1 & 0 & 0 & 0 & 0 & 1 \\
0 & 0 & 0 & 0 & 0 & 0 & 0 & 2 & 0 & 0 & 0 \\
0 & 0 & 0 & 0 & 0 & 0 & 0 & 0 & 2 & 0 & 0 \\
0 & 0 & 0 & 0 & 0 & 0 & 0 & 0 & -6 & -6 & -12
\end{pmatrix}
\begin{pmatrix}
L_a^\times \\ L_b^\times \\ L_e^\times \\ L_f^\times \\ L_h^\times \\ L_l^\times \\ L_n^\times \\ L_o^\times \\ L_p^\times \\ L_r^\times \\ L_s^\times
\end{pmatrix}
$$

The nullspace of the transpose of this matrix is spanned by $(3, 6, 24, 0, 6, 3, 12, 6, 3, 1)$, giving the only invariant linear combination,

$$\tag{4.17}$$

This gives the only independent minimal 3-invariant for $N = 4$.

Note that L_4 does not appear in the invariant. Indeed, it can be discarded immediately, since the unique Medusa associated with L_4 is
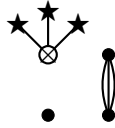
This Medusa has an empty vertex, which violates the lower bound on vertex degree.

4.4 Medusas and Total Derivative Relations

We have seen that Medusas play a central role in the search for P-invariants. It is thus worthwhile to discuss the key features of Medusas and to demonstrate how a total derivative relation consisting of loopless ×-graphs is constructed from a Medusa. Given any Medusa, $\rho^{(0)}(M)$ is in fact a total derivative relation, as can be seen from the following construction.

For fixed P and N, consider a Medusa M that contains $N(\star)$ $\star$-vertices. Then, by definition, it has a ×-vertex of degree $\deg(\times) = P + 1 - N(\star)$. Since the maximal degree of a ×-vertex is P, graphs in $\rho(M)$ contain at most $N(\star) - 1$ loops. Form a $\star$-graph $\Gamma^{(\ell)}$ from M by deleting $\ell \leq N(\star) - 1$ $\star$-vertices in M and then adding ℓ loops to the ×-vertex. By this definition, $M = \Gamma^{(0)}$. In the algebraic expression represented by $\Gamma^{(\ell)}$, the $N(\star) - \ell$ $\star$-vertices stand for $N(\star) - \ell$ partial derivatives acting on the whole term. Distributing $N(\star) - \ell - 1$ ∂'s over all ϕ's in this algebraic expression will result in a linear combination of total derivative terms. In the graphical representation, this is equivalent to acting ρ on $\Gamma^{(\ell)}$ but keeping fixed exactly one $\star$-vertex and its incident edge. Setting to zero all coefficients of graphs in the resulting linear combination, except for the ones containing exactly ℓ loops, generates a linear combination $L^{(\ell)}$ of $\star$-graphs, each containing exactly one $\star$-vertex. By construction,

$$\rho^{(0)}(M) = \rho \left(\sum_{\alpha=0}^{N(\star)-1} (-1)^\alpha L^{(\alpha)} \right). \tag{4.18}$$

The algebraic form of the RHS of (4.18) is explicitly a total derivative relation. For a rigorous treatment of the above discussion, refer to the appendix in [19].

As a simple example, we consider the Medusa M_7 referred to in (4.16). We have

For a second example, we consider $(P, N, \Delta) = (5, 3, 6)$ and the Medusa
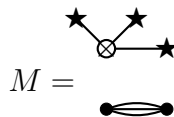
By (4.18), we obtain

$$\rho^{(0)}(M) = \rho \left(2 \, \text{} + 2 \, \text{} - 2 \, \text{} + \text{} \right).$$

This Medusa is involved in a 5-invariant that we will construct in Section 4.5.

4.5 Superposition of Graphs

In Section 4.1, we discovered an intriguing construction of the minimal 1-invariant for given N, which is a sum with equal coefficients of all possible trees with N vertices. A close study of the P-invariants with $P > 1$ in Section 4.2 also reveals an elegant structure in these invariants: They can all be decomposed as a *superposition* of equal-weight tree summations and *exact* invariants. Recall that an exact invariant is a linear combination that is invariant exactly, instead of up to a total derivative. In the graphical representation, a linear combination of graphs is an exact P_E-invariant if and only if all vertices are of degree larger than P_E. Each graph in an exact invariant is itself exactly invariant.

Next we illustrate "the superposition of linear combinations" by explicit examples. When appropriate, we will consider labeled graphs and only remove the labels at the end. Consider two labeled graphs,

$$\Gamma_1 = \text{} \qquad \Gamma_2 = \text{}$$

The superposition of Γ_1 and Γ_2 is defined to be the graph formed by taking all edges in Γ_2 and adding them to Γ_1, *i.e.*,

$$\Gamma_1 \cup \Gamma_2 = \text{}$$
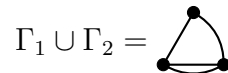
The superposition of two linear combinations, $L_A = \sum_{i=1}^{k_A} a_i \Gamma_i^A$ and $L_B = \sum_{i=1}^{k_B} b_i \Gamma_i^B$, of plain-graphs Γ_i^A, Γ_j^B with the same N, is defined as

$$L_A \cup L_B \equiv \sum_{i=1}^{k_A} \sum_{j=1}^{k_B} a_i \, b_j \, \Gamma_i^A \cup \Gamma_j^B.$$

In the following we present numerous examples of invariants constructed by superposing equal-weight tree summations and exact invariants for various P's. In fact, we prove the following theorem in [19]:

> — *for fixed N, the superposition of an exact P_E-invariant with the superposition of Q minimal loopless 1-invariants results in a P-invariant, provided $P_E + 2Q \geq P$.*[1]

---

[1] Note that this theorem also applies when $P_E < 0$, where we take an exact P_E-invariant for $P_E < 0$ to mean any linear combination of plain-graphs. In particular, the plain-graph consisting only of empty vertices is a P_E-invariant for any $P_E < 0$, and superposing this graph on any other is equivalent to not superposing anything at all.
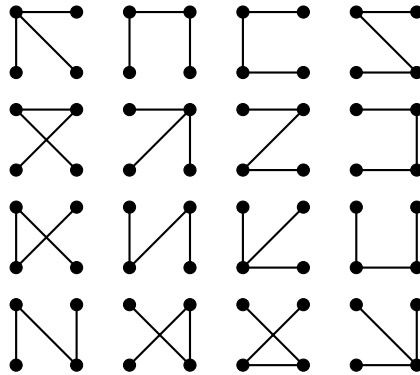
Figure 4.1: All 16 trees for $N = 4$.

We conjecture that the above result captures all P-invariants, up to total derivatives. In [19], we classified all exact invariants and all 1-invariants; therefore, it is straightforward to construct the P-invariants in the above statement for any specific case. We now proceed to construct several examples for minimal P-invariants to demonstrate how the superposition construction works; further examples and relevant mathematical proofs can be found in [19].

Case 1: $(P, N) = (3, 3)$.

For $P = 3$, the only independent minimal invariant for $N = 3$ is given in (4.11), which can be written as a superposition of two equal-weight tree summations:
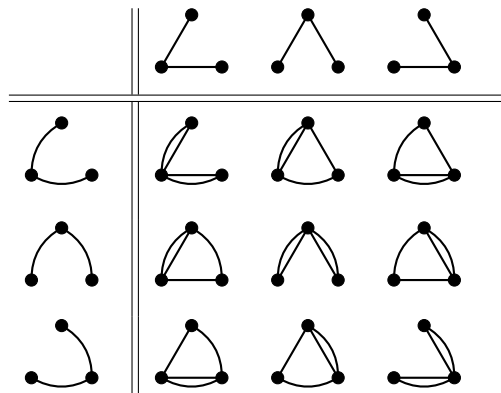
As we already pointed out, this 3-invariant happens to be the minimal 2-invariant as well.

Case 2: $(P, N) = (3, 4)$.

In Section 4.3 we found that (4.17) gives the only independent minimal 3-invariant for $N = 4$. It has the structure of a superposition of two sums with unit coefficients of all trees in Figure 4.1. As mentioned in Section 4.1, there are two isomorphism classes of $N = 4$
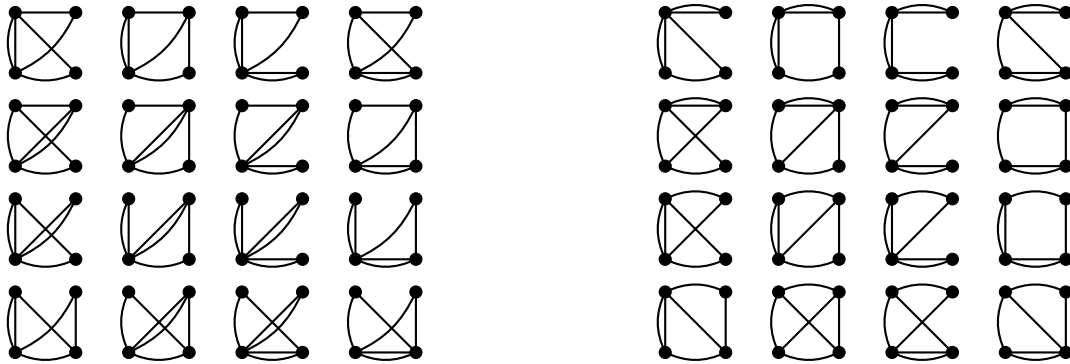
(a) Superposition of T_A and Figure 4.1.

(b) Superposition of T_B and Figure 4.1.

Figure 4.2: Superposition of graphs in (4.19) on trees in Figure 4.1.

trees:

$$T_A = \quad\quad\quad\quad T_B = \quad\quad\quad\quad (4.19)$$

Superposing these graphs on the $N = 4$ trees produces the graphs in Figure 4.2. If T and T' are isomorphic trees, then superposing T on the trees in Figure 4.1 produces 16 graphs which are isomorphic to the 16 graphs formed by superposing T' on the same trees. There are four trees in the isomorphism class of T_A and twelve for T_B. Therefore, we just have to give the 16 graphs in Figure 4.2a weight 4 and the 16 graphs in Figure 4.2b weight 12 and then add them all up. The result is (4.17) with an overall prefactor of 4. Again, we have already shown that this is the unique minimal 3-invariant for $N = 4$.

Case 3: $(P, N) = (5, 4)$.

The superposition of three equal-weight sums of $N = 4$ trees yields

Note that the sum of the coefficients is $4096 = 16^3$.

To facilitate the check of the invariance of the above linear combination, denoted as L, we provide the linear combination of Medusas L_M such that $\delta_5(L) = \rho^{(0)}(L_M)$:
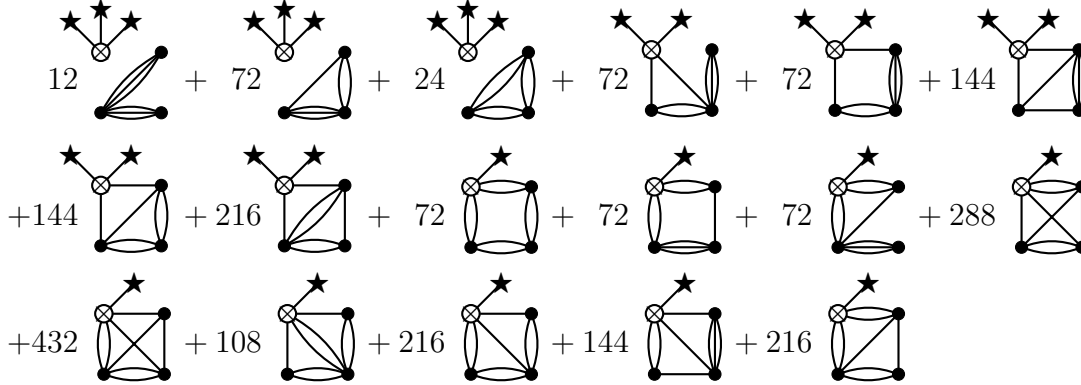
In general, superposing χ minimal loopless 1-invariants and then identifying all isomorphism graphs (so that all vertices are considered to be identical) results in a $P = 2\chi - 1$ invariants. It is quite difficult to see why this has to be true in the position space (whose proof can be found in the appendix in [19]). However, after Fourier transforming into the momentum space, the above statement becomes transparent. Consider a degree-P polynomial shift symmetry,

$$\phi(t, \mathbf{x}) \to \phi(t, \mathbf{x}) + a_{i_1 \cdots i_P} x^{i_1} \cdots x^{i_P} + \cdots . \tag{4.20}$$

In momentum space, we have

$$\widetilde{\phi}(\omega, \mathbf{k}) \to \phi(\omega, \mathbf{k}) + a_{i_1 \cdots i_P} \partial_{\mathbf{k}_{i_1}} \cdots \partial_{\mathbf{k}_{i_P}} \delta(\mathbf{k}) + \cdots . \tag{4.21}$$

Moreover, the Feynman rule derived from a P-invariant operator with n vertices constructed from χ copies of equal-weight sums of trees is simply

$$(\varepsilon_{i_1 \cdots i_n} \mathbf{k}_1^{i_1} \cdots \mathbf{k}_{n-1}^{i_n})^{2\chi}, \tag{4.22}$$

where we applied the conservation law of momentum, $\mathbf{k}_n = -\mathbf{k}_1 - \cdots - \mathbf{k}_{n-1}$ to elimintate $\mathbf{k}_n$ in the Feynman rule. This Feynman rule is manifestly invariant under the polynomial shift symmetry (4.21).

In this chapter, we have seen that the graphical language is very efficient not only for deriving theorems about our invariants, but also for stating the results. This graphical technique is important for two reasons. First, it is quite powerful: The translation of the classification problem into a graph-theory problem allows us to generate sequences of invariants for various values of P, number N of fields, the number 2Δ of spatial derivatives, and as a function of the spatial dimension D, in a way that is much more efficient than any "brute force" technique. Secondly, and perhaps more importantly, the graphical technique reveals

some previously hidden structure even in those invariants already known in the literature. For example, the known Galileon N-point invariants are given by the equal-weight sums of all labeled trees with N vertices! This hidden simplicity of the Galileon invariants is a feature previously unsuspected in the literature, and its mathematical explanation deserves further study. In addition, we also discovered patterns that allow the construction of higher polynomials from the superposition of graphs representing a collection of invariants of a lower degree – again a surprising result, revealing glimpses of intriguing connections among the *a priori* unrelated spaces of invariants across the various values of P, N and Δ.

Chapter 5

Cascading Multicriticality

In Chapter 2, we showed that the Type A-B dichotomy of nonrelativistic NG modes is further refined into two discrete families, labeled by a positive integer n: Type A_n NG modes are described by a single scalar with dispersion $\omega \sim k^n$ (and dynamical critical exponent $z = n$), while Type B_{2n} modes are described by a canonical pair and exhibit the dispersion relation $\omega \sim k^{2n}$ (and dynamical exponent $z = 2n$). These two families are technically natural, and therefore stable under renormalization in the presence of interactions [18]. As usual, such naturalness is explained by a new symmetry. For $n = 1$, the NG modes are protected by the well-known constant shift symmetry $\delta\phi(t, \mathbf{x}) = b$. The $n > 1$ theories enjoy shift symmetries by a degree-P polynomial in the spatial coordinates,

$$\delta\phi(t, \mathbf{x}) = b + b_i x^i + \cdots + b_{i_1 \ldots i_P} x^{i_1} \cdots x^{i_P}, \tag{5.1}$$

with suitable P. Away from the Type A_n and B_{2n} Gaussian fixed points, the polynomial shift symmetry is generally broken by most interactions. The lowest, least irrelevant interaction terms invariant under the polynomial shift were systematically discussed in Chapter 4 (also see [19, 57]). Such terms are often highly irrelevant compared to all the other possible interactions that break the symmetry.

Having established the existence of the multicritical Type A and B families of NG fixed points, in this chapter we study the dynamics of flows between such fixed points in interacting theories. We uncover a host of novel phenomena, involving large, technically natural hierarchies of scales, protected again by the polynomial shift symmetries. As a given theory flows between the short-distance and the long-distance regime, it can experience a natural cascade of hierarchies, sampling various values of the dynamical critical exponent z in the process. Such cascades represent an intriguing mechanism for evading some of the consequences of the relativistic Coleman-Hohenberg-Mermin-Wagner (CHMW) Theorem. In Chapter 3, we already encountered a first example that exhibits this novel behavior, in the context of condensed matter physics. In this chapter, we will further illustrate the the novelties of this cascading behavior with a series of examples.

5.1 Relativistic and Nonrelativistic CHMW Theorem

First recall that in relativistic systems, all NG bosons are of Type A_1, assuming that they exist as well-defined quantum objects. Whether or not they exist, and whether or not the corresponding symmetry can be spontaneously broken, depends on the spacetime dimension. This phenomenon is controlled by a celebrated theorem, discovered independently in condensed matter by Mermin and Wagner [58] and by Hohenberg [59], and in high-energy physics by Coleman [60]. We therefore refer to this theorem, in the alphabetical order, as the CHMW theorem.

The relativistic CHMW theorem states that the spontaneous breaking of global continuous internal symmetries is not possible in $1+1$ spacetime dimensions. The proof is beautifully simple. $1+1$ is the "lower critical dimension," where ϕ is formally dimensionless at the Gaussian fixed point. Quantum mechanically, this means that its propagator is logarithmically divergent, and we must regulate it by an IR regulator μ_{IR}:

$$
\begin{aligned}
\langle \phi(x)\phi(0) \rangle &= \int \frac{d^2 k}{(2\pi)^2} \frac{e^{ik\cdot x}}{k^2 + \mu_{\text{IR}}^2} \\
&\approx -\frac{1}{2\pi} \log(\mu_{\text{IR}}|x|) + \text{const.} + \mathcal{O}(\mu_{\text{IR}}|x|).
\end{aligned}
\tag{5.2}
$$

The asymptotic expansion in (5.2), valid for $\mu_{\text{IR}}|x| \ll 1$, shows that as we take $\mu_{\text{IR}} \to 0$, the propagator stays sensitive at long length scales to the IR regulator. We can still construct various composite operators from the derivatives and exponentials of ϕ, with consistent and finite renormalized correlation functions in the $\mu_{\text{IR}} \to 0$ limit, but the field ϕ itself does not exist as a quantum object. Since the candidate NG mode ϕ does not exist, the corresponding symmetry could never have been broken in the first place, which concludes the proof.

Going back to the general class of Type A_n NG modes, we find an intriguing nonrelativistic analog of the CHMW theorem. The dimension of $\phi(t, \mathbf{x})$ at the A_n Gaussian fixed point in $D+1$ dimensions – measured in the units of spatial momentum – is

$$
[\phi(t, \mathbf{x})]_{A_n} = \frac{D-n}{2}.
\tag{5.3}
$$

The Type A_n field ϕ is at its lower critical dimension when $D = n$. Its propagator also requires an infrared regulator. There are many ways how to introduce μ_{IR} in this case, for example by

$$
\langle \phi(t, \mathbf{x})\phi(0) \rangle = \int \frac{d\omega\, d^D \mathbf{k}}{(2\pi)^{D+1}} \frac{e^{i\mathbf{k}\cdot\mathbf{x} - i\omega t}}{\omega^2 + k^{2D} + \mu_{\text{IR}}^{2D}},
\tag{5.4}
$$

or by

$$
\langle \phi(t, \mathbf{x})\phi(0) \rangle = \int \frac{d\omega\, d^D \mathbf{k}}{(2\pi)^{D+1}} \frac{e^{i\mathbf{k}\cdot\mathbf{x} - i\omega t}}{\omega^2 + (k^2 + \mu_{\text{IR}}^2)^D}.
\tag{5.5}
$$

Either way, as we try to take $\mu_{\text{IR}} \to 0$, the asymptotics of the propagator again behaves logarithmically, both in space

$$\langle \phi(t, \mathbf{x})\phi(0) \rangle \approx -\frac{1}{(4\pi)^{D/2}\Gamma(D/2)} \log(\mu_{\text{IR}}|\mathbf{x}|) + \dots \qquad \text{for } |\mathbf{x}|^D \gg t \qquad (5.6)$$

and in time,

$$\langle \phi(t, \mathbf{x})\phi(0) \rangle \approx -\frac{1}{(4\pi)^{D/2}D\,\Gamma(D/2)} \log(\mu_{\text{IR}}^D t) + \dots \qquad \text{for } |\mathbf{x}|^D \ll t. \qquad (5.7)$$

Most importantly, the propagator remains sensitive to the infrared regulator μ_{IR}. Consequently, we obtain the nonrelativistic, multicritical version of the CHMW theorem for Type A NG modes and their associated symmetry breaking:

— *The Type A_n would-be NG mode $\phi(t, \boldsymbol{x})$ at its lower critical dimension $D = n$ exhibits a propagator which is logarithmically sensitive to the infrared regulator μ_{IR}, and therefore $\phi(t, \boldsymbol{x})$ does not exist as a quantum mechanical object. Consequently, no spontaneous symmetry breaking with Type A_n NG modes is possible in $D = n$ dimensions.*

By extension, this also invalidates all Type A_n would-be NG modes with $n > D$: Their propagator grows polynomially at long distances, destabilizing the would-be condensate and disallowing the associated symmetry breaking pattern.

In contrast, the dimension of the Type B_{2n} field is

$$[\phi(t, \mathbf{x})]_{B_{2n}} = \frac{D}{2},$$

and the lower critical dimension is $D = 0$. Hence, in all dimensions $D > 0$, the Type B_{2n} NG modes are free of infrared divergences and well-defined quantum mechanically for all $n = 1, 2, \dots$, and the *Type B nonrelativistic, multicritical CHMW theorem* is limited to the following statement:

— *the Type B_{2n} symmetry breaking is possible in any $D > 0$ and for any $n = 1, 2, \dots$.*

5.2 Cascading Multicriticality

Whereas in the relativistic case, all NG modes must always be of Type A_1, in nonrelativistic systems the existence of the Type A_n and B_{2n} families allows a much richer dynamical behavior.

For example, with the changing momentum or energy scales, a given NG mode can change from Type A_n (or B_{2n}) to Type $A_{n'}$ (or $B_{2n'}$) with $n \neq n'$, or it could change from Type A to Type B. The hierarchies of scales that open up in this process are naturally protected by the corresponding polynomial symmetries. One of the simplest cases is the Type A_n scalar with $n > 1$, whose polynomial shift symmetry of degree P is broken at some momentum

scale μ to the polynomial shift symmetry of degree $P - 2$, by some small amount $\varepsilon \ll 1$. This breaking modifies the dispersion relation to

$$\omega^2 \approx k^{2n} + \zeta_{n-1}^2 k^{2n-2}, \tag{5.8}$$

with $\zeta_{n-1}^2 \approx \varepsilon \mu^2$. Here, as in [4], we identify μ as the scale of naturalness. At a hierarchically much smaller scale, $\mu_\otimes \equiv \mu\sqrt{\varepsilon}$, the system exhibits a crossover, from Type A_n above $\mu_\otimes$ to Type A_{n-1} below $\mu_\otimes$. The technical naturalness of the large hierarchy $\mu_\otimes \ll \mu$ is protected by the restoration of the polynomial shift symmetry of degree P as $\varepsilon \to 0$.

In the special case of $n = D$, this crossover from Type A_D to Type A_{D-1} yields an intriguing mechanism for evading the naive conclusion of our CHMW theorem. For a large range of scales close to μ, the would-be NG mode can exhibit a logarithmic propagator. The hierarchically smaller scale $\mu_\otimes \ll \mu$ then serves as a natural IR regulator, allowing the NG mode to cross over to Type A_{D-1} at very long distances. Therefore, the mode is well-defined as a quantum mechanical object, despite the large hierarchy across which it behaves effectively logarithmically.

An interesting refinement of this scenario comes from breaking the polynomial symmetries hierarchically, in a sequence of partial breakings, from a higher polynomial symmetry of degree P to symmetries with degrees $P' < P$, $P'' < P'$, ..., all the way to constant shift. This gives rise to a cascading phenomenon, with a hierarchy of crossover scales $\mu \gg \mu' \gg \mu'' \gg \ldots$, separating plateaux governed by the fixed points with the dynamical exponent taking the corresponding different integer values. Again, such cascading hierarchies are technically natural, and protected by the underlying breaking pattern of the polynomial symmetries.

Before we illustrate this behavior in a series of examples, it is worth pointing out one very simple yet important feature of large hierarchies in nonrelativistic theories. Consider a theory dominated over some range of scales by the dispersion relation $\omega \approx k^n$, with $n > 1$. If we open up a large hierarchy of momentum scales $\mu \gg \mu'$ (say by N orders of magnitude), this hierarchy of momentum scales gets magnified into an even larger hierarchy (by nN orders of magnitude) in energy scales.

A Type-A Hierarchy. The first model that we use to illustrate the hierarchy is a relatively well-known system in $2+1$ dimensions: The $z = 2$ Gaussian model of a single Aristotelian scalar field $\phi(t, \mathbf{x})$, with a derivative 4-point self-interaction turned on [48, 61]:

$$S_2 = \frac{1}{2} \int dt d^2\mathbf{x} \left\{ \dot{\phi}^2 - (\partial^2 \phi)^2 - c^2 \partial_i \phi \partial_i \phi - g(\partial_i \phi \partial_i \phi)^2 \right\}.$$

This action contains all the marginal and relevant terms of the $z = 2$ fixed point consistent with the constant shift symmetry and the reflection symmetry $\phi \to -\phi$. At the $z = 2$ Gaussian fixed point, g is classically marginal, and breaks the polynomial shift symmetry of this fixed point to constant shift. Quantum corrections at one loop turn g marginally irrelevant [48].

This system allows a natural hierarchy of scales, stable under quantum corrections. At the naturalness scale μ, we can break the polynomial shift symmetry of the $z = 2$ fixed point to constant shifts by a small amount $\varepsilon_0 \ll 1$. This implies $g \sim \varepsilon_0$ and $c^2 \sim \varepsilon_0 \mu^2$, relations which can be shown to be respected by the loop corrections. In particular, c^2 can stay naturally small, much less than μ^2. The dispersion relation changes from $z = 2$ close to the high scale μ, to $z = 1$ around the much lower scale $\mu_1 \equiv \mu\sqrt{\varepsilon_0} \ll \mu$.

A Type-A/Type-B Hierarchy. The above example illustrates the cascading mechanism in the Type A case. Type B systems can form their own hierarchies, in the obvious generalization of the Type A cascades exemplified above. There is no analog of the lower critical dimension and the CHMW limit on n. Type A NG modes can also exhibit a flow to Type B. This behavior, albeit not new (see *e.g.* [62]), can be embedded as one step into the more general technically natural hierarchies of Type A or B as discussed above. In particular, the crossover to Type B can provide a new IR regulator of the Type A cascade at the lower critical dimension.

We shall illustrate this on the simplest Type A_1 example, although the full story is, of course, more general. Consider two would-be Type A NG fields, $\phi_{1,2}(t, \mathbf{x})$, in the vicinity of the $z = 1$ Gaussian fixed point

$$S_1 = \frac{1}{2} \int dt d^D \mathbf{x} \left\{ \dot{\phi}_1^2 + \dot{\phi}_2^2 - c_1^2 (\partial_i \phi_1)^2 - c_2^2 (\partial_i \phi_2)^2 \right\}.$$

For simplicity, we will set $c_1 = c_2 = 1$, although this is not necessary for our argument. Besides the rotations and translations of the two scalars, note two independent $\mathbb{Z}_2$ symmetries – the field reflection,

$$R : \ (\phi_1, \phi_2) \to (\phi_1, -\phi_2), \tag{5.9}$$

and the time reversal,

$$\mathcal{T} : \ t \to -t, \quad \phi_{1,2}(t, \mathbf{x}) \to \phi_{1,2}(-t, \mathbf{x}). \tag{5.10}$$

We can now turn on the Type B kinetic term,

$$S' = S_1 + \Omega \int dt d^D \mathbf{x} \left(\phi_1 \dot{\phi}_2 - \phi_2 \dot{\phi}_1 \right). \tag{5.11}$$

Ω now provides an IR regulator for the propagator. At that scale, the field reversal R and the time reversal $\mathcal{T}$ are broken to their diagonal subgroup. At energy scales below Ω, one of the would-be Type A NG modes survives and turns into the Type B NG mode, while the other would-be Type A mode develops a gap set by Ω. Note that in $1 + 1$ dimensions, the "no-go" consequences of the relativistic CHMW theorem are again naturally evaded by this hierarchy: A NG mode exists quantum mechanically after all, and symmetry breaking is possible, despite the fact that above the scale Ω, the two would-be Type A modes exhibit the logarithmic two-point function suggesting that symmetry breaking may not be possible.

The hierarchy between the Type A and Type B behavior is also protected by symmetries. In fact, the system has multiple symmetries that can do this job. One can rely on the

breaking pattern of the discrete symmetries R and $\mathcal{T}$ mentioned above. If the Type A system is Lorentz invariant, one can use Lorentz symmetry breaking to protect small Ω. More interestingly, without relying on the discrete or Lorentz symmetries, one can introduce a shift symmetry linear in time,

$$\delta\phi_{1,2} = b_{1,2}t. \tag{5.12}$$

While the Type A kinetic term is invariant under this symmetry, the Type B kinetic term is not. Breaking the linear shift symmetry to constant shifts allows the Type-A/Type-B crossover scale to be hierarchically smaller than the naturalness scale.

In these two examples, we have seen that the multicritical Type A_n and B_{2n} NG modes can experience technically natural cascading hierarchies of scales, protected by a hierarchy of polynomial shift symmetries. Perhaps the most interesting case is Type A with $n = D$, which according to our CHMW theorem exhibits logarithmic sensitivity to the IR regulator. In the relativistic case, this would prevent the symmetry breaking. We have shown that the Type A_D modes can experience a cascade to Type A_n with $n < D$ (or to Type B), which provides a natural IR regulator, thus making the symmetry breaking possible after all.

5.3 Prelude: Scalar Field Theory with Linear Shift Symmetry

In rest of this chapter, we introduce a new scalar field theory with linear shift symmetry, which not only illustrates the cascading hierarchy with multiple crossovers, but also exhibits additional intriguing renormalization properties of independent interest. The full analysis of the quantum properties of this theory will be discussed in details in Chapter 6; here we will only give a brief prelude of this theory and focus on the cascading behavior. In Chapter 7, we will apply this theory to address the Higgs mass hierarchy problem.

We impose two discrete symmetries: $\phi(t, \mathbf{x}) \to -\phi(t, \mathbf{x})$, and time reversal $\mathcal{T}$: $(t, \mathbf{x}) \to (-t, \mathbf{x})$, acting trivially on ϕ, $\mathcal{T} : \phi(t, \mathbf{x}) = \phi(-t, \mathbf{x})$. For our main interest, $\mathcal{T}$ is a bit of an overkill: It will be an "accidental" symmetry anyway. In $3+1$ dimensions, the Gaussian fixed point with $z = 3$ is described by

$$S_3 = \frac{1}{2} \int dt\, d^3\mathbf{x} \left\{ \dot{\phi}^2 - (\partial_i \partial_j \partial_k \phi)^2 \right\}. \tag{5.13}$$

We have normalized the field ϕ to set the coefficient in front of the kinetic term $\dot{\phi}^2$ to the canonical value of $1/2$, and the coefficient in front of the $(\partial^3\phi)^2$ term has been set to $1/2$ by the rescaling of space. The scalar field at the $z = 3$ Gaussian fixed point is dimensionless,

$$[\phi] = 0. \tag{5.14}$$

Thus, in $3+1$ spacetime dimensions, ϕ is at its lower critical dimension. In Chapter 3, this $z = 3$ fixed point is used to explain the T-linear resistivity in strange metals.

Next, we turn to the classification of all classically marginal and relevant interaction terms up to total derivative. First of all, just as in the relativistic non-linear sigma model

in $1+1$ dimensions, there would be an infinite number of such couplings. In order to reduce consistently to a finite number of independent couplings, we impose (at least) the constant shift symmetry. The sole exception will be the addition of the non-derivative quadratic gap term $m^2\phi^2$, which of course breaks the constant shift symmetry explicitly, but does so in the "softest possible way" without generating any self-interactions violating the constant shift symmetry.[1]

There are four marginal interaction terms invariant under the constant shift. It is convenient to represent them in the "loopless basis"[2]. We find three independent terms at four points,

$$\mathcal{O}_4^{(1)} = \partial_i\partial_j\partial_k\phi\,\partial_i\phi\,\partial_j\phi\,\partial_k\phi = \quad , \tag{5.15}$$

$$\mathcal{O}_4^{(2)} = \partial_i\phi\,\partial_i\partial_j\phi\,\partial_j\partial_k\phi\,\partial_k\phi = \quad , \tag{5.16}$$

$$\mathcal{O}_4^{(3)} = \partial_i\partial_j\phi\,\partial_i\partial_j\phi\,\partial_k\phi\,\partial_k\phi = \quad , \tag{5.17}$$

$$\tag{5.18}$$

and one at six points:

$$\mathcal{O}_6 = (\partial_i\phi\partial_i\phi)^3 = \quad . \tag{5.19}$$

The $z=3$ fixed point has three relevant terms which respect the constant shift symmetry: Two of them modify the free, Gaussian part of the theory,

$$\partial_i\phi\,\partial_i\phi, \qquad \partial_i\partial_j\phi\,\partial_i\partial_j\phi, \tag{5.20}$$

and the third one gives a four-point self-interaction,

$$\mathcal{W} \equiv (\partial_i\phi\partial_i\phi)^2. \tag{5.21}$$

Hence, the general action involving all the marginal and relevant couplings with constant shift symmetry (plus the gap term) can be written as

$$S = \frac{1}{2}\int dt\,d^3\mathbf{x}\left\{\dot\phi^2 - \sum_{s=0}^{3}\zeta_s^2(\partial_{i_1}\dots\partial_{i_s}\phi)^2 - w\mathcal{W} - \sum_{I=1}^{3}\lambda_3^{(I)}\mathcal{O}_3^{(I)} - g_3\mathcal{O}_3\right\}. \tag{5.22}$$

We have used the collective notation for ζ_s, with $\zeta_0 \equiv m$ and $\zeta_1 \equiv c$. The engineering dimensions of various parameters are

$$[\zeta_2^2] = \frac{2}{3}, \qquad [c^2] = \frac{4}{3}, \qquad [m^2] = 2. \tag{5.23}$$

---

[1]The low-energy observer with the relativistic prejudice might be inclined to call this term the "mass term," but we find the notion of a "gap term" more accurate.

[2]This refers to the terminology used in Chapter 4, as inherited from graph theory. The "loopless basis" is a representation in which whenever a $\partial^2 \equiv \partial_i\partial_i$ term acting on one ϕ is encountered, it is eliminated by one integration by parts. In the graphical representation, this means that the two end of an edge never join to the same vertex.

The couplings $\lambda_3^{(I)}$ and g_3 are all dimensionless.

Renormalization group properties of any Aristotelian scalar field theory will depend on possible hidden symmetries of the model. We already used the constant shift symmetry above, to restrict the number of independent marginal and relevant terms to a finite number. However, the structure of symmetries of the infinite hierarchy of Aristotelian-invariant operators that can appear in the action and are built out of n copies of ϕ and some number Δ of pairs of derivatives $\partial_i \cdots \partial_i \cdots$ is much more intricate. In our case of $z = 3$ in $3 + 1$ dimensions, polynomial shift symmetries pick out one renormalizable self-interaction term. We define infinitesimal polynomial shift transformations of ϕ,

$$\phi(\mathbf{x}, t) \rightarrow \phi(\mathbf{x}, t) + \delta\phi(\mathbf{x}, t), \tag{5.24}$$

where

$$\delta\phi(\mathbf{x}, t) = b_{i_1 \cdots i_P} x^{i_1} \cdots x^{i_P} + \ldots + b_i x^i + b_0. \tag{5.25}$$

The task of classifying all terms invariant under the polynomial shift transformation (5.25) of degree P up to a total derivative represents an intriguing mathematical problem, which effectively leads to new graph-theory cohomology groups. This problem was set up, and solved for some lower values of P and low-enough number of fields and derivatives, in Chapter 4.

Among all the 4-point and 6-point interaction terms in (5.22), there is a unique term which is invariant under linear shifts, up to a total derivative. As shown in Section 4.1, for a given number n of fields, there is a unique invariant under linear shift symmetry with the lowest number of derivatives (in high enough spacetime dimensions); moreover, this term has a very simple graphical representation – it is simply given by the equal-weight sum over all spanning trees with n vertices, when we treat the vertices as distinguishable. Following this rule, for $n = 4$ we thus get our unique 4-point 1-invariant,

$$\tag{5.26}$$

When we again treat the vertices as indistinguishable, this sum becomes

$$12\mathcal{O} \equiv 4 \,\raisebox{-0.4em}{\includegraphics[height=1.2em]{g1}} + 12 \,\raisebox{-0.4em}{\includegraphics[height=1.2em]{g2}} = 4 \,\mathcal{O}_4^{(1)} + 12 \,\mathcal{O}_4^{(2)}$$

$$= 4 \,\partial_i\partial_j\partial_k\phi \,\partial_i\phi \,\partial_j\phi \,\partial_k\phi + 12 \,\partial_i\phi \,\partial_i\partial_j\phi \,\partial_j\partial_k\phi \,\partial_k\phi. \tag{5.27}$$

Finally, here is the theory that will be the subject of our case study. Its action is given by (5.22), in which we set

$$\lambda_3^{(1)} = \lambda_3, \qquad \lambda_3^{(3)} = \frac{\lambda_3}{3}, \tag{5.28}$$

and all other non-Gaussian couplings to zero:

$$\lambda_2^{(2)} = 0, \qquad g_3 = 0, \qquad w = 0. \tag{5.29}$$

The total action is

$$S = \frac{1}{2} \int dt \, d^3\mathbf{x} \Big\{ \dot{\phi}^2 - \zeta_3^2 (\partial_i \partial_j \partial_k \phi)^2 - \zeta_2^2 (\partial_i \partial_j \phi)^2 - c^2 \partial_i \phi \, \partial_i \phi - m^2 \phi^2$$
$$- \lambda_3 \Big(\partial_i \phi \, \partial_i \partial_j \phi \, \partial_j \partial_k \phi \, \partial_k \phi + \frac{1}{3} \partial_i \phi \, \partial_j \phi \, \partial_k \phi \, \partial_i \partial_j \partial_k \phi \Big) \Big\}, \tag{5.30}$$

This model has intriguing renormalization group properties, which will be discussed in detail in Chapter 6. There is no wave-function renormalization of ϕ, and both λ_3 and c^2 satisfy a non-renormalization theorem to all orders in λ_3. This does not mean that the theory can be weakly coupled at all scales: The coefficient ζ_3^2 in (5.30) – which we set equal to 1 in the classical limit – is logarithmically divergent starting at two loops, and therefore ζ_3 runs with the RG scale. The effective coupling in the two-on-two scattering amplitude is not λ_3 but $\overline{\lambda} \equiv \lambda_3 / \zeta_3^3$, which runs due to the running of ζ_3. The two-loop beta function reveals that $\overline{\lambda}$ increases with increasing energy.

Having illustrated the quantum corrections, we can now study cascading hierarchies of symmetry breaking in this model, and confirm their technical naturalness. At some high scale μ, which will be our naturalness scale, and which we keep below μ_s, consider the following hierarchical breaking of polynomial symmetries: First, break the $P = 4$ symmetry of the $z = 3$ Gaussian fixed point to the $P = 2$ symmetry of the $z = 2$ fixed point by some small amount $\varepsilon_2 \ll 1$. Then break $P = 2$ to $P = 1$ by an even smaller amount $\varepsilon_1 \ll \varepsilon_2$. This pattern corresponds to

$$\zeta_3^2 \approx 1, \qquad \zeta_2^2 \approx \mu^2 \varepsilon_2, \qquad c^2 \approx \mu^4 \varepsilon_1, \qquad \lambda_3 \approx \varepsilon_1. \tag{5.31}$$

The dispersion relation cascades from $z = 3$ at high energy scales, to $z = 2$ at intermediate scales, to $z = 1$ at low scales.[3] Both the large hierarchies in (5.31) and the cascading behavior of the dispersion relation are respected by all loop corrections, and therefore are technically natural. This follows by inspection from the properties of the quantum corrections discussed above.

Our original motivation for this study of technical naturalness and hierarchies in spontaneous symmetry breaking came from quantum gravity and high-energy physics, especially in

---

[3]We can also break the linear shift symmetry to constant shifts, by some amount $\varepsilon_0 \ll \varepsilon_1$. This would generate the remaining classically marginal operators $\mathcal{O}_4^{(a)}$, $\mathcal{O}_6$ and the relevant operator $\mathcal{W}$, with coefficients of order ε_0 in the units of μ.

the context of nonrelativistic gravity [5, 6]. Besides extending our understanding of the general "landscape of naturalness," we expect that our results could find their most immediate applications in two other areas: In condensed matter physics, and in effective field theory of inflationary cosmology [63, 64, 65]. Both areas treat systems with nonrelativistic, Aristotelian symmetries similar to ours. In condensed matter, we have seen in Chapter 3 that the multicriticality of NG modes will affect their thermodynamic and transport properties: The Type A_3 modes at the lower critical dimension will exhibit resistivity linear in temperature T over the range of T dominated by the $z = 3$ dispersion (up to $T \log T$ corrections due to self-interactions). In the context of inflation, our self-interacting scalar field theories represent a new nonrelativistic variation on the theme of the Galileon [66], an extension of the $z = 2$ ghost condensate [67, 68], and of the $z = 3$ cosmological scalar theory of Mukohyama [7, 69]. Eventually, we are hoping that the lessons learned in the nonrelativistic arena will give new insights to the fundamental puzzles of naturalness in high-energy physics and gravity: The cosmological constant problem and the Higgs mass hierarchy problem.

Chapter 6

Nonrelativitic Renormalization: A Case Study

In this chapter, we continue the case study of the Aristotelian scalar field theory in $3 + 1$ dimensions introduced in the previous chapter. This theory exhibits intriguing quantum properties. Our focus is on the interplay between their renormalization group properties and the polynomial shift symmetries.

We consider the nonrelativistic quantum field theory of a single real scalar field $\phi(\mathbf{x}, t)$ in $3 + 1$ spacetime dimensions, whose action is given by (5.22), [1]

$$ S = \frac{1}{2} \int dt \, d^3\mathbf{x} \left\{ \dot{\phi}^2 - (\partial_i \partial_j \partial_k \phi)^2 - \zeta_2^2 (\partial_i \partial_j \phi)^2 - c^2 \partial_i \phi \, \partial_i \phi - m^2 \phi^2 - \lambda_3 \mathcal{O} \right\}, \qquad (6.1) $$

where

$$ \mathcal{O} = \partial_i \phi \, \partial_i \partial_j \phi \, \partial_j \partial_k \phi \, \partial_k \phi + \frac{1}{3} \partial_i \phi \, \partial_j \phi \, \partial_k \phi \, \partial_i \partial_j \partial_k \phi. \qquad (6.2) $$

This is the theory that will be the subject of our case study. This theory is renormalizable. Its short-distance behavior is controlled by the $z = 3$ Gaussian fixed point, where z is the dynamical critical exponent. Around this fixed point, λ_3 is a classically marginal coupling. Our statement of renormalizability in particular implies that no other combination of terms with up to four fields and up to six derivatives, besides the ones already in (6.2), are generated by loop corrections; this statement is an immediate consequence of the hidden linear shift symmetry of the system,

$$ \phi(t, \mathbf{x}) \rightarrow \phi(t, \mathbf{x}) + b_i x^i + b. \qquad (6.3) $$

The self-interaction term $\mathcal{O}$ may look familiar, it is closely related to one of the Galileons [66], at least formally. Physically, the role of the term is quite different: In the relativistic Galileon theory, the four-point self-interaction term is highly irrelevant from the viewpoint of the free relativistic massless scalar field theory, of dimension ten in mass units. In the theory with $\phi \rightarrow -\phi$ symmetry, it is the lowest-dimension, least-irrelevant self-interaction that preserves spacetime linear shift symmetry, and the theory is naturally viewed as an

---

[1] We simplify our notation by writing $(\partial_{i_1} \dots \partial_{i_s} \phi)(\partial_{i_1} \dots \partial_{i_s} \phi) \equiv (\partial_{i_1} \dots \partial_{i_s} \phi)^2$, etc.

effective field theory. In contrast, our spatial linear-shift invariant $\mathcal{O}$ is marginal, and in fact the only such invariant in a renormalizable theory with linear shift invariance. Moreover, the relativistic version of this term that appears in the relativistic Galileon contains six spacetime derivatives, which results in a very different dynamics and in particular a very different Hamiltonian. However, some formal features (for example, the structure of a non-renormalization theorem that we prove in this chapter) are somewhat similar between the two theories. Similar structures, including higher polynomial shift symmetries, have emerged in the study of amplitudes [70, 71].

In the following, we will show that the unique self-interaction coupling λ_3 satisfies a non-renormalization theorem to all loop orders. However, despite this non-renormalization of the coupling, the self-interaction strength does depend on scales, as a result of the non-trivial renormalization of the two-point function. In contrast to the relativistic case, there are several natural perspectives on the Callan-Symanzik equation and the process of the renormalization group flow, associated with the observer's freedom to choose how to relate time to space.

6.1   Observer-dependent Relations Between Space and Time

Throughout the thesis, we have been following the "additive convention" for referring to dimensions, whereby [...] is defined to be the *exponent* of the fundamental unit of scale (in our case, energy). This convention is common in high-energy physics, and more generally whenever one keeps track of only one type of dimension.

Occasionally it will prove illuminating to revert to a more elementary picture, in which the units of measurement of time and space are unrelated to each other. In this more fundamental picture, we have two independent dimensions: L for length of space, T for time. We will therefore express the dimension $\dim(\mathcal{O})$ of any object $\mathcal{O}$ multiplicatively, as the appropriate powers of T and L (instead of the additive convention, referring only to the scaling exponent as in the case of $[\ldots]$). with the power of L and T being the length and time dimension os the corresponding object. We can still choose to normalize the field such that its kinetic term $\dot\phi^2$ appears with the canonical prefactor of $1/2$, implying

$$\dim(\phi) = \frac{T^{1/2}}{L^{3/2}}. \tag{6.4}$$

Given this dimension of ϕ, the $(\partial_i\partial_j\partial_k\phi)^2$ term in the action is no longer of the same dimension as $\dot\phi^2$, and we need to introduce its own coupling ζ_3^2, of dimension

$$\dim(\zeta_3^2) = \frac{L^6}{T^2}. \tag{6.5}$$

Setting $\zeta_3^2 = 1$ would be one particular way how to relate time and space dimensions. It would reproduce the $z = 3$ scaling and reduce $\dim(\ )$ to the dimensions at the $z = 3$ fixed point [...].

It is important to note that the relation between time and space is observer dependent, and conversion factors may depend on the prejudice of a given observer as to the "correct" or "most natural" interpretation of the dynamics. We shall see several examples of such distinct observers, and distinct physical perspectives of the same system, throughout this chapter.

Different observers differ by their choice of a conversion factor that relates time and space. For example, when we wrote (6.1), we took the perspective of a "short-distance" observer, and chose to relate space to time by setting $\zeta_3 = 1$. In contrast, a low-energy observer may have the prejudice to interpret the system as approximately relativistic, and relate space to time by setting $c = 1$.

6.2 Hamiltonian Formalism and Vacuum Instability

Using the antisymmetric ε tensor, it is possible to re-write the interaction term (up to total derivatives) in a more compact form, as

$$\frac{\lambda_3}{2} \int dt\, d^3\mathbf{x} \left(\partial_i\phi\, \partial_i\partial_j\phi\, \partial_j\partial_k\phi\, \partial_k\phi + \frac{1}{3}\partial_i\phi\, \partial_j\phi\, \partial_k\phi\, \partial_i\partial_j\partial_k\phi \right)$$
$$= \frac{\lambda_3}{4!} \int dt\, d^3\mathbf{x}\ \varepsilon_{ijk}\varepsilon_{\ell mn}\partial_i\phi\, \partial_j\partial_\ell\phi\, \partial_k\partial_m\phi\, \partial_n\phi. \tag{6.6}$$

The equation of motion is:

$$\ddot{\phi} - (\partial^2)^3\phi + \zeta_2^2(\partial^2)^2\phi - c^2\partial^2\phi - \zeta_0^2\phi - \frac{\lambda_3}{6}\,\varepsilon_{ijk}\varepsilon_{\ell mn}\,\partial_i\partial_\ell\phi\, \partial_j\partial_m\phi\, \partial_k\partial_n\phi = 0. \tag{6.7}$$

Applying the Legendre transformation to (6.1), the Hamiltonian is

$$H = \frac{1}{2}\int d^3\mathbf{x} \left\{ \dot{\phi}^2 + (\partial_i\partial_j\partial_k\phi)^2 + \zeta_2^2(\partial_i\partial_j\phi)^2 + c^2(\partial_i\phi)^2 + m^2\phi^2 \right\} + H_{\text{int}}, \tag{6.8}$$

where

$$H_{\text{int}} = \frac{\lambda_3}{4!}\int d^3\mathbf{x}\ \varepsilon_{ijk}\varepsilon_{\ell mn}\partial_i\phi\, \partial_j\partial_\ell\phi\, \partial_k\partial_m\phi\, \partial_n\phi. \tag{6.9}$$

The energy is not bounded from below, for either sign of λ. We now demonstrate this by explicit constructions.

First, we consider the field configuration that is rotationally symmetric in its spatial coordinates, *i.e.*,

$$\phi(\mathbf{x}, t) = \phi(r, t), \qquad r = |\mathbf{x}|. \tag{6.10}$$

Plugging this ansatz into (6.9), we obtain

$$H_{\text{int}} = \frac{\pi\lambda_3}{3}\int_0^\infty (\phi')^4 \geq 0, \tag{6.11}$$

where

$$\phi' \equiv \frac{\partial}{\partial r}\phi(r, t). \tag{6.12}$$

The Hamiltonian is unbounded from above but bounded from below.

Next, we consider field configurations that break the spatial rotational symmetry. As a simple example, we take the ansatz

$$\phi(\mathbf{x}, t) = P(\rho, t) Z(x_3, t), \qquad \rho = |\mathbf{x}|. \tag{6.13}$$

Here, x_3 is the third component of $\mathbf{x}$. Plugging this ansatz into (6.9), we obtain

$$H_{\text{int}} = 2\pi\lambda_3 H_Z H_P, \tag{6.14}$$

where

$$H_Z \equiv \int_0^\infty dx_3 \, Z^2 (Z')^2 \geq 0, \qquad H_P \equiv \int_0^\infty d\rho \, P^2 P' P'', \tag{6.15}$$

and

$$Z' \equiv \frac{\partial}{\partial x_3} Z(x_3, t), \qquad P' \equiv \frac{\partial^n}{\partial \rho^n} P(\rho, t), \qquad n = 1, 2. \tag{6.16}$$

If we require that

$$P(\rho, t) = \frac{\rho_0 \rho}{\rho^2 + \rho_0^2}, \tag{6.17}$$

then,

$$H_P = -\frac{1}{20\rho_0^2} \leq 0. \tag{6.18}$$

Therefore, there exist both configurations such that H_{int} is greater or smaller than zero. By scaling ϕ up, the size of H_{int} can always surpass the quadratic terms and dominate the Hamiltonian. Hence, we reach the conclusion that the Hamiltonian is unbounded neither from below or above.

Assume that the couplings ζ_2^2, c^2 and m^2 have been chosen such that the dispersion relation is positive definite, then the theory is perturbatively stable around $\langle\phi\rangle = 0$. However, at nonzero λ, this state is non-perturbatively unstable, with the decay probability controlled by a bounce instanton [72, 73]. To derive the instanton action and hence the vacuum decay rate, we look for least-action solution of the equations of motion in imaginary time $\tau = it$,

$$\partial_\tau^2\phi - (\partial^2)^3\phi + \zeta_2^2(\partial^2)^2\phi - c^2\partial^2\phi - \zeta_0^2\phi - \frac{\lambda_3}{6}\varepsilon_{ijk}\varepsilon_{\ell mn}\,\partial_i\partial_\ell\phi\,\partial_j\partial_m\phi\,\partial_k\partial_n\phi = 0. \tag{6.19}$$

This type of equations of motion is sufficiently complicated and the analytic form of the dominant instanton is not known, but its contribution to the decay rate of the vacuum will be

$$\Gamma_{\text{vac}} \propto \exp\left(-\frac{C}{\lambda_3}\right), \tag{6.20}$$

with C positive and of order one. Is this factor C finite? Not if an IR regulator is absent, in which case the instanton action would in fact diverge logarithmically with the size of spacetime. However, C is finite in the presence of any IR regulator, even just $\zeta_2^2 \neq 0$, which in any case we know will be generated by quantum corrections.

It is often assumed that the least-action instanton will be the one with the largest group of spacetime symmetries. In relativistic systems, such instantons would be spherically symmetric in Euclidean spacetime, with symmetry $SO(D+1)$. In our case, the imaginary-time version of the Aristotelian spacetime still carries a preferred foliation by Euclidean leaves of constant τ, and the system is anisotropic between space and time. The largest spacetime symmetry that one can expect is thus the group $SO(D)$ of spatial rotations, times the $\mathbb{Z}_2$ time-reversal symmetry.

Further note that the energy is conserved, and through the slice of $\tau = 0$ should be zero. Interestingly, for $SO(3)$ invariant solutions, this can be used to show that when $\lambda > 0$ such an $SO(3)$-invariant instanton cannot exist, simply because $H_{\text{int}} \geq 0$ with the ansatz of spatial rotational invariance (see (6.11)). However, an instanton solutions can (and probably does) exist for $\lambda < 0$. The least-action instanton for $\lambda > 0$ must break spatial rotational symmetry, and we therefore expect its action to be larger than the action of the spherically symmetric instanton for the other sign of λ. This is sufficient for suppressing the tunneling.

If one wishes, the vacuum instability can be cured by embedding the model in a theory with the symmetries reduced to constant shifts. As a simple example at the classical level, we can turn on the marginal $\mathcal{O}_6$ operator, in which case the action becomes

$$S = \frac{1}{2} \int dt\, d^3\mathbf{x} \left\{ \dot{\phi}^2 - (\partial_i \partial_j \partial_k \phi)^2 - \lambda_3 \mathcal{O} - g_3 \mathcal{O}_6 \right\}. \tag{6.21}$$

We note that the potential

$$\mathcal{V} \equiv \frac{1}{2} \int d^3\mathbf{x} \left\{ (\partial_i \partial_j \partial_k \phi)^2 + \lambda_3 \mathcal{O} + g_3 \mathcal{O}_6 \right\} \tag{6.22}$$

can be written as a sum of complete squares for sufficiently large g_3: If $\lambda > 0$ and $\lambda_6 = \lambda^2/36$, then

$$\mathcal{V} = \frac{1}{2} \int d^3\mathbf{x} \left\{ \left(\partial_i \partial_j \partial_k \phi + \tfrac{1}{6}\lambda_3\, \partial_i \phi\, \partial_j \phi\, \partial_k \phi \right)^2 + \lambda_3 \left(\partial_i \phi\, \partial_i \partial_j \phi \right)^2 \right\} > 0; \tag{6.23}$$

If $\lambda_3 < 0$ and $g_3 = 5\lambda_3^2/18$, then

$$\mathcal{V} = \frac{1}{2} \int d^3\mathbf{x} \left\{ \frac{1}{10} \left[\partial_i \partial_j \partial_k \phi - \delta_{(ij}\partial_{k)}\partial^2 \phi + \frac{5\lambda_3}{3} \partial_i \phi\, \partial_j \phi\, \partial_k \phi \right]^2 \right.$$
$$\left. - \frac{\lambda_3}{15} \left(\delta_{(ij}\partial_{k)}\partial_\ell \phi\, \partial_\ell \phi \right)^2 - \lambda_3 \left(\partial_i \phi\, \partial_j \partial_k \phi \right)^2 \right\}, \tag{6.24}$$

where the symmetrization between spatial indices is defined to be $_{(ijk)} = {}_{ijk} + {}_{jki} + {}_{kij}$. By construction, for any $g_3 \geq 5\lambda_3^2/18$, the potential $\mathcal{V}$ can be written as a sum of squares. This condition is sufficient but not necessary: the bound on g_3 can be relaxed by considering a more general sum of complete squares while rewriting $\mathcal{V}$.

6.3   Quantum Corrections and Properties of Loop Diagrams

We will be interested in perturbation theory around uniform phases, not modulated phases. We assume that ζ_2^2, c^2 and m^2 are all positive definite.

First, the propagator

$$\frac{i}{\omega^2 - (\mathbf{k}^2)^3 - \zeta_2^2(\mathbf{k}^2)^2 - c^2\mathbf{k}^2 - m^2 + i\epsilon} \tag{6.25}$$

contains all the couplings that are present in the Gaussian limit of the theory. It depends on the spatial momentum $\mathbf{k}$ only through its magnitude, which we will denote by $k \equiv |\mathbf{k}|$ from now on.

The Feynman rules of this model involve one four-vertex, which can be simplified using the momentum conservation $\mathbf{k}_4 = -\mathbf{k}_1 - \mathbf{k}_2 - \mathbf{k}_3$ to

$$= -i\lambda\Big[k_1^2 k_2^2 k_3^2 + 2(\mathbf{k}_1 \cdot \mathbf{k}_2)(\mathbf{k}_2 \cdot \mathbf{k}_3)(\mathbf{k}_3 \cdot \mathbf{k}_1)$$
$$- k_1^2(\mathbf{k}_2 \cdot \mathbf{k}_3)^2 - k_2^2(\mathbf{k}_3 \cdot \mathbf{k}_1)^2 - k_3^2(\mathbf{k}_1 \cdot \mathbf{k}_2)^2\Big]. \tag{6.26}$$

Note that in this vertex each momentum appears quadratically, with no subleading terms. We can write it even more compactly with the use of the fully antisymmetric ϵ_{ijk} tensor: If for any three momenta $\mathbf{k}, \mathbf{p}, \mathbf{q}$ we define $[\mathbf{kpq}] \equiv \epsilon_{ijk}k_i p_j q_k$, our vertex becomes simply

$$- i\lambda[\mathbf{k}_1\mathbf{k}_2\mathbf{k}_3]^2. \tag{6.27}$$

This simple vertex structure is intimately related to the underlying symmetries: When translated into momentum space, the linear shift symmetry $\delta\phi(t, \mathbf{x}) = b_i x^i + b$ becomes a shift of the Fourier modes $\phi(t, \mathbf{k})$ by

$$\delta\phi(t, \mathbf{k}) = b_i \frac{\partial}{\partial \mathbf{k}_i}\delta(\mathbf{k}) + b\,\delta(\mathbf{k}). \tag{6.28}$$

Acting with this symmetry on any of the legs of the vertex produces zero, as the vertex is purely quadratic in each of the outside momenta.

Consider the $2N$-point function of ϕ with external momenta $\mathbf{k}_1, \mathbf{k}_2, \cdots, \mathbf{k}_{2N}$. All four-vertices in a 1PI loop diagram Γ_{2N} contain at least two internal legs. Therefore, for all four-vertices that contain external legs, one can always apply momentum conservation to eliminate one of the internal momenta. As a consequence, by (6.27), the momentum associated with each external leg will appear quadratically in the Feynman rule, and any 1PI diagram will be of the form

$$\Gamma_{2N} = \big(k_1^{i_1}k_1^{j_1}\big)\big(k_2^{i_2}k_2^{j_2}\big)\cdots\big(k_{2N}^{i_{2N}}k_{2N}^{j_{2N}}\big)\,\mathcal{I}_{i_1 j_1 i_2 j_2 \cdots i_{2N} j_{2N}}(\mathbf{k}_1, \mathbf{k}_2, \cdots, \mathbf{k}_{2N}), \tag{6.29}$$

which is at least of $4N$-th order in the external momenta. By power-counting, the superficial degree of divergence of the factor $\mathcal{I}$ is $\mathcal{D} = 6 - 4N$.

Equation (6.29) can be viewed as a direct consequence of the Ward-Takahashi (WT) identity for 1PI functional $\Gamma[\phi]$ from the linear shift symmetry. Let us consider the partition function $Z[J]$, a functional of the current J,

$$Z[J] = \int \mathcal{D}\phi \, \exp\left\{ -S[\phi] + \int dt \, d^3\mathbf{x} \, J(t,\mathbf{x})\phi(t,\mathbf{x}) \right\} \tag{6.30}$$

We would like to derive the WT identity by requiring that $Z[J]$ be invariant under the linear shift symmetry. The action $S[\phi]$ is invariant under the transformations (6.3) by design, and the only variation comes from the source term:

$$0 = \delta Z[J] = \int dt \, d^3\mathbf{x} \, J(t,\mathbf{x})(b_i x^i + b)Z[\phi]. \tag{6.31}$$

It is useful to rewrite (6.31) as

$$0 = \int dt \, d^3\mathbf{x} \, J(t,\mathbf{x}) \int dt' \, d^3\mathbf{x}'(b_i x'^i + b)\frac{\delta}{\delta\phi(t',\mathbf{x}')}\left(\frac{\delta W[J]}{\delta J(t,\mathbf{x})} \right), \tag{6.32}$$

where we have introduced $W[J] \equiv \ln Z[J]$, the generating functional of connected correlation functions. To derive the WT identity for the 1PI functional $\Gamma[\phi]$, we perform the following Legendre transformations,

$$\Gamma[\phi] = -W[J] + \int dt \, d^3\mathbf{x} \, J(t,\mathbf{x})\phi(t,\mathbf{x}), \qquad \phi(t,\mathbf{x}) = \frac{\delta W[J]}{\delta J(t,\mathbf{x})}. \tag{6.33}$$

Then (6.32) gives the WT identity for $\Gamma[\phi]$,

$$\int dt \, d^3\mathbf{x}(b_i x^i + b)\frac{\delta\Gamma[\phi]}{\delta\phi(t,\mathbf{x})} = 0. \tag{6.34}$$

In the momentum space, we have

$$\int d\omega \, d^3\mathbf{k} \left[b_i \partial_i \delta^{(3)}(\mathbf{k}) + b \, \delta^{(3)}(\mathbf{k}) \right] \frac{\delta\Gamma[\widetilde{\phi}]}{\delta\widetilde{\phi}(\omega,\mathbf{k})} = 0, \tag{6.35}$$

where $\widetilde{\phi}$ denotes the Fourier modes of ϕ. This implies that a $2N$-point 1PI function Γ_{2N} has to appear at least quadratically for the momenta carried by all external legs. This condition is satisfied by (6.29), which contains the fewest number of momenta.

Nonrenormalization Theorems. We now show that the theory with λ_3 as the only nonzero self-interaction is self-contained under renormalization and the parameters c^2, m^2 and λ_3 are not renormalized to any order in λ_3.

We first consider a two-point 1PI diagram Γ_2 of ϕ with external momenta $\mathbf{k}_1$ and $\mathbf{k}_2$, with $\mathbf{k}_1 = -\mathbf{k}_2 = \mathbf{k}$. This is the special case with $N = 1$ in (6.29):

$$\Gamma_2 = \left(k^{i_1} k^{j_1}\right)\left(k^{i_2} k^{j_2}\right) \mathcal{I}_{i_1 j_1 i_2 j_2}(\mathbf{k}). \tag{6.36}$$

The expression starts only at k^4, and will not contribute to k^2 and the constant – not only via divergent terms, but will not even produce a finite correction. Thus, c^2 and m^2 are not renormalized. This statement is again true to all orders in perturbation theory in λ_3. This proves the nonrenormalization theorems for c^2 and m^2.

The superficial degree of divergence of the factor $\mathcal{I}$ in (6.36) is $\mathcal{D} = 2$, which means that Γ_2 is quadratically divergent in the UV cutoff. We will deal with this divergence momentarily in this section.

Analogously, in the special case when $N = 2$, Γ_4 starts at the eighth order in the external momenta, implying that, at any loop order, there are neither divergent nor finite quantum corrections to λ_3. (The operator $\mathcal{O}$ contains 6 derivatives.) This proves the nonrenormalization theorem for λ_3. Furthermore, none of the operators $\mathcal{W}$, $\mathcal{O}_6$ or $\mathcal{O}_4^{(I)}$'s (containing no more than six derivatives) that would break the linear shift symmetry are generated by the loop corrections.

In general, for $N > 1$, the superficial degree of divergence of the factor $\mathcal{I}$ in (6.29) is $\mathcal{D} = 6 - 4N < 0$. Therefore, once the one-loop divergent correction to the propagator has been canceled by their own counterterm, the one-loop corrections to Γ_{2N} for $N > 1$ will all be finite. As usual, one then iterates this procedure, using the one-loop corrected propagator and four-point function to generate the two-loop correction to the propagator, and so on. Therefore, the factor $\mathcal{I}$ in (6.29) is finite to all loops for $N > 1$.

The only primitive divergent diagrams are those that contribute to the 1PI two-point function. Now, we compute the loop corrections to the propagator. First note that there is no wavefunction renormalization to all orders in perturbation theory, because all loop corrections will be proportional to at least k^4, as shown explicitly in (6.36).

We have noted that the factor $\mathcal{I}$ in (6.36) is quadratically divergent in the UV cutoff. Therefore, the coefficient ζ_2^2 in front of the k^4 term will receive a quadratic divergence. Moreover, expanding $\mathcal{I}$ in a Taylor series of $\mathbf{k}$ yields a logarithmically divergent correction to the coefficient ζ_3^2 (which is set to 1 classically) in front of the k^6 term.

First, we consider the one-loop diagram. Just as in the case of relativistic ϕ^4 theory, the loop integral is manifestly independent of $\omega, \mathbf{k}$. However, in our case, even more is true: This diagram vanishes identically,

$$\underset{\omega, \mathbf{k}}{\overset{\eta, \mathbf{p}}{\bigcirc}} = \frac{1}{2} \int \frac{d\eta}{2\pi} \frac{d^3\mathbf{p}}{(2\pi)^3} \frac{i(-i\lambda_3 [\mathbf{k}\mathbf{k}\mathbf{p}]^2)}{\eta^2 - \omega_{\mathbf{p}}^2 + i\epsilon} \equiv 0, \tag{6.37}$$

simply because the numerator $[\mathbf{k}\mathbf{k}\mathbf{p}]^2 \equiv 0$ is identically zero due to the antisymmetry of the bracket in its three arguments.

The first nonzero quantum correction to the inverse propagator comes at two loops. There is just one 1PI diagram, which we will refer to as the "sunset diagram:"

$$\xrightarrow{\omega,\mathbf{k}} \bigcirc \xrightarrow{\omega,\mathbf{k}} \tag{6.38}$$

The sunset diagram is carefully examined and evaluated in Appendix B. The result is

$$i\lambda_3^2 k^4 \left(A\, k^2 \log \Lambda + B\Lambda^2 + \text{finite} \right), \tag{6.39}$$

where Λ is the sharp cutoff places on the momenta carried by the internal legs. Coefficients A and B are real numbers estimated numerically in (B.42) and (B.27), respectively, $A < 0$ and $B > 0$. The finite term is non-singular at $k^2 = 0$ assuming that at least one of the infrared-regulating couplings c^2 or ζ_2^2 is non-zero, as shown in Appendix B. There is no contribution such as $(\log \Lambda)^2$ in (6.39), due to the simple fact that any subdiagram in the sunset diagram except for itself is finite.

In summary, even though there is no wavefunction renormalization of ϕ, two of the Gaussian couplings – ζ_2^2 and ζ_3^2 – do get renormalized when λ_3 is turned on. However, λ_3 itself satisfies a nonrenormalization theorem, to all loops.

6.4 Elementary Processes

In this section, we consider some elementary processes in the $\partial^6 \phi^4$-theory. In Section 6.2, we have discussed the vacuum decay and bounce instantons. In the following, we discuss two more processes: Particle decays and two-on-two scatterings. More details about scattering amplitudes in Aristotelian spacetime can be found in Appendix A.

Particle decay. The ϕ quanta exhibit an intriguing perturbative instability in the Aristotelian spacetime: Self-decay processes are kinematically allowed and a single particle acquires a non-zero decay width Γ. The lowest contribution to Γ comes from the imaginary part of the sunset diagram. By taking the cutting rule, this describes the decay of a single particle into three copies of itself.

As a simple example, consider an incoming particle with momentum $\mathbf{k}$ decaying into three copies of itself, with momentum $\mathbf{k}/3 + \mathbf{q}_i$, with $i = 1, \cdots, 3$, $\mathbf{q}_1 + \mathbf{q}_2 + \mathbf{q}_3 = 0$ and $|\mathbf{q}_i| = q$. Around the $z = 3$ fixed point, we assume the dispersion relation to be $\omega = \sqrt{k^6 + m^2}$. Then, the conservation law of energy enforces

$$\sqrt{k^6 + m^2} = 3\sqrt{\left(\frac{k^2}{9} + q^2\right)^3 + m^2}, \tag{6.40}$$

which can be satisfied for any $\mathbf{k}$ with

$$k \geq \left(\frac{81\, m^2}{10}\right)^{\frac{1}{6}}. \tag{6.41}$$

The ϕ quantum is absolutely stable at $\mathbf{k} \approx 0$ below the threshold. At small $|\mathbf{k}|$, there is a very sharp long-lived resonance. At large k, the decay width Γ can be obtained by calculating the imaginary part of the sunset diagram, which gives

$$\Gamma \sim \frac{\lambda_3^2}{\zeta_3^5} k^3. \tag{6.42}$$

In the more fundamental picture in which space and time are *a priori* unrelated, $\dim(\zeta_3) = L^3/T$ and $\dim(\lambda_3) = L^9/T^3$. Therefore, $\dim(\Gamma) = 1/T$, as expected. A more thorough exposition of decay rate calculation in Aristotelian spacetime can be found in Appendix A.

Particle scattering. We consider the two-on-two scattering. The incoming particles carry momenta $\mathbf{k}_1$ and $\mathbf{k}_2$; the outgoing particles carry momenta $\mathbf{k}_1'$ and $\mathbf{k}_2'$. At the tree level,

$$
\begin{aligned}
d\sigma =& \frac{d^3\mathbf{k}_1'}{(2\pi)^3} \frac{d^3\mathbf{k}_2'}{(2\pi)^3} \frac{\lambda_3^2[\mathbf{k}_1\mathbf{k}_2\mathbf{k}_1']^4}{2\omega_{\mathbf{k}_1} 2\omega_{\mathbf{k}_2} |v_1 - v_2|} \frac{1}{(2\omega_{\mathbf{k}_1}')(2\omega_{\mathbf{k}_2}')} \\
&\times (2\pi)^4 \delta\left(\omega_1 + \omega_2 - \omega_1' - \omega_2'\right) \delta^{(3)}\left(\mathbf{k}_1 + \mathbf{k}_2 - \mathbf{k}_1' - \mathbf{k}_2'\right).
\end{aligned}
\tag{6.43}
$$

Here $v_i = d\omega_{\mathbf{k}_1}/dk_1^{\|}$, $i = 1, 2$, with $k_i^{\|}$ the component of $\mathbf{k}_i$ parallel to the total incoming momentum $\mathbf{k}_1 + \mathbf{k}_2$. In the more fundamental picture in which space and time are *a priori* unrelated, $\dim(\lambda_3) = L^9/T^3$. Therefore, $\dim(d\sigma) = L^2$, as expected.

6.5 Renormalization from the High-Energy Perspective

Unlike in relativistic theories, there are at least two natural classes of observers already at the microscopic level:

- The *Aristotelian observers* fix the coordinates $(t, \mathbf{y})$ once and for all, find the non-renormalization of λ_3 but also the running of ζ_3^2, which lead to the running of the effective coupling $\overline{\lambda}$.

- The *Wilsonian observers*, during the process of integrating out a shell of modes, rescale the system to restore the normalization condition $\zeta_3^2 = 1$. This involves a rescaling of the spatial coordinates which depends on the RG scale. Their effective coupling runs.

When these two observers compare their notes with the Aristotelian observers, both see the same physics but in a slightly rescaled coordinate system.

In this section, we take the perspective of the Aristotelian observer use the Callan-Symanzik equations to compute the beta functions. To begin with, we define the normalization conditions. Consider $\Gamma^{(n)}(\omega_1, \mathbf{k}_1; \dots, \omega_n, \mathbf{k}_n)$. $\Gamma^{(2)}$ is only a function of $\omega \equiv \omega_1 = -\omega_2$ and $k^2 \equiv k_1^2 = k_2^2$. We impose four normalization conditions

$$\Gamma^{(2)}(\omega, k^2)\big|_\star = m^2, \qquad\qquad \frac{\partial \Gamma^{(2)}(\omega, k^2)}{\partial k^2}\bigg|_\star = c^2, \tag{6.44}$$

$$\frac{1}{2}\left.\frac{\partial^2\Gamma^{(2)}(\omega,k^2)}{(\partial k^2)^2}\right|_{\star} = \zeta_2^2, \qquad\qquad \frac{1}{3!}\left.\frac{\partial^3\Gamma^{(2)}(\omega,k^2)}{(\partial k^2)^3}\right|_{\star} = 1. \qquad (6.45)$$

These normalization conditions are chosen such that at the normalization point $\star$, the inverse propagator reproduces the expected behavior near the $z=3$ fixed point.

Our selection of the appropriate normalization point $\star$, and our choice of the renormalized couplings m^2, ζ_2 and c in the normalization conditions, will depend on the nature of any particular physics question we may address. For example, in a theory with a gap m, one natural choice of the normalization condition is the on-shell normalization. However, due to the presence of higher order terms in spatial momentum in the propagator, sometimes it is more convenient to choose an off-shell condition. A particularly useful choice for the normalization point $\star$ is

$$\star : (\omega^2, k^2) = (-M^6, 0), \qquad (6.46)$$

where M is the renormalization scale associated with the normalization point $\star$, $[M] = 1/3$ $(\dim(\phi) = 1/T^{1/3})$. We will stick to this normalization condition in the following discussion.

The four-point function gives the normalization of λ_3. Similarly to the two-point function, we must choose a normalization point $\star$, and then impose appropriate conditions guaranteeing that the four-point function reproduces the expected vertex structure. However, thanks to the nonrenormalization theorem for λ_3, we do not have to spend much time on this.[2]

In terms of the bare couplings, the action is

$$S = \frac{1}{2}\int dt\, d^3\mathbf{x}\Big\{\dot{\phi}_{\text{bare}}^2 - \zeta_{3,\text{bare}}^2(\partial_i\partial_j\partial_k\phi_{\text{bare}})^2 - \zeta_{2,\text{bare}}^2(\partial_i\partial_j\phi_{\text{bare}})^2 - \lambda_{3,\text{bare}}\mathcal{O}_{\text{bare}}\Big\}, \qquad (6.47)$$

where $\mathcal{O}_{\text{bare}}$ is given by $\mathcal{O}$ in (6.2) with ϕ replaced with ϕ_{bare}. We have set m^2 and c^2 to zero by invoking the nonrenormalization theorems. The renormalized action is

$$S = \frac{1}{2}\int dt\, d^3\mathbf{x}\Big\{\dot{\phi}^2 - \zeta_3^2(\partial_i\partial_j\partial_k\phi)^2 - \zeta_2^2(\partial_i\partial_j\phi)^2 - \lambda_3\mathcal{O}$$
$$- \delta_Z\dot{\phi}^2 - \delta_3(\partial_i\partial_j\partial_k\phi)^2 - \delta_2(\partial_i\partial_j\phi)^2 - \delta_\lambda\mathcal{O}\Big\}. \qquad (6.48)$$

We have introduced physical couplings, ζ_3, ζ_2 and λ_3, and counterterms, δ_Z, δ_3 and δ_2. Around the normalization point $\star$, the theory is regulated by the nonzero ω^2 in the IR. For simplicity, we would like to set ζ_2 to zero at the tree level. Since there is no field renormalization, $\delta_Z = 0$. δ_λ can be set to zero trivially, due to the nonrenormalization theorem for λ_3. To determine δ_2 and δ_3, we introduce the following renormalization conditions:

$$\frac{1}{2}\left.\frac{\partial^3\Gamma^{(2)}(\omega,k^2)}{(\partial k^2)^2}\right|_{\star} = 0, \qquad \frac{1}{3!}\left.\frac{\partial^3\Gamma^{(2)}(\omega,k^2)}{(\partial k^2)^3}\right|_{\star} = \zeta_3^2. \qquad (6.49)$$

The correction to the inverse two-point function up to two loops is given by

$$i\Pi^{(2)}(\omega,\mathbf{k}) = \;\text{—}\bigcirc\text{—}\; + \;\text{—}\otimes\text{—}\; + \cdots. \qquad (6.50)$$

---

[2]If one wishes, we could normalize to the equilateral tetrahedron point. (See Section 8.4 for details.)

All other loop diagrams that contribute up to the two-loop order vanish. In (B.52), the sunset diagram is evaluated to be

$$\overrightarrow{\omega,\mathbf{k}}\bigcirc\overrightarrow{\omega,\mathbf{k}} = \frac{i\lambda_3^2}{\zeta_3^4}k^4\left\{Ak^2\log\left(\zeta_3^{\frac{1}{3}}\Lambda/|\omega|^{\frac{1}{3}}\right) + B\Lambda^2 + \text{finite}\right\}, \qquad (6.51)$$

where

$$A \approx -1.13 \times 10^{-6} < 0, \qquad B > 0, \qquad (6.52)$$

and Λ is a UV momentum cutoff, $[\Lambda] = 1/3$ $(\dim(\Lambda) = 1/L)$. The counterterm is given by

$$\overrightarrow{\omega,\mathbf{k}}\,{}^{\otimes}\overrightarrow{\omega,\mathbf{k}} = -i\delta_3 k^6 - i\delta_2 k^4. \qquad (6.53)$$

Summing over the geomertic series, we obtain the exact inverse propagator:

$$\Gamma^{(2)} = \omega^2 - \zeta_3^2 k^6 + \Pi^{(2)}(\omega, \mathbf{k}). \qquad (6.54)$$

Imposing the renormalization conditions (6.49), we obtain

$$\delta_2 = \frac{\lambda_3^2}{\zeta_3^4}B\Lambda^2, \qquad \delta_3 = \frac{\lambda_3^2}{\zeta_3^4}A\log\left(\zeta_3^{\frac{1}{3}}\Lambda/M\right). \qquad (6.55)$$

Note that the argument of the log has dimension 1 in either measures ($[\ldots]$ or $\dim(\ )$), as desired. The two-point Green's function is

$$G^{(2)}(\omega, \mathbf{k}) = \frac{i}{\omega^2 - \zeta_3^2 k^6\left[1 - \zeta_3^{-6}\lambda_3^2 A\log\left(M/|\omega|^{\frac{1}{3}}\right)\right] + \mathcal{O}(\lambda_3^3)}. \qquad (6.56)$$

From the Callan-Symanzik equation,

$$\left(M\frac{\partial}{\partial M} + \beta\frac{\partial}{\partial \lambda_3} + \widetilde{\gamma}\zeta_3^2\frac{\partial}{\partial \zeta_3^2} + 2\gamma\right)G^{(2)} = 0, \qquad (6.57)$$

we obtain

$$\beta \equiv \frac{d\lambda_3}{d\log M} = 0 + \mathcal{O}(\lambda_3^3), \qquad \gamma = 0 + \mathcal{O}(\lambda_3^3), \qquad (6.58)$$

and

$$\widetilde{\gamma} \equiv \frac{d\log\zeta_3^2}{d\log M} = \frac{\lambda_3^2}{\zeta_3^6}A + \mathcal{O}(\lambda_3^3). \qquad (6.59)$$

This is interpreted as the anomalous dimension for ζ_3.

Next, we consider the four-point Green's function. Up to two-loop, the only divergent contribution to the four-point Green's function comes from the non-amputated diagram

$$(6.60)$$

The four-point Green's function is thus

$$G^{(4)}(\omega_i, \mathbf{k}_i) = \left(-i\lambda_3[\mathbf{k}_1\mathbf{k}_2\mathbf{k}_3]^2\right) G^{(2)}(\omega_1, \mathbf{k}_1)G^{(2)}(\omega_2, \mathbf{k}_2)G^{(2)}(\omega_3, \mathbf{k}_3)G^{(2)}(\omega_4, \mathbf{k}_4). \qquad (6.61)$$

From the Callan-Symanzik Equation,

$$\left(M\frac{\partial}{\partial M} + \beta\frac{\partial}{\partial \lambda_3} + \widetilde{\gamma}\zeta_3^2\frac{\partial}{\partial \zeta_3^2} + 4\gamma\right) G^{(4)} = 0, \qquad (6.62)$$

we obtain

$$\beta = 0 + \mathcal{O}(\lambda_3^4), \qquad \gamma = 0 + \mathcal{O}(\lambda_3^4). \qquad (6.63)$$

This result is expected: Since there is no field renormalization, $\gamma = 0$ should hold to all loop orders. Moreover, by the nonrenormalization for λ_3, $\beta = 0$ holds to all loop orders.

By applying the Callan-Symanzik equation for computing the beta functions, we fix the coordinates $(t, \mathbf{x})$ once and for all, which defines the *Aristotelian observers*. Those observers find the non-renormalization of λ_3 but also the running of ζ_3^2, indicated by (6.58). This leads to the running of the dimensionless quantity $\overline{\lambda}$, with respective to the smallness of which the theory can be expanded perturbatively.

The dispersion relation runs with changing energy. With increasing energy, ζ_3 decreases. The dispersion relation is

$$\omega^2 = \zeta_3^2 k^6 + \zeta_2^2 k^4. \qquad (6.64)$$

We have introduced ζ_2 as an IR regulator. Running to the UV, ζ_3 decreases, and the dispersion relation "closes up."

Despite the nonrenormalization theorem for λ_3, the physics does depend on the scale. In fact, the theory is not defined perturbatively with respect to λ_3, but instead an effective coupling constant

$$\overline{\lambda} \equiv \frac{\lambda_3}{\zeta_3^3}. \qquad (6.65)$$

Even though there holds the nonrenormalization theorem for λ_3, the coefficient ζ_3 receives renormalization, and thus the effective coupling $\overline{\lambda}$ runs. To show that $\overline{\lambda}$ is indeed the effective coupling constant of the theory, we present the following arguments:

- The coupling λ_3 is a dimensionless quantity at the $z = 3$ fixed point, *i.e.*, $[\lambda_3] = 0$. However, in a more elementary picture where the time and space have independent dimensions T and L, respectively, the coupling λ_3 develops a dimension $\dim(\lambda_3) = L^9/T^3$, which is not unit. In contrast, the quantity $\overline{\lambda}$ is dimensionless in both measures: $[\overline{\lambda}] = 0$, $\dim(\overline{\lambda}) = 1$.

- The actual expansion parameter of our perturbation theory is not λ_3 but $\overline{\lambda}$: A Feynman diagram with $2N$ external legs and L loops can be written as

$$\overline{\lambda}^L\left(\zeta_3^{N+1}\overline{\lambda}^{N-1}\right)\mathcal{I}\left(\Lambda, \omega/\zeta_3\right). \qquad (6.66)$$

Therefore, the loop-wise expansion is characterized by an expansion series of the effective coupling $\overline{\lambda}$.

- The scattering cross-section as a physical observable is controlled by $\overline{\lambda}$: For a tree level process, in the limit that the IR regulators are zero, the dispersion relation is $\omega = \zeta_3 k^3$, and the two-on-two cross section σ can be read off from (6.43):

$$d\sigma = \overline{\lambda}^2 \left\{ \frac{d^3\mathbf{k}_1'}{(2\pi)^3} \frac{d^3\mathbf{k}_2'}{(2\pi)^3} \frac{[\mathbf{k}_1\mathbf{k}_2\mathbf{k}_1']^4 (2\pi)^4 \delta(k_1^3 + k_2^3 - k_1'^3 - k_1'^3) \, \delta^{(3)}(\mathbf{k}_1 + \mathbf{k}_2 - \mathbf{k}_1' - \mathbf{k}_2')}{48 k_1^3 k_2^3 k_1'^3 k_2'^3 |k_1 k_1^\parallel - k_2 k_2^\parallel|} \right\},$$

where it is again $\overline{\lambda}$ that controls the size of σ.

By (6.58) and (6.63), the beta function for $\overline{\lambda}$ is

$$\overline{\beta} = -\frac{3}{2} A \overline{\lambda}^3. \tag{6.67}$$

Because $A < 0$, $\overline{\lambda}$ increases with increasing energy, and the theory becomes strongly coupled at very high scales.

It is intriguing to note that the running of the $\overline{\lambda}$ coupling to large values does not necessarily imply that the theory is UV incomplete. Recall that a single particle with momentum $\mathbf{k}$ with respect to the rest frame acquires a non-zero decay width. At large k, the decay rate behaves asymptotically as $\Gamma \sim \zeta_3 \overline{\lambda}^2 k^3$, in terms of the effective coupling $\overline{\lambda}$. The spectral function $A(\omega, \mathbf{k})$ for the self-interaction characterized by $\overline{\lambda}$ is given by [74]

$$A(\omega, \mathbf{k}) = \frac{1}{\pi} \frac{\omega_\mathbf{k} \Gamma}{(\omega^2 - \omega_\mathbf{k}^2)^2 + \omega_\mathbf{k}^2 \Gamma^2}. \tag{6.68}$$

At large k and not very small ζ_3, $\omega_\mathbf{k} \sim \zeta_3^2 k^3$. With increasing k, $\overline{\lambda}$ runs until it becomes of order 1, and the ratio $\omega_\mathbf{k}/\Gamma \sim \overline{\lambda}^2$ also approaches order 1, implying that the ϕ resonance becomes very wide. The scattering of individual quanta with very high k makes no sense: They decay rapidly into multiple soft quanta beforehand. Therefore, at high energies, the large values of $\overline{\lambda}$ anticipated by the RG equations cannot by measured by any two-on-two scattering, because there are only softer quanta that are available to scatter. It is possible that the theory self-completes in the UV via some non-Wilsonian mechanism similar to classicalization [75, 76]: Instead of the appearance of new degrees of freedom in the high energies, an arbitrarily small length scale is forbidden to probe due to the self-decay process, and the soft quanta may form a classical condensate. Since the speed of light c characterizes the scale above which the theory exhibits perturbative instability, it is conceivable that the UV physics above the momentum scale $\sqrt{c}$ is dual to the IR physics below $\sqrt{c}$; this is reminiscent of the UV/IR connection in the context of gravity.

6.6 Renormalization from the Wilsonian Perspective

From the perspectives of a Wilsonian observer, during the process of integrating out a shell of modes, one also rescales the system to restore the normalization condition $\zeta_3^2 = 1$.

In the Wilsonian approach, we consider the action

$$S = \frac{1}{2} \int dt\, d^3\mathbf{x} \left\{ \dot{\phi}^2 - (\partial_i \partial_j \partial_k \phi)^2 - \bar{\lambda}\mathcal{O} \right\}, \tag{6.69}$$

where $\bar{\lambda}$ will eventually turn out to be equivalent to λ_3/ζ_3^3 for the Aristotelian observers. In the previous sections, we applied the sharp cutoff on internal momenta, $\mathbf{p}$, $\mathbf{q}$ and $\mathbf{K} \equiv \mathbf{p} + \mathbf{q}$, and evaluated the sunset diagram. The sharp cutoffs are $|\mathbf{p}|, |\mathbf{q}|, |\mathbf{K}| < \Lambda$. Choose a fraction $0 < f < 1$. In the Wilsonian approach, we integrate out the high energy modes by restricting the momentum integral to be over the range

$$\left\{ (\mathbf{p}, \mathbf{q}) : 0 < |\mathbf{p}|, |\mathbf{q}|, |\mathbf{K}| < \Lambda \right\} \setminus \left\{ (\mathbf{p}, \mathbf{q}) : 0 < |\mathbf{p}|, |\mathbf{q}|, |\mathbf{K}| < f\Lambda \right\}. \tag{6.70}$$

The integration over this precise momentum shell is impractical to perform. However, we can take the advantage of the known result for the log divergence in the sunset diagram over the range $\{(\mathbf{p}, \mathbf{q}) : 0 < |\mathbf{p}|, |\mathbf{q}|, |\mathbf{K}| < \Lambda\}$,

$$= i\bar{\lambda}^2 \Im(\Lambda), \qquad \Im(\Lambda) = Ak^6 \log\left(\zeta_3^{\frac{1}{3}} \Lambda / |\omega|^{\frac{1}{3}} \right) + \cdots . \tag{6.71}$$

The high energy contribution to the low energy effective action from the integration over the momentum shell (6.70) is

$$\bar{\lambda}^2 \left[\Im(\Lambda) - \Im(f\Lambda) \right] = -\bar{\lambda}^2 Ak^6 \log f + \cdots . \tag{6.72}$$

The effective action obtained from integrating over the momentum shell can be written as

$$S_{\text{eff}} = \frac{1}{2} \int dt\, d^3\mathbf{x} \left\{ \dot{\phi}^2 - f^\Delta (\partial_i \partial_j \partial_k \phi)^2 - \bar{\lambda}\mathcal{O} \right\}, \tag{6.73}$$

where

$$\Delta \equiv \bar{\lambda}^2 A + \mathcal{O}(\bar{\lambda}^3). \tag{6.74}$$

To compare with the original action (6.69), we taking the following rescaling in (6.73):

$$\mathbf{k}' \equiv f^{-1}\mathbf{k}, \qquad t' \equiv f^z t, \qquad \mathbf{x}' \equiv f\mathbf{x}, \qquad \phi' \equiv f^{-\gamma}\phi. \tag{6.75}$$

Here z is the dynamical critical exponent and γ is the anomalous dimension of the scalar field. The rescaled action is

$$S_{\text{eff}} = \frac{1}{2} \int dt'\, d^3\mathbf{x}' \left\{ f^{2\gamma+z-3}(\partial_{t'}\phi')^2 - f^{2\gamma-z+3+\Delta}(\partial_i'\partial_j'\partial_k'\phi')^2 - \bar{\lambda}'\mathcal{O}' \right\}, \tag{6.76}$$

where

$$\bar{\lambda}_3' \equiv \bar{\lambda} f^{4\gamma-z+3}. \tag{6.77}$$

Here, $\partial'_i \equiv \partial/\partial(x')^i$. Requiring that the action (6.76) take the same form as (6.69), we obtain

$$z = 3 + \frac{1}{2}\bar{\lambda}^2 A + \mathcal{O}(\bar{\lambda}^3), \qquad \gamma = -\frac{1}{4}\bar{\lambda}^2 A + \mathcal{O}(\bar{\lambda}^3), \tag{6.78}$$

and

$$\bar{\lambda}' = \bar{\lambda} + \frac{3}{2}\bar{\lambda}^3 A \log(1/f) + \mathcal{O}(\bar{\lambda}^4). \tag{6.79}$$

Since $A < 0$, as one integrates out the high momentum shell, the coupling $\bar{\lambda}$ decreases and the field ϕ develops a positive anomalous dimension. $z < 3$, CHMW theorem is fine. The beta function for $\bar{\lambda}$ is defined to be

$$\bar{\beta} = \frac{d\bar{\lambda}}{d\log f} = -\frac{3}{2}\bar{\lambda}^3 A + \mathcal{O}(\bar{\lambda}^4). \tag{6.80}$$

This result matches (6.67) with $\zeta_3 = 1$.

From the perspectives of the Wilsonian observer, the effective coupling $\bar{\lambda}$ runs, and the theory also becomes strongly coupled at very high momentum scales. More interestingly, the anisotropy between space and time also changes, due to the rescaling of the spatial coordinates that depends on the RG scale. This is reflected in the correction to z in (6.78). When they compare their notes with the Aristotelian observers, both see the same physics but in a slightly rescaled coordinate system; such a rescaling of the coordinate system is the most evident by comparing the actions used by different observers.

According to the Aristotelian observer, the action can be written as

$$S = \frac{1}{2}\int dt\, d^3\mathbf{x}\left\{\dot{\phi}^2 - \zeta_3^2\left(\partial_i\partial_j\partial_k\phi\right)^2 - \lambda_3\mathcal{O}\right\} \tag{6.81}$$

We take the rescaling of spatial coordinates,

$$\mathbf{x}' \equiv \frac{\mathbf{x}}{\zeta_3^{1/3}}; \tag{6.82}$$

together with a rescaling of the field ϕ,

$$\phi' \equiv \zeta_3^{1/2}\phi, \tag{6.83}$$

we obtain a rescaled action,

$$S' = \frac{1}{2}\int dt\, d^3\mathbf{x}\left\{\dot{\phi}^2 - \left(\partial'_i\partial'_j\partial'_k\phi'\right) - \bar{\lambda}\mathcal{O}'\right\}, \tag{6.84}$$

where $\bar{\lambda} = \lambda_3/\zeta_3^3$, $\partial'_i \equiv \partial/\partial\mathbf{x}'^i$ and $\mathcal{O}'$ is the same as $\mathcal{O}$ with ∂ replaced by ∂' and ϕ replaced by ϕ'. This action S' is exactly the one taken by the Wilsonian observer.

6.7 Large N Expansion

In this section, we consider the $O(N)$ extension: ϕ^I, $I = 1, \cdots, N$. There is a unique dressing of the vertex by vector indices, and a unique $O(N)$ theory of an N-component scalar. In the momentum space, it is easy to see that there is a unique four-vertex, written as a direct product between the vertex structure given in (6.27) and Kronecker symbols with their indices symmetrized:

$$- i[\mathbf{pqk}]^2 \left(\delta^{IJ}\delta^{KL} + \delta^{IK}\delta^{JL} + \delta^{IL}\delta^{JK}\right) \tag{6.85}$$

In the position space, one can construct this unique four-vertex in the graphical representation, by adding a graphical structure representing the contractions between fields ϕ's in (5.26): Denoting the contraction between two fields, $(\phi^I \ldots \phi^I)$, by a dashed link, the unique invariant under the linear shift symmetry in its graphical representation is

$$\tag{6.86}$$

Treating the vertices as indistinguishable, this sum becomes

$$4\widetilde{\mathcal{O}} \equiv 4\left\{ \vcenter{\hbox{}} \right\}$$
$$= 4\Big[(\partial_i\phi \cdot \partial_i\partial_j\partial_k\phi)(\partial_j\phi \cdot \partial_k\phi) + (\partial_i\phi \cdot \partial_j\partial_k\phi)(\partial_k\phi \cdot \partial_i\partial_j\phi)$$
$$+ (\partial_i\phi \cdot \partial_i\partial_k\phi)(\partial_j\phi \cdot \partial_j\partial_k\phi) + (\partial_i\phi \cdot \partial_j\phi)(\partial_i\partial_k\phi \cdot \partial_j\partial_k\phi)\Big]. \tag{6.87}$$

Using the antisymmetric ε tensor, we can rewrite this interaction term (up to total derivatives) in a more compact form, as

$$\frac{\lambda_3}{2}\int dt\, d^3\mathbf{x}\, \widetilde{O} = \frac{\lambda_3}{8}\int dt\, d^3\mathbf{x}\, \varepsilon_{ijk}\varepsilon_{\ell mn}(\partial_i\phi \cdot \partial_j\partial_\ell\phi)(\partial_k\partial_m\phi \cdot \partial_n\phi)$$
$$= \frac{\lambda_3}{8}\int dt\, d^3\mathbf{x}\, \varepsilon_{ijk}\varepsilon_{\ell mn}(\partial_i\phi \cdot \partial_\ell\phi)(\partial_j\partial_m\phi \cdot \partial_k\partial_n\phi). \tag{6.88}$$

The action can be written as

$$S = \frac{1}{2}\int dt\, d^3\mathbf{x}\Big\{\dot{\phi} \cdot \dot{\phi} - \zeta_3^2\, \partial_i\partial_j\partial_k\phi \cdot \partial_i\partial_j\partial_k\phi - \lambda_3\, \widetilde{O}$$

$$- \zeta_2^2 \, \partial_i \partial_j \phi \cdot \partial_i \partial_j \phi - c^2 \partial_i \phi \cdot \partial_i \phi - m^2 \phi \cdot \phi \Big\}. \tag{6.89}$$

In the following, we show that the quantum correction to the propagator vanishes completely in the large N limit. Let us first take the rescaling of the field ϕ^I: $\phi^I \to N^{\frac{1}{2}} \phi^I$, and define the 't Hooft coupling, $\lambda_t = \lambda_3 N$. Therefore,

$$S = \frac{N}{2} \int dt \, d^3\mathbf{x} \Big\{ \dot{\phi} \cdot \dot{\phi} - \zeta_3^2 \, \partial_i \partial_j \partial_k \phi \cdot \partial_i \partial_j \partial_k \phi - \lambda_t \, \widetilde{O}$$

$$- \zeta_2^2 \, \partial_i \partial_j \phi \cdot \partial_i \partial_j \phi - c^2 \partial_i \phi \cdot \partial_i \phi - m^2 \phi \cdot \phi \Big\}. \tag{6.90}$$

Then, the propagator becomes

$$\frac{\delta^{IJ}}{N} \frac{i}{\omega^2 - \zeta_3^2 k^6 - \zeta_2^2 k^4 - c^2 k^2 - m^2}. \tag{6.91}$$

The four-vertex is

$$- N \lambda_t [\mathbf{pqk}]^2 \left(\delta^{IJ} \delta^{KL} + \delta^{IK} \delta^{JL} + \delta^{IL} \delta^{JK} \right). \tag{6.92}$$

Consider an amputated Feynman diagram with V vertices, I internal legs L independent loops. Note that $L = I - V + 1$. Each propagator will contribute one power of N and each vertex will contribute one power of $1/N$. Summing over N fields ϕ^I in a loop will contribute an extra N to the Feynman diagram. If there are ℓ loops that are summed over in a Feynman diagram, then the overall power in N is

$$V - I + \ell = 1 - L + \ell. \tag{6.93}$$

The diagram is of the leading order N if and only if there is way of contracting the indices of the fields ϕ^I such that $\ell = L$. Requiring $\ell = L$ forbids any overlapping subdiagrams and restricts the diagrams to be of the cactus-type, in which there is no internal leg that is contained in more than one loop.

Diagrammatically, the full propagator is denoted by a thick line and can be written as a geometric series of 1PI diagrams,

$$\tag{6.94}$$

where 1PI is a sum of all 1PI cactus diagrams. This induces the recursive relation

$$\tag{6.95}$$

which vanishes identically due to the linear shift symmetry, in analogy of (6.37). This implies a nonrenormalization theory in the large N limit for the couplings ζ_3^2 and ζ_2^2, in addition to the nonrenormalization theorems for c^2, m^2 and λ_t. We conclude that the theory is scale invariant if the relevant deformations ζ_2^2, c^2 and m^2 are turned off.

Moreover, both the nonperturbative decay rate of the vacuum and the perturbative decay width vanish in the large N limit:

$$\Gamma_{\text{vac}} \propto \exp\left(-NC/\overline{\lambda}_t\right) \to 0, \qquad \Gamma \sim \frac{1}{N}\zeta_3\overline{\lambda}_t^2|\mathbf{k}|^3 \to 0, \tag{6.96}$$

where $\overline{\lambda}_t \equiv \lambda_t/\zeta_3^3$. The theory becomes absolutely stable in the large N limit.

Looking for holographic duals [77, 78] for this theory in the large N limit might be instructive. Because of the $O(N)$ symmetry in the boundary theory, we expect the possible bulk theory defined in one higher dimensions to be a nonrelativsitic version of Vasiliev theories. Developing such holographic duals will be useful for further understanding both holography and nonrelativistic field theories. It is also intriguing to note that the relevant terms with coupling constants ζ_2^2, c^2 and m^2 are free to turn on, which may correspond to interesting deformations in the bulk gravity theory.

Chapter 7

Application: A Naturally Light Higgs

In Chapter 5, we have seen that nonrelativistic scalar field theories can exhibit a natural cascading hierarchy of scales, protected by a hierarchy of polynomial shift symmetries. Using the toy model that we introduced in Chapter 6, we argue that a high-energy cross-over to such nonrelativistic behavior naturally leads to light scalars, and thus represents a useful ingredient for technically natural resolutions of scalar mass hierarchies, perhaps even the Higgs mass hierarchy puzzle.

The 2012 discovery [1, 2] and the observed properties of the Higgs boson suggest that the Standard Model may be self-contained up to a very high scale. This intriguing possibility brings the naturalness puzzles back into renewed focus (see *e.g.* [79, 80]), and invites us to look for new ideas about naturalness. There are two perspectives on naturalness:

- Technical naturalness by 't Hooft. This is the notion that we have presented in §1.1 and have been working with throughout the thesis. This criteria of naturalness states that a parameter may be naturally small if setting it to zero leads to an enhanced symmetry.

- Naturalness criteria by Dirac. This is a stronger version of naturalness, which simply requires that there be no "unexplained" small numbers in Nature.

We would like to emphasize that our philosophy in through is to search for mechanisms which produce technical naturalness: explaining the permissibility of small numbers, but not necessarily their origin.

In the previous chapters, we have learned that the concept of technical naturalness exhibits many surprises in nonrelativistic settings. New symmetries emerge [18], and they protect new hierarchies of Nambu-Goldstone bosons with cascading scales of partial symmetry breaking [22]. In this chapter, we apply this phenomenon to relativistic scalars such as the Higgs, and investigate the possibility of a crossover to nonrelativistic physics at high energy scales and its influence on the naturalness of a small Higgs mass.

For gravity, nonrelativistic physics with possible fundamental anisotropies between space and time is beneficial for improving the short-distance behavior, possibly leading to a UV

complete theory [5, 6]. In contrast, there seem to be no similar benefits from viewing the Standard Model (SM) as a low-energy effective description of an underlying fundamentally nonrelativistic theory: The SM is already renormalizable and nearly UV complete (assuming that one can remedy the growth of the hypercharge coupling at high energies). However, an embedding of the SM into a nonrelativistic theory may be of interest, if it provides a way out of the Higgs mass hierarchy problem without ruining the observed Lorentz symmetry at accessible energies.

The essence of the naturalness problem of a light scalar with nonderivative self-interactions (such as the Higgs) can be succinctly illustrated by considering a single relativistic scalar $\Phi(x^\mu)$ in $3 + 1$ dimensions with action

$$S = \frac{1}{2} \int d^4x \left(\partial_\mu \Phi \partial^\mu \Phi - m^2 \Phi^2 - \frac{\lambda}{12} \Phi^4 \right). \tag{7.1}$$

We have presented this example in §1.1: Both nonderivative terms in (1.1) break the same, constant shift symmetry $\Phi \to \Phi + \delta\Phi$ with $\delta\Phi = b$, and therefore must be of the same order of smallness (measured by $\varepsilon \ll 1$) relative to the naturalness scale M,

$$m^2 \sim \varepsilon M^2, \qquad \lambda \sim \varepsilon. \tag{7.2}$$

This gives the following simple but important relation,

$$M \sim \frac{m}{\sqrt{\lambda}}, \tag{7.3}$$

which then implies the naturalness problem: m cannot be made arbitrarily smaller than M without λ being made correspondingly small to assure that the naturalness condition (1.3) hold. At typical values of λ not much smaller than 1, m will be of the order of the naturalness scale M, ruining the hierarchy. Note that this naturalness problem is present already before gauging.

Finding new ways around relations (1.2) without putting technical naturalness in jeopardy is the main goal of this chapter.

7.1 A Toy Model

For simplicity, and to highlight the novelties associated with nonrelativistic naturalness, let us consider a simple toy model first: The theory of a real scalar field $\phi(t, \mathbf{y})$ in $3 + 1$ dimensions, $\mathbf{y} = (y^i, i = 1, \ldots, 3)$, with Aristotelian spacetime symmetry. Our model was introduced in Chapter 5 and studied further in Chapter 6, and we summarize the relevant key points in the following.

We start with the free theory controlled at short distances by the Gaussian fixed point with dynamical exponent $z = 3$. The action is

$$S_2 = \frac{1}{2} \int dt\, d^3\mathbf{y} \left\{ \dot\phi^2 - \zeta_3^2 \partial_i\partial_j\partial_k\phi\, \partial_i\partial_j\partial_k\phi - \zeta_2^2 \partial_i\partial_j\phi\, \partial_i\partial_j\phi - c^2 \partial_i\phi\, \partial_i\phi - m^2\phi^2 \right\}. \tag{7.4}$$

The first two terms define the Gaussian $z = 3$ fixed point, and the remaining three terms are its relevant Gaussian deformations. Classically, we can set $\zeta_3^2 = 1$ by a one-time rescaling of space-time coordinates. We measure the dimensions in the units of energy; with the scaling of the $z = 3$ fixed point, we have,

$$[t] = -1, \qquad [y^i] = -1/3, \qquad [\partial_i] = 1/3, \tag{7.5}$$

and the field ϕ is dimensionless (*i.e.*, at its *lower critical dimension*). The dimensions of the relevant Gaussian couplings are

$$[\zeta_2^2] = 2/3, \qquad [c^2] = 4/3, \qquad [m^2] = 2. \tag{7.6}$$

To this free action, we add interaction terms S_{int} whose choice depends on the desired symmetries; in the simplest model, we take

$$S_{\text{int}} = -\frac{\lambda_3}{2} \int dt \, d^3\mathbf{y} \, \mathcal{O} - \frac{\lambda_0}{4!} \int dt \, d^3\mathbf{y} \, \phi^4, \tag{7.7}$$

where

$$\mathcal{O} = \partial_i\phi \, \partial_i\partial_j\phi \, \partial_j\partial_k\phi \, \partial_k\phi + \frac{1}{3}\partial_i\phi \, \partial_j\phi \, \partial_k\phi \, \partial_i\partial_j\partial_k\phi. \tag{7.8}$$

The four-point six-derivative self-coupling constant λ_3 is marginal ($[\lambda_3] = 0$). With Higgs applications in mind, we also added the nonderivative ϕ^4 self-interaction. In our microscopic theory, its coupling is relevant, $[\lambda_0] = 2$. Our theory with the interaction term given by (7.8) is power-counting renormalizable, since at the $z = 3$ fixed point $\mathcal{O}$ is the only marginal or relevant interaction term invariant under the linear shift symmetry. (With the symmetry reduced to the constant shifts, there would also be one relevant and three additional marginal interaction terms.) Our theory with the interaction term given by (7.8) is power-counting renormalizable, since at the $z = 3$ fixed point $\mathcal{O}$ is the only marginal or relevant interaction term invariant under the linear shift symmetry. With the symmetry reduced to the constant shifts, there would also be one relevant and three additional marginal interaction terms.

The theory with the linear-shift invariant interaction given by the λ_3 term in (7.7) (and with $\lambda_0 = 0$) exhibits intriguing quantum properties. The quantum behavior has been studied in details in the last chapter, and we will only briefly summarize the relevant part here. There is no wave-function renormalization of ϕ, and both λ_3 and c^2 satisfy a non-renormalization theorem to all orders in λ_3. This does not mean that the theory can be weakly coupled at all scales: The coefficient ζ_3^2 in (7.4) – which we set equal to 1 in the classical limit – is logarithmically divergent starting at two loops, and therefore ζ_3 runs with the renormalization-group scale. The effective coupling in the two-on-two scattering amplitude is not λ_3 but $\overline{\lambda} \equiv \lambda_3/\zeta_3^3$, which runs due to the running of ζ_3. The two-loop β function reveals that $\overline{\lambda}$ increases with increasing energy.

The theory exhibits interesting instabilities. First, note that the contribution of the λ_3 term in (7.7) to the Hamiltonian is unbounded both below and above. Assuming that the couplings in (7.4) have been chosen such that the dispersion relation is positive definite,

the theory is perturbatively stable around $\langle\phi\rangle = 0$. However, at nonzero λ_3, this state is non-perturbatively unstable, with the decay probability controlled by a bounce instanton [72, 73]. The analytic form of the dominant instanton is not known, but its contribution to the decay rate of the vacuum will be $\Gamma_{\text{vac}} \propto \exp(-C/\overline{\lambda})$, with C positive and of order one (assuming at least one of the infrared-regulating couplings m^2, c^2 or ζ_2^2 is non-zero). If one so desires, this vacuum instability can be cured by embedding this model into a (more complex but stable) theory with the symmetries reduced to constant shifts [23].

The ϕ quanta also exhibit an intriguing perturbative instability in the Aristotelian space-time: A single particle with a large enough momentum $\mathbf{k}$ with respect to the rest frame acquires a non-zero decay width Γ. This is the usual phenomenon of quasiparticle damping known from condensed matter. The leading contribution to Γ arises at two loops, and at large $\mathbf{k}$ goes as $\Gamma \sim \zeta_3 \overline{\lambda}^2 |\mathbf{k}|^3$. The ϕ quantum is absolutely stable at $\mathbf{k} \approx 0$; at small $|\mathbf{k}|$ above the threshold, we find a very sharp long-lived resonance. With increasing $|\mathbf{k}|$, $\overline{\lambda}$ runs until it becomes ~ 1 and the ϕ resonance becomes very wide. The scattering of individual quanta with very high $|\mathbf{k}|$ makes no sense: They decay rapidly into multiple soft quanta beforehand. Thus, one cannot simply argue that the running of the $\overline{\lambda}$ coupling to large values makes the theory UV incomplete: These large values of $\overline{\lambda}$ cannot be measured by any two-on-two scattering; only softer quanta are available to scatter and the theory may self-complete in a mechanism reminiscent of classicalization [75, 76]. In this chapter, we do not need any such completion and will use this model only up to a very high naturalness scale where the coupling will still be small.

7.2 Nonrelativistic vs Relativistic Observers and Naturalness

While the theory is unambiguously defined by its microscopic behavior around the $z = 3$ fixed point, its physical properties will look somewhat different to different observers.

Unlike in relativistic theories, there are at least two natural classes of observers already at the microscopic level. The *Aristotelian observers* fix the coordinates $(t, \mathbf{y})$ once and for all, find the non-renormalization of λ_3 but also the running of ζ_3^2, which lead to the running of the effective coupling $\overline{\lambda}$. The *Wilsonian observers*, during the process of integrating out a shell of modes, rescale the system to restore the normalization condition $\zeta_3^2 = 1$. This involves a rescaling of the spatial coordinates which depends on the RG scale. Their effective coupling runs. When they compare their notes with the Aristotelian observers, both see the same physics but in a slightly rescaled coordinate system.

At low energies, the lowest-derivative terms dominate. The higher-derivative terms are suppressed, and the system develops an accidental approximate Lorentz symmetry, with small Lorentz-violating corrections. Observers at those energies will find it natural to interpret the system relativistically. We shall refer to such observers as "low-energy relativistic observers." While for the microscopic observers c^2 is a relevant coupling, for the low-energy relativistic observers c appears to be a constant of nature, insofar as they cannot detect deviations from the constancy of c due to the small Lorentz-violating terms. Given their

relativistic prejudice, their natural coordinate frame is

$$x^0 = t, \qquad x^i = y^i/c. \tag{7.9}$$

Note that this gives the correct dimensions of a relativistic coordinate system, $[x^0] = [x^i] = -1$. In these coordinates, the low-energy relativistic observer finds the action of our system to be

$$
\begin{aligned}
S \;=\; & \frac{1}{2} \int d^4x \left\{ \nabla_\mu \Phi \nabla^\mu \Phi - m^2 \Phi - \frac{1}{12} \lambda_h \Phi^4 \right. \\
& \left. - \widetilde{\zeta}_3^2 (\nabla_i \nabla_j \nabla_k \Phi)^2 - \widetilde{\zeta}_2^2 (\nabla_i \nabla_j \Phi)^2 - \widetilde{\lambda}_3 \widetilde{\mathcal{O}} \right\}
\end{aligned}
\tag{7.10}
$$

where $\nabla_\mu \equiv \partial/\partial x^\mu$, $\Phi = c^{3/2}\phi$ is the scalar field properly rescaled to match the perspective of the relativistic observer, and $\widetilde{\mathcal{O}}$ is given by (7.8) with ∂ replaced by ∇ and ϕ by Φ. The low-energy parameters are given in terms of the microscopic parameters as follows. For the relativistic observer, the mass m of Φ is equal to the gap parameter m of the microscopic theory, and its nonderivative self-coupling is given by

$$\lambda_h = \lambda_0/c^3. \tag{7.11}$$

The remaining couplings in (7.10) are given in terms of the microscopic parameters by

$$\widetilde{\zeta}_3^2 = \zeta_3^2/c^6, \quad \widetilde{\zeta}_2^2 = \zeta_2^2/c^4, \quad \widetilde{\lambda}_3 = \lambda_3/c^9; \tag{7.12}$$

from the low-energy perspective, they represent irrelevant terms which violate Lorentz invariance.

In accord with the principles of causality, we require that technical naturalness hold at the level of the microscopic, nonrelativistic theory. Technically natural hierarchies with varying degrees of complexity are possible [22]. In the simplest, one ε controls the breaking of the linear shift symmetry to no shift symmetry at all, and all couplings are of order ε in units of the naturalness momentum scale μ. However, this crude pattern may be naturally refined: λ_3 and ζ_2^2 preserve linear shifts and can be controlled by their own smallness parameter: $\lambda_3 \sim \varepsilon_2$ and $\zeta_2^2 \sim \varepsilon_2 \mu^2$. At this stage, quantum corrections to c^2 will not be generated (due to the nonrenormalization theorem), and can be kept of order $\varepsilon_1 \ll \varepsilon_2$. Finally, the nonderivative terms break constant shift symmetry, and can be of order $\varepsilon_0 \ll \varepsilon_1$. We thus obtain a technically natural cascading hierarchy of scales. This cascade is associated with a natural hierarchy of crossover scales: At very high scales (around μ), the system is dominated by the $z = 3$ scaling, then it crosses at lower scales to a $z = 2$ regime, followed by another crossover to the $z = 1$ regime, until it finally reaches the lowest scales set by the gap m. Next we need to examine how this cascading hierarchy appears from the viewpoint of the low-energy relativistic observer.

We begin at the microscopic level, with the following, technically natural hierarchy of couplings,

$$\zeta_3^2 \sim 1, \qquad \lambda_3 \sim \varepsilon_2, \qquad \zeta_2^2 \sim \varepsilon_2 \mu^2,$$

$$c^2 \sim \varepsilon_1 \mu^4, \qquad m^2 \sim \lambda_0 \sim \varepsilon_0 \mu^6, \tag{7.13}$$

and

$$\varepsilon_0 \ll \varepsilon_1 \ll \varepsilon_2 \ll 1. \tag{7.14}$$

What are the sizes of the couplings that the low-energy relativistic observer will see? Plugging (7.13) into (7.11) and (7.12), and introducing the naturalness energy scale $M \equiv \mu^3$, we obtain

$$m^2 \sim \varepsilon_0 M^2, \qquad \lambda_h \sim \varepsilon_0/\varepsilon_1^{3/2} \tag{7.15}$$

for the scalar mass and self-coupling, and

$$\widetilde{\zeta}_3^2 \sim \frac{\varepsilon_0^2}{\varepsilon_1^3} \frac{1}{m^4}, \quad \widetilde{\zeta}_2^2 \sim \frac{\varepsilon_0 \varepsilon_2}{\varepsilon_1^2} \frac{1}{m^2}, \quad \widetilde{\lambda}_3 \sim \frac{\varepsilon_0^3 \varepsilon_2}{\varepsilon_1^{9/2}} \frac{1}{m^6} \tag{7.16}$$

for the irrelevant nonrelativistic corrections.

This is the central result of this chapter: In contrast to the standard relativistic relations (1.2), we now have a new small parameter ε_1 which controls c^2, modifies the relations to (7.15), and makes a technically natural large hierarchy of scales with sizable values of the coupling $\lambda_h \sim 1$ possible.

Finally, we would like to address another question: How important is it to embed the Higgs into a $z = 3$ theory? Can we choose the simpler $z = 2$ short-distance behavior, perhaps improving the prospects of a realistic gauging? Interestingly, the answer is no, if we insist on λ_h in (7.15) to be ~ 1: In the absence of $z = 3$ terms, the leading nonrelativistic corrections originate from $\zeta_2^2 \sim 1$, and they become important at unacceptably low energies $\ll m$. The $z = 2$ observer would be almost as mystified about the naturalness of a light Higgs as the relativistic observer. Thus, $z = 3$ is the lowest value of z in the microscopic system for which our mechanism with relations (7.15) and $\lambda_h \sim 1$ can work, without generating large Lorentz violations at low energies.

7.3 Towards the Higgs and the Standard Model

Now we would like to couple this naturally light scalar to the rest of the SM. We will assume the Higgs-less part of SM to be exactly relativistic until the coupling to the Higgs; the coupling will induce violations of Lorentz invariance that we wish to keep naturally small in order to conform to the stringent experimental bounds on Lorentz violations [81], and without spoiling the mass hierarchy.

For simplicity, we will continue working within the logical structure of our toy model, but the results are more universal, robust and model-independent. First, as noted in Section 6.7, our toy model can be extended to a unique theory with global $SO(N)$ symmetry with ϕ in the N. The case of $N = 4$ will correspond to the candidate Higgs; with the flip of the m^2 sign, ϕ will develop a condensate $\langle \phi \rangle = m/\sqrt{\lambda_0} \sim 1$.

Phenomenologically, we would like $m \sim M_{EW}$ of the order of the electroweak scale, while $M \sim M_X$ of the order of some high scale M_X, such as the Planck scale or a GUT scale. To illustrate our mechanism, we will try to go the whole hog and realize a hierarchy across 15 orders of magnitude, between the electroweak scale and the Planck scale. For numerical simplicity, we take $m \sim 1$ TeV and $M \sim 10^{18}$ GeV. At the same time, we want the Higgs self-coupling λ_h not too much smaller than ~ 1.

As a very simple and concrete example, take the following "10-20-30" model:

$$\varepsilon_2 \sim 10^{-10}, \qquad \varepsilon_1 \sim 10^{-20}, \qquad \varepsilon_0 \sim 10^{-30}. \tag{7.17}$$

From (7.15), we obtain

$$m/M \sim 10^{-15}, \quad \lambda_h \sim 1, \tag{7.18}$$

precisely as desired! (Smaller λ_h, say ~ 0.1, are easily arranged by small changes of (7.17).) Moreover, the irrelevant Lorentz-violating couplings (7.16) are pushed above the TeV scale:

$$\widetilde{\zeta}_3^2 \sim \frac{1}{m^4}, \quad \widetilde{\zeta}_2^2 \sim \frac{1}{m^2}, \quad \widetilde{\lambda}_3 \sim 10^{-10} \frac{1}{m^6}. \tag{7.19}$$

The $\widetilde{\zeta}^2$ couplings yield small nonrelativistic modifications of the Higgs dispersion relation $\omega^2 = m^2 + \mathbf{k}^2$ by higher power terms $|\mathbf{k}|^4$ and $|\mathbf{k}|^6$, representing the first observable signatures of the "new physics" that cures the hierarchy problem: the Higgs sector exhibits a crossover towards $z > 1$ at scales of order $m \sim 1$ TeV. Pushing the nonrelativistic corrections to higher scales should be possible in slightly more sophisticated versions of our simplest 10-20-30 scenario; for example, making $\lambda_h < 1$ further suppresses the size of $\widetilde{\zeta}_3^2$, since $\widetilde{\zeta}_3^2 \sim \lambda_h^2/m^4$; and $\widetilde{\zeta}_2^2$ can be suppressed by simply choosing a smaller ε_2.

We can couple the scalar ϕ to several species of relativistic fermions $\Psi_f(t, \mathbf{y})$, whose two chiralities we assume to be in distinct representations to prevent bare masses (as in the SM). In the microscopic theory, their dimension is $[\Psi_f] = 1/2$. Their relativistic kinetic term written in nonrelativistic coordinates is

$$\sum_f \int dt \, d^3\mathbf{y} \, (\Psi_f^\dagger \dot{\Psi}_f + c_f \overline{\Psi}_f \gamma^i \partial_i \Psi_f). \tag{7.20}$$

Before coupling to ϕ, all fermions see the same limiting speed, which we set equal to $c_f = c$. When we couple the fermions to ϕ, their dispersion relation acquires nonrelativistic corrections from Higgs loops; we need these to be small, without spoiling the Higgs mass hierarchy. The most relevant coupling of Ψ_f to ϕ is the Yukawa term

$$\sum_f Y_f \int dt \, d^3\mathbf{y} \, \overline{\Psi}_f \phi \Psi_f. \tag{7.21}$$

When non-zero, the Yukawa couplings Y_f break the constant shift symmetry of ϕ, and one may expect them all to be bounded from above by the parameter ε_0 which controls all the

other terms breaking the constant shift symmetry in the Higgs sector. (This is in the units of μ^3, since $[Y_f] = 1$.) However, there is some wiggling room: Detailed estimates of the Higgs loop corrections show that we can increase the range of the Yukawas to include the window from ε_0 to $\sqrt{\varepsilon_0}$, without spoiling the smallness of m^2 and λ_0. This requires that we also include the nonrelativistic terms $\zeta_{3f}\overline{\Psi}\gamma^i\partial_i\partial^2\Psi$ with $\zeta_{3f} \lesssim 1$ to the action (which will be generated by the Higgs loops anyway). This increase in the range of the Yukawas works because the corrections to m^2 and λ_0 due to fermionic loops are at least quadratic in Y_f's. Thus, the window of naturalness for the non-zero Yukawas has been extended to include $\varepsilon_0\mu^3 \lesssim Y_f \lesssim \sqrt{\varepsilon_0}\mu^3$, self-consistently requiring that $\zeta_{3f} \sim Y_f^2/m^2$ for each fermion.

The low-energy relativistic observer rewrites the theory in terms of the naturally normalized fermions $\psi_f(x^\mu) = c^{3/2}\Psi_f(t, \mathbf{y})$, and sees the Yukawa terms as

$$\sum_f y_f \int d^4x \, \Phi \, \overline{\psi}_f \psi_f, \tag{7.22}$$

with $y_f = Y_f/c^{3/2}$. The naturalness window for the Yukawas as seen by the relativistic observer extends to

$$y_f \lesssim \varepsilon_0^{1/2}/\varepsilon_1^{3/4}. \tag{7.23}$$

This extension past the naive bound $y_f \lesssim \varepsilon_0/\varepsilon_1^{3/4}$ is crucial: In our 10-20-30 scenario, the naive bound would require $y_f \lesssim 10^{-15}$, excluding all fermions. The extended bound (7.23) requires $y_f \lesssim 1$, a range which naturally accommodates the masses of all the known fermions, from the top quark at the upper bound, down to the likely values of the neutrino masses not too far above the naive bound. Thus, in the 10-20-30 scenario, all the SM fermion masses can be Dirac masses, in a technically natural way.

Next we couple the system to relativistic Yang-Mills fields. In the microscopic theory, this is done by covariantizing the derivatives to

$$D_t\phi \equiv \dot{\phi} + iea_0\phi, \qquad D_i\phi = \partial_i\phi + iea_i\phi. \tag{7.24}$$

We normalize the gauge fields such that when rewritten in the nonrelativistic language, their standard relativistic action is

$$\int dt\, d^3\mathbf{y} \left[\frac{1}{2}(\partial_i a_0 - \dot{a}_i + \ldots)^2 - (c^2/4)(\partial_i a_j - \partial_j a_i + \ldots)^2\right]. \tag{7.25}$$

Thus, we have $[a_i] = 0$, $[a_0] = 2/3$, and the gauge coupling is relevant, $[e] = 1/3$. The low-energy relativistic fields A_μ and the Yang-Mills coupling are related to these microscopic variables by $A_i = c^{3/2}a_i$, $A_0 = c^{1/2}a_0$, and $g_{\mathrm{YM}}^2 = e^2/c$.

What is the size of the Yang-Mills coupling g_{YM} seen by the low-energy observer? The microscopic gauge coupling e breaks the constant shift symmetry of ϕ. Hence, the gauge loops can be expected to correct m^2 by $\sim e^2\mu^4$. To maintain naturalness, this would require $e^2 \sim \varepsilon_0\mu^2$; the low-energy observer would then find the Yang-Mills coupling

$$g_{\mathrm{YM}} = e/c^{1/2} \sim \varepsilon_0^{1/2}/\varepsilon_1^{1/4}. \tag{7.26}$$

Unfortunately, if these estimates are accurate (*i.e.*, in the absence of additional cancellations or hidden symmetries), it would be very difficult to make $g_{\text{YM}} \sim 1$ while keeping $\lambda_h \sim 1$. In particular, in our simple 10-20-30 model the natural values of the gauge couplings come out unrealistically small, $g_{\text{YM}} \sim 10^{-10}$, implying unrealistically light gauge bosons. It is at present unclear whether these estimates can be improved to achieve a scenario with more realistic values of g_{YM}; this question would require a more detailed analysis of the interplay between polynomial shift symmetries and gauge symmetries, which will appear in [82].

In this chapter, we have presented a new mechanism leading to naturally light scalars whose nonderivative self-couplings can be large. Our results have been based on rather conservative estimates of the quantum corrections, ensuring but not necessarily optimizing naturalness. These estimates can certainly be further tightened, refined by invoking more symmetries, or otherwise improved. In particular, it should be noted that we have not relied on (nor included) the omnipresent loop suppression factors involving powers of $\sim 1/(16\pi^2)$. A more detailed investigation is needed before we can conclude whether our mechanism is a useful ingredient for resolving the Higgs mass hierarchy puzzle in the SM. It is clear, however, that our results about naturalness are relevant to other scalar fields, with or without gauge invariance, including the inflaton.

Chapter 8

Aristotelian $O(N)$ Nonlinear Sigma Model

In this chapter, we apply the techniques and intuitions that we have established in the previous chapters about the Aristotelian QFTs to a more complicated system: Aristotelian nonlinear sigma model (NLSM) with a nonlinearly realized $O(N)$ symmetry. This type of models has been mentioned in Section 2.3 to illustrate the naturalness of NG modes with higher-order dispersion relations. However, the details of the RG structure of Aristotelian NLSM remains as a challenging task. In this chapter, we continue this study and map out the RG structure of the Aristotelian $O(N)$ NLSM in $2 + 1$ dimensions.

One motivation for studying Aristotelian NLSMs comes from gravity. One may view the NLSM as a simple proxy for a gravity theory, without the added details of gauge invariance. The relativistic NLSM is a widely used toy model in high energy physics. For example, the NLSM with an arbitrary worldsheet is crucial to the construction of string theories. Moreover, in analogy with string theory, the $2 + 1$ dimensional NLSM at a Lifshitz fixed point, with dynamical critical exponent $z = 2$, and with a dynamical worldvolume can be used as a building block for a membrane theory [5]. The ground state of such a bosonic membrane theory considered in [5] at quantum criticality produces the partition function of the bosonic string theory in one lower dimension. However, again, the details of the quantum behavior of this membrane theory have not been explored.

Interest in Aristotelian NLSMs also arises from condensed matter physics. Systems with dynamical critical exponent $z \neq 1$, which lack Lorentz invariance, have been commonly discussed in many contexts ranging from quantum ferromagnets [83] to systems which are closely related to topological order [84]. Some particularly interesting classes of models with $z = 2$ are (generalized) Rokhsar-Kivelson models or quantum Lifshitz models in 2+1 dimensions [85, 86, 87]. An interesting feature of these models is the existence of a quantum multicritical point from which one can access a rich variety of phases. At the so-called Rokhsar-Kivelson (RK) points, the ground state wave functions (wave functionals) are given in terms of the Boltzmann weight of two-dimensional classical statistical mechanics models. For example, the original RK model studies the quantum dimer, an effective model which describes quantum spin liquid ground states. The ground state of this model is given in terms of the equal superposition of all dimer configurations. In particular, the $O(N)$ NLSM has

been widely studied in the context of critical phenomena and in condensed matter physics [88, 83]. $O(N)$ NLSMs with anisotropic scaling between time and space appear in numerous condensed matter contexts, such as the study of phase transitions and critical phenomena. For example, the $O(N)$ NLSM around a $z = 2$ Lifshitz fixed point, which is of interest in this chapter, can arise as a low-energy effective field theory of the quantum spherical models with competing interactions, which is important for describing phase transitions in some condensed matter systems [89, 90, 91].

In spite of the recent effort, for example in [43, 92], the full renormalization group flow of the $O(N)$ NLSM at the $z = 2$ Lifshitz fixed point in $2+1$ dimensions remains unknown. This $z = 2$ fixed point is protected by the quadratic shift symmetry [18] in the weak coupling limit. In this work, we provide a complete analysis of the RG flow of this theory in the full space of marginal and relevant couplings. One may view the present work as the first step towards a more ambitious goal: to generalize to the Aristotelian case the landmark calculation by Friedan of the one-loop beta function for a $1 + 1$ dimensional relativistic sigma model with target space an arbitrary Riemannian manifold [93].

In Section 8.1 we construct the classical action for the NLSM around a $z = 2$ Lifshitz fixed point in $2 + 1$ dimensions and discuss the boundedness of energy. In Section 8.2 we calculate the one-loop beta functions and study the RG structure. Unlike the relativistic NLSM, the NLSM around a $z = 2$ fixed point is not generically asymptotically free in the UV, but instead exhibits a more intricate RG structure. In particular, there exists an RG trajectory characterized by the detailed balance condition. In Section 8.8 we extend our control of the NLSM to the nonperturbative region by taking the large N limit. In terms of the 't Hooft coupling, the exact beta functions (to all loops) can be computed by summing over all cactus diagrams recursively, and they coincide with the one-loop beta functions in the large N limit, as in the relativistic case.

8.1   The Classical Theory

The target space of our anisotropic nonlinear sigma model is S^{N-1} equipped with the maximally symmetric metric. The model will be invariant under two classes of symmetries: the target-space isometry group $O(N)$, and the "worldvolume"[1] spacetime Aristotelian symmetry group.
where λ is a positive real constant scaling factor and z is the dynamical critical exponent. In addition, we will require both time and space reversal invariance.

One way to parametrize S^{N-1} is by using the fields by $n \equiv (n^\alpha), \alpha = 1, ..., N$, and requiring them to satisfy the constraint

$$n \cdot n = 1. \tag{8.1}$$

This system of fields makes the symmetries more manifest, but it is redundant in view of (8.1). We will mostly switch to a suitable set of $N - 1$ independent fields, representing a

---

[1]In $1 + 1$ dimensions this "worldvolume" reduces to the conventional worldsheet.

local coordinate system on S^{N-1}, by writing

$$n = (\pi^1, \ldots, \pi^{N-1}, \sigma) \tag{8.2}$$

where

$$\sigma = \sqrt{1 - \pi \cdot \pi}. \tag{8.3}$$

In this representation, $\pi \equiv (\pi^I)$, $I = 1, \ldots, N-1$, is a local coordinate system on S^{N-1}, covering the target manifold everywhere except at one point. We will call π the "Goldstone fields".

To write down an explicit action, we assume a $z = 2$ scaling in the UV regime. We will therefore focus on terms in the Lagrangian that are classically marginal or relevant around the Gaussian $z = 2$ fixed point in $2 + 1$ dimensions.[2] We will measure dimensions in the units of spatial length L and time T,

$$[\partial_i] = L^{-1}, \quad [\partial_t] = T^{-1}. \tag{8.4}$$

Since the magnitude of n is constrained to equal 1, it is natural to assign to n the classical scaling dimension of zero. In this measure, $[n] = 1$. At the $z = 2$ Gaussian fixed point, the dimension of the time derivative is twice the dimension of the spatial derivative,

$$T = L^2. \tag{8.5}$$

At this $z = 2$ fixed point in $2 + 1$ dimensions, classically marginal Lagrangian terms have scaling dimension 4 in L^{-1}, relevant operators have lower scaling dimension, and irrelevant ones have higher scaling dimension. We classify all independent classically marginal and relevant operators, up to total derivatives. To accomplish this, it is useful to note a few consequences of the imposed symmetries.

First, our requirement of time reversal invariance implies that the number of time derivatives in each term is even. Together with the condition of marginality or relevance, this means that each term contains either two time derivatives (and therefore no spatial derivatives), or no time derivatives. The full action in terms in imaginary time t (*i.e.*, in Euclidean signature) is thus given by

$$S = \frac{1}{g^2} \int dt \, d^2x \, (\mathcal{K} + \mathcal{V}), \tag{8.6}$$

where g is a coupling constant, the kinetic term $\mathcal{K}$ contains the terms with two time derivatives, and the potential term $\mathcal{V}$ contains the terms with no time derivatives. Immediately, one concludes that $\mathcal{K}$ must be purely quadratic. In fact, there is one unique kinetic term,

$$\mathcal{K} = \frac{1}{2} \dot{n} \cdot \dot{n}. \tag{8.7}$$

---

[2]More generally, we could allow for separate scaling in time and space, and only lock the corresponding scales together at a later stage. This "double scaling" would require a revision of some of the fundamentals of QFT. For example one would have to generalize the renormalization group to a two-parameter family of flows. The $O(N)$ invariant sigma model may be used as a playground for testing the viability of such ideas in a simple and controlled setting.

Next, we classify all contributions to the potential $\mathcal{V}$. There is one unique marginal term quadratic in n,

$$\mathcal{O} = \frac{1}{2}\partial^2 n \cdot \partial^2 n, \tag{8.8}$$

and one unique relevant term quadratic in n,

$$\mathcal{W} = \frac{1}{2}\partial_i n \cdot \partial_i n. \tag{8.9}$$

All other possible quadratic terms are related to the ones above via integration by parts. Insofar as boundary terms or global topological issues can be ignored, this completes the classification of quadratic terms.

This leaves terms that contain four spatial derivatives but include more than one inner product in the internal $O(N)$ index. Two of these terms contain only first spatial derivatives,

$$\mathcal{U}_1 = \frac{1}{8}\left(\partial_i n \cdot \partial_i n\right)^2, \qquad\qquad \mathcal{U}_2 = \frac{1}{4}\left(\partial_i n \cdot \partial_j n\right)\left(\partial_i n \cdot \partial_j n\right). \tag{8.10}$$

These are independent of each other for $N > 2$, and independent of the quadratic terms classified above, and therefore represent new interaction terms that can appear in the action. In addition, there are terms with at least one second derivative:

$$\left(\partial_i n \cdot \partial_j n\right)\left(n \cdot \partial_i\partial_j n\right), \quad \left(n \cdot \partial_i\partial_j n\right)\left(n \cdot \partial_i\partial_j n\right), \quad \left(\partial_i n \cdot \partial_i n\right)\left(n \cdot \partial^2 n\right), \quad \left(n \cdot \partial^2 n\right)^2.$$

The constraint $n \cdot n = 1$ implies

$$n \cdot \partial_i\partial_j n = -\partial_i n \cdot \partial_j n, \tag{8.11}$$

which can be used to reduce the above four terms to (8.10).

Finally, all terms with a third derivative and two inner products vanish identically, given the fact that the inner product not containing the third derivative must have only one spatial derivative, and that

$$\partial_i n \cdot n = 0. \tag{8.12}$$

To summarize, the full action, including all the independent marginal and relevant terms, is given by

$$S = \frac{1}{g^2}\int dt\, d^2x \left\{\mathcal{K} + \zeta^2\left[\mathcal{O} + \eta_1\mathcal{U}_1 + \eta_2\mathcal{U}_2\right] + c^2\mathcal{W}\right\}$$

$$= \frac{1}{2g^2}\int dt\, d^2x \left\{\dot{n}\cdot\dot{n} + \zeta^2\left[\partial^2 n \cdot \partial^2 n + \frac{\eta_1}{4}\left(\partial_i n \cdot \partial_i n\right)^2 + \frac{\eta_2}{2}\left(\partial_i n \cdot \partial_j n\right)\left(\partial_i n \cdot \partial_j n\right)\right]\right.$$

$$\left. + c^2\partial_i n \cdot \partial_i n\right\}. \tag{8.13}$$

This action is the same as the model examined in [43]. From the low-energy point of view, when $c^2 > 0$, the relevant term $\mathcal{W}$ supplies the missing part of the relativistic Lagrangian

for the S^{N-1} nonlinear sigma model in $2+1$ dimensions, expected to induce a flow in the infrared to the Gaussian fixed point with $z = 1$. When $c^2 < 0$, we expect the ground state to take the form of a modulated phase, spontaneously breaking spatial translation and rotation symmetries [94, 95]. We will focus on the $c^2 \geq 0$ case throughout this chapter. The classical dimensions of the fields and couplings are

$$[n] = 1, \quad [g^2] = [\zeta] = \frac{L^2}{T}, \quad [\eta_1] = [\eta_2] = 1, \quad [c] = \frac{L}{T}. \tag{8.14}$$

Around the $z = 2$ fixed point, where $T = L^2$, it is more conventional to define the scaling dimension, which is the power of L^{-1} of the ordinary dimension. The scaling dimensions of g^2, ζ, η_1 and η_2 are all 0, and c has scaling dimension 1.

For stability, we require that the potential term $\mathcal{V}$ be bounded from below. In the following we identify the conditions on the couplings that ensure that $\mathcal{V}$ is a sum of complete squares, which is a sufficient condition for the positive definiteness of the potential.[3] We focus on the case $N > 2$ in this section. Let us write the most generic potential which is a sum of complete squares as

$$\mathcal{V} = \frac{1}{2} \sum_{s=1}^{I} \left[a_s \delta_{ij} \partial^2 n + b_s \partial_i \partial_j n + c_s \delta_{ij} \left(n \cdot \partial^2 n \right) n + d_s \left(n \cdot \partial_i \partial_j n \right) n \right]^2, \tag{8.15}$$

where a_s, b_s, c_s and d_s, $s = 1, \ldots, I$ are real numbers. In (8.15) we have dropped the relevant deformation $\mathcal{W}$, which is taken to be positive since we have assumed $c^2 > 0$. By applying the identity (8.11), we obtain

$$\int dt\, d^2x\, \mathcal{V} = \frac{1}{2} \int dt\, d^2x \sum_s \left\{ A_s \partial^2 n \cdot \partial^2 n + B_s \left(\partial_i n \cdot \partial_i n \right)^2 + C_s \left(\partial_i n \cdot \partial_j n \right) \left(\partial_i n \cdot \partial_j n \right) \right\},$$

where

$$A_s = (a_s + b_s)^2 + a_s^2, \quad B_s = 2 \left[c_s^2 + (b_s + d_s + 2) c_s + d_s \right], \quad C_s = (b_s + d_s)^2 - b_s^2. \tag{8.16}$$

We further require $\sum_s A_s > 0$, i.e., not all a_s and b_s are zero. This condition is necessary for maintaining a physical dispersion relation dominated by the quadratic scaling. Classically, we normalize ζ to 1 by rescaling space and time coordinates. Then, comparing with (8.13), we obtain

$$\eta_1 = \frac{4 \sum_s B_s}{\sum_s A_s}, \quad \eta_2 = \frac{2 \sum_s C_s}{\sum_s A_s}. \tag{8.17}$$

Analyzing this set of equations result in the following bounds on η_1 and η_2:

$$\eta_2 \geq -4, \qquad \eta_1 + \eta_2 \geq -4, \qquad \eta_1 + 2\eta_2 \geq -4. \tag{8.18}$$

---

[3]This condition may not be necessary. We leave the more general case for future work.
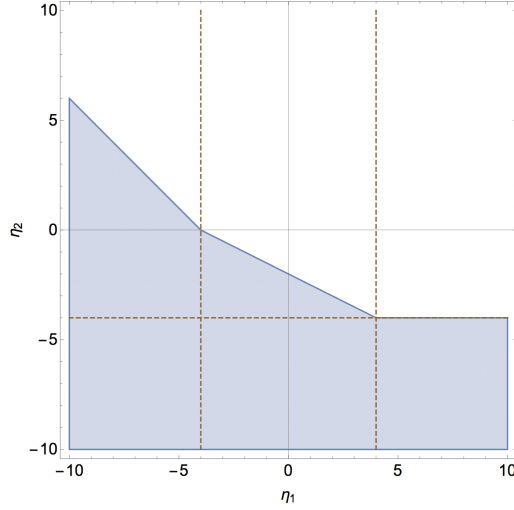
Figure 8.1: The potential is a sum of squares if (η_1, η_2) is in the white region. This ensures that the Hamiltonian is bounded from below in this region.

These are necessary conditions for the potential $\mathcal{V}$ to be expressed in terms of (8.15). The converse statement is also true: any η_1, η_2 satisfying these bounds can be written as a sum of squares.

Figure 8.1 shows the region in the η_1-η_2 plane where the energy is certainly bounded from below since the potential can be written as a sum of squares. At this point, we cannot exclude the possibility of a piece of the shaded region where the energy is bounded from below but the potential is not a sum of squares of the form (8.15). However, it is conceivable that in the shaded region the theory may exhibit interesting nonperturbative instabilities and consist instead of bounce instanton solutions [72, 73].

Finally, when expressed in terms of the non-redundant field π, the terms in the action take the following form. First, we have the terms which will contribute to the propagator – the two marginal terms that define the Gaussian fixed point,

$$\dot{n} \cdot \dot{n} = \dot{\pi} \cdot \dot{\pi} + \frac{1}{4} \frac{\left[\partial_t(\pi \cdot \pi)\right]^2}{1 - \pi \cdot \pi}, \tag{8.19}$$

and

$$\partial^2 n \cdot \partial^2 n = \partial^2 \pi \cdot \partial^2 \pi + \frac{1}{1 - \pi \cdot \pi} \left[\frac{1}{2}\partial^2(\pi \cdot \pi) + \frac{1}{4} \frac{\partial_i(\pi \cdot \pi)\partial_i(\pi \cdot \pi)}{1 - \pi \cdot \pi}\right]^2, \tag{8.20}$$

and the relevant deformation

$$\partial_i n \cdot \partial_i n = \partial_i \pi \cdot \partial_i \pi + \frac{1}{4} \frac{\partial_i(\pi \cdot \pi)\partial_i(\pi \cdot \pi)}{1 - \pi \cdot \pi}. \tag{8.21}$$

In addition, we have the two independent marginal terms that will only generate interactions,

$$(\partial_i n \cdot \partial_i n)^2 = \left\{\partial_i \pi \cdot \partial_i \pi + \frac{1}{4} \frac{\left[\partial_i(\pi \cdot \pi)\right]^2}{1 - \pi \cdot \pi}\right\}^2, \tag{8.22}$$

and

$$(\partial_i n \cdot \partial_j n)^2 = \left[\partial_i \pi \cdot \partial_j \pi + \frac{1}{4}\frac{\partial_i(\pi \cdot \pi)\partial_j(\pi \cdot \pi)}{1 - \pi \cdot \pi}\right]\left[\partial_i \pi \cdot \partial_j \pi + \frac{1}{4}\frac{\partial_i(\pi \cdot \pi)\partial_j(\pi \cdot \pi)}{1 - \pi \cdot \pi}\right]. \quad (8.23)$$

This form of the action in terms of the non-redundant components of the Goldstone field π makes the $O(N)$ symmetry less manifest, but it will be more practical for deriving Feynman rules and dealing with explicit loop calculations.

8.2   The Quantum Theory

We first focus on the quantum corrections near the Gaussian UV fixed point. In this regime, the theory is weakly coupled, and the standard techniques of perturbation theory and Feynman diagrams are applicable.

Before any serious loop calculation, we discus some formal aspects of the perturbative theory. We seek a regularization scheme that preserves the $O(N)$ symmetry. We will use dimensional regularization with minimal subtraction. One additional benefit of this scheme is that it automatically removes power law divergences. Nevertheless, dimensional regularization captures all logarithmic divergences, including those which arise as subleading divergences to power law divergences. Thus, we will be able to systematically focus only on the logarithmic divergences, which will simplify the loop calculation. Power law divergences, which are important for examining issues of naturalness, will be treated separately in Section 8.7.

Around the $z = 2$ fixed point, the propagator is

$$\mathcal{D}^{I_1 I_2}(\omega, \mathbf{k}) = \frac{g^2}{\omega^2 + \zeta^2 k^4 + c^2 k^2}\delta^{I_1 I_2}, \quad (8.24)$$

where $k = |\mathbf{k}|$. The relevant deformation $c^2 k^2$ acts as a natural $O(N)$-invariant IR regulator. The theory is free of IR divergences and is thus well-defined in perturbation theory. This is in contrast to the relativistic NLSM in two dimensions, where a lattice regularization is required for the IR divergence in order to preserve the $O(N)$ symmetry.[4]

The renormalizability of the $z = 2$ anisotropic NLSM follows in close analogy with the relativistic case. The action can be Taylor expanded with respect to the Goldstone fields π parametrizing the coset space $O(N)/O(N-1)$ which has the topology of a $(N-1)$-sphere S^{N-1} of unit radius. Since the scaling dimension of n is zero, the classical scaling dimension of π should also be zero, and the theory is borderline renormalizable by power counting. In terms of the Goldstone fields π^I, the $O(N-1)$ symmetry is linearly realized, which restricts the counterterms to be $O(N-1)$ invariant. However such counterterms can in general violate the nonlinearly realized $O(N)/O(N-1)$ symmetry. Regularizing the theory in a way that preserves the $O(N)$ symmetry of the action, a set of Ward-Takahashi (WT) identities

---

[4]Alternatively, one introduces a Zeeman term sourcing σ, which explicitly breaks the $O(N)$ invariance.

can be derived, as a consequence of the $O(N)$ symmetry of the correlation functions. This calculation is in complete analogy with the relativistic NLSM (see [88] for details). By solving the WT identities, it can be shown that the renormalized action is $O(N)$-invariant, but that the radius of S^{N-1} is also renormalized, which corresponds to a field rescaling. This demonstrates the renormalizability of the $z = 2$ anisotropic NLSM.[5]

In the following, we will apply dimensional regularization to calculate the RG equations by analytic continuation to $D + 1$ dimensions, where $D = 2 - \epsilon$. When we move away from $2 + 1$ to $(2 - \epsilon) + 1$ spacetime dimensions, the classical dimension of g^2 shifts:

$$[g^2] = \frac{L^{2-\epsilon}}{T}, \tag{8.25}$$

and the dimensions of all other parameters remain the same.

Recall the action derived in (8.13), which we write in terms of bare parameters:

$$S = \frac{1}{g_0^2} \int dt\, d^D x \left\{ \mathcal{K}_0 + \zeta_0^2 \left[\mathcal{O}_0 + (\eta_1)_0 \, (\mathcal{U}_1)_0 + (\eta_2)_0 \, (\mathcal{U}_2)_0 \right] + c_0^2 \mathcal{W}_0 \right\}. \tag{8.26}$$

Here, we have introduced the subscript 0 to emphasize that all couplings and fields are bare. The subscript 0 on the operators is short-hand notation for the same subscript on the π's contained in those operators. Note that we will work in Euclidean signature henceforth. The renormalized action in $D + 1$ dimensions can be written as

$$S = \frac{1}{\mu^\epsilon g^2 Z_g} \int dt\, d^D x \left\{ \mathcal{K} + \zeta^2 Z_\zeta \left(\mathcal{O} + \eta_1 Z_1 Z \mathcal{U}_1 + \eta_2 Z_2 Z \mathcal{U}_2 \right) + c^2 Z_c \mathcal{W} \right\}, \tag{8.27}$$

where μ is a momentum scale used to absorb the change in the dimension of g^2,

$$n = \left(\pi^I, \sigma \right) \tag{8.28}$$

and $\sigma = \sqrt{Z^{-1} - \pi \cdot \pi}$.

There are in total 6 counterterms, Z_g, Z_ζ, Z_1, Z_2, Z_c and Z, corresponding to g, ζ, η_1, η_2, c and the radius of S^{N-1}, respectively. Explicitly breaking the $O(N)$ symmetry by giving a mass to π^I or adding the Zeeman term $\int dt\, d^2 x\, h\, \sigma$, with h sourcing σ, results in no new renormalization constant. The bare fields and parameters are related to the renormalized ones via

$$\begin{aligned} &\pi_0 = Z^{1/2} \pi, & &\zeta_0^2 = Z_\zeta \zeta^2, & &c_0^2 = Z_c c^2; \\ &g_0^2 = \mu^\epsilon Z_g Z g^2, & &(\eta_1)_0 = Z_1 \eta_1, & &(\eta_2)_0 = Z_2 \eta_2. \end{aligned} \tag{8.29}$$

8.3 Feynman Rules

For developing the Feynman rules, it is useful to work directly in the broken phase with the π representation, which is intrinsic to the target manifold and does not invoke its embedding

---

[5]The proof of the renormalizability of the $z = 2$ NLSM is discussed in detail in [92].

into a higher dimensional space. In order to determine the propagator and the infinite series of $2j$-point vertices, we expand all terms in the Lagrangian in powers of π and its derivatives. We will be able to read off all of the one-loop renormalization properties of the theory by focusing on the two-point and four-point Green's functions only. Higher order correlation functions will just yield identical renormalization equations. The highest order in π that we would have to keep in this case is sixth-order, since this contributes to the one-loop renormalization of the four-point Green's function.

Keeping terms up to the sixth order in π, we obtain

$$\mathcal{K} = \mathcal{K}^{(2)} + Z\mathcal{K}^{(4)} + Z^2\mathcal{K}^{(6)} + \cdots , \tag{8.30a}$$

$$\mathcal{O} = \mathcal{O}^{(2)} + Z\mathcal{O}^{(4)} + Z^2\mathcal{O}^{(6)} + \cdots , \tag{8.30b}$$

for the two terms that contribute to the $z = 2$ Gaussian fixed point. Here,

$$\mathcal{K}^{(2)} = \frac{1}{2}\dot{\pi}\cdot\dot{\pi}, \qquad \mathcal{K}^{(4)} = \frac{1}{8}\left[\partial_t\left(\pi\cdot\pi\right)\right]^2, \qquad \mathcal{K}^{(6)} = \frac{1}{16}\partial_t(\pi\cdot\pi)\,\partial_t\left[(\pi\cdot\pi)^2\right], \tag{8.31a}$$

$$\mathcal{O}^{(2)} = \frac{1}{2}\partial^2\pi\cdot\partial^2\pi, \qquad \mathcal{O}^{(4)} = \frac{1}{8}\left[\partial^2(\pi\cdot\pi)\right]^2, \qquad \mathcal{O}^{(6)} = \frac{1}{16}\partial^2(\pi\cdot\pi)\,\partial^2\left[(\pi\cdot\pi)^2\right]. \tag{8.31b}$$

For the relevant deformation that induces the flow towards $z = 1$ in the Gaussian limit,

$$\mathcal{W} = \mathcal{W}^{(2)} + Z\mathcal{W}^{(4)} + Z^2\mathcal{W}^{(6)} + \cdots , \tag{8.32}$$

where

$$\mathcal{W}^{(2)} = \frac{1}{2}\partial_i\pi\cdot\partial_i\pi, \quad \mathcal{W}^{(4)} = \frac{1}{8}\partial_i(\pi\cdot\pi)\,\partial_i(\pi\cdot\pi), \quad \mathcal{W}^{(6)} = \frac{1}{16}\partial_i(\pi\cdot\pi)\,\partial_i\left[(\pi\cdot\pi)^2\right]. \tag{8.33}$$

The two remaining marginal terms are

$$\mathcal{U}_1 = \mathcal{U}_1^{(4)} + Z\mathcal{U}_1^{(6)} + \cdots , \qquad \mathcal{U}_2 = \mathcal{U}_2^{(4)} + Z\mathcal{U}_2^{(6)} + \cdots , \tag{8.34}$$

where

$$\mathcal{U}_1^{(4)} = \frac{1}{8}(\partial_i\pi\cdot\partial_i\pi)^2, \qquad\qquad \mathcal{U}_1^{(6)} = \frac{1}{16}(\partial_i\pi\cdot\partial_i\pi)\partial_j(\pi\cdot\pi)\,\partial_j(\pi\cdot\pi), \tag{8.35a}$$

$$\mathcal{U}_2^{(4)} = \frac{1}{4}(\partial_i\pi\cdot\partial_j\pi)(\partial_i\pi\cdot\partial_j\pi), \qquad \mathcal{U}_2^{(6)} = \frac{1}{8}(\partial_i\pi\cdot\partial_j\pi)\partial_i(\pi\cdot\pi)\,\partial_j(\pi\cdot\pi). \tag{8.35b}$$

Write $Z = 1 + \delta$, $Z_g = 1 + \delta_g$ and so on. We split up the action into the bare action, in which all of the Z factors are set to 1,

$$S_{\text{bare}}^{(2)} = \frac{1}{\mu^\epsilon g^2}\int dt\,d^D x\left\{\mathcal{K}^{(2)} + \zeta^2\mathcal{O}^{(2)} + c^2\mathcal{W}^{(2)}\right\}, \tag{8.36a}$$

$$S_{\text{bare}}^{(4)} = \frac{1}{\mu^\epsilon g^2}\int dt\,d^D x\left\{\mathcal{K}^{(4)} + \zeta^2\left[\mathcal{O}^{(4)} + \eta_1\mathcal{U}_1^{(4)} + \eta_2\mathcal{U}_2^{(4)}\right] + c^2\mathcal{W}^{(4)}\right\}, \tag{8.36b}$$

$$S_{\text{bare}}^{(6)} = \frac{1}{\mu^\epsilon g^2} \int dt\, d^D x \left\{ \mathcal{K}^{(6)} + \zeta^2 \left[\mathcal{O}^{(6)} + \eta_1 \mathcal{U}_1^{(6)} + \eta_2 \mathcal{U}_2^{(6)} \right] + c^2 \mathcal{W}^{(6)} \right\}, \qquad (8.36c)$$

and the remainder, collectively called the counterterm action,

$$S_{\text{ct}}^{(2)} = \frac{1}{\mu^\epsilon g^2} \int dt\, d^D x \left\{ -\delta_g \mathcal{K}^{(2)} + (\delta_\zeta - \delta_g) \zeta^2 \mathcal{O}^{(2)} + (\delta_c - \delta_g) c^2 \mathcal{W}^{(2)} \right\}, \qquad (8.37a)$$

$$S_{\text{ct}}^{(4)} = \frac{1}{\mu^\epsilon g^2} \int dt\, d^D x \left\{ (\delta - \delta_g) \mathcal{K}^{(4)} + (\delta + \delta_c - \delta_g) c^2 \mathcal{W}^{(4)} \right.$$
$$\left. + \zeta^2 \left[(\delta + \delta_\zeta - \delta_g) \mathcal{O}^{(4)} + (\delta + \delta_1 + \delta_\zeta - \delta_g) \eta_1 \mathcal{U}_1^{(4)} + (\delta + \delta_2 + \delta_\zeta - \delta_g) \eta_2 \mathcal{U}_2^{(4)} \right] \right\}. \qquad (8.37b)$$

There is no need to write down the sixth-order counterterm action because we will only calculate the one-loop renormalization of the propagator and the four-point vertices, not the six- or higher-point ones.

Next, we present the Feynman rules for the propagator, the four-point vertices and the six-point vertices. The propagator is

$$\mathcal{D}^{IJ} = \quad I \xrightarrow{\;\omega, \mathbf{k}\;} J \quad = \frac{\mu^\epsilon g^2 \delta^{IJ}}{\omega^2 + \zeta^2 k^4 + c^2 k^2}. \qquad (8.38)$$

Denote the Feynman rule for the 4-point vertex as

$$V_{I_1 I_2 I_3 I_4}^{(4)}(\omega_i, \mathbf{k}_i) = \quad \begin{array}{c} I_1 \quad\quad\quad I_2 \\ \omega_1, \mathbf{k}_1 \quad \quad \omega_2, \mathbf{k}_2 \\ \diagdown\!\!\!\!\diagup \\ \omega_3, \mathbf{k}_3 \quad \quad \omega_4, \mathbf{k}_4 \\ I_3 \quad\quad\quad I_4 \end{array} \quad , \qquad (8.39)$$

where the symbol $(\omega_i, \mathbf{k}_i)$ is short for $(\omega_1, \mathbf{k}_1; \omega_2, \mathbf{k}_2; \omega_3, \mathbf{k}_3; \omega_4, \mathbf{k}_4)$. We will suppress the I indices in $V^{(4)}$ in general. Then,

$$V^{(4)}(\omega_i, \mathbf{k}_i) = -\frac{1}{\mu^\epsilon g^2} \left[V_{\mathcal{K}}^{(4)} + \zeta^2 \left(V_{\mathcal{O}}^{(4)} + \eta_1 V_1^{(4)} + \eta_2 V_2^{(4)} \right) + c^2 V_{\mathcal{W}}^{(4)} \right], \qquad (8.40)$$

where

$$\mathcal{K}^{(4)}: \; V_{\mathcal{K}}^{(4)} = (\omega_1 + \omega_2)^2 \, \delta^{I_1 I_2} \delta^{I_3 I_4} + (2 \leftrightarrow 3) + (2 \leftrightarrow 4), \qquad (8.41a)$$

$$\mathcal{O}^{(4)}: \; V_{\mathcal{O}}^{(4)} = |\mathbf{v}k_1 + \mathbf{v}k_2|^4 \, \delta^{I_1 I_2} \delta^{I_3 I_4} + (2 \leftrightarrow 3) + (2 \leftrightarrow 4), \qquad (8.41b)$$

$$\mathcal{U}_1^{(4)}: \; V_1^{(4)} = (\mathbf{v}k_1 \cdot \mathbf{v}k_2)(\mathbf{v}k_3 \cdot \mathbf{v}k_4) \, \delta^{I_1 I_2} \delta^{I_3 I_4} + (2 \leftrightarrow 3) + (2 \leftrightarrow 4), \qquad (8.41c)$$

$$\mathcal{U}_2^{(4)}: \; V_2^{(4)} = \left[(\mathbf{v}k_1 \cdot \mathbf{v}k_3)(\mathbf{v}k_2 \cdot \mathbf{v}k_4) + (\mathbf{v}k_1 \cdot \mathbf{v}k_4)(\mathbf{v}k_2 \cdot \mathbf{v}k_3) \right] \delta^{I_1 I_2} \delta^{I_3 I_4}$$
$$+ (2 \leftrightarrow 3) + (2 \leftrightarrow 4), \qquad (8.41d)$$

$$\mathcal{W}^{(4)}\colon V_{\mathcal{W}}^{(4)} = |\mathbf{v}k_1 + \mathbf{v}k_2|^2 \, \delta^{I_1 I_2} \delta^{I_3 I_4} + (2 \leftrightarrow 3) + (2 \leftrightarrow 4). \tag{8.41e}$$

Similarly, denote the Feynman rule for the 6-point vertex as

$$V^{(6)}(\omega_i, \mathbf{k}_i) = \quad$$

$$= -\frac{1}{\mu^\epsilon g^2}\left[V_{\mathcal{K}}^{(6)} + \zeta^2 \left(V_{\mathcal{O}}^{(6)} + \eta_1 V_1^{(6)} + \eta_2 V_2^{(6)} \right) + c^2 V_{\mathcal{W}}^{(6)} \right], \tag{8.42}$$

where

$$\mathcal{K}^{(6)}\colon V_{\mathcal{K}}^{(6)} = (\omega_1 + \omega_2)^2 \, \delta^{I_1 I_2} \delta^{I_3 I_4} \delta^{I_5 I_6} + \cdots, \tag{8.43a}$$

$$\mathcal{O}^{(6)}\colon V_{\mathcal{O}}^{(6)} = |\mathbf{v}k_1 + \mathbf{v}k_2|^4 \, \delta^{I_1 I_2} \delta^{I_3 I_4} \delta^{I_5 I_6} + \cdots, \tag{8.43b}$$

$$\mathcal{U}_1^{(6)}\colon V_1^{(6)} = (\mathbf{v}k_1 \cdot \mathbf{v}k_2)(\mathbf{v}k_3 + \mathbf{v}k_4) \cdot (\mathbf{v}k_5 + \mathbf{v}k_6) \, \delta^{I_1 I_2} \delta^{I_3 I_4} \delta^{I_5 I_6} + \cdots, \tag{8.43c}$$

$$\mathcal{U}_2^{(6)}\colon V_2^{(6)} = \left[\mathbf{v}k_1 \cdot (\mathbf{v}k_3 + \mathbf{v}k_4)\right]\left[\mathbf{v}k_2 \cdot (\mathbf{v}k_5 + \mathbf{v}k_6)\right] \delta^{I_1 I_2} \delta^{I_3 I_4} \delta^{I_5 I_6} + \cdots, \tag{8.43d}$$

$$\mathcal{W}^{(6)}\colon V_{\mathcal{W}}^{(6)} = -|\mathbf{v}k_1 + \mathbf{v}k_2|^2 \, \delta^{I_1 I_2} \delta^{I_3 I_4} \delta^{I_5 I_6} + \cdots. \tag{8.43e}$$

Here, "$\cdots$" denotes the sum of fourteen terms obtained by permuting the numerical subscripts of the first term,

$$(4 \leftrightarrow 5) + (4 \leftrightarrow 6) + (2 \leftrightarrow 3) + (2 \leftrightarrow 3, 4 \leftrightarrow 5) + (2 \leftrightarrow 3, 4 \leftrightarrow 6)$$
$$+ (2 \leftrightarrow 4) + (2 \leftrightarrow 4, 3 \leftrightarrow 5) + (2 \leftrightarrow 4, 3 \leftrightarrow 6)$$
$$+ (2 \leftrightarrow 5) + (2 \leftrightarrow 5, 3 \leftrightarrow 6) + (2 \leftrightarrow 5, 4 \leftrightarrow 6)$$
$$+ (2 \leftrightarrow 6) + (2 \leftrightarrow 6, 3 \leftrightarrow 5) + (2 \leftrightarrow 6, 4 \leftrightarrow 5). \tag{8.44}$$

We will also need the Feynman rules for the counterterms. The counterterm contribution to two-point vertex is

$$V_{\text{c.t.}}^{(2)} = \quad I \xrightarrow{\omega, \mathbf{k}} \otimes \longrightarrow J \quad = -\frac{1}{\mu^\epsilon g^2} \delta^{IJ}\left[-\delta_g \omega^2 + (\delta_\zeta - \delta_g)\zeta^2 k^4 + (\delta_c - \delta_g)c^2 k^2 \right], \tag{8.45}$$

The counterterm contribution to the four-point vertex is

$$V_{\text{c.t.}}^{(4)} = \quad$$

$$= -\frac{1}{\mu^\epsilon g^2}\Big[(\delta - \delta_g)V_{\mathcal{K}}^{(4)} + (\delta + \delta_c - \delta_g)c^2 V_{\mathcal{W}}^{(4)}$$
$$+ \zeta^2(\delta + \delta_\zeta - \delta_g)V_{\mathcal{O}}^{(4)} + (\delta + \delta_1 + \delta_\zeta - \delta_g)\eta_1 V_1^{(4)} + (\delta + \delta_2 + \delta_\zeta - \delta_g)\eta_2 V_2^{(4)}\Big]. \tag{8.46}$$

8.4 Renormalization Conditions

We define the physical couplings ζ_*, c_*, g_*, η_1^* and η_2^* at the fiducial point where the external frequencies and momenta are zero. Since the field will be renormalized, the n-point Green's functions at the chosen fiducial point should be defined with respect to a new field π_*^I instead of the original field π, where

$$\pi_*^I = r\pi^I, \tag{8.47}$$

with r a coefficient determined by the renormalization conditions.

First, we define the inverse propagator to be $\Gamma^{I_1 I_2}(\omega, k^2)$. We impose the following three renormalization conditions,

$$\left.\frac{\partial \Gamma^{I_1 I_2}(\omega, k^2)}{\partial \omega^2}\right|_{\omega=0,\,k^2=0} = \frac{1}{\mu^\epsilon g_*^2}\delta^{I_1 I_2}, \tag{8.48a}$$

$$\left.\frac{1}{2}\frac{\partial^2 \Gamma^{I_1 I_2}(\omega, k^2)}{(\partial k^2)^2}\right|_{\omega=0,\,k^2=0} = \frac{\zeta_*^2}{\mu^\epsilon g_*^2}\delta^{I_1 I_2}, \tag{8.48b}$$

$$\left.\frac{\partial \Gamma^{I_1 I_2}(\omega, k^2)}{\partial k^2}\right|_{\omega=0,\,k^2=0} = \frac{c_*^2}{\mu^\epsilon g_*^2}\delta^{I_1 I_2}. \tag{8.48c}$$

Next, we would like to define the renormalization conditions for the amputated four-point 1PI vertex

$$\Gamma^{I_1 I_2 I_3 I_4}(\omega_i, \mathbf{k}_i) = \Gamma_s(\omega_i, \mathbf{k}_i)\delta^{I_1 I_2}\delta^{I_3 I_4} + \Gamma_t(\omega_i, \mathbf{k}_i)\delta^{I_1 I_3}\delta^{I_2 I_4} + \Gamma_u(\omega_i, \mathbf{k}_i)\delta^{I_1 I_4}\delta^{I_2 I_3}. \tag{8.49}$$

Denote the following four-point configuration by $\star$:

$$\star: \quad \omega_1 = \omega_2 = -\omega_3 = -\omega_4 = \frac{1}{2}\omega;$$
$$\mathbf{k}_1 = -\mathbf{k_2} = \mathbf{p}, \quad \mathbf{k}_3 = -\mathbf{k}_4 = \mathbf{q}, \quad \mathbf{p}\cdot\mathbf{q} = 0. \tag{8.50}$$

Note that

$$V_{\mathcal{K}}^{(4)}(\star) = \omega^2 \delta^{I_1 I_2}\delta^{I_3 I_4}, \tag{8.51a}$$

$$V_{\mathcal{O}}^{(4)}(\star) = \left(p^2 + q^2\right)^2 \left(\delta^{I_1 I_3}\delta^{I_2 I_4} + \delta^{I_1 I_4}\delta^{I_2 I_3}\right), \tag{8.51b}$$

$$V_1^{(4)}(\star) = p^2 q^2 \delta^{I_1 I_2}\delta^{I_3 I_4}, \tag{8.51c}$$

$$V_2^{(4)}(\star) = p^2 q^2 \left(\delta^{I_1 I_3}\delta^{I_2 I_4} + \delta^{I_1 I_4}\delta^{I_2 I_3}\right), \tag{8.51d}$$

$$V_{\mathcal{W}}^{(4)}(\star) = \left(p^2 + q^2\right)\left(\delta^{I_1 I_3}\delta^{I_2 I_4} + \delta^{I_1 I_4}\delta^{I_2 I_3}\right). \tag{8.51e}$$

The following renormalization condition will fix the field renormalization:

$$\frac{\partial \Gamma_s(\star)}{\partial \omega^2}\bigg|_{\omega=p^2=q^2=0} = \frac{1}{\mu^\epsilon g_*^2}, \tag{8.52}$$

We need two additional conditions to define η_1^* and η_2^*,

$$\frac{\partial^2 \Gamma_s(\star)}{\partial p^2 \partial q^2}\bigg|_{\omega=p^2=q^2=0} = \frac{\zeta_*^2}{\mu^\epsilon g_*^2} \eta_1^*, \tag{8.53}$$

$$\frac{\partial^2 \Gamma_t(\star)}{\partial p^2 \partial q^2}\bigg|_{\omega=p^2=q^2=0} = \frac{\zeta_*^2}{\mu^\epsilon g_*^2} (\eta_2^* + 2). \tag{8.54}$$

For convenience, we henceforth choose to set $\zeta_\star = 1$ by rescaling space and time coordinates.

8.5   One-Loop Beta Functions

The one-loop correction to the inverse propagator is

$$= -\frac{\delta^{I_1 I_2}}{4\pi\zeta\mu^\epsilon}\left\{\left[\omega^2 + \zeta^2 k^4 + (1-\eta)\, c^2 k^2\right]\left(\frac{1}{\epsilon} + \ell\right)\right\} + \mathfrak{f}, \tag{8.55}$$

where

$$\ell \equiv \log\left(\frac{\zeta\mu}{c}\right), \tag{8.56}$$

and

$$\eta \equiv \frac{N\eta_1 + (N+2)\eta_2 + 8}{4}. \tag{8.57}$$

Here, $\mathfrak{f}$ denotes finite pieces to be absorbed by counterterms.

The one-loop correction to the four-point vertex comes from the "candy diagram" and the "quadrupus diagram" (here, the candy diagram stands for the sum of the s-, t- and u-channels),
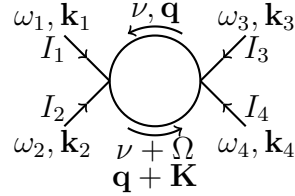
$$\tag{8.58}$$

Let $\Omega \equiv \omega_1 + \omega_2$ and $\mathbf{K} \equiv \mathbf{k}_1 + \mathbf{k}_2$. The quadrupus diagram is

$$= \frac{1}{2} \int \frac{d\nu}{2\pi} \frac{d^D q}{(2\pi)^D} \, V^{(6)}_{I_1 I_2 I_3 I_4 I_5 I_6}(\omega_1, \mathbf{k}_1; \omega_2, \mathbf{k}_2; \omega_3, \mathbf{k}_3; \omega_4, \mathbf{k}_4; \nu, \mathbf{q}; -\nu, -\mathbf{q}) \, \mathcal{D}^{I_5 I_6}(\nu, \mathbf{q}). \quad (8.59)$$

The *s*-channel candy diagram is
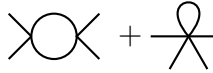
$$= \frac{1}{2} \int \frac{d\nu}{2\pi} \frac{d^D q}{(2\pi)^D} \, V^{(4)}_{I_1 I_2 I_5 I_6}(\omega_1, \mathbf{k}_1; \omega_2, \mathbf{k}_2; \nu, \mathbf{q}; -\nu - \Omega, -\mathbf{q} - \mathbf{K})$$

$$\times \mathcal{D}^{I_5 I_7}(\nu, \mathbf{q}) \, \mathcal{D}^{I_6 I_8}(\nu + \Omega, \mathbf{q} + \mathbf{K})$$

$$\times V^{(4)}_{I_3 I_4 I_7 I_8}(\omega_3, \mathbf{k}_3; \omega_4, \mathbf{k}_4; -\nu, -\mathbf{q}; \nu + \Omega, \mathbf{q} + \mathbf{K}). \quad (8.60)$$

Here $\Omega = \omega_1 + \omega_2$ and $\mathbf{K} = \mathbf{k}_1 + \mathbf{k}_2$. The *t*- and *u*-channel results can be obtained by cycling the indices. Summing over the three candy diagrams and one quadrupus diagram and keeping track of the $1/\epsilon$ contributions, we obtain

$$= -\frac{1}{32\pi\zeta\mu^\epsilon} \left[8N \left(V^{(4)}_{\mathcal{K}} + \zeta^2 V^{(4)}_{\mathcal{O}} \right) + \zeta^2 \left(f_1 \eta_1 V^{(4)}_1 + f_2 \eta_2 V^{(4)}_2 \right) \right.$$

$$\left. + 8(\eta - N)c^2 V^{(4)}_{\mathcal{W}} \right] \left(\frac{1}{\epsilon} + \ell \right) + \mathfrak{f}, \quad (8.61)$$

where f_1 and f_2 are functions of η_1 and η_2 given by

$$f_1 = -\frac{1}{\eta_1} \left[(2N + 3)\eta_1^2 + 4(N + 3)\eta_1\eta_2 + (N + 10)\eta_2^2 + 8\eta_1 + 48\eta_2 - 16 \right], \quad (8.62a)$$

$$f_2 = -\frac{1}{\eta_2} \left[\eta_1^2 + 8\eta_1\eta_2 + (N + 10)\eta_2^2 + 24\eta_1 + 32\eta_2 + 80 \right]. \quad (8.62b)$$

The two-point 1PI contribution to the one-loop order is

$$\Pi \, \delta^{I_1 I_2} = \quad \text{(diagram)} \quad + \quad \text{(diagram)} \quad , \quad (8.63)$$

where

$$\Pi = -\frac{1}{\mu^\epsilon g^2} \left\{ \left[\frac{g^2}{4\pi\zeta} \left(\frac{1}{\epsilon} + \ell \right) - \delta_g \right] \omega^2 + \left[\frac{g^2}{4\pi\zeta} \left(\frac{1}{\epsilon} + \ell \right) + \delta_\zeta - \delta_g \right] \zeta^2 k^4 \right.$$

$$\left. + \left[\frac{(1 - \eta)g^2}{4\pi\zeta} \left(\frac{1}{\epsilon} + \ell \right) + \delta_c - \delta_g \right] c^2 k^2 \right\} + \mathcal{O}(g^2). \quad (8.64)$$

Switching to the physical fields π_*, the geometric sum in the Schwinger-Dyson equation gives the exact physical inverse propagator,

$$\Gamma^{I_1 I_2}(\omega, k^2) = \frac{1}{r^2 \mu^\epsilon g^2} \left(\omega^2 + \zeta^2 k^4 + c^2 k^2 - \mu^\epsilon g^2 \Pi \right) \delta^{I_1 I_2}. \tag{8.65}$$

We require $r = 1$, $g_* = g$, $\zeta_* = \zeta$ and $c_* = c$ at $\ell = 0$ (i.e., $\mu = c_*/\zeta_*$). Then, the renormalization conditions in (8.48) imply

$$\delta_\zeta = 0 + \mathcal{O}\left(g^4\right), \tag{8.66a}$$

$$\delta_g = \frac{g^2}{4\pi \zeta \epsilon} + \mathcal{O}\left(g^4\right), \tag{8.66b}$$

$$\delta_c = \frac{g^2 \eta}{4\pi \zeta \epsilon} + \mathcal{O}\left(g^4\right), \tag{8.66c}$$

and

$$g_*^2 = r^2 g^2 \left(1 - \frac{g^2 \ell}{4\pi \zeta}\right) + \mathcal{O}\left(g^6\right), \tag{8.67a}$$

$$1 = \zeta_*^2 = \zeta^2 + \mathcal{O}\left(g^4\right), \tag{8.67b}$$

$$c_*^2 = c^2 \left(1 - \frac{g^2 \ell \, \eta}{4\pi \zeta}\right) + \mathcal{O}\left(g^4\right). \tag{8.67c}$$

Therefore we observe that there is no renormalization to ζ at the one-loop level.

In terms of the physical field π_*, the amputated four-point 1PI function is

$$\begin{aligned}
\Gamma^{I_1 I_2 I_3 I_4}(\omega_i, \mathbf{k}_i) = &-\frac{1}{r^4 \mu^\epsilon g^2} \left[1 + \frac{N g^2}{4\pi}\left(\frac{1}{\epsilon} + \ell\right) + (\delta - \delta_g)\right] \left(V_{\mathcal{K}}^{(4)} + V_{\mathcal{O}}^{(4)}\right) \\
&- \frac{\eta_1}{r^4 \mu^\epsilon g^2} \left[1 + \frac{g^2 f_1}{32\pi}\left(\frac{1}{\epsilon} + \ell\right) + \delta + \delta_1 - \delta_g\right] V_1^{(4)} \\
&- \frac{\eta_2}{r^4 \mu^\epsilon g^2} \left[1 + \frac{g^2 f_2}{32\pi}\left(\frac{1}{\epsilon} + \ell\right) + \delta + \delta_2 - \delta_g\right] V_2^{(4)} \\
&- \frac{c^2}{r^4 \mu^\epsilon g^2} \left[1 + \frac{(N + \eta) g^2}{4\pi}\left(\frac{1}{\epsilon} + \ell\right)\right] V_{\mathcal{W}}^{(4)} + \mathcal{O}\left(g^2\right). \tag{8.68}
\end{aligned}$$

The renormalization conditions in (8.52) imply

$$\delta = -\frac{(N-1)g^2}{4\pi \epsilon} + \mathcal{O}\left(g^4\right), \qquad \delta_i = \frac{(8N - f_i)g^2}{32\pi \epsilon} + \mathcal{O}\left(g^4\right), \quad i = 1, 2, \tag{8.69}$$

and

$$g_*^2 = r^4 g^2 \left(1 - \frac{N g^2 \ell}{4\pi}\right) + \mathcal{O}\left(g^6\right). \tag{8.70}$$

Together with (8.67a) we obtain

$$r = 1 + \frac{(N-1)g^2\ell}{8\pi} + \mathcal{O}\left(g^4\right), \tag{8.71}$$

which is related to the anomalous dimension of π via

$$\gamma \equiv \frac{d\log r}{d\ell} = \frac{(N-1)g^2}{8\pi} + \mathcal{O}\left(g^4\right). \tag{8.72}$$

Moreover,

$$g_*^2 = g^2\left[1 + \frac{(N-2)g^2\ell}{4\pi}\right] + \mathcal{O}\left(g^6\right). \tag{8.73}$$

Since g_* is the physical coupling defined at a fiducial point, it is independent of ℓ. Hence, the beta function for g is

$$\beta_{g^2} \equiv \frac{dg^2}{d\log\mu} = -\frac{(N-2)g^4}{4\pi} + \mathcal{O}\left(g^6\right). \tag{8.74}$$

We further require $\eta_i^* = \eta_i$, $i = 1, 2$ at $\ell = 0$. The renormalization conditions in (8.53) set

$$\eta_i^* = \eta_1\left[1 - \frac{(8N - f_i)g^2\ell}{32\pi}\right], \quad i = 1, 2. \tag{8.75}$$

The terms $\mathcal{O}^{(4)}$ and $\mathcal{W}^{(4)}$ serve as consistency checks.

Requiring that c_* in (8.67c) and η_i^* in (8.75) be independent of ℓ, and taking (8.74) into account, we obtain the following set of RG equations:

$$\beta_{\eta_i} \equiv \frac{d\eta_i}{d\log\mu} = \frac{F_i g^2}{32\pi} + \mathcal{O}\left(g^4\right), \quad i = 1, 2, \tag{8.76a}$$

$$\gamma_{c^2} \equiv \frac{d\log c^2}{d\log\mu} = \frac{g^2}{16\pi}\left[N\eta_1 + (N+2)\eta_2 + 8\right] + \mathcal{O}(g^4), \tag{8.76b}$$

where

$$F_1 = (2N+3)\eta_1^2 + 4(N+3)\eta_1\eta_2 + (N+10)\eta_2^2 + 8(N+1)\eta_1 + 48\eta_2 - 16, \tag{8.77}$$
$$F_2 = \eta_1^2 + 8\eta_1\eta_2 + (N+10)\eta_2^2 + 24\eta_1 + 8(N+4)\eta_2 + 80. \tag{8.78}$$

If one also keeps track of terms linear in ϵ, the only beta function that is modified is β_{g^2}:

$$\beta_{g^2} = \epsilon - \frac{(N-2)g^4}{4\pi} + \mathcal{O}\left(g^4\right). \tag{8.79}$$

In the next section we will demonstrate that $\beta_{\eta_i} = 0$ if $\eta_1 = -4$ and $\eta_2 = 0$, in which case the theory is said to be at the detailed balance (if c is tuned to be zero). If one further set

$$g^2 = g_c^2 \equiv \sqrt{\frac{4\pi\epsilon}{N-2}}, \quad N \neq 2, \tag{8.80}$$

then the theory becomes scale invariant at the one-loop level. In the large N limit this scale invariance becomes exact. A systematic study of the critical exponents associated with this Wilson-Fisher fixed point and its application in condensed matter systems is of future interest.

A particularly simple case is when $N = 2$, which provides a consistency check of the beta functions we calculated previously. In this case, one can parametrize the field in terms of an angular variable:

$$n = (\cos\theta, \sin\theta), \tag{8.81}$$

which has unit Jacobian on the circle and therefore introduces no nontrivial measure terms to the path integral. Then,

$$\dot{n} \cdot \dot{n} = \dot{\theta}^2, \qquad \partial^2 n \cdot \partial^2 n = (\partial^2\theta)^2 + (\partial_i\theta\,\partial_i\theta)^2, \qquad \partial_i n \cdot \partial_i n = \partial_i\theta\,\partial_i\theta,$$

$$(\partial_i n \cdot \partial_i n)^2 = (\partial_i n \cdot \partial_j n)(\partial_i n \cdot \partial_j n) = (\partial_i\theta\,\partial_i\theta)^2. \tag{8.82a}$$

The action becomes

$$S = \frac{1}{2g^2} \int dt\, d^2x \left\{ \dot{\theta}^2 + \zeta^2 \left[\partial^2\theta\,\partial^2\theta + \frac{\eta}{2}(\partial_i\theta\,\partial_i\theta)^2 \right] + c^2 \partial_i\theta\,\partial_i\theta \right\}, \tag{8.83}$$

which demonstrates that the self-interaction of the field θ is characterized not by η_1 and η_2 separately, but by the particular combination η given in (8.57). In particular, $\eta = 0$ describes a Gaussian fixed point.

Of course, one can transform to angular coordinates analogously for any $N \geq 3$ as well, but there would be nontrivial measure terms in that case and the action does not simplify as it does for the $N = 2$ case.

The above analysis is borne out in the previous calculations of the beta functions. In $2 + 1$ dimensions, at $N = 2$, the beta function of g vanishes. This is in analogy with the relativistic NLSM in $1 + 1$ dimensions. However, the renormalization group flows of c^2, η_1 and η_2 are nontrivial:

$$\gamma_{c^2} = \frac{g^2}{8\pi}(\eta_1 + 2\eta_2 + 4) + \mathcal{O}(g^4), \tag{8.84}$$

$$\beta_{\eta_1} = \left(7\eta_1^2 + 20\eta_1\eta_2 + 12\eta_2^2 + 24\eta_1 + 96\eta_2 - 16\right)\frac{g^2}{32\pi} + \mathcal{O}(g^4), \tag{8.85}$$

$$\beta_{\eta_2} = \left(\eta_1^2 + 8\eta_1\eta_2 + 12\eta_2^2 + 24\eta_1 + 48\eta_2 + 80\right)\frac{g^2}{32\pi} + \mathcal{O}(g^4). \tag{8.86}$$

However, when $N = 2$, η_1 and η_2 are no longer independent couplings. Indeed, as found above, the appropriate coupling is η. One finds

$$\beta_\eta = \frac{1}{2}\beta_{\eta_1} + \beta_{\eta_2} = \frac{9}{16\pi}g^2\eta^2. \tag{8.87}$$

In particular, when η is set to zero, all beta functions vanish. Boundedness of the Hamiltonian from below requires $\eta \geq 0$, or $\eta_1 + 2\eta_2 + 4 \geq 0$.

At the Gaussian fixed point with $\eta = 0$, one can set the relevant coupling c^2 to be naturally small, in which case one has the purely $z = 2$ Gaussian fixed point action. This action enjoys a quadratic shift symmetry [18],

$$\theta \to \theta + b_{ij} x^i x^j, \tag{8.88}$$

where b_{ij} is a symmetric tensor and x^i are spatial coordinates. This is the underlying symmetry that protects the smallness of c^2 and η simultaneously. This theory describes a natural Type A Nambu-Goldstone boson (NGB) with a quadratic dispersion relation. These types of NGB do not violate time reversal symmetry and each is associated with one broken symmetry generator.

8.6 Asymptotic Trajectories

In this subsection we study the structure of the RG trajectories described by the RG equations (8.74) and (8.76). We will focus on the marginal operators in the action. In fact, the relevant deformation can be set to zero naturally in the weak-coupling limit, where the free theory is protected by a quadratic shift invariance. We will address this in more detail later in Section 8.7. The canonically normalized action is

$$S_{\text{marginal}} = \frac{1}{2} \int dt\, d^2x \Big\{ \left(\dot{\pi} \cdot \dot{\pi} + \partial^2 \pi \cdot \partial^2 \pi \right) + \frac{u_3}{4} \left[\left[\partial_t \left(\pi \cdot \pi \right) \right]^2 + \left[\partial^2 \left(\pi \cdot \pi \right) \right]^2 \right]$$
$$+ \frac{u_1}{4} \left(\partial_i \pi \cdot \partial_i \pi \right)^2 + \frac{u_2}{2} \left(\partial_i \pi \cdot \partial_j \pi \right) \left(\partial_i \pi \cdot \partial_j \pi \right) + \cdots \Big\}, \tag{8.89}$$

where we defined

$$u_1 \equiv \eta_1 g^2, \quad u_2 \equiv \eta_2 g^2, \quad u_3 \equiv g^2 \geq 0. \tag{8.90}$$

These are the couplings that control the strength of various interactions. For the one-loop approximation to be valid, we require that $u_1, u_2, u_3 \ll 1$. The corresponding one-loop RG equations are

$$\dot{u}_i = M_i, \quad i = 1, 2, 3, \tag{8.91}$$

where

$$\dot{u}_i \equiv \frac{du_i}{dt}, \quad t \equiv \frac{\ell}{32\pi}, \quad i = 1, 2, 3. \tag{8.92}$$

and

$$M_1 = (2N + 3)u_1^2 + 4(N + 3)u_1 u_2 + (N + 10)u_2^2 + 24u_1 u_3 + 48u_2 u_3 - 16u_3^2,$$
$$M_2 = u_1^2 + 8u_1 u_2 + (N + 10)u_2^2 + 24u_1 u_3 + 48u_2 u_3 + 80u_3^2, \tag{8.93}$$
$$M_3 = -8(N - 2)u_3^2 \leq 0.$$

Here we denoted the RG time by t, which is not to be conflated with the ordinary time or the Mandelstam t variable. The solution for u_3 is

$$u_3(t) = \frac{u_{30}}{1 + 8(N-2)u_{30}t}. \tag{8.94}$$

We have taken the initial RG time to be zero at which point u_3 takes the value u_{30}. $N = 2$ is a special case discussed earlier. For $N > 2$ and any $u_{30} \geq 0$, we have that $u_3 \to 0$ in the UV ($t \to \infty$) and u_3 will become strongly coupled as it flows towards the IR. For $N > 2$, the equations have only one fixed point, the Gaussian fixed point at $(u_1, u_2, u_3) = (0, 0, 0)$.

We would like to study the behavior of the above set of RG equations around the Gaussian fixed point with $u_1 = u_2 = u_3 = 0$. Our approach is to search for the simple RG trajectories that are straight rays. We then linearize around these simple RG trajectories to discover the behaviour of the nearby trajectories. This allows us to determine the stability of these simple trajectories as they approach the fixed point. We refer the readers to [96] for more details on RG equations with more than two couplings and [97] for quasi-linear systems, but we will review this procedure briefly here.

Let us start by examining this simple family of RG trajectories that are straight rays that either point towards or away from the Gaussian fixed point. We parametrize these trajectories as

$$u_1 = \frac{u_{10}}{1-at}, \quad u_2 = \frac{u_{20}}{1-at}, \quad u_3 = \frac{u_{30}}{1-at}, \tag{8.95}$$

where $a \neq 0$ and u_{i0}, $i = 1, 2, 3$ are constants and at least one of u_{i0} is nonzero. Furthermore, u_{i0} are the values that u_i take at the initial RG times $t = 0$. Depending on whether a is positive or negative, we divide these straight-line rays into two types, namely:

- UV asymptotic trajectories (UVAT): For $a < 0$. The range of t is $\left(\frac{1}{a}, \infty\right)$. The theory approaches the critical point at $t \to \infty$, *i.e.*, the theory is asymptotically free in the UV along any UVAT.

- IR asymptotic trajectories (IRAT): For $a > 0$. The range of t is $\left(-\infty, \frac{1}{a}\right)$. The theory approaches the critical point at $t \to -\infty$, *i.e.*, the theory is asymptotically free in the IR along any IRAT.

Plugging (8.95) back into (8.91), we obtain

$$au_{i0} = M_i \Big|_{u_j = u_{j0}}, \quad i, j = 1, 2, 3, \tag{8.96}$$

with M given in (8.93). It is always possible to rescale a by making a different choice of the initial RG time $t = 0$ along the RG trajectory. In what follows, we always choose $a = -1$ for the UVATs and $a = 1$ for the IRATs.

Next, to analyze the stability of an asymptotic trajectory, we take a small deviation v_i, $i = 1, 2, 3$ away from the trajectory as follows:

$$u_i = \frac{u_{i0} + v_i}{1 - at}. \tag{8.97}$$

Substituting this change of variables back into (8.91), we obtain the linearized equations

$$\frac{dv_i}{d\tau} = \sum_{j=1}^{3} \left(\left. \frac{\partial M_i}{\partial u_j} \right|_{u_k = u_{k0}} - a\delta_i^j \right) v_j + \mathcal{O}\left(v^2\right), \quad i, j, k = 1, 2, 3. \tag{8.98}$$

where $\tau \equiv -\frac{1}{a}\ln(1 - at)$.

The dimension of the manifold of stability around a UVAT is the number of negative eigenvalues of the matrix $\left. \frac{\partial M^i}{\partial u^j} \right|_{u_k = u_{k0}} + \delta_j^i$. For an IRAT, this is the number of positive eigenvalues of the matrix $\left. \frac{\partial M^i}{\partial u^j} \right|_{u_k = u_{k0}} - \delta_j^i$. The stability manifold will always contain the trajectory itself.

We solve the equations $-u_{i0} = M_i \Big|_{u_j = u_{j0}}$, with M_i given in (8.93). We will omit the subindex 0 in the following and simply write $-u_i = M_i$. There are two solutions for u_3:

$$u_3 = 0, \qquad\qquad u_3 = \frac{1}{8(N-2)}. \tag{8.99}$$

Subtracting the u_2- from the u_1-equation allows one to solve for u_2 in terms of u_1 and u_3:

$$u_2\left[1 - 4(N+1)u_1\right] = 2(N+1)u_1^2 + u_1 - 96u_3^2. \tag{8.100}$$

We now examine the solutions to this equation. Note that at the special value $u_1 = \frac{1}{4(N+1)}$ this equation degenerates and u_2 drops out entirely. The solution $u_3 = 0$ does not satisfy the resulting equation, in this case. The solution $u_3 = \frac{1}{8(N-2)}$ does work, but only at the particular value $N = 8$. In this special case, one finds two real solutions for u_2 to either the u_1- or u_2-equation after plugging in the specific values for u_1 and u_3. The solutions are

$$N = 8: \qquad (u_1, u_2, u_3) = \left(\frac{1}{36}, \frac{-5 \pm \sqrt{7}}{81}, \frac{1}{48} \right). \tag{8.101}$$

Having dispensed of the special case $u_1 = \frac{1}{4(N+1)}$, we now assume $u_1 \neq \frac{1}{4(N+1)}$. Solving for u_2 in (8.100) and plugging back into the UVAT equations yields an equation for u_1 and u_3. When $u_3 = 0$, the remaining equation for u_1 reads

$$u_1\left[1 - (N-17)u_1 - 4(N-2)(N+1)u_1^2 + 4(N-2)(N+1)^2 u_1^3\right] = 0. \tag{8.102}$$

Here, $u_1 = 0$ just yields the trivial solution. On the other hand, the cubic equation has one real solution for $N \leq 47$ and three real solutions for $N \geq 48$, which is determined by noting that the discriminant of the cubic equation has a zero at $N \approx 47.55$.

For $u_3 = \frac{1}{8(N-2)} \neq 0$, the same analysis of the corresponding cubic equation shows that there is one real solution for $N = 3, 4, 5$, whereas for $N = 6, 7$ and $N > 8$, there are 3 real solutions for u_1, each with a corresponding value of u_2. In the special case of $N = 8$, two of the solutions for u_1 coincide, leaving just two real solutions for u_1, namely $u_1 = \frac{5}{36}$ and $u_1 = \frac{1}{36}$. The value $u_1 = \frac{5}{36}$ has the corresponding u_2 value $u_2 = -\frac{1}{9}$. The value

$u_1 = \frac{1}{36}$ is actually the special case considered earlier in (8.101), which has two values of u_2 and therefore there are still three real solutions for $N = 8$ in this case. In addition to the solutions to the cubic equation, we find one other solution that exists for all $N \geq 2$:

$$(u_1, u_2, u_3) = \frac{1}{8(N-2)}(-4, 0, 1). \tag{8.103}$$

In fact, this solution corresponds to imposing a detailed balance condition. This condition often reduces to the requirement that the part of the action that depends only on spatial derivatives take the form of the square of the equation of motion of an associated Euclidean theory in one lower dimension.

In the case of our sigma model, requiring that the theory satisfy the detailed balance condition with respect to the relativistic S^{N-1} nonlinear sigma model means that the potential term should be

$$\frac{1}{2g^2} \int dt \, d^2x \, g_{IJ}(\pi) \Delta\pi^I \Delta\pi^J, \tag{8.104}$$

where

$$g_{IJ}(\pi) = \delta_{IJ} + \frac{\pi^I \pi^J}{1 - \pi \cdot \pi} \tag{8.105}$$

is the round metric on the unit S^{N-1} in the π^I coordinate system, and Δ is the covariant Laplacian on the Goldstone fields,

$$\Delta\pi^K \equiv \partial^2\pi^K + \Gamma^K{}_{IJ}\partial_i\pi^I\partial_i\pi^J. \tag{8.106}$$

Since the Riemannian connection of g_{IJ} is given by

$$\Gamma^K{}_{IJ} = \delta_{IJ}\pi^K + \frac{\pi^I\pi^J\pi^K}{1 - \pi \cdot \pi} = g_{IJ}(\pi)\pi^K, \tag{8.107}$$

the expression for $\Delta\pi^K$ simplifies to

$$\Delta\pi^K = \left(\partial^2 + \mathcal{W}\right)\pi^K. \tag{8.108}$$

Comparing $\partial^2 n \cdot \partial^2 n$ and $g_{IJ}(\pi)\,\Delta\pi^I\,\Delta\pi^J$, we find that these two terms differ by an additive factor of $\mathcal{W}^2$. Hence, in terms of the fields n, the theory at detailed balance corresponds to the action

$$S_{\text{db}} = \frac{1}{2g^2} \int dt \, d^2x \left\{ \dot{n} \cdot \dot{n} + \zeta^2 \left[\left(\partial^2 n \cdot \partial^2 n\right) - (\partial_i n \cdot \partial_i n)^2 \right] \right\}. \tag{8.109}$$

This is a special case of our general action, with

$$\eta_1 = -4, \quad \eta_2 = 0, \quad c = 0, \tag{8.110}$$

which is indeed the $u_3 \neq 0$ UVAT that exists for all N in (8.103).

When $u_3 \neq 0$, it is instructive to consider the flow in (η_1, η_2, u_3) space. Since the beta functions of η_1 and η_2 are proportional to $u_3 = g^2$ in (8.76), the slices at fixed $u_3 > 0$ in

the three-dimensional RG phase diagram are identical to each other except for their RG time scale. Therefore, it is sufficient to analyze the flow lines projected onto any such plane. In Figure 8.2, we plot the RG flow in this plane as well as the nullclines when $\beta_{\eta_1} = 0$ (solid curve) and when $\beta_{\eta_2} = 0$ (thick dashed curve). These nullclines intersect at points on UVATs. Note the horizontal alignment of two of these intersections at the special value $N = 8$ in agreement with the previous analysis. There is also an interesting switching in the branching pattern of the $\beta_{\eta_1} = 0$ nullcline from $N = 14$ and $N = 15$. For $N = \infty$, the $\beta_{\eta_2} = 0$ nullcline limits to two horizontal lines at $\eta_2 = 0$ and $\eta_2 = -8$ and the four intersection points become $(\eta_1, \eta_2) = (0,0), (-4,0), (4,-8)$ and $(8,-8)$.[6] The RG structure becomes even more transparent in the η_+-η_2 plane, where $\eta_+ = \eta_1 + \eta_2$, which is presented in Figure 8.3. In Figure 8.3, arrows on the flow lines point towards the UV. Solid curve is $\beta_{\eta_1} = 0$ nullcline, thick dashed curve is $\beta_{\eta_2} = 0$ nullcline. Their intersections are points on UVATs with stability manifolds of dimension 1 (green), 2 (blue) and 3 (red). The vertical black line for $N = 8$ shows the horizontal alignment of two trajectories. The branching pattern of the solid nullclines switches between $N = 14$ and $N = 15$. The theory is UV complete along the stream line on the η_1-η_2 plane that connects the upper blue point and the green point.

In summary, we have found three UVATs for $3 \le N \le 5$, five for $6 \le N \le 47$ and seven for $N \ge 48$. Let us now analyze the stability of these trajectories as we approach the fixed point.

The stability matrix for each UVAT has at least one eigenvalue of -1 (the stable direction corresponding to moving along the trajectory towards the fixed point). It turns out that in this case, the UVATs with $u_3 = 0$ always have at least one unstable direction (the stability matrix always turns out to have an eigenvalue of -1). Presumably this corresponds to the unstable flow towards negative u_3.

The detailed balance UVAT with $(u_1, u_2, u_3) = \frac{1}{8(N-2)}(-4, 0, 1)$ has a stability matrix with eigenvalues $(-1, -\frac{N}{N-2}, 1)$ and therefore always has a 2-dimensional stability manifold. We can analyze the stability of the other trajectories numerically. These are indicated in Figure 8.2 by red, blue or green dots. A red dot indicates a trajectory with a stability manifold of dimension 3 (the two dimensions of the plane are attractive towards the point and the direction, $u_3 = g^2$, perpendicular to the plane is the direction of the trajectory itself, which is always attractive). The blue dots indicate trajectories with stability manifolds of dimension 2. The green dot indicates a trajectory with stability manifold of dimension one.

Putting all these results together, we get the following:

- For $3 \le N \le 5$, there are three UVATs. The $u_3 = 0$ solution has a one-dimensional stability manifold. The trajectory $(u_1, u_2, u_3) = \frac{1}{8(N-2)}(-4, 0, 1)$ (detailed balance) has

---

[6]Some UVATs lie outside the region where the potential is a sum of squares. Some flows leave and others enter this region. Perhaps the region is augmented in an N-dependent way. Otherwise, in some regions of parameter space, it would seem that the theory predicts its own IR or UV demise.

(a) $N = 5$

(b) $N = 6$

(c) $N = 8$

(d) $N = 14$

(e) $N = 15$

(f) $N = \infty$
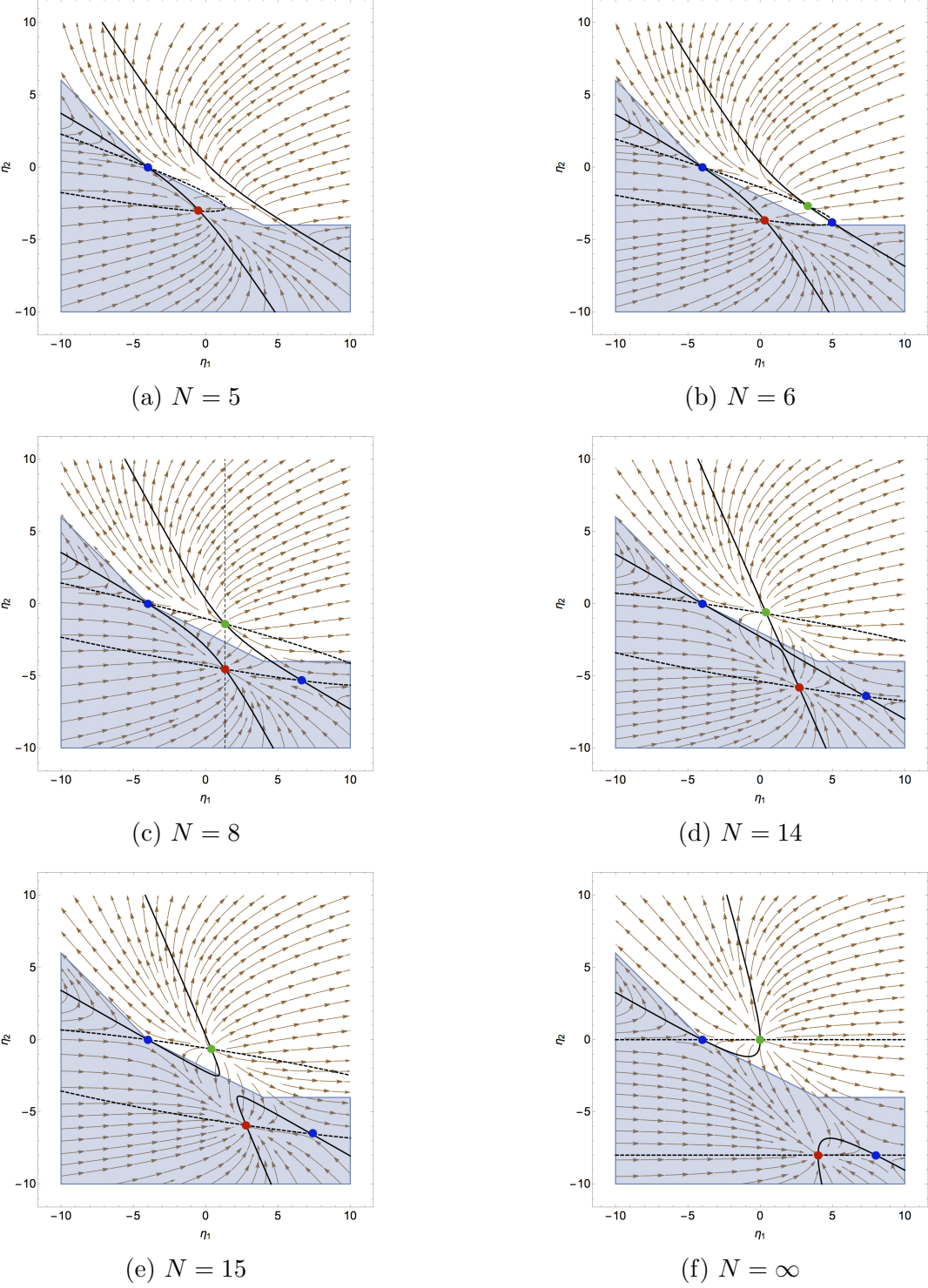
Figure 8.2: RG flow lines projected in the η_1-η_2 plane.

(a) $N = 5$

(b) $N = 8$

(c) $N = 15$

(d) $N = \infty$
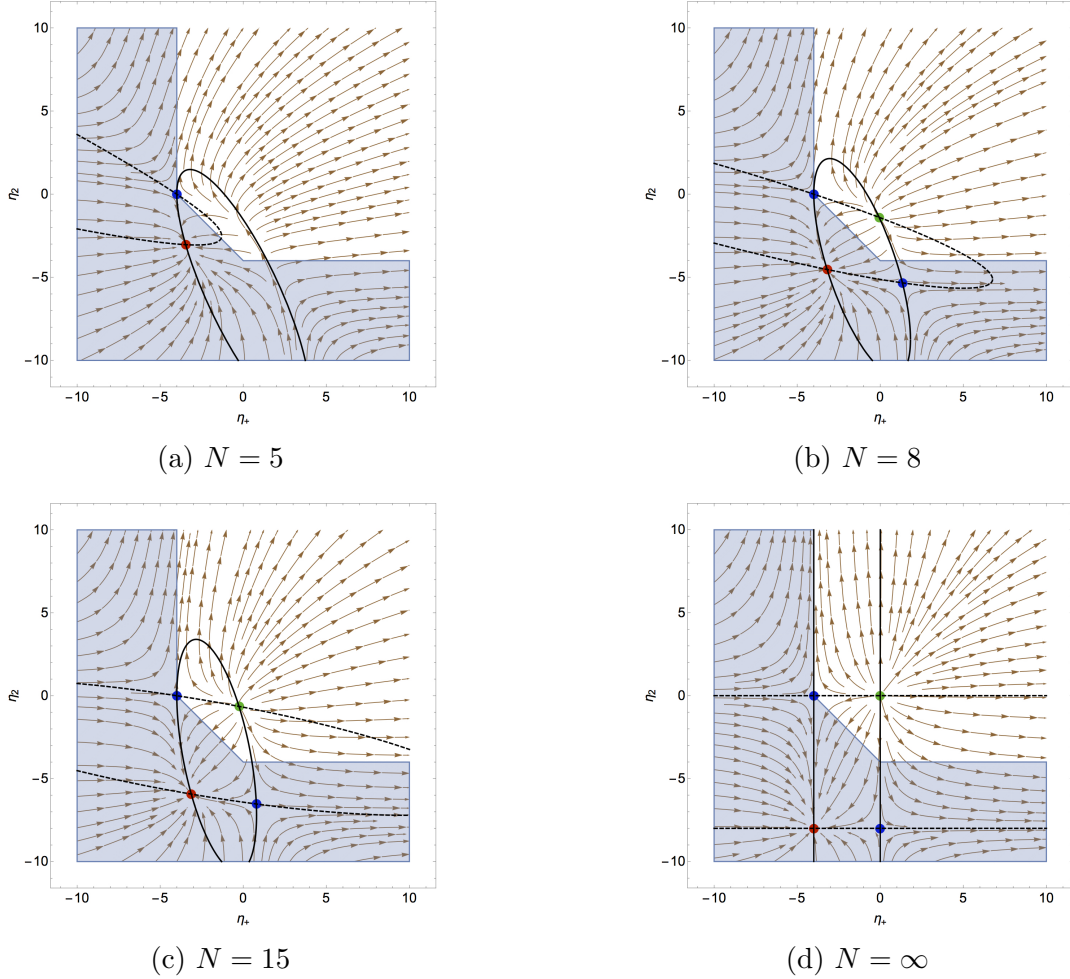
Figure 8.3: RG flow lines projected in the η_+-η_2 plane, $\eta_+ = \eta_1 + \eta_2$.

a two-dimensional stability manifold (blue dot). The other $u_3 = \frac{1}{8(N-2)}$ solution (red dot) has a three-dimensional stability manifold.

- For $6 \leq N \leq 47$, there are five UVATs. The $u_3 = 0$ solution and the $u_3 = \frac{1}{8(N-2)}$ trajectory indicated with a green dot have one-dimensional stability manifolds. There are two trajectories with two-dimensional stability manifolds (blue dots). There is one trajectory with a three-dimensional stability manifold (red dot).

- For $N \geq 48$, there are seven UVATs. In addition to the case $6 \leq N \leq 47$, there are now two more $u_3 = 0$ solutions. One of these has a one-dimensional manifold of stability and the other has a two-dimensional manifold of stability.

The four UVATs plotted on the η_1-η_2 plane in Figure 8.2 will approach the Gaussian fixed point when u_3 decreases along the RG flow towards the UV, which indicates the potential

existence of a UV asymptotically free region. However, most of the RG trajectories that approach the Gaussian fixed point in the UV will escape the sum-of-square region for large enough RG time, except for the UVAT at detailed balance and the green UVAT, and by continuity every point along the stream line on the η_1-η_2 plane that connects these two points. In the large N limit, this arc lies along the dashed curve.

Solving the equations $u_i = M_i$ with the restriction $u_3 \geq 0$ gives only one solution for u_3, which is $u_3 = 0$. One solves for u_2 in terms of u_1:

$$u_2 = \frac{u_1 - 2(N+1)u_1^2}{1 + 4(N+1)u_1}. \tag{8.111}$$

There is no solution for which the denominator above vanishes. Plugging this back into the IRAT equations yields, as before, a cubic equation for u_1, which has one real solution for $3 \leq N \leq 47$ and three real solutions for $N \geq 48$.

In summary, there is one IRAT for $3 \leq N \leq 47$ and three IRATs for $N \geq 48$. The fact that we have always found at least one IRAT means that there are some values of the couplings for which the theory is not asymptotically free.

The stability matrix for each IRAT has at least one eigenvalue of 1 (the stable direction corresponding to moving along the trajectory from the fixed point). Since $u_3 = 0$, the IRATs always have at least one unstable direction (the stability matrix always has an eigenvalue of -1). We can analyze the stability of the each trajectory numerically, with the following results.

- For $3 \leq N \leq 47$, there is one IRAT having a one-dimensional manifold of stability (an isolated trajectory). Nearby trajectories do not originate from the free fixed point.

- For $N \geq 48$, there are three IRATs, one having a two-dimensional manifold of stability and two having a one-dimensional manifold of stability.

We emphasize that the above discussion is only valid in the regime in the vicinity of the critical point, where all (u_1, u_2, u_3) couplings are sufficiently small. There are however two novelties that do not arise in relativistic theories:

- Self-decay processes are kinematically allowed in theories with higher z's. However, at the one-loop level, there is no diagram contributing to the decay rate, and thus a one-particle state is stable at one-loop level. At two-loops, there will be nonzero decay rate from the imaginary part of the sunset diagram $\!-\!\bigcirc\!-\!$. In the deep UV this decay rate will be comparable to the energy scale and there will not exist any long-living particles, unless the theory is asymptotically free, in which case the decay rate will be suppressed by the smallness of the coupling. It is possible that the theory UV completes in a non-Wilsonian way in the regime where the theory is strongly coupled, for example, by decaying into many soft quanta and creating some classical object reminiscent of the classicalization phenomenon [75].

- In the deep IR, the relevant operator $\mathcal{W}$ becomes more and more dominant and the theory cascades towards $z = 1$ [18]. At the momentum scale much smaller than c, the theory becomes approximately relativistic. This natural flow towards a relativistic fixed point in the IR is guaranteed by the quadratic shift symmetry in play.

In Figure 8.2, there are trajectories leaving or entering the shaded region, in which the action cannot be written as a sum of complete squares. In fact, there exists a large region within which the trajectories are asymptotically free in the UV but run across the sum-of-squares border. This indicates possible nonperturbative instabilities since the potential is not guaranteed to be bounded from below. However, the decay rate for the theory to leave a false vacuum is presumably suppressed by the smallness of the coupling constant g^2 as in [23], for example.

On the other hand, it is still possible that the configurations in the shaded region do not actually exhibit instability. In the case that at some energy scale Λ_{UV} the RG trajectory signals UV instability, the effective description as a NLSM may break down before reaching Λ_{UV} and the theory should be already replaced by its UV completion; in the case that at some energy scale Λ_{IR} the RG trajectory signals IR instability, the theory may have cascaded to a lower value of z beforehand.

8.7 The Power Law Divergence

By power counting, the one-loop correction to the two-point Green's function is quadratically divergent. Higher power law divergences will be cancelled by the path integral measure.[7] In the above analysis, we applied dimensional regularization so all power law divergences are regularized to zero. However, to examine issues of naturalness, it is necessary to explicitly calculate the size of these power law divergences. In the sharp cutoff regularization scheme, the quadratic divergence is cancelled by introducing the corresponding counterterm. The contribution from the relevant term $\mathcal{W}$ can naturally be set to zero if and only if the quadratically divergent contribution to c^2 vanishes exactly.

To extract the quadratic divergence in the two-point Green's function, let us introduce the UV cutoff Λ for the momentum. Then,

$$\underset{\bigcirc}{\underline{}} = -\frac{k^2\Lambda^2}{8\pi}\delta^{I_1 I_2}\left[N\eta_1 + (N+2)\eta_2 + 8\right] = -\frac{\eta k^2\Lambda^2}{2\pi}\,\delta^{I_1 I_2}. \qquad (8.112)$$

Therefore, c^2 can be set to zero naturally if and only if

$$N\eta_1 + (N+2)\eta_2 + 8 = 4\eta = 0, \qquad N\beta_{\eta_1} + (N+2)\beta_{\eta_2} = 4\beta_\eta = 0. \qquad (8.113)$$

When $N = 2$, $\eta = 0$ implies $\beta_\eta = 0$ and so the vanishing of the quadratic divergence is preserved under RG flow. However, this is no longer true at any other value of N and in

---

[7]The role that the measure terms play here is qualitatively very similar to the relativistic case [88].

general c^2 does indeed receive a quadratic divergence[8]:

$$\delta c^2 = \frac{\eta g^2 \Lambda^2}{2\pi} = \frac{g^2 \Lambda^2}{8\pi} \left[N\eta_1 + (N+2)\eta_2 + 8 \right].$$ (8.114)

Despite the quadratic divergence to c^2, it is however natural to set c to zero in the weak coupling limit. If we view the NLSM as a low energy effective field theory, we can apply the enhanced quadratic shift symmetry (8.88) on π^I in the free-field limit. The symmetry transformation in analogy of (8.88) is

$$\pi^I \to \pi^I + b^I_{ij} x^i x^j.$$ (8.115)

We further define the naturalness scale μ at which the quadratic shift symmetry is broken. Then, restoring the dimensions, we have

$$g^2 = \mathcal{O}(\varepsilon), \quad c^2 = \mathcal{O}(\varepsilon \mu^2),$$ (8.116)

which predicts

$$c^2 = \mathcal{O}(g^2 \mu^2).$$ (8.117)

In the small g^2 regime of the weakly-coupled NLSM, c^2 can be naturally much smaller than the naturalness scale. We refer the readers to [18] for further details.

Based on (8.116), we can argue that the theory flows towards a relativistic theory in the deep IR, with the nonrelativistic effects being relevant only at the momentum scale set by c. From a low energy perspective, due to one's prejudice favoring Lorentz symmetry, it is convenient to introduce a redefinition of spacetime coordinates,

$$y^i \equiv c^{-1} x^i, \quad \nabla_i \equiv \frac{\partial}{\partial y^i}.$$ (8.118)

Therefore, the effective action from the relativistic observer's perspective is

$$\widetilde{S} = \frac{c^2}{2g^2} \int dt\, d^2y \Big\{ \nabla_\mu n \cdot \nabla^\mu n$$

$$+ \frac{\zeta^2}{c^4} \left[\nabla^2 n \cdot \nabla^2 n + \eta_1 \left(\nabla_i n \cdot \nabla_i n \right)^2 + \eta_2 \left(\nabla_i n \cdot \nabla_j n \right) \left(\nabla_i n \cdot \nabla_j n \right) \right] \Big\},$$ (8.119)

where,

$$\nabla_\mu = \left(\frac{\partial}{\partial_t}, \nabla_i \right).$$ (8.120)

The new coupling is $g^2/c^2 = \mathcal{O}(1/\mu^2)$. The nonrelativistic effects come from the second line in (8.119) become negligible at the momentum scale much lower than c.

---

[8]A similar result is reported in [43], in which δc^2 is claimed to be zero for all N's at $\eta_1 = 4$ and $\eta_2 = -4$ (note the differences in our notations). However, these values of η_1 and η_2 are not preserved under RG flow, which invalidates the claim to asymptotic freedom in [43].

It is also interesting to examine the quadratic divergence at the detailed balance point, where we have $\eta_1 = -4$ and $\eta_2 = 0$ given by (8.103) and the beta functions for η_1 and η_2 vanish. The quadratic divergence (8.112) is still present for $N > 2$,

$$\underset{\displaystyle \rule{0pt}{0pt}}{\bigcirc} = \frac{k^2 \Lambda^2}{2\pi} (N - 2) \, \delta^{I_1 I_2}. \tag{8.121}$$

This quadratic divergence can be exactly cancelled by adding in fermionic degrees of freedom and making the theory supersymmetric [98].

8.8 The Large N Limit

We can extend control over the theory beyond weak coupling in g by considering the large N limit with the 't Hooft coupling $\lambda_t = g^2 N$ held fixed. In terms of the physical field π_*, the action is

$$S = \frac{N}{\mu^\epsilon Z_g \lambda_t} \int dt \, d^2x \Big\{ \mathcal{K}_* + \zeta^2 Z_\zeta \big(\mathcal{O}_* + \eta_1 Z_1 Z \mathcal{U}_1^* + \eta_2 Z_2 Z \mathcal{U}_2^* \big) + c^2 Z_c \mathcal{W}_* \Big\}. \tag{8.122}$$

In terms of π, the operators can be expanded to all orders as follows:

$$\mathcal{K} = \frac{1}{2} \dot{\pi} \cdot \dot{\pi} + \frac{1}{8} \sum_{n=0}^{\infty} Z^{n+1} (\pi \cdot \pi)^n \left[\partial_t (\pi \cdot \pi) \right]^2, \tag{8.123}$$

$$\mathcal{O} = \frac{1}{2} \partial^2 \pi \cdot \partial^2 \pi + \frac{1}{8} \sum_{n=0}^{\infty} Z^{n+1} (\pi \cdot \pi)^n \, \partial^2 (\pi \cdot \pi) \left\{ \partial^2 (\pi \cdot \pi) + Z(n+1) \left[\partial_i (\pi \cdot \pi) \right]^2 \right\}$$

$$+ \frac{1}{64} \sum_{n=0}^{\infty} Z^{n+1} (n+1)(n+2) (\pi \cdot \pi)^n \left[\partial_i (\pi \cdot \pi) \, \partial_i (\pi \cdot \pi) \right]^2, \tag{8.124}$$

$$\mathcal{W} = \frac{1}{2} \partial_i \pi \cdot \partial_i \pi + \frac{1}{8} \sum_{n=0}^{\infty} Z^{n+1} (\pi \cdot \pi)^n \, \partial_i (\pi \cdot \pi) \, \partial_i (\pi \cdot \pi), \tag{8.125}$$

$$\mathcal{U}_1 = \frac{1}{8} \left(\partial_i \pi \cdot \partial_i \pi \right)^2 + \frac{1}{16} \sum_{n=0}^{\infty} Z^{n+2} (\pi \cdot \pi)^n \left[\partial_i (\pi \cdot \pi) \right]^2 \left(\partial_j \pi \cdot \partial_j \pi \right)$$

$$+ \frac{1}{128} \sum_{n=0}^{\infty} Z^{n+3} (n+1) (\pi \cdot \pi)^n \left[\partial_i (\pi \cdot \pi) \, \partial_i (\pi \cdot \pi) \right]^2, \tag{8.126}$$

$$\mathcal{U}_2 = \frac{1}{4} \left(\partial_i \pi \cdot \partial_j \pi \right)^2 + \frac{1}{8} \sum_{n=0}^{\infty} Z^{n+2} (\pi \cdot \pi)^n \, \partial_i (\pi \cdot \pi) \, \partial_j (\pi \cdot \pi) \left(\partial_i \pi \cdot \partial_j \pi \right)$$

$$+ \frac{1}{64} \sum_{n=0}^{\infty} Z^{n+3} (n+1) (\pi \cdot \pi)^n \left[\partial_i (\pi \cdot \pi) \, \partial_i (\pi \cdot \pi) \right]^2. \tag{8.127}$$

The operators with the subscript "$*$" can be obtained by replacing π with π_*/r. To leading order in the large N limit, only cactus diagrams need be summed over, which can be done recursively.

In the following we derive the beta functions to all loops by summing over all cactus diagrams. First, we focus on the two-point Green's function. There are only two interactions contributing in the large N limit,

$$(\partial_i \pi_* \cdot \partial_i \pi_*)^2, \quad (\partial_i \pi_* \cdot \partial_j \pi_*)(\partial_i \pi_* \cdot \partial_j \pi_*). \tag{8.128}$$

The propagator is

$$\underline{\hspace{1cm}} = \frac{\delta^{I_1 I_2}}{N} \frac{r^2 \mu^\epsilon Z_g \lambda_t}{\omega^2 + Z_\zeta \zeta^2 k^4 + Z_c c^2 k^2}. \tag{8.129}$$

The four-point vertex is

$$-\frac{N Z Z_\zeta \zeta^2}{r^4 \mu^\epsilon Z_g \lambda_t} \left(Z_1 \eta_1 \mathcal{U}_1^{(4)} + Z_2 \eta_2 \mathcal{U}_2^{(4)} \right), \tag{8.130}$$

where a superscript (4) indicates the part of the potential involving the four-point interaction. Diagrammatically, the exact two-point function can be written as a geometric series of 1PI diagrams,

$$\blacksquare = \frac{\delta^{I_1 I_2}}{N} \frac{\mu^\epsilon \lambda_*}{\omega^2 + \zeta^2 k^4 + c^2 k^2} = \underline{\hspace{0.5cm}} + -\!\!\boxed{\text{1PI}}\!\!- + -\!\!\boxed{\text{1PI}}\!\!-\!\!\boxed{\text{1PI}}\!\!- + \cdots, \tag{8.131}$$

where 1PI is a sum of all 1PI cactus diagrams. Therefore, one derives the recursive relation

$$-\!\!\boxed{\text{1PI}}\!\!- = \underline{\hspace{0.4cm}}\!\!\varnothing\!\!\underline{\hspace{0.4cm}} \tag{8.132}$$

Denote the amputated 1PI two-point function as $\delta^{I_1 I_2}\Pi$. Then, (8.132) implies

$$\Pi = \frac{N}{16\pi\zeta} \frac{Z Z_\zeta}{r^2 \mu^\epsilon Z_g} (Z_1 \eta_1 + Z_2 \eta_2) c^2 k^2 \left(\frac{1}{\epsilon} + \ell \right), \tag{8.133}$$

where

$$\ell \equiv \log \left(\frac{\zeta_* \mu}{c_*} \right). \tag{8.134}$$

Therefore,

$$\blacksquare = \frac{\delta^{I_1 I_2}}{N} \frac{r^2 \mu^\epsilon Z_g \lambda_t}{\omega^2 + \zeta^2 Z_\zeta k^4 + \left(Z_c c^2 k^2 - \frac{\mu^\epsilon Z_g \lambda_t}{N} \Pi \right)}. \tag{8.135}$$

There is no divergence to be absorbed by Z_g or Z_ζ. Take $r = 1$, $\lambda_* = \lambda$ and $c_* = c$ at $\ell = 0$. The renormalization conditions in (8.48) imply

$$Z_g = 1, \quad Z_\zeta = 1, \tag{8.136}$$

and

$$\lambda_* = r^2 \lambda_t, \quad 1 = \zeta_* = \zeta. \tag{8.137}$$

Moreover,

$$c_*^2 = Z_c c^2 - \frac{\lambda_t}{16\pi\zeta} Z \left(Z_1 \eta_1 + Z_2 \eta_2 \right) c^2 \left(\frac{1}{\epsilon} + \ell \right). \tag{8.138}$$

Now, we compute the four-point Green's function for π_*^I. The tree level vertex is

$$\math:X = -\frac{NZ}{r^4 \mu^\epsilon \lambda_t} \left[\mathcal{K}^{(4)} + \mathcal{O}^{(4)} + Z_1 \eta_1 \mathcal{U}_1^{(4)} + Z_2 \eta_2 \mathcal{U}_2^{(4)} + Z_c c^2 \mathcal{W}^{(4)} \right]. \tag{8.139}$$

Since Z_c has been obtained from the two-point calculation and the $\mathcal{W}$ vertex does not contribute to any divergent corrections of other four-point terms, $\mathcal{K}^{(4)}$, $\mathcal{O}^{(4)}$, $\mathcal{U}_1^{(4)}$ and $\mathcal{U}_2^{(4)}$, we will thus exclude the $\mathcal{W}^{(n)}$, $n \geq 4$ interactions in the following calculation. We start with the infinite sum of multi-headed quadrupus diagrams:

$$\math:X = \math:X + \math:Y + \math:Z + \cdots \tag{8.140}$$

all of which are of the cactus-type. There are exactly two types of vertices that have nonzero contributions to such multi-headed quadrupus diagrams:

$$(\pi_* \cdot \pi_*)^n \left[\partial_t (\pi_* \cdot \pi_*) \right]^2, \quad (\pi_* \cdot \pi_*)^n \left[\partial^2 (\pi_* \cdot \pi_*) \right]^2. \tag{8.141}$$

An n-headed quadrupus diagram yields

$$-\frac{N}{\mu^\epsilon \lambda_t} \frac{Z^{n+1}}{r^{2n+4}} \left\{ \frac{\lambda_*}{4\pi} \left(\frac{1}{\epsilon} + \ell \right) \right\}^n \left[\mathcal{K}^{(4)} + \mathcal{O}^{(4)} \right], \quad n \geq 1. \tag{8.142}$$

Then,

$$\begin{aligned} \math:X = &-\frac{NZ}{r^4 \mu^\epsilon \lambda_t} \frac{1}{1 - \frac{Z\lambda_*}{4\pi r^2} \left(\frac{1}{\epsilon} + \ell \right)} \left[\mathcal{K}^{(4)} + \mathcal{O}^{(4)} \right] \\ &- \frac{NZ}{r^4 \mu^\epsilon \lambda_t} \left[Z_1 \eta_1 \mathcal{U}_1^{(4)} + Z_2 \eta_2 \mathcal{U}_2^{(4)} \right]. \end{aligned} \tag{8.143}$$

The exact four-point vertex at large N comes from the sum of all cactus diagrams

$$\math:X = \math:X + \math:XX + \math:XXX + \cdots = \math:X + \math:XX \tag{8.144}$$

where

$$\math:X = -\frac{N}{\mu^\epsilon \lambda_*} \left[\mathcal{K}^{(4)} + \mathcal{O}^{(4)} + \eta_1 \mathcal{U}_1^{(4)} + \eta_2 \mathcal{U}_2^{(4)} \right]. \tag{8.145}$$

Further note that

$$\text{\raisebox{0pt}{\includegraphics}} = \frac{NZ}{32\pi\mu^\epsilon} \frac{\lambda_t}{\lambda_*} \left(\frac{1}{\epsilon} + \ell\right) \left\{ \left[2Z_1\eta_1(\eta_1^* + \eta_2^*) + Z_2\eta_2(2\eta_1^* + \eta_2^*)\right]\mathcal{U}_1^{(4)} \right.$$

$$\left. + Z_2\eta_2\eta_2^*\,\mathcal{U}_2^{(4)} \right\}. \qquad (8.146)$$

The renormalization condition (8.52) requires

$$Z = \frac{\lambda_*}{\lambda_t\left[1 + \frac{\lambda_*}{4\pi}\left(\frac{1}{\epsilon} + \ell\right)\right]}, \qquad (8.147)$$

where we have applied $r^2 = \lambda_*/\lambda_t$ from (8.137). At $\ell = 0$ we have $\lambda_* = \lambda_t$ and thus

$$Z = \frac{1}{1 + \frac{\lambda_t}{4\pi\epsilon}}, \qquad (8.148)$$

which further implies

$$\lambda_* = \frac{\lambda_t}{1 - \frac{\lambda_t}{4\pi}\ell}, \qquad r^2 = \frac{1}{1 - \frac{\lambda_t}{4\pi}\ell}. \qquad (8.149)$$

Take $\eta_i^* = \eta_i$, $i = 1, 2$ at $\ell = 0$. The renormalization conditions in (8.53) require

$$Z_1 = \frac{1 + \frac{\lambda_t}{32\pi\epsilon}\frac{\eta_2}{\eta_1}(\eta_1 + \eta_2)}{1 - \frac{(\eta_1+\eta_2)\lambda_t}{16\pi\epsilon}} Z_2, \qquad Z_2 = \frac{1}{1 - \frac{\eta_2\lambda_t}{32\pi\epsilon}}\frac{1}{Z}, \qquad (8.150)$$

and

$$\eta_1^* = \frac{1 - \frac{\lambda_t}{32\pi}\frac{\eta_2}{\eta_1}(\eta_1 + \eta_2)\ell}{1 + \frac{\lambda_t}{16\pi}(\eta_1 + \eta_2)\ell}\frac{\eta_2^*}{\eta_2}\eta_1, \qquad \eta_2^* = \frac{1}{1 + \frac{\eta_2\lambda_t}{32\pi}\ell}\frac{\lambda_t}{\lambda_*}\eta_2. \qquad (8.151)$$

Set $c_* = c$ at $\ell = 0$. Plugging (8.147) and (8.150) back into (8.138) gives

$$Z_c = \frac{1}{1 - \frac{\lambda_t}{16\pi\epsilon}(\eta_1 + \eta_2)}, \qquad (8.152)$$

and

$$c_*^2 = \frac{c^2}{1 + \frac{(\eta_1+\eta_2)\lambda_t}{16\pi}\ell}. \qquad (8.153)$$

Finally, require the physical coupling to be independent of ℓ in (8.137), (8.149), (8.150) and (8.153), we obtain the exact beta functions,

$$\beta_{\lambda_t} = -\frac{\lambda_t^2}{4\pi}, \qquad (8.154)$$

$$\beta_{\eta_1} = \frac{\lambda_t}{32\pi}\left(2\eta_1^2 + 4\eta_1\eta_2 + \eta_2^2 + 8\eta_1\right), \qquad (8.155)$$

$$\beta_{\eta_2} = \frac{\lambda_t}{32\pi}\eta_2(\eta_2 + 8), \tag{8.156}$$

$$\gamma_{c^2} = \frac{\lambda_t}{16\pi}(\eta_1 + \eta_2), \tag{8.157}$$

while the anomalous dimension for π is given by

$$\gamma \equiv \frac{d\log r}{d\ell} = \frac{\lambda_t}{4\pi}. \tag{8.158}$$

These exact RG equations match the one-loop beta functions in Section 8.5. This matching is exactly the same as occurs in the large N limit of the relativistic NLSM.

From (8.148), (8.150) and (8.152) it is clear that the couplings that control the strength of the operators are λ_t, $u_1 \equiv \eta_1\lambda_t$, $u_2 \equiv \eta_2\lambda_t$ and c^2. Note that

$$\beta_{u_1} = \frac{1}{32\pi}\left(2u_1^2 + 4u_1u_2 + u_2^2\right), \tag{8.159a}$$

$$\beta_{u_2} = \frac{1}{32\pi}u_2^2. \tag{8.159b}$$

It is convenient to change into the set of couplings (u, u_2, λ_t), where $u \equiv u_1 + u_2$, in terms of which the beta functions are

$$\beta_{\lambda_t} = -\frac{\lambda_t^2}{4\pi}, \quad \beta_u = \frac{u^2}{16\pi^2}, \quad \beta_{u_2} = \frac{u_2^2}{32\pi^2}, \tag{8.160}$$

which can be solved exactly by

$$\lambda_t = \left(\frac{1}{\lambda_{t0}} + \frac{t}{4\pi}\right)^{-1}, \quad u = \left(\frac{1}{u_0} - \frac{t}{16\pi}\right)^{-1}, \quad u_2 = \left(\frac{1}{u_{20}} - \frac{t}{32\pi}\right)^{-1}, \tag{8.161}$$

where λ_{t0}, u_0 and u_{20} are initial conditions for λ_t, u and u_2, respectively. The theory is asymptotically free in the UV only if $u_0 \leq 0$ and $u_{20} \leq 0$. However, the conditions given in (8.18) that allow the potential to be written as a sum of squares require

$$u_2 \geq -4\lambda_t, \quad u \geq -4\lambda_t, \quad u + u_2 \geq -4\lambda_t. \tag{8.162}$$

If one starts with $\lambda_{t0} \geq 0$, $u_0 \leq 0$ and $u_{20} \leq 0$ that respect the above inequalities, even though the second inequality will be always preserved, the other two inequalities will be violated at a sufficiently large t, unless $u_{20} = 0$ is satisfied exactly. Additionally, in the large N limit, the decay rate is at least suppressed by N^{-1}. In conclusion, the theory is asymptotically free in the UV if one starts with the initial data that satisfies

$$0 \geq u_{10} \geq -4\lambda_{t0}, \quad u_{20} = 0. \tag{8.163}$$

It is also interesting to note that the quadratically divergent contribution to c^2 is

$$\delta c^2 = \frac{\Lambda^2}{8\pi}(u_1 + u_2). \tag{8.164}$$

Furthermore, δc^2 in (8.164) is exactly zero if and only if $u_1 + u_2 = 0$, which is preserved by the RG flow. Setting $u_1 = -u_2 \equiv -\widetilde{u}$,

$$\beta_{\widetilde{u}} = \frac{1}{32\pi}\widetilde{u}^2. \tag{8.165}$$

In order for the entire flow to satisfy the bounds on η_1 and η_2 given in (8.18), we require $\widetilde{u} \geq 0$. In the IR, λ_t increases while u_1 and u_2 decrease to zero, and the theory becomes

$$S = \frac{N}{\lambda_t} \int dt\, d^2\mathbf{x} \left\{ \mathcal{K} + \mathcal{O} \right\}. \tag{8.166}$$

Again, there is a hidden quadratic shift symmetry protecting this action. To make this symmetry manifest, we consider the NLSM as a low energy effective field theory which is completed by a linear sigma model (LSM) in the UV. This has been addressed in [18], which we review in the following. Consider the LSM in $2 + 1$ dimensions for a $O(N)$ vector field ϕ^α, $\alpha = 1, 2, \cdots, N$ in the broken phase with a spatially uniform condensate, which we take to lie along the N-th component such that $\langle \phi^N \rangle = v$. Let us write

$$\phi^\alpha = \left(\Pi^I, v + \Sigma \right), \quad I = 1, 2, \cdots, N - 1. \tag{8.167}$$

We further require Π^I satisfying the quadratic shift symmetry,

$$\Pi^I \to \Pi^I + a_{ij}^I x^i x^j, \tag{8.168}$$

similarly to (8.88). This restricts the LSM to be

$$S_{\text{LSM}} = \frac{1}{2} \int dt\, d^2\mathbf{x} \left\{ \dot{\phi} \cdot \dot{\phi} + \partial^2\phi \cdot \partial^2\phi \right\}. \tag{8.169}$$

In terms of the variables,
$$\phi^\alpha = r \left(\pi^I, \sqrt{1 - \pi \cdot \pi} \right), \tag{8.170}$$

and integrating out the gapped radial field $r - v$ in (8.169) gives (8.166) classically. In the large N limit, these two theories become the same at the quantum level.

In this chapter we discussed aspects of the $2 + 1$ dimensional nonlinear sigma model at a $z = 2$ Lifshitz fixed point. After constructing the theory in Section 8.1, we examined the conditions imposed on the couplings by requiring that the potential be a sum of complete squares. Then, we studied the one-loop quantum behavior of the system and obtained the beta functions for all couplings. A perturbatively stable asymptotically free region is identified. Due to the quadratic shift symmetry that simultaneously protects the smallness of the coupling constant g and the speed of light c, the theory can naturally flow towards a $z = 1$ fixed point in the IR and appears to be relativistic for low energy observers. The detailed balance condition is preserved under RG flow if $c = 0$. At detailed balance, the theory can be supersymmetrized, borrowing from the methods of stochastic quantization, which enjoys the

Parisi-Sourlas supersymmetry [98]. In the equilibrium limit, this theory corresponds to the topological harmonic sigma model [99]. The connection between the nonrelativistic NLSM and the topological harmonic sigma model is somewhat analogous to the connection between the (2+1) dimensional Rokhsar-Kivelson model and the 2-dimensional statistical mechanical models of dimers. Finally, we extended the beta function calculation to all loop order in the large N limit by summing over all cactus diagrams, which is further cross-checked in a nonperturbative manner by applying the steepest descent method.

In $(2-\epsilon)+1$ dimensions, there exists a scale-invariant fixed point at the critical coupling constant if the theory is also taken to be at detailed balance. This conformal fixed point may be important for the study of critical phenomena in Aristotelian-type theories.

Another interesting future direction is to include topological terms. In (2+1) dimensions, the $O(5)$ and $O(4)$ NLSMs can be augmented with the Wess-Zumino-Witten (WZW) term, and the θ term, respectively. These theories have been discussed, *e.g.*, in the context of deconfined quantum criticality, the quantum spin Hall effect (topological insulators), and graphene. (See, for example, [100, 101, 102, 103]). While the effect of the Wess-Zumino-Witten term in (1+1)-dimensional NLSMs and principal chiral models have been well-understood, *e.g.*, it is known that the $O(3)$ NLSM in (1+1) dimensions with a topological θ term ($\theta = \pi$) flows to a nontrivial fixed point, *i.e.*, a $SU(2)_1$ WZW theory [104], relatively little is known in higher dimensions. It is noted that one cannot develop a controlled RG calculation of the relativistic $O(5)$ NLSM in (2+1) dimensions with the WZW term [105]. On the other hand, the Aristotelian $O(N)$ NLSM studied in this work may provide a natural and convenient platform to study the effects of the topological term. It is expected that there is a nontrivial fixed point describing a (2+1)-dimensional CFT. [9]

---

[9]In a recent work [106], the effects of the WZW term in a relativistic NLSM in (2+1) dimensions were studied in the large N limit. To have a well-controlled RG calculation and a well-defined topological term, they chose to work with Grassmannian manifolds as their target space.

Chapter 9

Quantization of Hořava Gravity in $2 + 1$ Dimensions

Throughout the thesis, we mainly worked with Aristotelian QFTs of scalars. Even in this very simple case, mapping out the role of technical naturalness in nonrelativistic systems with Aristotelian spacetime symmetries has led to many surprises. In this last chapter of the thesis, we extend our study of nonrelativistic naturalness to systems with gauge symmetries, in particular to gravity. In these more complicated systems with gauge symmetries, we expect more interesting surprises to appear.

The Aristotelian spacetime is the ground-state solution to Hořava gravity. Considerable effort has been devoted to the study of Hořava gravity since it was introduced in [5, 6]. Being renormalizable by naïve power counting, Hořava's theory constitutes a candidate for an ultraviolet-complete theory of quantum gravity. In spite of some work [107, 108, 109, 110], nonetheless, as yet there have been no fully satisfactory quantum computations; in fact, perturbative renormalizability of one version — the "projectable" model — was established only recently [111].

The purpose of the present chapter is to take a step forward in understanding quantum corrections to Hořava gravity by making a careful computation of a one-loop quantity working in non-singular gauges. (What we mean by this is explained in Sections 9.2 and 9.4.) More specifically, the model we consider is $z = 2$ projectable Hořava gravity in $2 + 1$ dimensions, and the quantity we compute is the anomalous dimension of the cosmological constant.[1]

Hořava gravity is constructed so that, at high energies, the classical action has anisotropic scale invariance with the dynamical critical exponent z:

$$t \to b^z \, t, \qquad \mathbf{x} \to b \, \mathbf{x}. \tag{9.1}$$

As our interest is in $z = 2$, we take the engineering dimensions of the time and space

---

[1]In anisotropic models, the effective coefficients of the temporal and spatial kinetic terms can scale differently — *i.e.*, the dispersion relation runs with scale. This running can be captured by fixing the form in which either the energy or the spatial momentum appears in the dispersion relation. We compute the anomalous dimension of Λ with respect to a normalization condition that fixes the form of the spatial momentum contribution.

coordinates to be

$$[t] = -1, \qquad [\mathbf{x}] = -\frac{1}{2}. \tag{9.2}$$

In this convention, energy is of dimension one. The $z = 2$ theory is renormalizable in $2+1$ dimensions [111].

The spacetime manifold is equipped with a foliation by leaves of codimension one, corresponding to the surfaces of constant time. Its geometry is naturally parametrized using the ADM variables – a spatial scalar N (the lapse), a spatial vector N_i (the shift), and a spatial metric g_{ij}. The classical scaling dimensions of the fields are

$$[N] = 0, \qquad [N_i] = \frac{1}{2}, \qquad [g_{ij}] = 0. \tag{9.3}$$

The gauge symmetries are the diffeomorphisms that preserve the foliation. We parametrize the infinitesimal transformations by (Z, X^i),

$$\delta t = Z(t), \qquad \delta x^i = X^i(t, \mathbf{x}), \tag{9.4}$$

that act on the fields by

$$\delta N = \partial_t(Z\,N) + X^k \nabla_k N, \tag{9.5a}$$
$$\delta N^i = \partial_t(Z\,N^i) + (\partial_t - N^k \nabla_k) X^i + X^k \nabla_k N^i, \tag{9.5b}$$
$$\delta g_{ij} = Z \dot{g}_{ij} + \nabla_i X_j + \nabla_j X_i. \tag{9.5c}$$

A proper understanding of Hořava gravity requires a careful treatment of its gauge fixing. To this end, it is useful to begin with the simplest model possible. It is tempting to begin with the conformal case in $2+1$ dimensions, because it has no local propagating degrees of freedom. Unfortunately, not only does it require the "non-projectable" version of the theory, which has second class constraints and their attendant difficulties, but also it raises the thorny issue of gauge anomalies for the Weyl symmetry.

A more modest starting point is "projectable" Hořava gravity in $2+1$ dimensions. Projectability is the condition that $N = N(t)$ be a function of time but not of space, so that it is constant on each spatial slice. We assume this condition for the remainder of this chapter. The $2+1$ dimensional projectable case is more than just a toy model for understanding the qualitative behavior of the more realistic $3+1$ dimensional non-projectable theory. Mapping out the renormalization group structure of the projectable theory is important to further understand the phases of gravity, both in the context of Hořava gravity and the Causal Dynamical Triangulation approach to quantum gravity [112, 113].

The action is written in terms of quantities invariant under those diffeomorphisms preserving the foliation of spacetime, namely scalars built from the intrinsic and extrinsic curvatures of the leaves of the foliation and their covariant derivatives. The intrinsic curvature of a two-dimensional leaf is completely determined by its spatial Ricci scalar R. The extrinsic curvature is captured by the tensor

$$K_{ij} = \frac{1}{2N}(\dot{g}_{ij} - \nabla_i N_j - \nabla_j N_i), \tag{9.6}$$

where ∇_i is the covariant derivative with respect to g_{ij}. The most general $z = 2$ action invariant under (9.5) is

$$S = \frac{1}{\kappa^2} \int dt\, d^2\mathbf{x}\, N\sqrt{g} \left\{ K_{ij}K^{ij} - \lambda K^2 - \gamma R^2 + \rho R - 2\Lambda \right\}, \tag{9.7}$$

where $K = g^{ij}K_{ij}$. Since $\int d^2\mathbf{x}\sqrt{g}R$ is a topological invariant in two dimensions, ρ does not appear in the local equations of motion, but only in the global Hamiltonian constraint arising from time reparametrization symmetry. As a result ρ cannot contribute to the perturbative beta function, and so we drop this term in what follows.[2]

In general dimension, projectable Hořava gravity has a transverse traceless tensor mode and a scalar mode. Requiring the tensor polarizations to have a good dispersion relation around flat space then implies that $\gamma > 0$. Requiring the dispersion of the scalar also to be healthy imposes the constraint

$$\lambda < \frac{1}{2} \quad \text{or} \quad \lambda > 1. \tag{9.8}$$

In $2+1$ dimensions, however, there are no tensor modes. We then have the option of setting γ to be negative when $\frac{1}{2} < \lambda < 1$. The propagating spectrum of the theory is then healthy, at least classically. We do not worry about this explicitly in what follows, although our final result makes sense in this parameter region.

In this chapter, we will compute contributions to the effective action using the background field method. In this method, fields are split into a sum of two terms: a classical background value, and quantum fluctuations of typical size $\hbar^{1/2}$. For the action (9.7), the role of $\hbar$ is played by κ^2. This leads us to expand

$$N = \overline{N} + \kappa\, n, \qquad N^i = \overline{N}^i + \kappa\, n^i, \qquad g_{ij} = \overline{g}_{ij} + \kappa\, h_{ij}, \tag{9.9}$$

where $\overline{N}$, $\overline{N}^i$ and $\overline{g}_{ij}$ are background fields and n, n^i and h_{ij} are fluctuations around the given background. Gauge transformations can also be expanded in powers of κ,

$$Z = \overline{Z} + \kappa\, \zeta, \qquad X^i = \overline{X}^i + \kappa\, \xi^i, \tag{9.10}$$

with $(\overline{Z}, \overline{X}^i)$ the background diffeomorphisms, and (ζ, ξ^i) the physical gauge symmetries of the quantum fluctuations. Due to the projectability condition, we can use $(\overline{Z}, \overline{X}^i)$ to set

$$\overline{N} = 1, \qquad \overline{N}^i = 0. \tag{9.11}$$

In this gauge, the action of ζ and ξ^i (to linear order in κ) is

$$\delta n = \dot{\zeta} + O(\kappa), \tag{9.12a}$$

---

[2]On the other hand, it may very well contribute to the full non-perturbative beta function through instanton corrections. Also note that, while it cannot contribute to the perturbative beta function, in principle ρ itself may have a non-zero perturbative beta function that depends only on the other couplings in the theory. For dimensional reasons, however, its beta function vanishes at one loop. (See Section 9.6.)

$$\delta n^i = \dot{\xi}^i + O(\kappa), \tag{9.12b}$$

$$\delta h_{ij} = \overline{\nabla}_i \xi_j + \overline{\nabla}_j \xi_i + O(\kappa). \tag{9.12c}$$

Here, $\overline{\nabla}_i$ denotes the Christoffel connection for $\overline{g}_{ij}$. We can use ζ to set $n \equiv 0$; since n is independent of space and so has only one degree of freedom per spatial slice, it does not contribute divergences. For our purposes, therefore, we can ignore the contribution from n to the path integral.

In the following, we will work only on backgrounds that are time-independent. We express the partition function in terms of functional determinants by integrating out the quantum fluctuations n_i and h_{ij}, and the gauge-fixing ghost modes. The one-loop effective action is then evaluated using heat kernel techniques. This will allow us to compute some (but not all) of the one-loop beta functions in the theory. To fully understand the RG properties of the theory at weak coupling (and in particular, determine whether the theory is asymptotically free), it is necessary to evaluate the heat kernel on background geometries with a time-dependent metric. We leave this to future work.

Previous work on the one-loop effective action in gravity with anisotropic scaling [114] overlooked crucial contributions from the gauge-fixing sector of the theory, a problem exacerbated by dropping from the partition function altogether singular determinants that did not cancel out in their analysis. We show that such confusion can be avoided by an appropriate choice of gauge. The gauge-fixing methods we developed have, in the meantime, appeared in a more general form in the work of [111], which applied them to show the renormalizablility of projectable Hořava gravity. We take advantage of their more general gauge in Section 9.2 for reasons of clarity, although the bulk of our computation uses our more restrictive original gauge.

Section 9.1 and Section 9.2 develops the gauge-fixing method and field parametrizations we use in the remainder of this chapter in the simpler context of linearized theories. Before embarking on the gravitational calculation, we begin in Section 9.1 with a warm-up – free $U(1)$ gauge theory in $D+1$ dimensions with $z=2$ scaling at short distances. One natural choice in this context, used in [115], is temporal gauge. Here, we utilize a gauge choice that manifestly respects the $z=2$ scaling symmetry. Generalizing this gauge-fixing procedure to the gravitational case will lead us in Section 9.2 to the same sort of gauge-fixing condition used by [111] in proving perturbative renormalizability of projectable Hořava gravity. Section 9.3 uses these results to compute the dependence of the one-loop effective action on the cosmological constant, which illustrates how the effective action can depend on gauge, and how to extract the correct gauge-invariant effective action.

Section 9.4 turns to computations in curved space using the background field method. There, we compute the partition function on static on-shell curved backgrounds ($\overline{R} = \text{const}$, $\partial_t \overline{g}_{ij} = 0$) supported by non-vanishing Λ. Working with an on-shell background enables us to systematically disentangle the physical and unphysical modes and observe explicitly the cancellation of the unphysical modes among themselves. We give an explicit expression for the physical dispersion relation, which generalizes the flat space result. We normalize

the gravitational field such that γ/κ^4 is constant at all energy scales. With respect to this choice of normalization condition, we are able to determine the anomalous dimension of Λ. Extracting the beta functions for γ, λ and κ requires working on backgrounds that depend on time, which we leave to future research.

9.1 Aristotelian $U(1)$ Gauge Theory

In gauge theories exhibiting an anisotropic scaling symmetry of the form $(t, \mathbf{x}) \mapsto (b\,t, b^{1/z}\mathbf{x})$, it is desirable to choose a gauge-fixing condition that respects this symmetry. This is especially true in models at their critical dimension, for which standard gauges – in particular, Lorenz gauge – may not be renormalizable.

In some simple cases (*e.g.,* free Maxwell theory), there is no problem with singular gauges, such as the temporal or Coulomb gauges, which are in fact invariant under the scaling symmetry for any value of z. When the theory is coupled to gravity, however, such gauges can become problematic. For example, in temporal gauge the Faddeev-Popov determinant is $\det(\partial_t)$. While in the flat case this determinant can be dropped, in the gravitational case it couples non-trivially and should not be ignored. However, such operators have no dependence on large spatial momenta, leading to uncontrolled ultraviolet divergences. Moreover, this problem persists in both dimensional regularization and heat-kernel based methods. Such gauges therefore give rise to ambiguities, which need to be resolved in a manner consistent with BRST symmetry. From a more pedestrian perspective, our strategy ensures that the gauge-fixing Lagrangian, which is quadratic in the gauge-fixing condition, is of the same order in derivatives as the original Lagrangian. Thus, the two can be combined more seamlessly.

In the first two sections, our goal is to introduce[3] such gauges in linearized $z = 2$ gravity. In this section, we illustrate the process in free anisotropic $U(1)$ gauge theory. This serves as a warm-up to the second case of $z = 2$ projectable Hořava gravity in $2 + 1$ dimensions linearized around flat space in the next section. We will apply these results to make a simple quantum computation. Section 9.4 will be concerned with the generalization to static backgrounds in the background field method.

We begin with free $U(1)$ gauge theory in $D+1$ dimensions exhibiting $z = 2$ scaling in the UV and $z = 1$ in the IR. The gauge field is a $U(1)$ connection on Aristotelian spacetime [23]. The time and space components, A_0 and A_i ($i = 1, \cdots, D$), have gauge transformations,

$$\delta A_0 = \dot{\zeta}, \qquad \delta A_i = \partial_i \zeta, \tag{9.13}$$

with $\zeta(t, \mathbf{x})$ an arbitrary scalar function. The invariant field strengths are

$$E_i = \dot{A}_i - \partial_i A_0, \qquad F_{ij} = \partial_i A_j - \partial_j A_i. \tag{9.14}$$

---

[3]The gauges we use in this chapter also appeared in the work of [111], where they were used to demonstrate the perturbative renormalizability of projectable Hořava gravity. We originally arrived at them as a way to remove singular behavior in the background field formalism while preserving anisotropic Weyl invariance.

At the ultraviolet $z = 2$ Gaussian fixed point, the engineering dimensions of the gauge fields are

$$[A_0] = \frac{D}{4}, \qquad [A_i] = \frac{D}{4} - \frac{1}{2}. \tag{9.15}$$

The basic most generic action with this scaling in the UV that is invariant under both the spacetime and gauge symmetries (including parity and time-reversal) is

$$S = \int dt \, d^D \mathbf{x} \Big\{ \frac{1}{2} E_i E_i - \frac{1}{4} \partial_k F_{ij} \partial_k F_{ij} - \frac{1}{4} v^2 F_{ij} F_{ij} \Big\}, \tag{9.16}$$

where v is the "speed of light" in the infrared.

In components, the action becomes

$$S = \frac{1}{2} \int dt \, d^D \mathbf{x} \Big\{ \partial_i A_0 \partial_i A_0 + \dot{A}_i \dot{A}_i - 2 \dot{A}_i \partial_i A_0 - A_i \left(\partial^2 - v^2 \right) \left(\delta_{ij} \partial^2 - \partial_i \partial_j \right) A_j \Big\}$$
$$= \frac{1}{2} \int dt \, d^D \mathbf{x} \left(A_0 \quad A_i \right) S^{(2)} \begin{pmatrix} A_0 \\ A_j \end{pmatrix}, \tag{9.17}$$

where

$$S^{(2)} = \begin{pmatrix} -\partial^2 & \partial_j \partial_t \\ \partial_t \partial_i & \mathcal{O} \delta_{ij} + (\partial^2 - v^2) \partial_i \partial_j \end{pmatrix}, \tag{9.18}$$

and $\mathcal{O}$ is the generalized d'Alebertian operator,

$$\mathcal{O} = -\partial_t^2 - \partial^4 + v^2 \partial^2. \tag{9.19}$$

A natural $z = 2$ generalization of the Lorenz gauge is given by the gauge-fixing functional

$$f[A] = \dot{A}_0 - (-\partial^2 + v^2) \partial_i A_i. \tag{9.20}$$

To quantize the theory with this gauge-fixing, we should further introduce a pair of fermionic ghosts (b, c), a bosonic auxiliary field Φ, and the fermionic BRST differential s acting on the fields as

$$s A_0 = \dot{c}, \qquad s A_i = \partial_i c, \qquad s b = \Phi, \qquad s\Phi = sc = 0. \tag{9.21}$$

A generalized $\mathcal{R}_\xi$ gauge-fixing action based on (9.20) can now be obtained from a gauge-fixing fermion of the form

$$\Psi = \int dt \, d^D \mathbf{x} \, b \Big\{ \frac{1}{2} \mathcal{D}\Phi - f[A] \Big\}. \tag{9.22}$$

Note that, unlike standard $\mathcal{R}_\xi$ gauge, if we wish to avoid introducing dimensionful parameters then $\mathcal{D}$ must be a differential operator of dimension one. The BRST-exact action is

$$s\Psi = \int dt \, d^D \mathbf{x} \Big\{ \frac{1}{2} \Phi \mathcal{D}\Phi - \Phi f[A] + b\mathcal{O}c \Big\}, \tag{9.23}$$

The resulting BRST-invariant gauge-fixed action is

$$S_{\text{BRST}} = S + s\Psi, \tag{9.24}$$

giving the quantum partition function

$$\mathcal{Z} = \int \mathcal{D}\{A_0, A_i, b, c, \Phi\} \, e^{iS_{\text{BRST}}}. \tag{9.25}$$

As in the case of the standard $\mathcal{R}_\xi$-gauge procedure, the partition function is independent of $\mathcal{D}$.

Setting $\mathcal{D} = -\partial^2 + v^2$ is a particularly nice choice, as it eliminates the cross-terms between A_0 and A_i, after integrating out Φ. Redefining the A_0 field via $A_0 \to \sqrt{\mathcal{D}} \, A_0$ results in a Jacobian $\mathcal{J}_{A_0} = (\det \mathcal{D})^{1/2}$, which cancels the factor of $(\det \mathcal{D})^{-1/2}$ produced by the integral over Φ. The action then becomes

$$S_{\text{BRST}}[A_0, A_i, b, c] = \int dt \, d^D\mathbf{x} \left\{ -\frac{1}{2} A_0 \mathcal{O} A_0 + \frac{1}{2} A_i \mathcal{O} A_i + b \mathcal{O} c \right\}. \tag{9.26}$$

The overall sign in front of the piece quadratic in A_0 in (9.26) is negative, so we must Wick rotate A_0 when we rotate t. The partition function evaluates to

$$\mathcal{Z} = (\det \mathcal{O})^{-\frac{D-1}{2}}. \tag{9.27}$$

This represents $D - 1$ physical propagating modes with dispersion relation

$$\omega^2 = k^4 + v^2 k^2. \tag{9.28}$$

Before we move on to Hořava gravity, we make the following comment. As in the Lorentz-invariant theory, one can diagonalize the kinetic operator of (9.17) explicitly in field space, without gauge-fixing. There is one pure gauge mode on which the operator vanishes completely. There is also one unphysical mode which gets a wrong-sign dispersion relation. The rest of the modes should then reproduce the correct dispersion relation (9.28).

9.2 Hořava Gravity Around Flat Space

We now turn to the linearization of $z = 2$ projectable Hořava gravity in $(2 + 1)$ dimensions around flat space, with $\bar{g}_{ij}$ in (9.9) set to δ_{ij}. The flat background is on-shell if the cosmological constant Λ is set to zero. However, since we are also interested in the Λ dependence of the off-shell effective action, we will allow for a nonzero Λ.

The action is that of (9.7), with $\rho = 0$. The quadratic part[4] of the action is

$$S_{\text{quad}} = \int dt \, d^2\mathbf{x} \left\{ \frac{1}{4} \left(\dot{h}_{ij}\dot{h}_{ij} - \lambda \dot{h}^2 \right) - \dot{h}_{ij}\partial_i n_j + \lambda \, \dot{h}\partial_i n_i + \frac{1}{2}\partial_i n_j \partial_i n_j - \left(\lambda - \frac{1}{2} \right)(\partial_i n_i)^2 \right.$$

---

[4]Since we are interested in the effective action, we drop the linear part, which is non-vanishing when $\Lambda \neq 0$.

$$- \gamma(\partial_i\partial_j h_{ij} - \partial^2 h)^2 + \frac{\Lambda}{4}(2h_{ij}h_{ij} - h^2)\Big\}$$

$$= \frac{1}{2}\int dt\, d^2\mathbf{x}\, \begin{pmatrix} n_i & h_{ik}\end{pmatrix} S^{(2)}\begin{pmatrix} n_j \\ h_{j\ell}\end{pmatrix}, \tag{9.29}$$

where $h \equiv h_{ii}$, and the matrix $S^{(2)}$ is the second functional derivative of the action. Explicitly,

$$S^{(2)} = \begin{pmatrix} S^{(2)}_{nn} & S^{(2)}_{nh} \\ S^{(2)}_{hn} & S^{(2)}_{hh}\end{pmatrix}, \tag{9.30}$$

with

$$S^{(2)}_{nn} = -\delta_{ij}\partial^2 + (2\lambda - 1)\partial_i\partial_j, \tag{9.31a}$$

$$S^{(2)}_{nh} = \left[S^{(2)}_{hn}\right]^{\dagger} = \frac{1}{2}\big(\delta_{ij}\partial_\ell + \delta_{i\ell}\partial_j - 2\lambda\delta_{j\ell}\partial_i\big)\partial_t, \tag{9.31b}$$

$$S^{(2)}_{hh} = -\frac{1}{4}\big(\delta_{ij}\delta_{k\ell} + \delta_{i\ell}\delta_{jk} - 2\lambda\delta_{ik}\delta_{j\ell}\big)\partial_t^2 + \frac{\Lambda}{2}\big(\delta_{ij}\delta_{k\ell} + \delta_{i\ell}\delta_{jk} - \delta_{ik}\delta_{j\ell}\big)$$
$$- 2\gamma\left[\delta_{ik}\delta_{j\ell}\partial^4 - (\delta_{ik}\partial_j\partial_\ell + \delta_{j\ell}\partial_i\partial_k)\partial^2 + \partial_i\partial_j\partial_k\partial_\ell\right]. \tag{9.31c}$$

Intuitively, one can think of this theory as "adding a spatial index" to the $U(1)$ gauge theory of the previous section: n_i is analogous to A_0, and h_{ij} to A_i. Likewise, the gauge-fixing functional f_i, ghost fields b_i and c_i, and bosonic auxiliary field Φ_i all carry a spatial index. The BRST differential s acts as

$$sn_i = \dot{c}_i, \qquad sh_{ij} = \partial_i c_j + \partial_j c_i, \qquad sb_i = \Phi_i, \qquad s\Phi_i = sc_i = 0. \tag{9.32}$$

In analogy with the $U(1)$ theory, we choose the gauge-fixing fermion

$$\Psi = \int dt\, d^2\mathbf{x}\, b_i\Big\{\frac{1}{2}\mathcal{D}_{ij}\Phi_j - f_i\Big\}, \tag{9.33}$$

where $\mathcal{D}_{ij}$ is some spatial differential operator of dimension one, and f_i is a gauge-fixing functional. As pointed out in [111], the most general such operator is

$$\mathcal{D}_{ij} = -\mathfrak{u}_1\delta_{ij}\partial^2 - \mathfrak{u}_2\,\partial_i\partial_j\,, \tag{9.34}$$

where $\mathfrak{u}_1$ and $\mathfrak{u}_2$ are constants.

The analog of the gauge-fixing condition (9.20) reads $f_i = \dot{n}_i - \mathcal{D}_{ijk}h_{jk}$, where $\mathcal{D}_{ijk}$ is a spatial differential operator of energy dimension $\frac{3}{2}$ (e.g., containing three spatial derivatives). Forcing the cross-terms between n_i and h_{ij} to vanish upon integrating out Φ_i uniquely determines $\mathcal{D}_{ijk}$ to be $\mathcal{D}_{ijk} = \mathcal{D}_{ij}\partial_k - \lambda\delta_{jk}\mathcal{D}_{i\ell}\partial_\ell$:

$$f_i = \dot{n}_i - \mathcal{D}_{ij}(\partial_k h_{jk} - \lambda\partial_j h)$$
$$= \dot{n}_i + \mathfrak{u}_1\,\partial^2\partial_j h_{ij} + \mathfrak{u}_2\,\partial_i\partial_j\partial_k h_{jk} - \lambda\mathfrak{u}\,\partial^2\partial_i h, \tag{9.35}$$

where $\mathfrak{u} = \mathfrak{u}_1 + \mathfrak{u}_2$. As before, the final result is independent of the particular choice of $\mathcal{D}_{ijk}$.

The analog of the BRST-exact action (9.23) is

$$S' = s\Psi = \int dt\, d^2\mathbf{x} \left\{ \frac{1}{2}\Phi_i \mathcal{D}_{ij}\Phi_j - \Phi_i f_i[h,n] + b_i \mathcal{O}_{ij} c_j \right\}, \tag{9.36}$$

where

$$\begin{aligned}
\mathcal{O}_{ij} &= -\delta_{ij}\partial_t^2 + \mathcal{D}_{ik}\big[\delta_{jk}\partial^2 - (2\lambda-1)\partial_j\partial_k\big] \\
&= \delta_{ij}\big(-\partial_t^2 - \mathfrak{u}_1\partial^4\big) + 2\big[(\lambda - \tfrac{1}{2})\mathfrak{u}_1 + (\lambda-1)\mathfrak{u}_2\big]\partial^2\partial_i\partial_j.
\end{aligned} \tag{9.37}$$

We can immediately read off the ghost partition function,

$$\mathcal{Z}_{\text{ghost}} = \det \mathcal{O}_{ij} = (\det \mathcal{O}_g)(\det \widetilde{O}_g), \tag{9.38}$$

where

$$\mathcal{O}_g = -\partial_t^2 - 2\mathfrak{u}(1-\lambda)\partial^4, \qquad\qquad \widetilde{\mathcal{O}}_g = -\partial_t^2 - \mathfrak{u}_1\partial^4. \tag{9.39}$$

The rest of the action, after integrating out Φ_i, called the "effective" part, reads

$$S_{\text{eff}}[n_i, h_{ij}] = \frac{1}{2}\int dt\, d^2\mathbf{x} \left\{ -n_i S^{(2)}_{ij} n_j + h_{ij} S^{(2)}_{ijk\ell} h_{k\ell} \right\}, \tag{9.40}$$

where

$$S^{(2)}_{ij} = \mathcal{D}^{-1}_{ik} \mathcal{O}_{kj}, \tag{9.41a}$$

$$\begin{aligned}
S^{(2)}_{ijk\ell} &= \frac{1}{4}(\delta_{ik}\delta_{j\ell} + \delta_{i\ell}\delta_{jk})(-\partial_t^2 + 2\Lambda) - \frac{1}{4}\delta_{ij}\delta_{k\ell}(-2\lambda\partial_t^2 - 4\lambda^2\mathcal{D}_{mn}\partial_m\partial_n + 8\gamma\partial^4 + 2\Lambda) \\
&\quad - 2\gamma\partial_i\partial_j\partial_k\partial_\ell + 2\gamma(\delta_{ij}\partial_k\partial_\ell + \delta_{k\ell}\partial_i\partial_j)\partial^2 \\
&\quad + \frac{1}{4}(\mathcal{D}_{ik}\partial_j\partial_\ell + \mathcal{D}_{i\ell}\partial_j\partial_k + \mathcal{D}_{jk}\partial_i\partial_\ell + \mathcal{D}_{j\ell}\partial_i\partial_k) \\
&\quad - \frac{\lambda}{2}\big[\delta_{ij}(\mathcal{D}_{km}\partial_\ell + \mathcal{D}_{\ell m}\partial_k) + \delta_{k\ell}(\mathcal{D}_{im}\partial_j + \mathcal{D}_{jm}\partial_i)\big]\partial_m.
\end{aligned} \tag{9.41b}$$

Note that various field components need to be Wick-rotated as well as the time when performing the path integral. The contribution of n_i to the partition function is

$$\mathcal{Z}_n = \big(\det S^{(2)}_{ij}\big)^{-1/2} = (\det \mathcal{D}_{ik})^{1/2} (\det \mathcal{O}_{ij})^{-1/2}. \tag{9.42}$$

Next, we compute the contribution to the partition function from h_{ij}. We first decompose h_{ij} as

$$h_{ij} = H_{ij} + \frac{1}{2}h\delta_{ij}, \tag{9.43}$$

where $H_{ii} = 0$. We decompose H_{ij} further as

$$H_{ij} = H_{ij}^{\perp} + \partial_i \eta_j + \partial_j \eta_i + \left(\partial_i \partial_j - \frac{1}{2} \delta_{ij} \partial^2 \right) \sigma, \tag{9.44}$$

with constraints

$$H_{ii}^{\perp} = 0, \qquad\qquad \partial_j H_{ij}^{\perp} = 0, \qquad\qquad \partial_i \eta_i = 0. \tag{9.45}$$

In two spatial dimensions, the transverse traceless component $H_{ij}^{\perp}$ has no local degrees of freedom, and in flat space is forced by boundary conditions to vanish. Furthermore, in two dimensions, one can parametrize η_i as

$$\eta_i = \epsilon_{ij} \partial_j \eta. \tag{9.46}$$

Thus, H_{ij} is finally parametrized as

$$H_{ij} = (\epsilon_{ik} \partial_j + \epsilon_{jk} \partial_i) \partial_k \eta + \left(\partial_i \partial_j - \frac{1}{2} \delta_{ij} \partial^2 \right) \sigma. \tag{9.47}$$

We require the Jacobian for this change of variables. The Jacobian for (9.43) is a constant. The Jacobian for (9.47) is computed in Appendix D,

$$\mathcal{J}_H = \left[\det(-\partial^2) \right]^2. \tag{9.48}$$

We can eliminate this Jacobian altogether by changing variables from η and σ to

$$\widetilde{\eta} = \partial^2 \eta, \qquad\qquad \widetilde{\sigma} = \partial^2 \sigma. \tag{9.49}$$

The action for $\widetilde{\eta}$ is just

$$S_{\widetilde{\eta}} = \frac{1}{2} \int dt\, d^2\mathbf{x}\, \widetilde{\eta}\, S_{\widetilde{\eta}}^{(2)} \widetilde{\eta}, \tag{9.50}$$

where

$$S_{\widetilde{\eta}}^{(2)} = -\partial_t^2 - \mathfrak{u}_1 \partial^4 + 2\Lambda = \widetilde{\mathcal{O}}_g + 2\Lambda. \tag{9.51}$$

Therefore, the contribution of $\widetilde{\eta}$ to the partition function is

$$\mathcal{Z}_{\widetilde{\eta}} = \left(\det S_{\widetilde{\eta}}^{(2)} \right)^{-1/2} = \frac{1}{\sqrt{\det\left(\widetilde{\mathcal{O}}_g + 2\Lambda \right)}}. \tag{9.52}$$

Meanwhile, h and $\widetilde{\sigma}$ remain coupled via the action

$$S_{h\widetilde{\sigma}} = \frac{1}{2} \int dt\, d^2\mathbf{x} \begin{pmatrix} h & \widetilde{\sigma} \end{pmatrix} S_{h\widetilde{\sigma}}^{(2)} \begin{pmatrix} h \\ \widetilde{\sigma} \end{pmatrix}, \tag{9.53}$$

where

$$S_{h\widetilde{\sigma}}^{(2)} = \frac{1}{2} \begin{pmatrix} -\left(\frac{1}{2} - \lambda\right)\partial_t^2 - \left[\gamma + 2\left(\frac{1}{2} - \lambda\right)^2 \mathfrak{u}\right]\partial^4 & \left[\gamma - \left(\frac{1}{2} - \lambda\right)\mathfrak{u}\right]\partial^4 \\ \left[\gamma - \left(\frac{1}{2} - \lambda\right)\mathfrak{u}\right]\partial^4 & -\frac{1}{2}\left[\partial_t^2 + (2\gamma + \mathfrak{u})\partial^4 - 2\Lambda\right] \end{pmatrix}. \tag{9.54}$$

The matrix $S_{h\widetilde{\sigma}}^{(2)}$ is diagonal only for the choice

$$\mathfrak{u} = \frac{\gamma}{\frac{1}{2} - \lambda}. \tag{9.55}$$

For general gauge parameters, $S_{h\widetilde{\sigma}}^{(2)}$ can't be diagonalized locally. When $\Lambda = 0$, however, the determinant itself factorizes neatly,

$$\mathcal{Z}_{h\widetilde{\sigma}}\Big|_{\Lambda=0} = \frac{1}{\sqrt{\left(\det \mathcal{O}_g\right)\left(\det \mathcal{O}_{\text{phys}}\right)}}, \tag{9.56}$$

where

$$\mathcal{O}_{\text{phys}} = -\left(\frac{1}{2} - \lambda\right)\partial_t^2 - 2\gamma\left(1 - \lambda\right)\partial^4. \tag{9.57}$$

The operator $\mathcal{O}_{\text{phys}}$ is independent of the gauge-fixing parameters $\mathfrak{u}_1$ and $\mathfrak{u}_2$.

In summary, the modes corresponding to the various dispersion relations are

$$h, \widetilde{\sigma}, n_i \text{ and ghost} : \mathcal{O}_g = -\partial_t^2 - 2\left(1 - \lambda\right)\mathfrak{u}\partial^4, \tag{9.58a}$$

$$\widetilde{\eta}, n_i \text{ and ghost} : \widetilde{\mathcal{O}}_g = -\partial_t^2 - \mathfrak{u}_1\partial^4, \tag{9.58b}$$

$$h, \widetilde{\sigma} : \mathcal{O}_{\text{phys}} = -\left(\frac{1}{2} - \lambda\right)\partial_t^2 - 2\gamma\left(1 - \lambda\right)\partial^4. \tag{9.58c}$$

For these to have the right sign dispersion relation requires

$$\mathfrak{u}_1 > 0, \qquad (1 - \lambda)\mathfrak{u} > 0. \tag{9.59}$$

Note that the "nice gauge" of [111] is when all three of the dispersions, including the unphysical ones, are actually identical. This condition is satisfied if and only if

$$\mathfrak{u}_1 = 2\gamma\frac{1 - \lambda}{\frac{1}{2} - \lambda}, \qquad\qquad \mathfrak{u} = \frac{\gamma}{\frac{1}{2} - \lambda}. \tag{9.60}$$

Finally, the total on-shell partition function is the product of (9.38), (9.42), (9.52), (9.56) and the extra factor of $(\det \mathcal{D}_{ij})^{-1/2}$ from integration over Φ_i. The result simplifies greatly,

$$\mathcal{Z}\Big|_{\Lambda=0} = \frac{1}{\sqrt{\det \mathcal{O}_{\text{phys}}}}. \tag{9.61}$$

This represents one physical degree of freedom, with dispersion relation

$$\omega^2 = 2\gamma\frac{1 - \lambda}{\frac{1}{2} - \lambda}k^4. \tag{9.62}$$

This dispersion relation is healthy when $\lambda > 1$ or $\lambda < \frac{1}{2}$. Note that this degree of freedom is a linear combination of h and $\widetilde{\sigma}$. Therefore, it will not be captured entirely if one neglects everything except the trace component of h_{ij}, as was done in [114]. When $\lambda > 1$ (and $\gamma > 0$), the overall sign in front of (9.61) is negative and we must Wick rotate the field[5] corresponding to $\mathcal{O}_{\text{phys}}$.

Once again, this dispersion relation can be derived without regard to a specific gauge-fixing procedure, as in the case of the $U(1)$ gauge theory.

9.3 Effective Action with a Nonzero Cosmological Constant

Let us calculate the contribution to the determinants of first order in Λ. Our object of study is the effective action $\Gamma(\varphi)$, where φ denotes the expectation values of all fields Φ of the gravitational theory. Expanding in $\hbar$,

$$\Gamma(\varphi) = S(\varphi) + \hbar\Gamma_1(\varphi) + O(\hbar^{3/2}),\tag{9.63}$$

by standard methods the one-loop quantum effective action takes the form[6]

$$\Gamma_1(\varphi) = \frac{i}{2}\text{tr}\log S^{(2)}(\varphi),\tag{9.64}$$

where

$$S^{(2)}(\varphi) = \frac{\delta^2 S(\Phi)}{\delta\Phi\delta\Phi}\bigg|_{\Phi=\varphi}\tag{9.65}$$

is the second functional derivative of S. Since this is a gauge theory, we must also include ghost contributions after gauge-fixing, leading to the standard expression

$$\Gamma_1(\varphi) = \frac{i}{2}\text{tr}\log S^{(2)} - i\,\text{tr}\log\mathcal{D}_{\text{ghost}}.\tag{9.66}$$

Note that the only dimensionful parameter present is Λ itself, with dimension $[\Lambda] = 2$. As a result, the only contribution Λ can have to the logarithmic divergence (and therefore to the one-loop beta functions) is proportional to Λ. To evaluate it, it therefore suffices to evaluate the first derivative of the partition function $\mathcal{Z}$ with respect to Λ. Separating out the Λ dependence of $S^{(2)}$,

$$S^{(2)} = M + \Lambda M^{(\Lambda)},\tag{9.67}$$

we can write

$$\log\det S^{(2)} = \text{tr}\log S^{(2)} = \text{tr}\log M + \Lambda\,\text{tr}\big(M^{-1}M^{(\Lambda)}\big) + O(\Lambda^2).\tag{9.68}$$

---

[5]In general, this field is some combination of h and $\widetilde{\sigma}$. In the "nice" gauge (9.60), this field is just h.

[6]This is not sufficient to define a gauge invariant effective action [116]. The full treatment of defining a gauge invariant off-shell effective action is beyond the scope of this thesis. Instead, we will make use of a field redefinition $\bar{g}_{ij} \to C\,\bar{g}_{ij}$, which will turn out to be sufficient for our purposes.

$M^{(\Lambda)}$ has contributions only from the $\widetilde{\eta}$ and $(h, \widetilde{\sigma})$ sectors. Collecting the corresponding objects, from (9.50) and (9.53), we have

$$M = \begin{pmatrix} M_{\widetilde{\eta}} & 0 \\ 0 & M_{h\widetilde{\sigma}} \end{pmatrix}, \qquad M^{(\Lambda)} = \begin{pmatrix} M_{\widetilde{\eta}}^{(\Lambda)} & 0 \\ 0 & M_{h\widetilde{\sigma}}^{(\Lambda)} \end{pmatrix}, \tag{9.69}$$

where

$$M_{\widetilde{\eta}} = -\partial_t^2 - \mathfrak{u}_1 \partial^4, \qquad M_{\widetilde{\eta}}^{(\Lambda)} = 2, \qquad M_{h\widetilde{\sigma}}^{(\Lambda)} = \frac{1}{2}\begin{pmatrix} 0 & 0 \\ 0 & 1 \end{pmatrix}, \tag{9.70}$$

$$M_{h\widetilde{\sigma}} = \frac{1}{2}\begin{pmatrix} -\left(\frac{1}{2} - \lambda\right)\partial_t^2 - \left[\gamma + 2\left(\frac{1}{2} - \lambda\right)^2 \mathfrak{u}\right]\partial^4 & \left[\gamma - \left(\frac{1}{2} - \lambda\right)\mathfrak{u}\right]\partial^4 \\ \left[\gamma - \left(\frac{1}{2} - \lambda\right)\mathfrak{u}\right]\partial^4 & -\frac{1}{2}\left[\partial_t^2 + (2\gamma + \mathfrak{u})\partial^4\right] \end{pmatrix}. \tag{9.71}$$

Evaluating the relevant traces, we obtain the integral form

$$\mathrm{tr}\left[M^{-1}M^{(\Lambda)}\right] = \int dt\, d^2\mathbf{x} \sum_{I=1}^{3} A_I \int \frac{d\omega\, d^2\mathbf{k}}{(2\pi)^3} G_I(\omega, \mathbf{k}), \tag{9.72}$$

with propagators

$$G_I(\omega, \mathbf{k}) = \frac{1}{\omega^2 - \alpha_I^2 k^4} \tag{9.73}$$

and constants

$$\alpha_1^2 = \mathfrak{u}_1, \qquad \alpha_2^2 = 2\mathfrak{u}(1 - \lambda), \qquad \alpha_3^2 = 4\gamma\frac{1 - \lambda}{1 - 2\lambda}; \tag{9.74}$$

$$A_1 = 2, \qquad A_2 = \frac{1}{1 - \lambda}, \qquad A_3 = \frac{1 - 2\lambda}{1 - \lambda}. \tag{9.75}$$

Here, $I = 1$ corresponds to the $\widetilde{\eta}$ contribution, while $I = 2, 3$ arise from the $(h, \widetilde{\sigma})$ sector.

Later on in this chapter we will use heat kernel methods, which preserve diffeomorphism invariance. It is difficult to use the heat kernel here, however, because we have not diagonalized $M_{h,\widetilde{\sigma}}$. (Note, however, that in the diagonal "nice" gauge this is not a problem.) Although it breaks gauge symmetry and modifies the infrared behavior of the theory, to extract the coefficient of the logarithmic divergence it suffices to use a cutoff regularization. We integrate over all ω and introduce a cutoff k_* in k. In addition, the denominators have an implicit $+i\varepsilon$, specifying the appropriate Wick rotatation $\omega = i\omega_E$. The integrals evaluate to

$$\int \frac{d\omega\, d^2\mathbf{k}}{(2\pi)^3} G_I(\omega, \mathbf{k}) = \frac{1}{4\pi i}\frac{\log k_*}{\alpha_I} + (\text{finite}), \tag{9.76}$$

giving the final result

$$\frac{\partial}{\partial\Lambda}\log\det S^{(2)}|_{\Lambda=0,\mathrm{div}} = \frac{\log k_*}{4\pi i}\left\{\frac{2}{\sqrt{\mathfrak{u}_1}} + \frac{1}{1 - \lambda}\frac{1}{\sqrt{2\mathfrak{u}(1 - \lambda)}} + \frac{1}{2\sqrt{\gamma}}\left(\frac{1 - 2\lambda}{1 - \lambda}\right)^{3/2}\right\}. \tag{9.77}$$

The contribution of Λ to the effective action (9.66) is therefore

$$\Gamma_{1,\mathrm{div}}(\overline{R}=0) = \frac{\log k_*}{8\pi}\left\{ \frac{2}{\sqrt{\mathfrak{u}_1}} + \frac{1}{\sqrt{2\mathfrak{u}}}\frac{1}{(1-\lambda)^{3/2}} + \frac{1}{2\sqrt{\gamma}}\left(\frac{1-2\lambda}{1-\lambda}\right)^{3/2} \right\}\int dt\, d^2\mathbf{x}\,\Lambda. \quad (9.78)$$

This is obviously gauge-dependent. As we will discuss in Section 9.6, this gauge dependence should be eliminated by a field strength redefinition for the background metric $\overline{g}_{ij}$,

$$\overline{g}_{ij} \to C\,\overline{g}_{ij}. \quad (9.79)$$

We will utilize this field redefinition in the subsequent section in order to extract the key gauge-independent information.

9.4 Time-independent Curved Background

In time-independent backgrounds ($\dot{\overline{g}}_{ij}=0$), the background values of the extrinsic curvature and the Riemann tensor are $\overline{K}_{ij} = 0$ and $\overline{R}^i{}_{jk\ell} = \overline{R}^i{}_{jk\ell}(\mathbf{x})$, respectively. In two spatial dimensions, the Riemann tensor is determined by the scalar curvature,

$$\overline{R}^i{}_{jk\ell}(\mathbf{x}) = \frac{1}{2}\overline{R}\big[\delta^i_k\,\overline{g}_{j\ell}(\mathbf{x}) - \delta^i_\ell\,\overline{g}_{jk}(\mathbf{x})\big]. \quad (9.80)$$

By dimensional analysis, the only divergence sensitive to $\overline{\nabla}_i\overline{R}$ that can appear in the effective action is $\overline{\Box}\overline{R}$, which is a total derivative. Therefore, it suffices to take $\overline{R}$ to be constant.

Consider the action (9.7) with the coupling constant ρ set to zero,

$$S = \frac{1}{\kappa^2}\int dt\, d^2\mathbf{x}\,N\sqrt{g}\big\{K_{ij}K^{ij} - \lambda K^2 - \gamma R^2 - 2\Lambda\big\}. \quad (9.81)$$

We now expand each term in this action to quadratic order in κ. With

$$K_{ij} = \frac{1}{2}\kappa\left(\dot{h}_{ij} - \overline{\nabla}_i n_j - \overline{\nabla}_j n_i\right) + O\big(\kappa^2\big), \quad (9.82)$$

we have

$$N\sqrt{g}K_{ij}K^{ij} = \frac{1}{4}\kappa^2\sqrt{\overline{g}}\left(\dot{h}_{ij}\dot{h}^{ij} - 4\overline{\nabla}^i n^j\dot{h}_{ij} + 2\overline{\nabla}^i n^j\overline{\nabla}_i n_j + 2\overline{\nabla}^i n^j\overline{\nabla}_j n_i\right) + O\big(\kappa^3\big), \quad (9.83a)$$

$$N\sqrt{g}K^2 = \frac{1}{4}\kappa^2\sqrt{\overline{g}}\left(\dot{h}^2 - 4\dot{h}\overline{\nabla}^i n_i + 4\overline{\nabla}^i n_i\overline{\nabla}^j n_j\right) + O\big(\kappa^3\big). \quad (9.83b)$$

Moreover,

$$N\sqrt{g}\,R^2$$
$$= \sqrt{\overline{g}}\,\overline{R}^2 + \kappa\sqrt{\overline{g}}\,\overline{R}\left[2\overline{\nabla}^i(\overline{\nabla}^j h_{ij} - \overline{\nabla}_i h) - \tfrac{1}{2}\overline{R}\,h\right]$$

$$+ \kappa^2 \sqrt{\overline{g}} \left\{ \left(\overline{\nabla}^i \overline{\nabla}^j h_{ij} - \overline{\nabla}^2 h \right)^2 + \overline{R}^2 \left(\tfrac{3}{4} h^{ij} h_{ij} - \tfrac{1}{8} h^2 \right) \right.$$

$$+ \overline{R} \left[\tfrac{3}{2} \overline{\nabla}_k h_{ij} \overline{\nabla}^k h^{ij} - \overline{\nabla}_i h_{jk} \overline{\nabla}^k h^{ij} + 2 \overline{\nabla}_i h \overline{\nabla}^j h^i_j - 2(\overline{\nabla}^j h_{ji})^2 \right.$$

$$\left. \left. - \tfrac{1}{2} \left(\overline{\nabla}_i h \right)^2 + 2 h^{ij} \overline{\nabla}_i \overline{\nabla}_j h - 2 h^{ij} \left(\overline{\nabla}_j \overline{\nabla}_k h^k_i + \overline{\nabla}_k \overline{\nabla}_j h^k_i - \overline{\nabla}^2 h_{ij} \right) \right] \right\}$$

$$+ O(\kappa^3) , \tag{9.84}$$

and

$$N \sqrt{\overline{g}} \, \Lambda = \sqrt{\overline{g}} \, \Lambda \left\{ 1 + \tfrac{1}{2} \kappa \, h + \tfrac{\kappa^2}{8} \left(h^2 - 2 h^{ij} h_{ij} \right) \right\} + O(\kappa^3). \tag{9.85}$$

The action can be put on-shell by imposing the equation of motion for the background field $\overline{g}_{ij}$. This essentially sets the cosmological constant to be

$$\Lambda = \frac{1}{2} \gamma \overline{R}^2 . \tag{9.86}$$

Plugging (9.86) back into the action eliminates the tadpole terms linear in κ. The on-shell action is

$$S = \frac{1}{\kappa^2} \int dt \, d^2\mathbf{x} \, N \sqrt{\overline{g}} \left\{ K_{ij} K^{ij} - \lambda K^2 - \gamma \left(R^2 + \overline{R}^2 \right) \right\} . \tag{9.87}$$

Considering such an on-shell action enables us to observe explicit cancellations between ghosts and non-physical modes, reducing the computation of the effective action to that of a single scalar functional determinant.

We offer one caveat: since we do not impose the constraint equation generated by the gauge choice $n = 0$, by "on shell" we actually mean the background satisfies the g_{ij} equations of motion. To render the background (9.86) fully on-shell requires imposing the further condition $\rho = 2\gamma \overline{R}$. As noted in the introduction, however, neither the lapse nor the value of ρ affects the local divergences, and therefore we can ignore both in the computation at hand.

We now turn to the problem of gauge-fixing. We will apply the BRST formalism. Instead of classifying the most general gauge-fixing conditions, let us take a more minimalistic approach and construct a gauge-fixing condition such that the cross terms between n_i and h_{ij} cancel in the BRST action. For this purpose, it is sufficient to set the gauge-fixing functional f_i to

$$f_i = \dot{n}_i - D_1 \overline{\nabla}^j h_{ij} - D_2 \overline{\nabla}_i h . \tag{9.88}$$

Here D_1 and D_2 are local operators of dimension one, which we will take to be linear combinations of the diffeomorphism-invariant objects $\overline{R}$ and $\overline{\square} \equiv \overline{\nabla}_i \overline{g}^{ij} \overline{\nabla}_j$. As we reviewed in Section 9.2, equation (9.88) is not the most general gauge choice consistent with background diffeomorphism invariance: for example, one may also include in f_i terms of the form

$$\overline{\nabla}_i \overline{\nabla}_j \overline{\nabla}_k h^{jk} . \tag{9.89}$$

In the zero curvature limit, this extra term is the same as the $\mathfrak{u}_2$ term in (9.35). In the flat case, if one requires that nonphysical modes have a right sign dispersion relation, the conditions derived in (9.59) must be satisfied. For $\lambda > 1$, a nonzero $\mathfrak{u}_2$ is indispensable for these conditions to hold. On an on-shell background, the one-loop contributions from nonphysical modes cancel exactly in the partition function, and it is not necessary to include (9.89) in the gauge-fixing condition. When on-shell, we can focus on $\lambda < \frac{1}{2}$ and adopt the simpler gauge-fixing condition in (9.88). Evaluating the partition function will result in a gauge invariant expression that is analytically continuable to $\lambda > 1$.

BRST quantization proceeds by introducing a ghost field c^i associated to the generator of infinitesimal diffeomorphisms. The BRST differential s acts on the physical fields in the same way as the linearized diffeomorphisms in (9.12):

$$ s n_i = \dot{c}_i + O(\kappa), \qquad s h_{ij} = \overline{\nabla}_i c_j + \overline{\nabla}_j c_i + O(\kappa). \tag{9.90} $$

We also require a cohomologically trivial BRST pair (b_i, Φ_i), with fermi and bose statistics respectively. The ghost sector has BRST variations

$$ s b_i = \Phi_i \,, \qquad s \Phi_i = 0 \,, \qquad s c_i = O(\kappa) \,. \tag{9.91} $$

Gauge-fixing actions are given by the BRST differential of a gauge-fixing fermion. We take the gauge-fixing fermion

$$ \Psi = - \int dt \, d^2\mathbf{x} \sqrt{\bar{g}} \, b^i \Big\{ \dot{n}_i - D_1 \overline{\nabla}^j h_{ij} - D_2 \overline{\nabla}_i h - \frac{1}{2} \mathcal{D} \Phi_i \Big\} \,, \tag{9.92} $$

which gives the BRST-exact action

$$ s\Psi = - \int dt \, d^2\mathbf{x} \sqrt{\bar{g}} \, \Phi^i \Big\{ \dot{n}_i - D_1 \overline{\nabla}^j h_{ij} - D_2 \overline{\nabla}_i h - \frac{1}{2} \mathcal{D} \Phi_i \Big\} $$
$$ + \int dt \, d^2\mathbf{x} \sqrt{\bar{g}} \, b^i \Big\{ \ddot{c}_i - D_1 \overline{\nabla}^j \overline{\nabla}_i c_j - D_1 \overline{\square} c_i - 2 D_2 \overline{\nabla}_i \overline{\nabla}^j c_j \Big\} \,. \tag{9.93} $$

This action is associated to a gauge-fixing condition of the form (9.88), except that we have replaced the δ-function type by a gauge of generalized $\mathcal{R}_\xi$ type. We have introduced auxiliary fields Φ^i of dimension $\frac{1}{2}$ and a local operator $\mathcal{D}$ of dimension 1. We choose the following expression for the operator $\mathcal{D}$:

$$ \mathcal{D} = -\mathfrak{u}_1 (\overline{\square} + \mathfrak{v} \overline{R}). \tag{9.94} $$

We intentionally keep the real parameters $\mathfrak{v}$ and $\mathfrak{u}_1$ which depend on the gauge choice. Physical results must be independent of their values, giving a check of the final result.

The full BRST-invariant action is

$$ S_{\text{BRST}} = S + s\Psi = S + S_{\text{g.f.}} + S_{\text{ghost}}, \tag{9.95} $$

where

$$ S_{\text{g.f.}} = - \int dt \, d^2\mathbf{x} \sqrt{\bar{g}} \, \Phi^i \Big\{ \dot{n}_i - D_1 \overline{\nabla}^j h_{ij} - D_2 \overline{\nabla}_i h - \frac{1}{2} \mathcal{D} \Phi_i \Big\}, \tag{9.96} $$

and

$$S_{\text{ghost}} = -\int dt\, d^2\mathbf{x} \left\{ b_i \dot{c}^i - \left(\overline{\nabla}_i D_1 b_j + \overline{g}_{ij} \overline{\nabla}_k D_2 b^k \right) \left(\overline{\nabla}^i c^j + \overline{\nabla}^j c^i \right) \right\}. \tag{9.97}$$

The BRST partition function is

$$\mathcal{Z}_{\text{BRST}} = \int \mathscr{D}\{n_i, h_{ij}, b_i, c_i, \Phi_i\}\, e^{i S_{\text{BRST}}}. \tag{9.98}$$

Next, let us integrate out the auxiliary field Φ_i in S_{BRST}. Since Φ_i only appears in $S_{\text{g.f.}}$, we can focus on the following piece in the partition function,

$$\mathcal{Z}_\Phi \equiv \int \mathscr{D}\Phi_i\, e^{i S_{\text{g.f.}}}. \tag{9.99}$$

Here, Φ_i is not dynamical and can be eliminated by imposing its equation of motion,

$$\Phi_i = \mathcal{D}^{-1} \left(\dot{n}_i - D_1 \overline{\nabla}^j h_{ij} - D_2 \overline{\nabla}_i h \right). \tag{9.100}$$

The resulting action after eliminating Φ_i in $S_{\text{g.f.}}$ is

$$-\frac{1}{2} \int dt\, d^2\mathbf{x} \sqrt{\overline{g}} \left(\dot{n}^i - D_1 \overline{\nabla}^j h^i_j - D_2 \overline{\nabla}^i h \right) \mathcal{D}^{-1} \left(\dot{n}_i - D_1 \overline{\nabla}^k h_{ik} - D_2 \overline{\nabla}_i h \right). \tag{9.101}$$

From now on, we will take $S_{\text{g.f.}}$ to denote the expression (9.101), even though it is different from the original expression in (9.96).

Integrating out Φ_i in the partition function (9.99) also contributes a functional determinant. To evaluate this determinant, we first make the change of variables

$$\Phi_i = \overline{\nabla}_i \phi + \overline{\varepsilon}_{ij} \overline{\nabla}^j \widetilde{\phi}, \tag{9.102}$$

with $\overline{\varepsilon}_{ij} = \sqrt{\overline{g}}\, \epsilon_{ij}$ the covariant Levi-Civita symbol for $\overline{g}$. The Jacobian is given by (D.10) in Appendix D,

$$\mathcal{J} = \det\left(-\overline{\Box} \right). \tag{9.103}$$

In terms of ϕ and $\widetilde{\phi}$, the part of (9.96) that is quadratic in Φ_i can be written as

$$S^{(2)}_{\Phi_i} = \frac{1}{2} \int dt\, d^2\mathbf{x} \sqrt{\overline{g}} \left\{ \phi \overline{\nabla}_i \mathcal{D} \overline{\nabla}^i \phi + \widetilde{\phi} \overline{\nabla}_i \mathcal{D} \overline{\nabla}^i \widetilde{\phi} \right\}. \tag{9.104}$$

To derive that the cross term between ϕ and $\widetilde{\phi}$ is zero, we used the form (9.94) of $\mathcal{D}$ and applied Identity 1 in Appendix C. Therefore,

$$\int \mathscr{D}\{\phi, \widetilde{\phi}\}\, e^{i S^{(2)}_{\Phi_i}} = \left(\det\nolimits_{\Phi_i} \mathcal{D} \right)^{-1/2}, \tag{9.105}$$

where the functional determinant is evaluated to be

$$\det{}_{\Phi_i} \mathcal{D} = \left[\det\left(\overline{\nabla}_i \mathcal{D} \overline{\nabla}^i \right) \right]^2 . \tag{9.106}$$

Therefore, the final expression for the Φ_i contribution (9.99) is

$$\mathcal{Z}_\Phi = \mathcal{J}_\Phi e^{i S_{\text{g.f.}}} , \tag{9.107}$$

where $S_{\text{g.f}}$ is given by (9.101) and

$$\mathcal{J}_\Phi = \frac{\det\left(-\overline{\Box} \right)}{\sqrt{\det{}_{\Phi_i} \mathcal{D}}} = \frac{1}{\left(\det |\mathfrak{u}_1| \right) \det\left[-\overline{\Box} - \left(\mathfrak{v} + \frac{1}{2} \right) \overline{R} \right]}. \tag{9.108}$$

We applied Identity 1 for the second equality in (9.108).

Finally, we determine the operators D_1 and D_2 in (9.92) by requiring that the cross terms between n_i and h_{ij} cancel in the sum $S + S_{\text{g.f.}}$, with $S_{\text{g.f.}}$ set to the expression in (9.101). The kinetic contribution in the action S comes from

$$S_{\mathcal{K}} = \frac{1}{\kappa^2} \int dt \, d^2\mathbf{x} \sqrt{g} \left\{ K_{ij} K^{ij} - \lambda K^2 \right\}.$$

The part contained in $S_{\mathcal{K}}$ that is quadratic in terms of the fluctuations is

$$\frac{1}{4} \int dt \, d^2\mathbf{x} \sqrt{\overline{g}} \left\{ \dot{h}_{ij} \dot{h}^{ij} - \lambda \dot{h}^2 - 4 \dot{n}^i \left(\overline{\nabla}^j h_{ij} - \lambda \overline{\nabla}_i h \right) \right.$$
$$\left. + 2 \left[\overline{\nabla}^i n^j \overline{\nabla}_i n_j + \overline{\nabla}^i n^j \overline{\nabla}_j n_i - 2\lambda (\overline{\nabla}^i n_i)^2 \right] \right\}. \tag{9.109}$$

The cross terms in $S_{\mathcal{K}}$ are

$$- \int dt \, d^2\mathbf{x} \sqrt{\overline{g}} \, \dot{n}^i \left(\overline{\nabla}^j h_{ij} - \lambda \overline{\nabla}_i h \right) . \tag{9.110}$$

The contributions to the cross terms from $S_{\text{g.f.}}$ are

$$\int dt \, d^2\mathbf{x} \sqrt{\overline{g}} \, \dot{n}^i \left(\mathcal{D}^{-1} D_1 \overline{\nabla}^j h_{ij} + \mathcal{D}^{-1} D_2 \overline{\nabla}_i h \right) \tag{9.111}$$

These two contributions, (9.110) and (9.111), cancel if

$$D_1 = -\frac{1}{\lambda} D_2 = \mathcal{D}. \tag{9.112}$$

Since $\mathcal{D}$ has been defined in (9.94), this fixes both D_1 and D_2.

The integration over the ghosts in the partition function can be treated separately. From (9.97) we obtain

$$S_{\text{ghost}} = - \int dt \, d^2\mathbf{x} \left\{ \dot{b}_i \dot{c}^i - \left(\overline{\nabla}_i D_1 b_j + \overline{g}_{ij} \overline{\nabla}_k D_2 b^k \right) \left(\overline{\nabla}^i c^j + \overline{\nabla}^j c^i \right) \right\}. \tag{9.113}$$

We would like to evaluate the partition function

$$\mathcal{Z}_{\text{ghost}} \equiv \int \mathscr{D}\{b_i, c_i\} \, e^{iS_{\text{ghost}}}. \tag{9.114}$$

Let us reparametrize the ghosts c_i and the anti-ghosts b_i by

$$c_i = \overline{\nabla}_i c + \overline{\varepsilon}_{ij} \overline{\nabla}^j \widetilde{c}, \qquad b_i = \overline{\nabla}_i b + \overline{\varepsilon}_{ij} \overline{\nabla}^j \widetilde{b}. \tag{9.115}$$

Similar to (9.103) but for fermions instead of bosons, these changes of variables give rise to the Jacobian

$$\mathcal{J}_{\text{ghost}} = \frac{1}{\left[\det\left(-\Box\right)\right]^2}. \tag{9.116}$$

In terms of the fields b, $\widetilde{b}$, c and $\widetilde{c}$, the ghost action becomes

$$S_{\text{ghost}} = \int dt \, d^2\mathbf{x} \sqrt{\overline{g}} \left\{ b \, \overline{\Box} \mathcal{O}_g \, c + \widetilde{b} \, \overline{\Box} \widetilde{\mathcal{O}}_g \, \widetilde{c} \right\}, \tag{9.117}$$

where

$$\mathcal{O}_g = -\partial_t^2 - 2\mathfrak{u}_1 \left[(1-\lambda)\overline{\Box} + \tfrac{1}{2}\overline{R} \right] \left[\overline{\Box} + \left(\mathfrak{v} + \tfrac{1}{2} \right) \overline{R} \right], \tag{9.118}$$

$$\widetilde{\mathcal{O}}_g = -\partial_t^2 - \mathfrak{u}_1 \left(\overline{\Box} + \overline{R} \right) \left[\overline{\Box} + \left(\mathfrak{v} + \tfrac{1}{2} \right) \overline{R} \right]. \tag{9.119}$$

Therefore,

$$\mathcal{Z}_{\text{ghost}} = \left(\det \mathcal{O}_g \right) \left(\det \widetilde{\mathcal{O}}_g \right). \tag{9.120}$$

Now, we would like to come back to examine the non-ghost part in the action S_{BRST}, namely, the combined contribution from $S + S_{\text{g.f.}}$.

It is useful to take the following decomposition of the metric fluctuation h_{ij} such that

$$h_{ij} = H_{ij} + \frac{1}{2}\overline{g}_{ij} h, \tag{9.121}$$

where H_{ij} is a traceless 2-tensor, and

$$H_{ij} = H_{ij}^{\perp} + \overline{\nabla}_i \eta_j + \overline{\nabla}_j \eta_i + \overline{\nabla}_i \overline{\nabla}_j \sigma - \frac{1}{2}\overline{g}_{ij} \overline{\Box}\sigma, \tag{9.122}$$

where

$$\overline{g}^{ij} H_{ij}^{\perp} = 0, \qquad \overline{\nabla}^j H_{ij}^{\perp} = 0, \qquad \overline{\nabla}^i \eta_i = 0. \tag{9.123}$$

Note that the quantum field $H_{ij}^{\perp}$ is both traceless and divergenceless. In $2+1$ dimensions, $H_{ij}^{\perp}$ encodes only global information about the geometry of the spatial slice (the moduli of the Riemann surface), and carries no local degrees of freedom. Therefore, we can drop $H_{ij}^{\perp}$ without affecting the beta functions. The constraint on η_i can be solved by parametrizing η_i as

$$\eta_i = \overline{\varepsilon}_{ij} \overline{\nabla}^j \eta. \tag{9.124}$$

The Jacobian from the transformation (9.122) is computed in (D.15),

$$\mathcal{J}_H = \det\left[\Box\left(\Box + \overline{R}\right)\right]. \tag{9.125}$$

Under the decomposition (9.122), we have

$$S + S_{\text{g.f.}} = S_n + S_\eta + S_{h\sigma}, \tag{9.126}$$

where

$$S_n = \frac{1}{2}\int dt\, d^2\mathbf{x}\sqrt{\overline{g}}\, n_i \left\{ \overline{g}^{ij}\left[-\mathfrak{u}_1^{-1}\left(\Box + \mathfrak{v}\overline{R}\right)^{-1}\partial_t^2 - \Box\right] - \overline{\nabla}^j\overline{\nabla}^i + 2\lambda\overline{\nabla}^i\overline{\nabla}^j \right\} n_j, \tag{9.127a}$$

$$S_\eta = \frac{1}{2}\int dt\, d^2\mathbf{x}\sqrt{\overline{g}}\, \eta\, \Box\left(\Box + \overline{R}\right)\left\{ -\partial_t^2 - \mathfrak{u}_1\left(\Box + \overline{R}\right)\left[\Box + \left(\mathfrak{v} + \tfrac{1}{2}\right)\overline{R}\right] \right\}\eta, \tag{9.127b}$$

$$S_{h\sigma} = \frac{1}{4}\int dt\, d^2\mathbf{x}\sqrt{\overline{g}}\, h\left\{ -\left(\tfrac{1}{2} - \lambda\right)\partial_t^2 - \gamma\left(\Box + \overline{R}\right)^2 - 2\mathfrak{u}_1\left(\tfrac{1}{2} - \lambda\right)^2\Box\left[\Box + \left(\mathfrak{v} + \tfrac{1}{2}\right)\overline{R}\right] \right\}h$$

$$+ \frac{1}{8}\int dt\, d^2\mathbf{x}\sqrt{\overline{g}}\, \sigma\,\Box\left(\Box + \overline{R}\right)\left\{ -\partial_t^2 - 2\gamma\Box\left(\Box + \overline{R}\right) - \mathfrak{u}_1\left(\Box + \overline{R}\right)\left[\Box + \left(\mathfrak{v} + \tfrac{1}{2}\right)\overline{R}\right] \right\}\sigma$$

$$+ \frac{1}{2}\int dt\, d^2\mathbf{x}\sqrt{\overline{g}}\, \sigma\,\Box\left(\Box + \overline{R}\right)\left\{ \gamma\left(\Box + \overline{R}\right) - \mathfrak{u}_1\left(\tfrac{1}{2} - \lambda\right)\left[\Box + \left(\mathfrak{v} + \tfrac{1}{2}\right)\overline{R}\right] \right\}h. \tag{9.127c}$$

The full one-loop BRST partition function can be written as

$$\mathcal{Z}_{\text{BRST}} = \mathcal{J}_\Phi\,\mathcal{J}_H\,\mathcal{Z}_{\text{ghost}}\,\mathcal{Z}_n\,\mathcal{Z}_\eta\,\mathcal{Z}_{h\sigma}, \tag{9.128}$$

where

$$\mathcal{Z}_n = \int \mathscr{D}n_i\, e^{iS_n}, \qquad \mathcal{Z}_\eta = \int \mathscr{D}\eta\, e^{iS_\eta}, \qquad \mathcal{Z}_{h\sigma} = \int \mathscr{D}\{h,\sigma\}\, e^{iS_{h\sigma}}. \tag{9.129}$$

For $\mathfrak{u}_1 > 0$ (and $\lambda < \tfrac{1}{2}$), we must Wick rotate n_i as well as the time when performing the path integral.

First, let us focus on $\mathcal{Z}_n$. We decompose n_i into scalar components ν and $\widetilde{\nu}$ as follows,

$$n_i = \overline{\nabla}_i\left[\Box + \left(\mathfrak{v} + \tfrac{1}{2}\right)\overline{R}\right]\nu + \overline{\varepsilon}_{ij}\overline{\nabla}^j\left[\Box + \left(\mathfrak{v} + \tfrac{1}{2}\right)\overline{R}\right]\widetilde{\nu}. \tag{9.130}$$

We choose this particular decomposition in order to make the action (9.127a) local. The corresponding Jacobian is

$$\mathcal{J}_n = \det\left\{ \left(-\Box\right)\left[\Box + \left(\mathfrak{v} + \tfrac{1}{2}\right)\overline{R}\right]^2 \right\}. \tag{9.131}$$

Under this parametrization, we obtain

$$S_n = -\frac{1}{2\mathfrak{u}_1}\int dt\, d^2\mathbf{x}\sqrt{\overline{g}}\left\{ \nu\,\Box\left[\Box + \left(\mathfrak{v} + \tfrac{1}{2}\right)\overline{R}\right]\mathcal{O}_g\,\nu + \widetilde{\nu}\,\Box\left[\Box + \left(\mathfrak{v} + \tfrac{1}{2}\right)\overline{R}\right]\widetilde{\mathcal{O}}_g\,\widetilde{\nu} \right\}. \tag{9.132}$$

Collecting these results gives the partition function of n_i,

$$\mathcal{Z}_n = \frac{\left(\det |\mathfrak{u}_1|\right) \det\left[-\overline{\Box} - \left(\mathfrak{v} + \frac{1}{2}\right)\overline{R}\right]}{\sqrt{\left(\det \mathcal{O}_g\right)\left(\det \widetilde{\mathcal{O}}_g\right)}}. \tag{9.133}$$

Contributions from η, σ and h can be read off of the actions (9.127b-9.127c) (in the h, σ sector the differential operator is a 2×2 matrix, whose determinant we take directly) and give

$$\mathcal{Z}_\eta = \frac{1}{\sqrt{\det\left[\overline{\Box}\left(\overline{\Box} + \overline{R}\right)\right]}} \frac{1}{\sqrt{\det \widetilde{\mathcal{O}}_g}}, \tag{9.134a}$$

$$\mathcal{Z}_{h\sigma} = \frac{1}{\sqrt{\det\left[\overline{\Box}\left(\overline{\Box} + \overline{R}\right)\right]}} \frac{1}{\sqrt{\left(\det \mathcal{O}_g\right)\left(\det \mathcal{O}_{\text{phys}}\right)}}, \tag{9.134b}$$

where

$$\mathcal{O}_{\text{phys}} = -\left(\frac{1}{2} - \lambda\right)\partial_t^2 - 2\gamma\left(\overline{\Box} + \overline{R}\right)\left[(1 - \lambda)\overline{\Box} + \frac{1}{2}\overline{R}\right]. \tag{9.135}$$

9.5   Reduction to Physical Spectrum

Let us collect the results that we have derived above. The BRST partition function $\mathcal{Z}_{\text{BRST}}$ is given by

$$\mathcal{Z}_{\text{BRST}} = \mathcal{J}_\Phi \, \mathcal{J}_H \, \mathcal{Z}_{\text{ghost}} \, \mathcal{Z}_n \, \mathcal{Z}_\eta \, \mathcal{Z}_{h\sigma}, \tag{9.136}$$

where,

$$\mathcal{J}_\Phi = \frac{1}{\left(\det |\mathfrak{u}_1|\right) \det\left[-\overline{\Box} - \left(\mathfrak{v} + \frac{1}{2}\right)\overline{R}\right]}, \qquad \mathcal{J}_H = \det\left[\overline{\Box}\left(\overline{\Box} + \overline{R}\right)\right], \tag{9.137}$$

and

$$\mathcal{Z}_{\text{ghost}} = \left(\det \mathcal{O}_g\right)\left(\det \widetilde{\mathcal{O}}_g\right), \tag{9.138a}$$

$$\mathcal{Z}_n = \frac{\left(\det |\mathfrak{u}_1|\right) \det\left[-\overline{\Box} - \left(\mathfrak{v} + \frac{1}{2}\right)\overline{R}\right]}{\sqrt{\left(\det \mathcal{O}_g\right)\left(\det \widetilde{\mathcal{O}}_g\right)}}, \tag{9.138b}$$

$$\mathcal{Z}_\eta = \frac{1}{\sqrt{\det\left[\overline{\Box}\left(\overline{\Box} + \overline{R}\right)\right]}} \frac{1}{\sqrt{\det \widetilde{\mathcal{O}}_g}}, \tag{9.138c}$$

$$\mathcal{Z}_{h\sigma} = \frac{1}{\sqrt{\det\left[\overline{\Box}\left(\overline{\Box} + \overline{R}\right)\right]}} \frac{1}{\sqrt{\left(\det \mathcal{O}_g\right)\left(\det \mathcal{O}_{\text{phys}}\right)}}. \tag{9.138d}$$

The operators $\mathcal{O}_g$, $\mathcal{O}_{\widetilde{g}}$ and $\mathcal{O}_{\mathrm{phys}}$ take the form

$$\mathcal{O}_g = -\partial_t^2 - 2\mathfrak{u}_1\left[(1-\lambda)\,\overline{\Box} + \tfrac{1}{2}\overline{R}\right]\left[\overline{\Box} + \left(\mathfrak{v}+\tfrac{1}{2}\right)\overline{R}\right], \tag{9.139a}$$

$$\widetilde{\mathcal{O}}_g = -\partial_t^2 - \mathfrak{u}_1\left(\overline{\Box} + \overline{R}\right)\left[\overline{\Box} + \left(\mathfrak{v}+\tfrac{1}{2}\right)\overline{R}\right], \tag{9.139b}$$

$$\mathcal{O}_{\mathrm{phys}} = -\left(\tfrac{1}{2}-\lambda\right)\partial_t^2 - 2\gamma\left(\overline{\Box}+\overline{R}\right)\left[(1-\lambda)\,\overline{\Box} + \tfrac{1}{2}\overline{R}\right]. \tag{9.139c}$$

The full BRST partition function reduces to

$$\mathcal{Z}_{\mathrm{BRST}} = \frac{1}{\sqrt{\det \mathcal{O}_{\mathrm{phys}}}}. \tag{9.140}$$

It is reassuring that the final result is gauge independent and all singular prefactors simply cancel. This partition function counts exactly one physical degree of freedom. On the other hand, on an off-shell background there is no reason to expect the result to reduce to a single functional determinant, and the analysis would be more difficult.

While the preceding discussion is formally correct, some care must be taken with analytic continuation to ensure that the path integral converges properly. Requiring that $\widetilde{\mathcal{O}}_g$ give rise to a sensible dispersion relation gives $\mathfrak{u}_1 > 0$; for $\mathcal{O}_g$, this requires that $\lambda < 1$. However, both of these operators drop out in the final BRST partition function, and the singular behavior for $\mathcal{O}_g$ (when $\lambda > 1$) can be fixed by modifying the gauge-fixing condition (9.88). Working on-shell gives us the luxury of ignoring this issue: both the operators $\mathcal{O}_g$ and $\widetilde{O}_g$ cancel out in the final BRST partition function.

All that remains is the determinant of $\mathcal{O}_{\mathrm{phys}}$ in (9.140), whose evaluation requires an appropriate choice of contour. The coefficient of ∂_t^2 in $\mathcal{O}_{\mathrm{phys}}$ has a healthy sign for $\lambda < 1/2$, in which case the standard contour will do. For $\lambda > 1$ on the other hand, when we perform Wick rotation we must also rotate the field; this is perhaps not surprising, since a similar rotation must be done for the scale factor in general relativity to get a well-defined Euclidean path integral.

In momentum space, we obtain the following dispersion relation for the physical degree of freedom:

$$\omega^2 = 2\gamma\,\frac{1-\lambda}{\tfrac{1}{2}-\lambda}\left(k^2 - \overline{R}\right)\left\{k^2 - \frac{1}{2\left(1-\lambda\right)}\overline{R}\right\}. \tag{9.141}$$

Note that there are values such that the right-hand side is negative, indicating instability. On the sphere ($\overline{R} > 0$), at most one unstable mode can arise, namely the zero-momentum mode which is unstable for $\lambda > 1$.[7] More troubling is the case where $\lambda > 1$ and $\overline{R} < 0$, since as $\lambda \to 1^+$, the range of momenta with unstable dispersion will grow arbitrarily large. Nonetheless, provided that the UV scale is much larger than $\overline{R}/(1-\lambda)$ this will not affect the divergences of the theory, and so for the purposes of computing the beta function we can ignore any instabilities in the low momentum modes.

---

[7]In fact, the zero-momentum mode is always projected out when we take into account the lapse constraint. We should note, however, that our background only satisfies the lapse constraint for a particular choice of ρ.

9.6 Evaluation of the Heat Kernel and Renormalization

It remains to compute the determinant of (9.140), which we will do using zeta function regularization. The real time quantum effective action is

$$\Gamma(\varphi) = S(\varphi) + \hbar \Gamma_1(\varphi) + O(\hbar^2), \tag{9.142}$$

where

$$\Gamma_1(\varphi) = \frac{i}{2} \mathrm{tr} \log \left\{ S^{(2)}/k_*^4 \right\}, \tag{9.143}$$

and

$$S^{(2)} \equiv - \left(\tfrac{1}{2} - \lambda \right)^{-1} \mathcal{O}_{\mathrm{phys}} = \partial_t^2 + 2\gamma \frac{1-\lambda}{\frac{1}{2}-\lambda} \left(\overline{\Box} + \overline{R} \right) \left[\overline{\Box} + \frac{\overline{R}}{2(1-\lambda)} \right]. \tag{9.144}$$

Here, we have introduced a (spatial) momentum scale k_*, with $[k_*] = \frac{1}{2}$.

The zeta function $\zeta(s)$ for the operator $S^{(2)}$ is defined in terms of the eigenvalues λ_m of $S^{(2)}$ by

$$\zeta(s) = k_*^{4s} \sum_m \frac{1}{\lambda_m^s}, \tag{9.145}$$

so that

$$\log \det S^{(2)} = - \frac{d}{ds} \zeta(s) \Big|_{s=0} = -\zeta'(0). \tag{9.146}$$

To evaluate divergences, we will use the standard heat kernel representation

$$\zeta(s) = \frac{k_*^{4s}}{\Gamma(s)} \int_0^\infty d\tau \, \tau^{s-1} \, \mathrm{Tr} \, e^{-\tau \, S^{(2)}}, \tag{9.147}$$

which gives us the following representation of the one-loop effective action,

$$\begin{aligned} \Gamma_1 &= \frac{1}{2i} \zeta'(0) \\ &= \frac{1}{2} \frac{d}{ds} \Big|_{s=0} \frac{k_*^{4s}}{\Gamma(s)} \int dt \, d^2\mathbf{x} \int_0^\infty d\tau \, \tau^{s-1} \, \mathcal{I}(\tau; t, \mathbf{x}), \end{aligned} \tag{9.148}$$

where

$$\mathcal{I}(\tau; t, \mathbf{x}) = -i \, \langle t, \mathbf{x} | \, e^{-\tau \, S^{(2)}} \, | t, \mathbf{x} \rangle. \tag{9.149}$$

Our background is a product geometry $\mathbb{R} \times M_2$, so we decompose $|t, \mathbf{x}\rangle = |t\rangle \otimes |\mathbf{x}\rangle$. Expanding $|t\rangle$ in Fourier modes allows us to write

$$\mathcal{I}(\tau; t, \mathbf{x}) = -i \int \frac{d\omega}{2\pi} e^{i\omega t} e^{-\tau \partial_t^2} e^{-i\omega t} \, \mathcal{I}_{A\mathcal{V}}(\tau; \mathbf{x}). \tag{9.150}$$

Here we have defined $\mathcal{I}_\mathcal{O}(\tau; \mathbf{x}) = \langle \mathbf{x} | e^{-\tau \mathcal{O}} | \mathbf{x} \rangle$ for any spatial differential operator $\mathcal{O}$ and set

$$A = 2\gamma \frac{1-\lambda}{\frac{1}{2}-\lambda}, \qquad \mathcal{V} = \left(\overline{\Box} + \overline{R} \right) \left[\overline{\Box} + \frac{\overline{R}}{2(1-\lambda)} \right]. \tag{9.151}$$

Note that the ω-integral converges after Wick rotation ($\widetilde{t} \equiv it$, $\widetilde{\omega} \equiv -i\omega$). Performing the integral over the frequency,

$$\int_{-\infty}^{\infty} \frac{d\omega}{2\pi} e^{-i\omega t} e^{-\tau \partial_t^2} e^{i\omega t} = i \int_{-\infty}^{\infty} \frac{d\widetilde{\omega}}{2\pi} e^{-\tau \widetilde{\omega}^2} = \frac{i}{\sqrt{4\pi\tau}}, \tag{9.152}$$

we obtain

$$\mathcal{I}(\tau; t, \mathbf{x}) = \frac{1}{\sqrt{4\pi\tau}} \mathcal{I}_{A\mathcal{V}}(\tau; \mathbf{x}). \tag{9.153}$$

By rescaling $\tau \to \tau/A$, we obtain

$$\Gamma_1 = \frac{1}{2} \int dt\, d^2\mathbf{x} \left. \frac{d}{ds} \right|_{s=0} \frac{k_*^{4s}}{A^s \Gamma(s)} \int_0^{\infty} d\tau\, \tau^{s-1} \mathcal{I}(\tau; t, \mathbf{x}), \tag{9.154}$$

and

$$\mathcal{I}(\tau; t, \mathbf{x}) = \frac{A^{\frac{1}{2}}}{\sqrt{4\pi\tau}} \mathcal{I}_{\mathcal{V}}(\tau; \mathbf{x}). \tag{9.155}$$

The spatial term $\mathcal{I}_{\mathcal{V}}$ can be evaluated by using the results of [117], which computed the divergent contributions due to operators of the form

$$\mathcal{V} = \overline{\Box}^2 + V^{ij}\overline{\nabla}_i\overline{\nabla}_j + T^i\overline{\nabla}_i + X. \tag{9.156}$$

In our case,

$$V^{ij} = \overline{g}^{ij}\overline{R}\frac{\frac{3}{2} - \lambda}{1 - \lambda}, \qquad T^i = 0, \qquad X = \frac{\overline{R}^2}{2(1-\lambda)}. \tag{9.157}$$

Expanding $\mathcal{I}_{\mathcal{V}}$ in powers of τ defines the Seeley-Gilkey coefficients,

$$\mathcal{I}_{\mathcal{V}}(\tau; \mathbf{x}) = \sqrt{\overline{g}} \sum_{m=0}^{\infty} a_m(\mathbf{x}) \tau^{\frac{m-1}{2}}. \tag{9.158}$$

The logarithmic divergence comes from the $m = 2$ term. The computation of the Seeley-Gilkey coefficient a_2 of [117] yields for $T^i = 0$,

$$a_2 = \frac{1}{16\sqrt{\pi}} \left\{ \frac{1}{16} \left(\overline{g}^{ij}V_{ij}\right)^2 + \frac{1}{8}V_{ij}V^{ij} + \frac{1}{6}\left(\overline{g}^{ij}V_{ij}\right)\overline{R} - \frac{1}{3}V_{ij}\overline{R}^{ij} - 2X \right\} = \frac{\gamma^2 \overline{R}^2}{8\sqrt{\pi}A^2}. \tag{9.159}$$

The log divergence can be evaluated by introducing a cutoff μ^{-4} for the τ-integral, which gives

$$\left. \frac{d}{ds} \right|_{s=0} \frac{k_*^{4s} A^{\frac{1}{2}-s}}{\Gamma(s)} \int_0^{\mu^{-4}} d\tau\, \tau^{s-1} \to \sqrt{A} \log\left(\frac{k_*^4}{A\mu^4}\right) + (\text{finite}). \tag{9.160}$$

Inserting this into the expression for Γ_1 gives the one-loop logarithmic divergence of the effective action on our background:

$$\Gamma_{1,\text{log}}\left(\gamma \overline{R}^2 = 2\Lambda\right) = \frac{\sqrt{2\gamma}}{32\pi} \left(\frac{\frac{1}{2} - \lambda}{1 - \lambda}\right)^{\frac{3}{2}} \log k_* \int dt\, d^2\mathbf{x} \sqrt{\overline{g}}\, \overline{R}^2. \tag{9.161}$$

So far, we have evaluated the one-loop effective action over two different background geometries, both of which are described by a time-independent metric:

- The Aristotelian spacetime with a nonzero cosmological constant $\Lambda \neq 0$. This background geometry is off-shell, *i.e.*, the background metric does not satisfy the associated background equations of motion. The effective action was evaluated in (9.78). The covariant expression is

$$\Gamma_{1,\log}(\overline{R} = 0) = Y_\Lambda \int dt\, d^2\mathbf{x}\, \overline{N} \sqrt{\overline{g}}\, 2\Lambda, \tag{9.162}$$

where

$$Y_\Lambda \equiv \frac{1}{16\pi} \left\{ \frac{2}{\sqrt{\mathfrak{u}_1}} + \frac{1}{\sqrt{2\mathfrak{u}}} \frac{1}{(1-\lambda)^{\frac{3}{2}}} + \frac{1}{2\sqrt{\gamma}} \left(\frac{1-2\lambda}{1-\lambda} \right)^{\frac{3}{2}} \right\} \log k_* + O(\kappa^2) \tag{9.163}$$

contains gauge dependence. Although (9.163) was computed using a sharp cutoff, the coefficient of the logarithmic divergence is universal, so we can use this result in studying the logarithmic divergence that arose in zeta function regularization.

- A background geometry with a time-independent metric but a nonvanishing Riemann tensor. We study the on-shell action with Λ set to be

$$\Lambda = \frac{1}{2}\gamma \overline{R}^2. \tag{9.164}$$

The effective action is given in (9.161):

$$\Gamma_{1,\log}(\gamma \overline{R}^2 = 2\Lambda) = Y \int dt\, d^2\mathbf{x}\, \overline{N} \sqrt{\overline{g}}\, \gamma \overline{R}^2, \tag{9.165}$$

where

$$Y \equiv \frac{1}{32\pi} \sqrt{\frac{2}{\gamma}} \left(\frac{\frac{1}{2} - \lambda}{1 - \lambda} \right)^{\frac{3}{2}} \log k_* + O(\kappa^2). \tag{9.166}$$

This result is on-shell, and therefore guaranteed to be gauge-independent.

Since Y_Λ is gauge-dependent, we cannot use Y_Λ by itself to extract physically meaningful information. Our goal will be to eliminate this gauge dependence and identify a physical quantity that can be extracted from Y.

We begin by examining the effective action evaluated on an off-shell time-independent background. We expand to one-loop order, keeping only the logarithmic divergence:

$$\Gamma = S + \Gamma_{1,\log} + \cdots, \tag{9.167}$$

where

$$S = \frac{1}{\kappa^2} \int dt\, d^2\mathbf{x}\, \overline{N} \sqrt{\overline{g}} \left\{ \overline{K}_{ij} \overline{K}^{ij} - \lambda \overline{K}^2 - \gamma \overline{R}^2 - 2\Lambda \right\}. \tag{9.168}$$

Note that $\overline{K}_{ij} = 0$ for a time-independent background. From (9.162) and (9.165), we obtain

$$\Gamma_{1,\log} = \int dt\, d^2\mathbf{x}\, \overline{N}\sqrt{\overline{g}}\left\{\gamma(Y - Y_\Lambda)\,\overline{R}^2 + 2Y_\Lambda\Lambda\right\}. \tag{9.169}$$

The effective action Γ on a time-independent background can be written as

$$\Gamma = \frac{1}{\kappa^2}\int dt\, d^2\mathbf{x}\, \overline{N}\sqrt{\overline{g}}\left\{-\gamma\left[1 - \kappa^2(Y - Y_\Lambda)\right]\overline{R}^2 - 2\Lambda\left(1 - \kappa^2 Y_\Lambda\right)\right\} + \cdots. \tag{9.170}$$

As we noted, the naïve off-shell effective action (9.170) depends on our choice of gauge parameters. In fact, as a function on the space of background metrics, the effective action is gauge-independent, but the parametrization of field space can depend on gauge. Such dependence can therefore be removed by a field redefinition. (For example, see [118, 116].) In general, these field redefinitions could include curvature terms. In our case, however, for dimensional reasons it suffices to rescale the metric. Under the rescaling,

$$\overline{g}_{ij} \to C\,\overline{g}_{ij}, \tag{9.171}$$

we have

$$\sqrt{\overline{g}} \to C\sqrt{\overline{g}}, \quad \overline{K}_{ij} \to C\overline{K}_{ij}, \quad \overline{R} \to C^{-1}\overline{R}, \quad \Lambda \to \Lambda. \tag{9.172}$$

Under this rescaling, the effective action becomes

$$\Gamma = \frac{1}{\kappa^2}\int dt\, d^2\mathbf{x}\, \overline{N}\sqrt{\overline{g}}\left\{-C^{-1}\left[1 - \kappa^2(Y - Y_\Lambda)\right]\gamma\overline{R}^2 - 2C\left(1 - \kappa^2 Y_\Lambda\right)\Lambda\right\} + \cdots. \tag{9.173}$$

To extract beta functions requires specifying a normalization condition that fixes the field rescaling. First, let us choose the normalization condition such that the coefficient of the $\overline{R}^2$ term is set to one. This fixes the field rescaling C to be

$$C = \frac{\gamma}{\kappa^2}\left[1 - \kappa^2(Y - Y_\Lambda)\right], \tag{9.174}$$

thereby turning the effective action into

$$\Gamma = \int dt\, d^2\mathbf{x}\, \overline{N}\sqrt{\overline{g}}\left\{-\overline{R}^2 - 2(1 - \kappa^2 Y)\Omega\right\} + \cdots, \tag{9.175}$$

where we have defined

$$\Omega \equiv \frac{\gamma\Lambda}{\kappa^4}. \tag{9.176}$$

Indeed, the gauge-dependent contribution Y_Λ drops out altogether from this last expression. The factor $(1 - \kappa^2 Y)$ can be absorbed into the renormalization of Ω. We are working in bare perturbation theory, so that the physical coupling Ω_{ph} is related to the bare coupling Ω by $\Omega_{\text{ph}} = (1 - \kappa^2 Y)\Omega$. Then, the anomalous dimension of Ω is

$$\delta_\Omega \equiv -\frac{d\log\Omega_{\text{ph}}}{d\log k_*} = \frac{1}{16\pi}\sqrt{\frac{\kappa^4}{2\gamma}}\left(\frac{\frac{1}{2} - \lambda}{1 - \lambda}\right)^{\frac{3}{2}} + O(\kappa^4). \tag{9.177}$$

It is interesting to note that the running of Ω is independent of any field rescaling defined in (9.171). A simple analysis is helpful for understanding this observation. Throughout this chapter, we have taken the scaling dimensions of time and spatial coordinates to be -1 and $-\frac{1}{2}$, respectively. In a more fundamental picture introduced in Section 6.1, however, we assign two independent dimensions, T to time, and L to length of space. In this latter convention, we have

$$\dim(\kappa^2) = T^{-1}L^2, \qquad \dim(\gamma) = T^{-2}L^4, \qquad \dim(\Lambda) = T^{-2}. \tag{9.178}$$

Therefore,

$$\dim(\Omega) = T^{-2}, \tag{9.179}$$

which suggests that Ω is independent of a rescaling of spatial coordinates. Further note that the rescaling of $\overline{g}_{ij}$ can be absorbed completely into a rescaling of spatial coordinates. Hence Ω should not change under the field redefinition of the spatial metric.

As we have seen in (9.177), an off-shell time-independent background provides us with only one piece of RG information. There are, however, three couplings, κ, γ and Λ, in the action evaluated on a time-independent background. Since we have the freedom of choosing a normalization condition to fix the field redefinition, not all these three couplings are independent. By an appropriate choice of the normalization condition, we can at least separate the flow of one coupling constant. Again, we would like to adapt a normalization condition to the spatial curvature term and extract the beta function for the cosmological constant.

Instead of using (9.174), let us first take C to be

$$C = \kappa^2 \left[1 + \kappa^2 C_1 + O(\kappa^4) \right], \tag{9.180}$$

thereby turning the effective action (9.173) into

$$\Gamma = \int dt \, d^2\mathbf{x} \, \overline{N} \sqrt{\overline{g}} \left\{ -\left[1 - \kappa^2(Y - Y_\Lambda + C_1) \right] \frac{\gamma}{\kappa^4} \overline{R}^2 - 2\left[1 - \kappa^2(Y_\Lambda - C_1) \right] \Lambda \right\} + \cdots. \tag{9.181}$$

Note that $\dim(\gamma/\kappa^4) = 1$ by (9.178), which motivates us to take a simple choice of the normalization condition by fixing γ/κ^4 to be constant at all scales. Then,

$$C_1 = Y_\Lambda - Y, \tag{9.182}$$

and the gauge-independent effective action becomes

$$\Gamma = \int dt \, d^2\mathbf{x} \, \overline{N} \sqrt{\overline{g}} \left\{ -\frac{\gamma}{\kappa^4} \overline{R}^2 - 2(1 - \kappa^2 Y)\Lambda \right\} + \cdots. \tag{9.183}$$

In bare perturbation theory, we require that the physical couplings γ_{ph}, κ_{ph} and Λ_{ph} satisfy

$$\frac{\gamma_{\text{ph}}}{\kappa_{\text{ph}}^4} = \frac{\gamma}{\kappa^4}, \qquad \Lambda_{\text{ph}} = (1 - \kappa^2 Y)\Lambda. \tag{9.184}$$

Therefore, the beta function for γ/κ^4 vanishes, while the anomalous dimension for the cosmological constant is

$$\delta_\Lambda \equiv -\frac{d\log\Lambda_{\mathrm{ph}}}{d\log k_*} = \frac{1}{16\pi}\sqrt{\frac{\kappa^4}{2\gamma}}\left(\frac{\frac{1}{2}-\lambda}{1-\lambda}\right)^{\frac{3}{2}} + O(\kappa^4). \qquad (9.185)$$

For $\gamma > 0$ and $\lambda > 1$ or $\lambda < \frac{1}{2}$, δ_Λ is real and positive. It is interesting to note that when $\lambda = \frac{1}{2}$, which is required for Weyl symmetry, δ_Λ vanishes at one-loop order. When λ approaches 1, which is required for Lorentz symmetry to be realized, the one-loop expression for δ_Λ blows up, reflecting the strong coupling problem of the $\lambda \to 1$ limit [119]. Of course, we are still far from determining if the theory is asymptotically free. One will have to evaluate the heat kernel for time-dependent background geometries to map out the full RG structure.

As a final comment, we note that there is no logarithmically divergent contribution to the coupling in front of the term

$$\int dt\, d^2\mathbf{x}\, \overline{N}\sqrt{\overline{g}}\,\overline{R}. \qquad (9.186)$$

This can be seen as follows. Since the UV properties are controlled by the terms with the most derivatives, we can view Λ purely as a coupling constant and expand in a power series of Λ. Since ρ does not contribute to the differential operator $\mathcal{O}_{\mathrm{phys}}$, Λ is the only dimensionful parameter that can arise in the one-loop divergence. The contribution of lowest dimension, linear in Λ, has dimension two, and so cannot appear in the coefficient for $\overline{R}$. Hence, (9.186) cannot appear at all in the logarithmic divergence at one loop.

9.7 Discussions and Outlooks

This chapter dealt with the computation of quantum corrections in the simplest version of critical Hořava gravity, the $z = 2$ projectable theory in $2+1$ dimensions. Working in a gauge with two free parameters, we computed the quantum effective action in two different cases. The first was flat space with $\Lambda \neq 0$; this is an off-shell background, and we saw that the naïve result was gauge dependent. This gauge dependence is however ephemeral: the effective action in gauge theory can be gauge-dependent, provided the gauge dependence can be eliminated by a field redefinition.

On the other hand, for an on-shell background field an infinitesimal field redefinition leaves the value of the action invariant (since the action is stationary under any variation), and therefore the result (if correct) must be gauge independent. Working on the time-independent on-shell background $\mathbb{R} \times S^2$ or $\mathbb{R} \times H^2$ with $\gamma\overline{R}^2 = 2\Lambda$, we find a gauge-independent effective action, as expected. Using this action, we are able to extract one of the one-loop beta functions.

The main result here is therefore equation (9.185), which captures the flow of the cosmological constant Λ at one loop order in $z = 2$ Hořava gravity in $2+1$ dimensions, as defined relative to a metric normalization such that γ/κ^4 is constant at all scales.

We focused on the flow of this variable for several reasons, which are all rooted in the fact that our computation is based on the effective action for on-shell, time-independent backgrounds. Working on-shell has several advantages, notably the automatic gauge invariance of the quantum effective action. We furthermore saw an explicit reduction of the partition function to only the physical degree of freedom in the one-loop partition function. This simplification can be traced to the on-shell condition. In this way, the computation of the on-shell effective action could be reduced to the functional determinant of a single scalar operator.

Time independence had the further virtue of allowing us to reduce our computations to known properties of the heat kernels of higher order relativistic differential operators. And as a background field computation, of course, this can all be done using only the divergences in a single "vacuum bubble" diagram, without having to compute vertices explicitly.

One pays a price for working on time-independent backgrounds, however: divergences in the effective action proportional to K_{ij} are invisible. This means that out of the four couplings[8] of the model — λ, κ, γ and Λ — that played a role here, we can only determine the flow of one. (Note that not all of these coefficients are physically meaningful. For example, in the text we rescaled g_{ij} to make one coupling take a value of our choosing.)

In order to compute the remaining beta functions, one must relax one of these restrictions. The full computation can in principle be done entirely on-shell, provided we allow time-dependent backgrounds. This approach runs into one of two possible difficulties. The first is that of finding explicit classical backgrounds on which to work. The simplest backgrounds are cosmological backgrounds of FLRW type, in which case $\overline{K}_{ij}$ is pure trace. Imposing the trace constraint reduces the number of beta functions that can be computed by one; to obtain the complete flow of the theory would still require backgrounds on which $\overline{K}_{ij}$ is not pure trace.

If we accept this limitation, we run into the second complication, that in pure Hořava gravity such backgrounds are de Sitter-like. As a result they suffer from large contributions to the effective action from temporal boundaries (the boundary area grows at about the same rate as the bulk volume), which makes it difficult to distinguish the boundary and bulk contributions to the effective action.

Even after overcoming these difficulties there remains a potentially troublesome point. Our methods expressed the determinant in the $(h, \widetilde{\sigma})$ sector as a product,

$$\det \mathcal{O}_{h\widetilde{\sigma}} = \det(\mathcal{O}_g \mathcal{O}_{\text{phys}}) = (\det \mathcal{O}_g)(\det \mathcal{O}_{\text{phys}}), \qquad (9.187)$$

after which we cancel against $\mathcal{O}_g$ coming from the ghost sector. This requires the product identity $\det(AB) = (\det A)(\det B)$, but this identity runs into difficulties in the infinite-dimensional case. These can be surmounted straightforwardly when $[A, B] = 0$ (as was the case for us), but it is more problematic when $[A, B] \neq 0$, as occurs in the time-dependent case, and leads to ambiguities in the result. (For one discussion of this issue, see [120].)

---

[8]There is a fifth, ρ, but as we saw above it receives no logarithmic divergences at one loop.

These problems point to a general need for more flexible methods to compute loop effects in Hořava gravity. In the end, it may turn out that the only viable method is to work on perturbative backgrounds, performing explicit expansions of the heat kernel of a matrix differential operator.

For many purposes, the most interesting class of Hořava gravities are the *non-projectable* theories, which relax the constraint $\nabla_i N = 0$ and allow $N = N(t, \mathbf{x})$ to depend on space. For example, in phenomenological applications the non-projectable variant requires much less fine tuning to be consistent with observational constraints [121, 122]. From a more conceptual point of view, the "conformal" variants – those invariant under anisotropic Weyl symmetry [5] — are also of considerable interest. We here briefly summarize the extension of our methods to these models, and discuss some of the new challenges that arise.

The novelty arising in the non-projectable theory is that once N has local fluctuations, it gives rise to a new constraint. Because the number of additional constraints equals the number of additional fields (one in both cases) the number of propagating degrees of freedom remains unchanged, but the details of the spectrum and the gravitational interaction are modified.

In the computation of the one-loop effective action, the non-projectability leads to two new features that should be handled carefully. The first is that $\overline{N}$ cannot be set to 1 by a gauge transformation, and therefore needs to be incorporated appropriately into the gauge-fixing conditions. The second is that the second-class constraint is non-linear, and so its measure needs to be defined carefully. The question of whether the right approach is to solve directly for the Dirac bracket, or to use the ghost formalism of [123], or whether there exists a simple prescription giving the correct contributions to the path integral, we leave for future work.

Now for the conformal case. For certain choices of parameters in the gravitational action, an additional local symmetry arises: anisotropic Weyl invariance. This is a symmetry under a Weyl scaling

$$N \mapsto \Omega^z N \qquad N_i \mapsto \Omega^2 N_i \qquad g_{ij} \mapsto \Omega^2 g_{ij} \tag{9.188}$$

where $\Omega = \Omega(t, \mathbf{x})$ is an arbitrary function. In this case, at the classical level the second-class constraint of N is replaced by a first-class constraint, which eliminates the scalar degree of freedom entirely. The question of whether this symmetry can survive at the quantum level is of considerable interest, particularly in $2+1$ dimensions, where conformal Hořava gravity has no propagating degrees of freedom and therefore provides a useful analog of three dimensional Einstein gravity, with its importance in addressing the conceptual issues of quantum gravity.

In some ways, the conformal case bears similarities to the projectable theory, in that we can gauge fix $\overline{N} = 1$ if we like. On the other hand, to answer questions about the preservation of conformal symmetry, it is important to choose a gauge-fixing condition that is invariant under background Weyl transformations.[9] In particular, if we want to study whether Weyl symmetry is anomalous, we should *not* gauge-fix $\overline{N} = 1$, and instead work in a more general background gauge. This requires us to modify the gauge-fixing conditions.

---

[9]This is analogous to the situation in relativistic Weyl gravity in $3 + 1$ dimensions, see [124].

One important difference in the conformal case is that to preserve background Weyl symmetry, the gauge fixing must respect $z = 2$ scaling. The type of gauge fixing used here and in [111] makes this possible. It is this consideration that initially led us to the gauge-fixing used earlier in the chapter. We note that background Weyl invariance requires some new features in the gauge-fixing condition, in particular in that $\overline{N}$ and n must be included to construct an appropriate Weyl-invariant object.

Beyond its interest as a toy model, the study of the conformal theory is relevant to the problem of quantum membranes [5]. The path integral for relativistic quantum membranes is not renormalizable, putting a theory of fundamental relativistic quantum membranes out of reach. This is reflected in the Polyakov action formalism in the non-renormalizability of three-dimensional gravity. With $z = 2$ scaling, on the other hand, the Polyakov action becomes power-counting renormalizable. In this picture, the critical membrane theory would become conformal Hořava gravity coupled to a $z = 2$ non-linear sigma model. The crucial question of whether such critical membrane theories exist, or whether a Weyl anomaly spoils criticality, we leave to future research.

Chapter 10

Conclusions

In this thesis, we examine the naturalness puzzles phrased in a simple model: Relativistic EFTs of a single scalar. We take an intriguing twist to such relativistic EFTs by considering nonrelativistic short-distance completions that preserve Lorentz invariance in the low energies. In this study, we discover a series of surprises in the study of Aristotelian scalar field theories, which leads to some new ingredients for some of those long-standing puzzles of naturalness.

In the context of spontaneous symmetry breaking, we study Aristotelian linear and nonlinear sigma models and classify nonrelativsitic NG modes. We find that the constant shift symmetry is extended to polynomial shift symmetries, which protects the technical naturalness of NG modes with a higher-order dispersion. This discovery leads to a generalization of the relativistic CHMW theorem to multicritical cases in lower critical dimension. By breaking the polynomial shift symmetries in a hierarchy, we find novel cascading phenomena with large hierarchies between the scales at which the values of z change, leading to an evasion of the "no-go" consequences of the relativistic CHMW theorem.

With potential applications to naturalness puzzles in mind, we continue to a case study of a 3+1 dimensional self-interacting single-scalar field theory with linear shift symmetry around a $z = 3$ Gaussian fixed point, which exhibits a nonrenormalization theorem for the speed of light. At high energies the theory becomes strongly coupled and exhibits increasingly large decay width and may self-complete in a mechanism reminiscent of classicalization. In the large-N limit, its $O(N)$ vector extension defines a stable and conformal theory, which suggests possible higher-spin holographic duals. It will be also fascinating to understand what role the polynomial shift symmetries could play in the context of the AdS/CFT correspondence.

Based on this case study and taking advantages of the cascading scales of the partial symmetry breaking, we propose a "10-20-30" model in which a high-energy cross-over to such nonrelativistic behavior may provide a useful ingredient for a technically natural resolution of the Higgs mass hierarchy problem: The scalar in this theory is naturally light! Introducing Yukawa couplings to fermions in this 10-20-30 scenario, the masses of all Standard Model fermions can be Dirac in a technically natural way. Such self-interacting scalar field theories also represent a new nonrelativistic variation on the models of inflation.

After establishing the polynomial shift symmetry in the continuum theory, we discretize this symmetry on a periodic lattice, aiming for potential applications in condensed matter systems. We then generalize the EFT classification of the electron-phonon interactions in metals by replacing the acoustic phonons by multicritical phonons with a higher dispersion, protected by these new discrete symmetries. By calculating the resistivity of the metal as a function of temperature T in the Bloch-Boltzmann transport theory, we find that the system of $z = 3$ multicritical phonons, which cascades to conventional $z = 1$ phonons in low energies, gives resistivity linear in T (with a $T \log T$ correction) in $3 + 1$ dimensions. This provides new insights into the study of strange metals and probably the high-T_c superconductivity.

The classification of lowest-dimensional operators invariant under the polynomial shift symmetry of degree P is an intricate cohomological question in the sense of the coset construction. However, in a novel graph-theoretical representation that we develop, the structure of such invariants reveals its elegancy: In the $P = 1$ case (essentially Galileons), they are interpreted as an equal-weight sum over all labeled trees with fixed vertices; higher P-invariants are constructed from superposing graphs that represent invariants of lower P's. Some special cases of such new higher P-invariants are connected to the study of the soft limits in EFTs.

To illustrate the naturalness of NG modes with higher-order dispersion relations, we used intensively Aristotelian $O(N)$ nonlinear sigma model. The study of Aristotelian NLSMs is interesting on its own from both the formal side and condensed matter physics. We apply the techniques picked up along our studies of Aristotelian scalar field theories to the $2 + 1$ dimensional $O(N)$ NLSM at a $z = 2$ Lifshitz fixed point and obtain its full one-loop beta-functions. In the large-N limit, we solve this theory to all loops by summing over cactus diagrams recursively. This calculation can be viewed as a first step towards the generalization to the Aristotelian case of the landmark calculation by Friedan of the one-loop beta function for a $1 + 1$ dimensional relativistic NLSM; such generalization may form a useful building block of a nonrelativistic M-theory. On the other hand, the Aristotelian $O(N)$ NLSM may provide new features to critical phenomena. Moreover, turning on Wess-Zumino terms in such Aristotelian NLSMs may also introduce interesting twists to the study of topological insulators.

Another motivation for our systematic study of scalar field theories with Aristotelian symmetry comes from the attempt to understand the quantum behaviors of Hořava gravity. Mapping out the quantum structure of nonrelativistic gravity theories and investigating the role of naturalness in the context of gravity remain an outstanding challenge, which could benefit the study of AdS/CFT correspondence for nonrelativistic systems, as well as our understanding of the phase structure revealed in the Causal Dynamical Triangulation approach in quantum gravity. A prototype example is the $2+1$ dimensional Hořava gravity at a $z = 2$ Lifshitz fixed point, which is also potentially useful as a worldvolume theory for describing membranes at quantum criticality. We study quantum corrections to projectable Hořava gravity with $z = 2$ scaling in $2 + 1$ dimensions. Using the background field method, we utilize a non-singular gauge to compute the anomalous dimension of the cosmological constant at one loop, in a normalization adapted to the spatial curvature term. It will be interesting

to generalize this calculation to nonprojectable cases, which could be important for both formal and phenomenological reasons. Despite of these efforts, nonrelativistic naturalness in Aristotelian QFTs beyond single scalars and its implications to important naturalness puzzles, such as the cosmological constant problem, remains largely mysterious and deserves future exploration.

Appendix A

Scattering Amplitudes in Aristotelian Spacetime

In this appendix, we study the decay rates and the scattering cross-sections in the Aristotelian spacetime. We will revert to the more fundamental picture where space and time are *a priori* unrelated, and will keep track of the double dimensions dim( ) (introduced in Chapter 6) of all quantities throughout.

A.1 Decay Rates

The derivation of the decay rates follows closely the derivation in the relativistic case, which we review as follows. We enclose the system in a cubic box with volume V; finite time length T. We work in general $3+1$ dimensions. Mode expansion of the real field $\Phi(t, \mathbf{x})$:

$$\Phi(t, \mathbf{x}) = \frac{1}{\sqrt{V}} \sum_{\mathbf{k}} \frac{1}{\sqrt{2\omega_{\mathbf{k}}}} \left\{ a_{\mathbf{k}} e^{-i(\omega_{\mathbf{k}} - \mathbf{k} \cdot \mathbf{x})} + a_{\mathbf{k}}^{\dagger} e^{i(\omega_{\mathbf{k}} t - \mathbf{k} \cdot \mathbf{x})} \right\}. \tag{A.1}$$

Commutation relation:

$$[a_{\mathbf{k}}, a_{\mathbf{k}'}^{\dagger}] = \delta_{\mathbf{k}, \mathbf{k}'}. \tag{A.2}$$

To compute the decay rate of a particle with frequency $\omega_{\mathbf{k}}$ and momentum $\mathbf{k}$ in the Aristotelian spacetime, we need to compute the transition amplitude for the process $\mathbf{k} \to \{\mathbf{k}_f\} \equiv \mathbf{k}_1, \cdots, \mathbf{k}_n$ (frequencies are $\omega_{\mathbf{k}}, \{\omega_f\} = \{\omega_{\mathbf{k}_1}, \cdots, \omega_{\mathbf{k}_n}\}$):

$$\mathcal{A} = \frac{1}{V^{\frac{n+1}{2}}} \sum_{\mathbf{k}, \{\mathbf{k}_f\}} \frac{1}{\sqrt{(2\omega) \prod_f (2\omega_f)}} \int dt \, d^3\mathbf{x} \, (i\mathcal{M}) \, \langle \{\mathbf{k}_f\} | a_{\mathbf{k}_1}^{\dagger} \cdots a_{\mathbf{k}_n}^{\dagger} a_{\mathbf{k}} | \mathbf{k} \rangle$$

$$\times \exp \left\{ i \left(\omega_{\mathbf{k}} - \sum_f \omega_f \right) t - i \left(\mathbf{k} - \sum_f \mathbf{k}_f \right) \cdot \mathbf{x} \right\}$$

$$= \frac{i\mathcal{M}}{V^{\frac{n+1}{2}} \sqrt{(2\omega) \prod_f (2\omega_f)}} (2\pi)^4 \delta \left(\omega_{\mathbf{k}} - \sum_f \omega_f \right) \delta^{(3)} \left(\mathbf{k} - \sum_f \mathbf{k}_f \right). \tag{A.3}$$

Here $\mathcal{M}$ is the amplitude, $\mathcal{M} = \mathcal{M}(\mathbf{k} \to \{\mathbf{k}_f\})$. Note that within the finite Aristotelian spacetime with 4-volume VT, we have

$$\left[(2\pi)^4 \delta\left(\omega_{\mathbf{k}} - \sum_f \omega_f\right) \delta^3\left(\mathbf{k} - \sum_f \mathbf{k}_f\right)\right]^2 = (2\pi)^4 \delta\left(\omega_{\mathbf{k}} - \sum_f \omega_f\right) \delta^{(3)}\left(\mathbf{k} - \sum_f \mathbf{k}_f\right) VT,$$

and the differential decay width is given by the product of the transition rate $|\mathcal{A}|^2/T$ and the number of the final states:

$$d\Gamma \equiv \frac{|\mathcal{A}|^2}{T} \prod_f \frac{V d^3\mathbf{k}_f}{(2\pi)^3}, \tag{A.4}$$

Hence, the differential decay width in the Aristotelian spacetime is

$$d\Gamma = \frac{1}{2\omega_{\mathbf{k}}} \left(\prod_f \frac{d^3\mathbf{k}_f}{(2\pi)^3} \frac{1}{2\omega_{\mathbf{k}_f}}\right) |\mathcal{M}(\mathbf{k} \to \{\mathbf{k}_f\})|^2 (2\pi)^4 \delta\left(\omega_{\mathbf{k}} - \sum_f \omega_f\right) \delta^{(3)}\left(\mathbf{k} - \sum_f \mathbf{k}_f\right). \tag{A.5}$$

Since it gives the probability of decay per unit time, its dimension is $\dim(\Gamma) = 1/T$.

A.2 Example: Self-decay in $2+1$ Dimensions

The calculation for the imaginary part of the sunset diagram to obtain the decay rate in the $\partial^6 \Phi^4$ theory is quite involved and it is difficult to have analytical control on it. (It is, however, not difficult to use standard method to estimate the decay width in high energies, and the result is given in (6.42).) To illustrate the structure of the self-decay rate more explicitly, let us consider the following simpler theory in $2+1$ dimensions, in which the decay rate can be computed analytically:

$$S = \frac{1}{2} \int dt\, d^2\mathbf{x} \left\{\dot{\phi}^2 - \left(\partial_i \partial_j \phi\right)^2 - c^2 \partial_i \phi\, \partial_i \phi - m^2 \phi^2 - \lambda_3 \partial_i \phi\, \partial_j \phi\, \partial_i \partial_j \phi\right\}. \tag{A.6}$$

This action describes a renormalizable QFT, due to its underlying linear shift symmetry. We have turned on the gap term that breaks the linear shift symmetry in the softest way. The λ_3-term breaks the reflection symmetry $\phi \to -\phi$. Up to total derivatives, the interaction with a λ_3 coupling can be written as

$$\int dt\, d^3\mathbf{x}\, \partial_i \phi\, \partial_j \phi\, \partial_i \partial_j \phi = \frac{1}{3} \int dt\, d^3\mathbf{x}\, \varepsilon_{ij} \varepsilon_{k\ell} \partial_i \phi\, \partial_j \phi\, \partial_k \partial_\ell \phi. \tag{A.7}$$

It is convenient to write the Feynman propagator as

$$\frac{i}{\omega^2 - (\omega_{\mathbf{k}} - i\varepsilon)^2}, \tag{A.8}$$

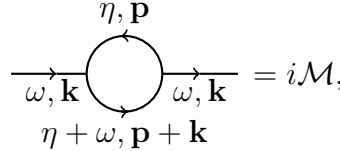where $\omega_{\mathbf{k}}^2 = k^4 + c^2 k^2 + m^2 > 0$ for a positive m^2. The 3-vertex is

$$-i\lambda_3 \left\{(\mathbf{k} \cdot \mathbf{p})(\mathbf{k} \cdot \mathbf{q}) + (\mathbf{p} \cdot \mathbf{q})(\mathbf{p} \cdot \mathbf{k}) + (\mathbf{q} \cdot \mathbf{k})(\mathbf{q} \cdot \mathbf{p})\right\}. \tag{A.9}$$

Applying the conservation law of momenta, $\mathbf{q} = -\mathbf{k} - \mathbf{p}$, we obtain

$$-i\lambda_3 \left\{ k^2 p^2 - (\mathbf{k} \cdot \mathbf{p})^2 \right\} = -i\lambda_3 [\mathbf{kp}]^2, \tag{A.10}$$

where $[\mathbf{kp}] = \varepsilon_{ij} \mathbf{k}^i \mathbf{p}^j$.

Consider the one-loop correction to the propagator,

$$= i\mathcal{M}, \tag{A.11}$$

where

$$i\mathcal{M} = \frac{1}{2} \int \frac{d\eta}{2\pi} \frac{d^2\mathbf{p}}{(2\pi)^2} \frac{i^2 \left\{ -i\lambda_3 [\mathbf{kp}]^2 \right\}^2}{\left[\eta^2 - (\omega_{\mathbf{p}} - i\varepsilon)^2 \right] \left[(\eta + \omega)^2 - (\omega_{\mathbf{p+k}} - i\varepsilon)^2 \right]}. \tag{A.12}$$

We impose the positive energy condition that $\omega > 0$. We are interested in the imaginary part of $\mathcal{M}$, which is associated with the decay width. We start with performing the integral over η along the real axis. We take the analytic continuation of η to the complex plane. The integrand has two poles in the upper half complex plane, namely,

$$\eta = -\omega_{\mathbf{p}} + i\varepsilon, \ -\omega - \omega_{\mathbf{p+k}} + i\varepsilon. \tag{A.13}$$

We complete the integration contour by including a semicircle that encloses the upper half plane. By Cauchy's theorem, we obtain

$$\mathcal{M} = -\frac{\lambda_3^2}{4} \int \frac{d^2\mathbf{p}}{(2\pi)^2} \frac{[\mathbf{kp}]^4}{\omega_{\mathbf{p}} \omega_{\mathbf{p+k}} (\omega - \omega_{\mathbf{p}} + \omega_{\mathbf{p+k}})}$$
$$\times \left\{ \frac{\omega_{\mathbf{p+k}}}{\omega - \omega_{\mathbf{p}} - \omega_{\mathbf{p+k}} + 2i\varepsilon} + \frac{\omega_{\mathbf{p}}}{\omega + \omega_{\mathbf{p}} + \omega_{\mathbf{p+k}} - 2i\varepsilon} \right\}. \tag{A.14}$$

By the Sokhotski-Plemelj theorem,

$$\frac{1}{x \pm i\varepsilon} = \mathcal{P} \left(\frac{1}{x} \right) \mp i\pi \delta(x), \tag{A.15}$$

we obtain

$$\mathbb{I}m\mathcal{M} = -\frac{\pi\lambda_3^2}{4} \int \frac{d^2\mathbf{p}}{(2\pi)^2} [\mathbf{kp}]^4 \frac{\omega_{\mathbf{p}} \delta(\omega + \omega_{\mathbf{p}} + \omega_{\mathbf{p+k}}) - \omega_{\mathbf{p+k}} \delta(\omega - \omega_{\mathbf{p}} - \omega_{\mathbf{p+k}})}{\omega_{\mathbf{p}} \omega_{\mathbf{p+k}} (\omega - \omega_{\mathbf{p}} + \omega_{\mathbf{p+k}})}.$$

Because $\omega > 0$, we obtain

$$\mathbb{I}m\mathcal{M} = \frac{\pi\lambda_3^2}{8} \int \frac{d^2\mathbf{p}}{(2\pi)^2} \frac{[\mathbf{kp}]^4}{\omega_{\mathbf{p}} \omega_{\mathbf{p+k}}} \delta(\omega - \omega_{\mathbf{p}} - \omega_{\mathbf{p+k}}), \tag{A.16}$$

which can be rewritten as

$$\mathbb{I}m\mathcal{M} = -\frac{\lambda_3^2}{4}\int\frac{d\eta}{2\pi}\frac{d^2\mathbf{p}}{(2\pi)^2}[\mathbf{kp}]^4(-2\pi i)\theta(E_1)\delta(E_1^2 - \omega_{\mathbf{p}}^2)(-2\pi i)\theta(E_2)\delta(E_2^2 - \omega_{\mathbf{p+k}}^2), \quad (A.17)$$

where $E_1 = -\eta$ and $E_2 = \eta+\omega$, the exactly the energies of the two outgoing on-shell particles. The expression (A.17) is expected from the usually optical theorem: The imaginary part of the one-loop diagram is equal to the square of the absolute value of the amplitude into two particles.

Next, we would like to evaluate (A.16) and calculate the decay width. Let us start with writing $\mathbf{p}$ as

$$\mathbf{p} = -u\,\mathbf{k} - \mathbf{q}, \qquad \mathbf{k}\cdot\mathbf{q} = 0. \quad (A.18)$$

Therefore,

$$\omega = \sqrt{k^4 + c^2 k^2 + m^2}, \quad (A.19)$$

$$\omega_{\mathbf{p}} = \sqrt{(u^2 k^2 + q^2)^2 + c^2(u^2 k^2 + q^2) + m^2}, \quad (A.20)$$

$$\omega_{\mathbf{p+k}} = \sqrt{\left[(1-u)^2 k^2 + q^2\right]^2 + c^2\left[(1-u)^2 k^2 + q^2\right] + m^2}. \quad (A.21)$$

We denote $q \equiv |\mathbf{q}|$. Note that when $u > 1$ or $u < 0$, $\omega_{\mathbf{p}}+\omega_{\mathbf{p+k}} > \omega$, violating the conservation law of energy, $\omega = \omega_{\mathbf{p}} + \omega_{\mathbf{p+k}}$, imposed by the Dirac delta in (A.16). Therefore, we can at least restrict the integration range over u to $0 \leq u \leq 1$. Then, (A.16) can be further rewritten as

$$\mathbb{I}m\mathcal{M} = \frac{\lambda_3^2 k^5}{32\pi}\int_0^1 du \frac{q^4}{\omega_{\mathbf{p}}\omega_{\mathbf{p+k}}\left(\partial_q\omega_{\mathbf{p}} + \partial_q\omega_{\mathbf{p+k}}\right)}\bigg|_{q=q_0}, \quad (A.22)$$

where q_0 is the real solution of q such that the conservation law of energy holds, *i.e.*,

$$\omega - \omega_{\mathbf{p}} - \omega_{\mathbf{p+k}}\big|_{q=q_0} = 0. \quad (A.23)$$

For the value of u at which there is no real solution for q, the integrand in (A.22) is understood to be set to zero.

At high energies, $q^2 \gg c^2$ and $q^4 \gg m^2$, we obtain the asymptotic behavior

$$\mathbb{I}m\mathcal{M} = \frac{\lambda_3^2}{1024}k^4 + \mathcal{O}(k^2). \quad (A.24)$$

In this high momentum limit, $\omega_{\mathbf{k}} \sim k^2$, and the total decay width is

$$\Gamma = \frac{1}{\omega_{\mathbf{k}}}\mathbb{I}m\mathcal{M} = \frac{\lambda_3^2}{1024}k^2 + \mathcal{O}(k^0). \quad (A.25)$$

At low momentum, the behavior is more complicated. When $k^4 < 4m^2$, the integral (A.22) is exactly zero, since there is no real solution q_0, and the decay width is zero; therefore, the particle is absolutely stable at momentum with $k^4 < 4m^2$. At $k^4 = 4m^2$, there is a unique

solution $q_0 = 0$ if and only if $u = \frac{1}{2}$; when $k^4 > 4m^2$, the integral in (A.22) yields nonzero value.

In the limit $m \to 0$, the imaginary part of $\mathcal{M}$ is nonzero for any $k > 0$ (and for any u with $0 < u < 1$). In the low momentum limit, $k \ll c$, we have

$$\mathbb{I}m\mathcal{M} = \frac{3\sqrt{3}\,\lambda_3^2}{4480\pi c^6} k^{10} + \mathcal{O}(k^7). \tag{A.26}$$

In this low energy limit with m set to 0, $\omega_{\mathbf{k}} \sim ck$, and the total decay width is

$$\Gamma = \frac{3\sqrt{3}\lambda_3^2}{4480\pi c^7} k^9 + \mathcal{O}(k^6). \tag{A.27}$$

At $\mathbf{k} = 0$, the particle is absolutely stable.

A.3   Cross-sections

The scattering cross-section can be straightforwardly written down as follows,

$$d\sigma = \frac{1}{2\omega_{\mathbf{k}_1} 2\omega_{\mathbf{k}_2} |v_1 - v_2|} \left(\prod_f \frac{d^3 \mathbf{k}_f}{(2\pi)^3} \frac{1}{2\omega_{\mathbf{k}_f}} \right) \left| \mathcal{M}(\mathbf{k}_1, \mathbf{k}_2 \to \{\mathbf{k}_f\}) \right|^2$$
$$\times (2\pi)^4 \delta\left(\omega - \sum_f \omega_f\right) \delta^{(3)}\left(\mathbf{k} - \sum_f \mathbf{k}_f\right). \tag{A.28}$$

Here $\mathbf{k}_1$ and $\mathbf{k}_2$ denote the incoming momenta and $\{\mathbf{k}_f\}$ denotes the outgoing momenta. We have defined the "longitudinal velocities," v_1 and v_2, with

$$v_i \equiv \frac{d\omega_{\mathbf{k}_i}}{dk_i^{\parallel}}, \quad , i = 1, 2, \tag{A.29}$$

with $\mathbf{k}_i^{\parallel}$ is the component of $\mathbf{k}_i$ that is parallel to the direction of the total incoming momentum $\mathbf{k}_1 + \mathbf{k}_2$. Just as in the relativistic case, the cross-section is of dimension $[\sigma] = L^2$.

Appendix B

Evaluation of The Sunset Diagram

In this appendix, we evaluate the following "sunset diagram" defined in Chapter 6 (refer to (6.38)),

$$
\overrightarrow{\omega,\mathbf{k}}\,\bigcirc\,\overrightarrow{\omega,\mathbf{k}} \;=\; \frac{1}{3!}\int \frac{d\eta}{2\pi}\frac{d\nu}{2\pi}\frac{d^3\mathbf{p}}{(2\pi)^3}\frac{d^3\mathbf{q}}{(2\pi)^3}\frac{i^3(-i\lambda[\mathbf{kpq}])^2}{(\eta^2-\omega_\mathbf{p}^2)(\nu^2-\omega_\mathbf{q}^2)[(\omega+\eta+\nu)^2-\omega_{\mathbf{k+p+q}}^2]}.
$$

(B.1)

Performing the Wick rotation by taking $\eta \to i\eta$, $\nu \to i\nu$ and $\omega \to i\omega$, the sunset diagram in (B.1) becomes

$$
\overrightarrow{\omega,\mathbf{k}}\,\bigcirc\,\overrightarrow{\omega,\mathbf{k}} = i\lambda^2\Im,
$$

(B.2)

where

$$
\Im \equiv \frac{1}{3!}\int \frac{d\eta}{2\pi}\frac{d\nu}{2\pi}\frac{d^3\mathbf{p}}{(2\pi)^3}\frac{d^3\mathbf{q}}{(2\pi)^3}\frac{[\mathbf{kpq}]^4}{(\eta^2+\omega_\mathbf{p}^2)(\nu^2+\omega_\mathbf{q}^2)[(\omega+\eta+\nu)^2+\omega_{\mathbf{k+p+q}}^2]}.
$$

(B.3)

We will henceforth stick to this imaginary time convention throughout the discussion in this appendix. It is convenient to define $k \equiv |\mathbf{k}|$, $p \equiv |\mathbf{p}|$, $q \equiv |\mathbf{q}|$ and $K \equiv |\mathbf{K}|$.

Relevant couplings in the dispersion relation $\omega_\mathbf{k}$ provide an IR regulator. Most generically,

$$
\omega_\mathbf{k}^2 = \zeta_3^2 k^6 + \zeta_2^2 k^4 + c^2 k^2 + m^2.
$$

(B.4)

The integral $\Im$ is finite in the IR as long as at least one of the IR-regulating terms, ζ_2, c, or ζ_0, is turned on. It is sufficient to show that (B.3) is IR finite if c and ζ_0 are zero but ζ_2^2 is nonzero, such that

$$
\omega_\mathbf{k} = k^4(k^2 + \zeta_2^2).
$$

(B.5)

Let us examine the integral (B.3) at zero frequency, $\omega = 0$. Apply (B.20) to perform the integrals over the frequencies in (B.3), we obtain

$$
\Im = \int \frac{d^3\mathbf{p}}{(2\pi)^3}\frac{d^3\mathbf{q}}{(2\pi)^3}\frac{[\mathbf{kpq}]^4}{4\,\omega_\mathbf{p}\,\omega_\mathbf{q}\,\omega_{\mathbf{k+K}}}\frac{1}{\omega_\mathbf{p}+\omega_\mathbf{q}+\omega_{\mathbf{k+K}}}
$$

$$< \int \frac{d^3\mathbf{p}}{(2\pi)^3} \frac{d^3\mathbf{q}}{(2\pi)^3} \frac{[\mathbf{kpq}]^4}{4\,\omega_\mathbf{p}\,\omega_\mathbf{q}\,\omega_{\mathbf{k+K}}} \frac{1}{2\sqrt{\omega_\mathbf{p}\,\omega_\mathbf{q}}}$$

$$< \frac{1}{8} \int \frac{d^3\mathbf{p}}{(2\pi)^3} \frac{d^3\mathbf{q}}{(2\pi)^3} \frac{[\mathbf{kp(k+K)}][\mathbf{k(k+K)q}][\mathbf{kpq}]^2}{p^3 q^3 |\mathbf{k+K}|^2}. \tag{B.6}$$

It is understood that the integrals over $\mathbf{p}$ and $\mathbf{q}$ are cut off appropriated in the UV. To show that $\Im$ is convergent in the IR, it is sufficient to show that the integrand in the second line in (B.6) is nonsingular:

$$\frac{[\mathbf{kp(k+K)}][\mathbf{k(k+K)q}][\mathbf{kpq}]^2}{p^3 q^3 |\mathbf{k+K}|^2} \leq k^4. \tag{B.7}$$

This proves that $\Im/k^4$ is finite with the choice of $\omega_\mathbf{k}$ in (B.5). A similar proof shows that the integral is IR finite if ζ_2, c and m are set to zero but the external frequency ω is nonzero.

The integral $\Im$ has a superficial quadratically UV divergent. We would like to study the behavior of $\Im$ around the fiducial point in the imaginary time, $\omega^2 = M^6$ and $k^2 = 0$. One can take a first look at the UV divergences by expanding the integral in a Taylor series in k^2:

$$\Im(\omega^2, \mathbf{k}) = \Im_0 + \Im_1 k^2 + \Im_2 k^4 + \Im_3 k^6 + \cdots, \tag{B.8}$$

where $\widetilde{\omega} \equiv \omega/\zeta_3$. By inspection, we see that $\Im_0$ and $\Im_1$ vanish identically. The first non-zero coefficients are $\Im_2$ and $\Im_3$, which can be expected to be quadratically and logarithmically divergent with the spatial momentum cutoff, respectively. All the higher-order terms denoted by "$\cdots$" will be finite.

Since we are setting the renormalization condition around $\omega^2 = M^6 \neq 0$, for practical purposes, we will treat ω^2 as an IR regulator and set ζ_2^2, c^2 and m^2 to zero. Under the change of variables,

$$\eta \to \zeta_3 \eta, \qquad \nu \to \zeta_3 \nu, \tag{B.9}$$

(B.3) can be written as

$$\Im \equiv \frac{1}{3!\zeta_3^4} \int \frac{d\eta}{2\pi} \frac{d\nu}{2\pi} \frac{d^3\mathbf{p}}{(2\pi)^3} \frac{d^3\mathbf{q}}{(2\pi)^3} \frac{[\mathbf{kpq}]^4}{(\eta^2 + p^6)(\nu^2 + q^6)[(\widetilde{\omega} + \eta + \nu)^2 + |\mathbf{k+p+q}|^6]}. \tag{B.10}$$

For simplicity, we will set ζ_3 to 1 in the following calculation. The dependence on ζ_3 can be easily recovered in the final results. Let us define $\mathbf{K} \equiv \mathbf{p}+\mathbf{q}$ and $\mathbf{X} \equiv \mathbf{p} \times \mathbf{q}$. Expanding with respective to the smallness of k^6/ω^2 in $\Im$, we obtain the expression of $\Im_2$ and $\Im_3$ in (B.8):

$$\Im_2 = \frac{1}{6k^4} \int \frac{d\eta}{2\pi} \frac{d\nu}{2\pi} \frac{d^3\mathbf{p}}{(2\pi)^3} \frac{d^3\mathbf{q}}{(2\pi)^3} \frac{(\mathbf{k} \cdot \mathbf{X})^4}{(\eta^2 + p^6)(\nu^2 + q^6)\big[(\omega + \eta + \nu)^2 + K^6\big]}, \tag{B.11}$$

$$\Im_3 = \frac{1}{2k^6} \int \frac{d\eta}{2\pi} \frac{d\nu}{2\pi} \frac{d^3\mathbf{p}}{(2\pi)^3} \frac{d^3\mathbf{q}}{(2\pi)^3} \frac{(\mathbf{k} \cdot \mathbf{X})^4}{(\eta^2 + p^6)(\nu^2 + q^6)}$$

$$\times \left\{ \frac{12(\mathbf{k} \cdot \mathbf{K})^2 K^8}{[(\omega + \eta + \nu)^2 + K^6]^3} - \frac{4(\mathbf{k} \cdot \mathbf{K})^2 K^2 + k^2 K^4}{[(\omega + \eta + \nu)^2 + K^6]^2} \right\}. \tag{B.12}$$

In order to evaluate these divergent terms $\Im_2$ and $\Im_3$, we first choose our cutoff prescription. We will start with applying a sharp cutoff Λ on the spatial momenta carried by internal legs in the sunset diagram, restricting the range of integration in (B.3) to be

$$-\infty < \eta, \nu < \infty, \quad 0 \le p, q, K \le \Lambda. \tag{B.13}$$

Later in Appendix B.3, we will investigate the application of the Pauli-Villars regularization to (B.3).

B.1   The k^4 Counterterm

First we evaluate $\Im_2$, the divergent coefficient of the k^4 term in (B.8). The following identity is useful for reducing the index structure:

$$\int d^3\mathbf{p} \, d^3\mathbf{q} \, X^i X^j X^k X^\ell F(p, q, K) = \frac{1}{15} \delta^{ijk\ell} \int d^3\mathbf{p} \, d^3\mathbf{q} \, X^4 F(p, q, K), \tag{B.14}$$

where $F(p, q, K)$ is an arbitrary function of p, q and K, and

$$\delta^{ijk\ell} \equiv \delta^{ij}\delta^{k\ell} + \delta^{ik}\delta^{j\ell} + \delta^{i\ell}\delta^{jk}. \tag{B.15}$$

Applying (B.14) to (B.11) yields

$$\Im_2 = \frac{1}{30} \int \frac{d\eta}{2\pi} \frac{d\nu}{2\pi} \frac{d^3\mathbf{p}}{(2\pi)^3} \frac{d^3\mathbf{q}}{(2\pi)^3} \frac{X^4}{(\eta^2 + p^6)(\nu^2 + q^6)\left[(\omega + \eta + \nu)^2 + K^6\right]}. \tag{B.16}$$

Next, we derive some useful integrals for performing the η and ν integrals on (B.16). Define

$$J(\omega, x, y) \equiv \int_{-\infty}^{\infty} d\omega' \frac{1}{(\omega'^2 + x^2)[(\omega' + \omega)^2 + y^2]}, \tag{B.17}$$

where ω, x and y are real numbers and $x, y > 0$. We further take the analytical continuation of ω' in (B.17) to the complex plane. The integrand has two poles in the upper half plane, namely:

$$\omega' = ix, \ -\omega + iy. \tag{B.18}$$

We complete the integration contour by including a semicircle that encloses the upper half plane. By Cauchy's theorem, we obtain

$$J(\omega, x, y) = 2\pi i \left\{ \frac{1}{(2ia)[(\omega + ix)^2 + y^2]} + \frac{1}{[(\omega - iy)^2 + x^2](2iy)} \right\}$$

$$= \frac{\pi}{\omega + i(x - y)} \left\{ \frac{1}{x[\omega + i(x + y)]} + \frac{1}{y[\omega - i(x + y)]} \right\}$$

$$= \frac{\pi(x+y)}{xy[\omega^2 + (x+y)^2]}. \tag{B.19}$$

Applying (B.19) recursively, we obtain (assuming $x, y, z > 0$)

$$
\begin{aligned}
I_1(\omega, x, y, z) &\equiv \int \frac{d\eta}{2\pi} \frac{d\nu}{2\pi} \frac{1}{(\eta^2 + x^2)(\nu^2 + y^2)[(\omega + \eta + \nu)^2 + z^2]} \\
&= \int \frac{d\eta}{2\pi} \frac{1}{2\pi} \frac{J(\omega + \eta, y, z)}{\eta^2 + x^2} \\
&= \int \frac{d\eta}{2\pi} \frac{y+z}{2yz(\eta^2 + x^2)[(\omega+\eta)^2 + (y+z)^2]} \\
&= \frac{y+z}{4\pi yz} J(\omega, x, y+z) \\
&= \frac{x+y+z}{4xyz[\omega^2 + (x+y+z)^2]}.
\end{aligned}
\tag{B.20}
$$

Applying (B.20) to (B.16), we obtain

$$\Im_2 = \frac{1}{120} \int \frac{d^3\mathbf{p}}{(2\pi)^3} \frac{d^3\mathbf{q}}{(2\pi)^3} \frac{X^4}{p^3 q^3 K^3} \frac{p^3 + q^3 + K^3}{[\omega^2 + (p^3 + q^3 + K^3)^2]}. \tag{B.21}$$

It is useful to further rewrite (B.21) as

$$
\begin{aligned}
\Im_2 &= \frac{1}{120} \int \frac{d^3\mathbf{p}}{(2\pi)^3} \frac{d^3\mathbf{q}}{(2\pi)^3} \frac{X^4}{p^3 q^3 K^3} \frac{1}{p^3 + q^3 + K^3} \\
&\quad - \frac{1}{120} \int \frac{d^3\mathbf{p}}{(2\pi)^3} \frac{d^3\mathbf{q}}{(2\pi)^3} \frac{X^4}{p^3 q^3 K^3} \frac{\omega^2}{\omega^2 + (p^3 + q^3 + K^3)^2} \\
&= \Im_{0,2} + \text{finite},
\end{aligned}
\tag{B.22}
$$

where

$$\Im_{0,2} = \frac{1}{120} \int \frac{d^3\mathbf{p}}{(2\pi)^3} \frac{d^3\mathbf{q}}{(2\pi)^3} \frac{X^4}{p^3 q^3 K^3} \frac{1}{p^3 + q^3 + K^3} \tag{B.23}$$

is power-counting quadratically divergent in Λ. Note that the integral over $\mathbf{q}$ is convergent in the UV, we will thus extend the domain for $\mathbf{q}$ to $q \in [0, \infty)$. Applying the following change of variable in (B.23),

$$\mathbf{x} \equiv \frac{\mathbf{q}}{p}, \tag{B.24}$$

we obtain

$$\Im_{0,2} \lesssim \frac{1}{120} \int \frac{d^3\mathbf{p}}{(2\pi)^3} \frac{d^3\mathbf{x}}{(2\pi)^3} \frac{x \sin^4\theta}{p\overline{K}^3} \frac{1}{1 + x^3 + \overline{K}^3} = \frac{\mathfrak{C}_{0,2}}{120(2\pi)^4} \Lambda^2, \tag{B.25}$$

where $\overline{K} = \sqrt{1 + x^2 + 2x\cos\theta}$ and θ is the angle between $\mathbf{p}$ and $\mathbf{q}$. Furthermore,

$$\mathfrak{C}_{0,2} = \int_0^\infty dx \int_0^\pi d\theta \, \frac{x^3 \sin^5\theta}{\overline{K}^3 \left(1 + x^3 + \overline{K}^3\right)}. \tag{B.26}$$

Numerical evaluation yields $\mathfrak{C}_{0,2} \approx 0.254$. Hence,

$$\mathfrak{I}_{0,2} = B\Lambda^2 + \text{finite}, \tag{B.27}$$

where B is a positive real number and

$$B \lesssim \frac{\mathfrak{C}_{0,2}}{1920\pi^4} \approx 1.36 \times 10^{-6}. \tag{B.28}$$

The precise value for B largely depends on how one chooses the UV cutoff and does not have a universal meaning. However, the sign of B is insensitive to the choice of cutoff.

B.2   The k^6 Counterterm

Next we evaluate $\mathfrak{I}_3$, the divergent coefficient of the k^6 term in (B.12). To reduce the index structure in (B.12), in addition to the identity (B.14), we note the following identity:

$$\int d^3\mathbf{p} \, d^3\mathbf{q} \, X^i X^j X^k X^\ell K^m K^n F(p, q, K)$$

$$= \frac{1}{210} \left(7\delta^{ijk\ell}\delta^{mn} - \delta^{ijk\ell mn}\right) \int d^3\mathbf{p} \, d^3\mathbf{q} \, X^4 K^2 F(p, q, K), \tag{B.29}$$

where $F(p, q, K)$ is an arbitrary function of p, q and K, and

$$\delta^{ijk\ell mn} \equiv \delta^{ijk\ell}\delta^{mn} + \delta^{mjk\ell}\delta^{in} + \delta^{imk\ell}\delta^{jn} + \delta^{ijm\ell}\delta^{kn} + \delta^{ijkm}\delta^{\ell n}. \tag{B.30}$$

Applying (B.14) and (B.29) to (B.12), we obtain

$$\mathfrak{I}_3 = \frac{1}{70} \int \frac{d\eta \, d\nu}{2\pi \, 2\pi} \frac{d^3\mathbf{p}}{(2\pi)^3} \frac{d^3\mathbf{q}}{(2\pi)^3} \frac{X^4 K^4}{(\eta^2 + p^6)(\nu^2 + q^6)}$$

$$\times \left\{ \frac{12K^6}{[(\omega + \eta + \nu)^2 + K^6]^3} - \frac{11}{[(\omega + \eta + \nu)^2 + K^6]^2} \right\}. \tag{B.31}$$

To perform the integrals over the frequencies η and ν for (B.31), we derive the following integrals from (B.20):

$$I_2(\omega, x, y, z) = \int \frac{d\eta \, d\nu}{2\pi \, 2\pi} \frac{1}{(\eta^2 + x^2)(\nu^2 + y^2)[(\omega + \eta + \nu)^2 + z^2]^2}$$

$$\equiv -\frac{1}{2z} \frac{\partial}{\partial z} I_1(\omega, x, y, z)$$

$$= \frac{\omega^2(x+y) + (x+y+2z)(x+y+z)^2}{8xyz^3 \left[\omega^2 + (x+y+z)^2\right]^2}, \tag{B.32}$$

and

$$\begin{aligned}
I_3(\omega, x, y, z) &= \int \frac{d\eta}{2\pi} \frac{d\nu}{2\pi} \frac{1}{(\eta^2 + \omega_x^2)(\nu^2 + y^2)[(\omega + \eta + \nu)^2 + z^2]^3} \\
&= -\frac{1}{2z} \frac{\partial}{\partial z} I_2(\omega, x, y, z) \\
&= \frac{3\omega^2(x+y)\left[\omega^2 + 2(x+y+z)(x+y+2z)\right]}{16xyz^5 \left[\omega^2 + (x+y+z)^2\right]^3} \\
&\quad + \frac{(x+y+z)^3\left[3(x+y)^2 + 9(x+y)z + 8z^2\right]}{16xyz^5 \left[\omega^2 + (x+y+z)^2\right]^3}.
\end{aligned} \tag{B.33}$$

Applying (B.32) and (B.33) to (B.31), we obtain

$$\begin{aligned}
\Im_3 = \frac{1}{280} \int \frac{d^3\mathbf{p}}{(2\pi)^3} \frac{d^3\mathbf{q}}{(2\pi)^3} \frac{X^4 K}{p^3 q^3} &\left\{ \frac{12(p^3 + q^3 + K^3)^3}{\left[\omega^2 + (p^3 + q^3 + K^3)^2\right]^3} \right. \\
&\left. - \frac{(p^3 + q^3 + K^3)(2p^3 + 2q^3 + 11K^3)}{K^3 \left[\omega^2 + (p^3 + q^3 + K^3)^2\right]^2} - \frac{p^3 + q^3}{K^6 \left[\omega^2 + (p^3 + q^3 + K^3)^2\right]} \right\}.
\end{aligned} \tag{B.34}$$

Here $\Im_3$ is a function of ω and some the momentum cutoff scale Λ. The divergent part in $\Im_3$ is by power counting logarithmic in Λ. Since the sunset diagram does not contain any divergent subdiagrams, we expect $\Im_3$ to take the form,

$$\Im_3 = A \log\left(\Lambda/|\omega|^{\frac{1}{3}}\right) + \text{finite}, \tag{B.35}$$

where A is a constant to be evaluated in the following.

First, we evaluate A by a shortcut method: We set ω to zero but introduce an IR cutoff for $\mathbf{p}$ such that $\mu_{\text{IR}} \leq p \leq \Lambda$. Since the integral over $\mathbf{q}$ is convergent, we also extend the integral over $\mathbf{q}$ to $q \in [0, \infty)$. Then, (B.34) is simplified to

$$\Im_3 = \frac{1}{280} \int \frac{d^3\mathbf{p}}{(2\pi)^3} \frac{d^3\mathbf{q}}{(2\pi)^3} \frac{X^4}{p^3 q^3 K^5} \frac{K^6 - 3K^3(p^3 + q^3) - (p^3 + q^3)^2}{(p^3 + q^3 + K^3)^3}. \tag{B.36}$$

Applying the following change of variable in (B.36):

$$x \equiv \frac{q}{p}, \tag{B.37}$$

we obtain

$$\Im_3 = \frac{1}{280} \int \frac{d^3\mathbf{p}}{(2\pi)^3} \frac{d^3\mathbf{x}}{(2\pi)^3} \frac{x \sin^4\theta}{p^3 \overline{K}^5} \frac{\overline{K}^6 - 3\overline{K}^3(1 + x^3) - (1 + x^3)^2}{\left(1 + x^3 + \overline{K}^3\right)^3}$$

$$= \frac{\mathfrak{C}_3}{2240\pi^4} \log\left(\frac{\Lambda}{\mu_{\mathrm{IR}}}\right), \tag{B.38}$$

where θ is the angle between $\mathbf{p}$ and $\mathbf{q}$ and $\overline{K} = \sqrt{1 + x^2 + 2x\cos\theta}$. Furthermore,

$$\mathfrak{C}_3 = \int_0^\infty dx \int_0^\pi d\theta \, \sin^5\theta \, \frac{x^3}{\overline{K}^5} \frac{\overline{K}^6 - 3\overline{K}^3(1+x^3) - (1+x^3)^2}{\left(1 + x^3 + \overline{K}^3\right)^3}. \tag{B.39}$$

The integral in (B.39) can be performed numerically, yielding

$$\mathfrak{C}_3 \approx -0.24715. \tag{B.40}$$

Therefore,

$$\Im_3 = A \log\Lambda + \text{finite}, \tag{B.41}$$

where

$$A = \frac{\mathfrak{C}_{0,3}}{2240\pi^4} \approx -1.13 \times 10^{-6}. \tag{B.42}$$

Next, we perform the integral (B.34) for nonzero ω^2. We find it the most convenient to modify the integration domain for $\mathbf{p}$ and $\mathbf{q}$ into

$$\left\{(\mathbf{p},\mathbf{q}) : 0 \le p^2 + q^2 \le \Lambda^2\right\}. \tag{B.43}$$

Rewrite (B.34) as

$$\Im_3 = \frac{1}{2240\pi^4} \int dp \, dq \int_0^\pi d\theta \, \sin^5\theta \, G_3(\omega^2, p, q, K). \tag{B.44}$$

where θ is the angle between $\mathbf{p}$ and $\mathbf{q}$, $K = \sqrt{p^2 + q^2 + 2pq\cos\theta}$, and

$$G_3(\omega^2, p, q, K) \equiv p^3 q^3 K \left\{ \frac{12(p^3 + q^3 + K^3)^3}{\left[\omega^2 + (p^3 + q^3 + K^3)^2\right]^3} - \frac{(p^3 + q^3 + K^3)(2p^3 + 2q^3 + 11K^3)}{K^3\left[\omega^2 + (p^3 + q^3 + K^3)^2\right]^2} \right.$$
$$\left. - \frac{p^3 + q^3}{K^6\left[\omega^2 + (p^3 + q^3 + K^3)^2\right]} \right\}. \tag{B.45}$$

Then, we apply the following change of variables:

$$p = \Lambda\ell\cos\psi, \qquad q = \Lambda\ell\sin\psi, \tag{B.46}$$

where

$$0 \le \ell \le 1, \qquad 0 \le \psi \le \frac{\pi}{2}. \tag{B.47}$$

Therefore,

$$\Im_3 = \frac{1}{2240\pi^4} \, \mathfrak{C}\left(\Lambda/|\omega|^{\frac{1}{3}}\right), \tag{B.48}$$

where the function $\mathfrak{C}(x)$ is given by

$$\mathfrak{C}(x) \equiv \int_0^1 \frac{d\ell}{\ell} \int_0^{\frac{\pi}{2}} d\psi \int_0^\pi d\theta \, \sin^5\theta \, G_3\big((x\ell)^{-6}, \cos\psi, \sin\psi, \widetilde{K}\big), \tag{B.49}$$

where $\widetilde{K} \equiv \sqrt{1 + \cos\theta \sin(2\psi)}$. From the result we derived by the shortcut method in (B.41), we expect that $\lim_{x\to 0}[\mathfrak{C}(x)/\log x]$ be equal to $\mathcal{C}_3$ defined in (B.39), due to the universality of the logarithmic divergences. By numerical evaluation, we obtain

$$\lim_{x\to\infty} \frac{\mathfrak{C}(x)}{\log x} \approx -0.24715. \tag{B.50}$$

This is indeed the same numerics by evaluating $\mathfrak{C}_3$ in (B.39). Finally, we obtain

$$\mathfrak{I}_3 = A\log\big(\Lambda/|\omega|^{\frac{1}{3}}\big) + \text{finite}, \tag{B.51}$$

with A given by (B.42). Combining this result with (B.27) and recovering the dependence on ζ_3, we obtain

$$\overrightarrow{\omega,\mathbf{k}}\,\bigcirc\,\overrightarrow{\omega,\mathbf{k}} = \frac{i\lambda^2}{\zeta_3^4}k^4\left\{Ak^2\log\big(\zeta_3^{\frac{1}{3}}\Lambda/|\omega|^{\frac{1}{3}}\big) + B\Lambda^2 + \text{finite}\right\}, \tag{B.52}$$

where

$$A \approx -1.13 \times 10^{-6}, \quad B \lesssim 1.36 \times 10^{-6}. \tag{B.53}$$

B.3 The Pauli-Villars Regularization

We would like to apply the Pauli-Villars regularization by taking the following substitution of the propagator in (B.55):

$$\frac{1}{\omega^2 + \omega_\mathbf{k}^2} \rightarrow \frac{1}{\omega^2 + \omega_\mathbf{k}^2} - \frac{1}{\omega^2 + \omega_\mathbf{k}^2 + \Lambda^6}. \tag{B.54}$$

Then, (B.55) becomes

$$\mathfrak{I} \equiv \frac{1}{3!}\int \frac{d\eta}{2\pi}\frac{d\nu}{2\pi}\frac{d^3\mathbf{p}}{(2\pi)^3}\frac{d^3\mathbf{q}}{(2\pi)^3}\,[\mathbf{kpq}]^4$$
$$\times \left(\frac{1}{\eta^2 + \omega_\mathbf{p}^2} - \frac{1}{\eta^2 + \omega_\mathbf{p}^2 + \Lambda^6}\right)\left(\frac{1}{\nu^2 + \omega_\mathbf{q}^2} - \frac{1}{\nu^2 + \omega_\mathbf{q}^2 + \Lambda^6}\right)$$
$$\times \left[\frac{1}{(\omega + \eta + \nu)^2 + \omega_{\mathbf{k}+\mathbf{p}+\mathbf{q}}^2} - \frac{1}{(\omega + \eta + \nu)^2 + \omega_{\mathbf{k}+\mathbf{p}+\mathbf{q}}^2 + \Lambda^6}\right]. \tag{B.55}$$

Taking $\omega_\mathbf{p}^2 = p^6$, $\omega_\mathbf{q}^2 = q^6$ and $\omega_{\mathbf{k}+\mathbf{p}+\mathbf{q}}^2 = |\mathbf{k} + \mathbf{p} + \mathbf{q}|^6$, expanding (B.55) in a Taylor series in k^2, and reducing the index structure we obtain

$$\mathfrak{I}(\omega^2, \mathbf{k}) = \mathfrak{I}_2 k^4 + \mathfrak{I}_3 k^6 + \cdots, \tag{B.56}$$

where

$$\Im_2 = \frac{1}{30} \int \frac{d\eta}{2\pi} \frac{d\nu}{2\pi} \frac{d^3\mathbf{p}}{(2\pi)^3} \frac{d^3\mathbf{q}}{(2\pi)^3} X^4$$

$$\times \left(\frac{1}{\eta^2 + p^6} - \frac{1}{\eta^2 + p^6 + \Lambda^6} \right) \left(\frac{1}{\nu^2 + q^6} - \frac{1}{\nu^2 + q^6 + \Lambda^6} \right)$$

$$\times \left[\frac{1}{(\omega + \eta + \nu)^2 + K^6} - \frac{1}{(\omega + \eta + \nu)^2 + K^6 + \Lambda^6} \right], \tag{B.57a}$$

$$\Im_3 = \frac{1}{70} \int \frac{d\eta}{2\pi} \frac{d\nu}{2\pi} \frac{d^3\mathbf{p}}{(2\pi)^3} \frac{d^3\mathbf{q}}{(2\pi)^3} X^4 K^4$$

$$\times \left(\frac{1}{\eta^2 + p^6} - \frac{1}{\eta^2 + p^6 + \Lambda^6} \right) \left(\frac{1}{\nu^2 + q^6} - \frac{1}{\nu^2 + q^6 + \Lambda^6} \right)$$

$$\times \left\{ 12K^6 \left(\frac{1}{[(\eta + \nu + \omega)^2 + K^6]^3} - \frac{1}{[(\eta + \nu + \omega)^2 + K^6 + \Lambda^6]^3} \right) \right.$$

$$\left. - 11 \left(\frac{1}{[(\eta + \nu + \omega)^2 + K^6]^2} - \frac{1}{[(\eta + \nu + \omega)^2 + K^6 + \Lambda^6]^2} \right) \right\}. \tag{B.57b}$$

Note that $\Im_2$ is a convergent integral and only contribute to finite pieces. We will then focus on $\Im_3$. Applying the integrals (B.32) and (B.33), we obtain

$$\Im_3 = \frac{1}{2240\pi^4} \int dp\, dq \int_0^\pi d\theta \sin^4\theta\, G_3(\omega^2, p, q, K, \Lambda), \tag{B.58}$$

where θ is the angle between $\mathbf{p}$ and $\mathbf{q}$, $K = \sqrt{p^2 + q^2 + 2pq\cos\theta}$, and

$$G_3(\omega^2, p, q, K, \Lambda) = p^6 q^6 K^4 \left\{ f(p, q, K) - f(p_\Lambda, q, K) - f(p, q_\Lambda, K) - f(p, q, K_\Lambda) \right.$$

$$\left. + f(p, q_\Lambda, K_\Lambda) + f(p_\Lambda, q, K_\Lambda) + f(p_\Lambda, q_\Lambda, K) - f(p_\Lambda, q_\Lambda, K_\Lambda) \right\}. \tag{B.59}$$

We have introduced the following definitions:

$$p_\Lambda \equiv \left(p^6 + \Lambda^6\right)^{\frac{1}{6}}, \quad q_\Lambda \equiv \left(q^6 + \Lambda^6\right)^{\frac{1}{6}}, \quad K_\Lambda \equiv \left(K^6 + \Lambda^6\right)^{\frac{1}{6}}, \tag{B.60}$$

and

$$f(x, y, z) = \frac{1}{x^3 y^3 z^9} \left\{ \frac{12K^6(x^3 + y^3 + z^3)^3}{\left[\omega^2 + (x^3 + y^3 + z^3)^2\right]^3} + \frac{(x^3 + y^3)(9K^6 - 11z^6)}{2z^6\left[\omega^2 + (x^3 + y^3 + z^3)^2\right]} \right.$$

$$\left. + \frac{(x^3 + y^3 + z^3)\left[9K^6(x^3 + y^3) - 11z^6(x^3 + y^3 + z^3)\right]}{z^3\left[\omega^2 + (x^3 + y^3 + z^3)^2\right]^2} \right\}. \tag{B.61}$$

It is useful to take the following change of variables:

$$p = \Lambda\ell\cos\psi, \quad q = \Lambda\ell\sin\psi, \tag{B.62}$$

where

$$0 < \ell < \infty, \quad 0 < \psi < \frac{\pi}{2}. \tag{B.63}$$

Then,

$$\Im_3 = \frac{1}{2240\pi^4} \overline{\mathfrak{C}}\left(\Lambda/|\omega|^{\frac{1}{3}}\right). \tag{B.64}$$

where

$$\overline{\mathfrak{C}}(x) \equiv \int_0^\infty \frac{d\ell}{\ell} \int_0^{\frac{\pi}{2}} d\psi \int_0^\pi d\theta \sin^5\theta \, G_3\left((x\ell)^{-6}, \cos\psi, \sin\psi, \widetilde{K}, \ell^{-1}\right). \tag{B.65}$$

Here, $\widetilde{K} \equiv \sqrt{1 + \cos\theta\sin(2\psi)}$. Numerical evaluation yields

$$\lim_{x\to\infty} \frac{\overline{\mathfrak{C}}(x)}{\log x} \approx -0.24715. \tag{B.66}$$

As expected, this is the same as (B.50).

Appendix C

Useful Formulas in Hořava Gravity

In this appendix, we prove a number of formulas which are useful in expanding out the action of Hořava gravity around curved space, in order to facilitate the derivations in Chapter 9. The identities are understood to hold under integration and thus we set all total derivatives to zero. Finally, we take the background to have constant curvature $\overline{R}$.

Recall that we decompose the spatial metric fluctuation as

$$h_{ij} = H_{ij} + \frac{1}{2}h\,\overline{g}_{ij}, \tag{C.1}$$

where $h = \overline{g}^{ij}h_{ij}$ and $\overline{g}^{ij}H_{ij} = 0$. Furthermore, we decompose H_{ij} as

$$H_{ij} = H_{ij}^{\perp} + \overline{\nabla}_i\eta_j + \overline{\nabla}_j\eta_i + \left(\overline{\nabla}_i\overline{\nabla}_j - \frac{1}{2}\overline{g}_{ij}\overline{\Box}\right)\sigma, \tag{C.2}$$

where $\overline{g}^{ij}H_{ij}^{\perp} = 0$, $\overline{\nabla}^j H_{ij}^{\perp} = 0$ and $\overline{\nabla}^i\eta_i = 0$. In two dimensions, we set $H_{ij}^{\perp}$ to zero and $\eta_i = \overline{\varepsilon}_{ij}\overline{\nabla}^j\eta$ for some scalar η.

Identity 1. $\overline{\Box}\overline{\nabla}_i\Phi = \overline{\nabla}_i\left(\overline{\Box} + \frac{\overline{R}}{2}\right)\Phi$, *where* Φ *is a scalar.*

Identity 2. $\overline{\nabla}^j H_{ij} = \overline{\varepsilon}_{ij}\overline{\nabla}^j(\overline{\Box} + \overline{R})\eta + \frac{1}{2}\overline{\nabla}_i(\overline{\Box} + \overline{R})\sigma$.

This identity is derived below:

$$
\begin{aligned}
\overline{\nabla}^j H_{ij} &= \overline{\varepsilon}_{jk}\overline{\nabla}^j\overline{\nabla}_i\overline{\nabla}^k\eta + \overline{\varepsilon}_{ik}\overline{\Box}\overline{\nabla}^k\eta + \left(\overline{\nabla}^j\overline{\nabla}_i\overline{\nabla}_j - \frac{1}{2}\overline{\nabla}_i\overline{\Box}\right)\sigma \\
&= \overline{\varepsilon}_{jk}\left(\overline{\nabla}_i\overline{\nabla}^j\overline{\nabla}^k + \overline{R}^k{}_{\ell}{}^j{}_i\overline{\nabla}^\ell\right)\eta + \overline{\varepsilon}_{ij}\overline{\Box}\overline{\nabla}^j\eta + \left(\overline{\nabla}_i\overline{\nabla}^j\overline{\nabla}_j - \overline{R}^k{}_j{}^j{}_i\overline{\nabla}_k - \frac{1}{2}\overline{\nabla}_i\overline{\Box}\right)\sigma \\
&= \overline{\varepsilon}_{jk}\frac{\overline{R}}{2}\left(\overline{g}^{kj}\overline{g}_{\ell i} - \delta_i^k\delta_\ell^j\right)\overline{\nabla}^\ell\eta + \overline{\varepsilon}_{ij}\overline{\Box}\overline{\nabla}^j\eta + \frac{1}{2}\overline{\nabla}_i\overline{\Box}\sigma - \frac{\overline{R}}{2}(\overline{g}^{kj}\overline{g}_{ji} - \delta_i^k\delta_j^j)\overline{\nabla}_k\sigma \\
&= \left(\overline{\Box} + \frac{\overline{R}}{2}\right)\overline{\nabla}^j\eta + \frac{1}{2}\overline{\nabla}_i(\overline{\Box} + \overline{R})\sigma \\
&= \overline{\varepsilon}_{ij}\overline{\nabla}^j(\overline{\Box} + \overline{R})\eta + \frac{1}{2}\overline{\nabla}_i(\overline{\Box} + \overline{R})\sigma. \tag{C.3}
\end{aligned}
$$

Identity 3. $\overline{\nabla}^i\overline{\nabla}^j H_{ij} = \frac{1}{2}\overline{\Box}(\overline{\Box} + \overline{R})\sigma$. *This follows immediately from Identity 2.*

Identity 4. $\overline{\nabla}_i\overline{\Box}^n\overline{\nabla}^i\Phi = \overline{\Box}\left(\overline{\Box} + \frac{\overline{R}}{2}\right)^n\Phi$, *where Φ is a scalar and n is a non-negative integer.*

In practice, we will only need this identity up to $n = 2$. However, it is not much more difficult to prove it in general via induction using Identity 1.

Identity 5. $H_{ij}\overline{\nabla}^i\overline{\Box}^n\overline{\nabla}_k H^{jk} = \eta\mathcal{O}\eta + \frac{1}{4}\sigma\mathcal{O}\sigma$, *where $\mathcal{O} = \overline{\Box}(\overline{\Box} + \overline{R})^2\left(\overline{\Box} + \frac{\overline{R}}{2}\right)^n$. This follows directly from Identities 2 and 4.*

Identity 6. *For vectors Φ_i and $\widetilde{\Phi}_i$,*

$$\Phi_i\overline{\nabla}_j\overline{\Box}^{n+1}\overline{\nabla}^j\widetilde{\Phi}^i = \Phi_i\left(\overline{\Box} + \frac{\overline{R}}{2}\right)\overline{\nabla}_j\overline{\Box}^n\overline{\nabla}^j\widetilde{\Phi}^i + \overline{R}\left(\Phi_i\overline{\nabla}^j\overline{\Box}^n\overline{\nabla}^i\widetilde{\Phi}_j - \Phi_i\overline{\nabla}^i\overline{\Box}^n\overline{\nabla}^j\widetilde{\Phi}_j\right), \quad \text{(C.4a)}$$

$$\Phi_i\overline{\nabla}^j\overline{\Box}^{n+1}\overline{\nabla}^i\widetilde{\Phi}_j = \Phi_i\left(\overline{\Box} + \frac{\overline{R}}{2}\right)\overline{\nabla}^j\overline{\Box}^n\overline{\nabla}^i\widetilde{\Phi}_j + \overline{R}\left(\Phi_i\overline{\nabla}_j\overline{\Box}^n\overline{\nabla}^j\widetilde{\Phi}^i - \Phi_i\overline{\nabla}^i\overline{\Box}^n\overline{\nabla}^j\widetilde{\Phi}_j\right). \quad \text{(C.4b)}$$

From (C.4) *we obtain*

$$\Phi_i\left(\overline{g}^{ij}\overline{\nabla}_k\overline{\Box}^{n+1}\overline{\nabla}^k + \overline{\nabla}^j\overline{\Box}^{n+1}\overline{\nabla}^i\right)\widetilde{\Phi}_j$$

$$= \Phi_i\left(\overline{\Box} + \tfrac{3}{2}\overline{R}\right)^{n+1}\left(\overline{g}^{ij}\overline{\Box} + \overline{\nabla}^j\overline{\nabla}^i\right)\widetilde{\Phi}_j - 2\overline{R}\sum_{m=0}^{n}\Phi_i\left(\overline{\Box} + \tfrac{3}{2}\overline{R}\right)^{n-m}\overline{\nabla}^i\overline{\Box}^m\overline{\nabla}^j\widetilde{\Phi}_j. \quad \text{(C.5)}$$

Identity 7. *Applying Identity 6 on the vectors $\eta_i = \overline{\varepsilon}_{ij}\overline{\nabla}^j\eta$ and $\overline{\nabla}_i\sigma$ yields*

$$\eta_i\overline{\nabla}_j\overline{\Box}^n\overline{\nabla}^j\eta^i + \eta_i\overline{\nabla}^j\overline{\Box}^n\overline{\nabla}^i\eta_j = \eta\overline{\Box}(\overline{\Box} + \overline{R})(\overline{\Box} + 2\overline{R})^n\eta, \quad \text{(C.6a)}$$

$$\sigma\overline{\nabla}_i\overline{\nabla}_j\overline{\Box}^n\overline{\nabla}^j\overline{\nabla}^i\sigma - \frac{1}{2}\sigma\overline{\Box}^{n+2}\sigma = \frac{1}{2}\sigma\overline{\Box}(\overline{\Box} + \overline{R})(\overline{\Box} + 2\overline{R})^n\sigma. \quad \text{(C.6b)}$$

Identity 8. $H_{ij}\overline{\Box}^n H^{ij} = 2\eta\mathcal{O}\eta + \frac{1}{2}\sigma\mathcal{O}\sigma$, *where $\mathcal{O} = \overline{\Box}(\overline{\Box} + \overline{R})(\overline{\Box} + 2\overline{R})^n$. This follows directly from Identity 7.*

Appendix D

Jacobians in Path Integrals

Here, as an appendix to Chapter 9, we review the computation of a partition function under the change of variables $\Phi = F\Psi$, for some linear differential operator F that is often, but not always, local. The path integral for Φ is defined with respect to a measure on the space of field configurations, which in the background field method we take to be covariant with respect to background diffeomorphisms. It is natural to define the measure in terms of a metric G_Φ on this space. For example, if Φ_i has a spatial index, the inner product of two infinitesimal variations $\delta\Phi^{(1)}$ and $\delta\Phi^{(2)}$ takes the form

$$G_\Phi(\delta\Phi^{(1)}, \delta\Phi^{(2)}) = \langle \delta\Phi^{(1)}, \delta\Phi^{(2)} \rangle_\Phi = \int dt\, d^2\mathbf{x}\, \sqrt{\bar{g}}\, \bar{g}^{ij} \delta\Phi_i^{(1)} \delta\Phi_j^{(2)}\,. \tag{D.1}$$

The path integral can schematically be written[1]

$$\int d\Phi \sqrt{\det G_\Phi}\, e^{iS_\Phi}\,. \tag{D.2}$$

The metric is not covariant under a change of variables; instead, the measure transforms as

$$d\Phi \sqrt{\det G_\Phi} = d\Psi \sqrt{\det G_\Psi} \sqrt{\det \mathcal{O}_F}, \tag{D.3}$$

where

$$\mathcal{O}_F = G_\Psi^{-1} F^\intercal G_\Phi F. \tag{D.4}$$

The operator $\mathcal{O}_F$ is computed by setting

$$\langle \delta\Phi, \delta\Phi \rangle_\Phi = \langle \delta\Psi, \mathcal{O}_F \delta\Psi \rangle_\Psi\,. \tag{D.5}$$

The Jacobian is then expressed as $\mathcal{J}_F = \sqrt{\det \mathcal{O}_F}$.

As an example, let us consider the Jacobian for the transformation

$$\Phi_i = \overline{\nabla}_i \phi + \bar{\varepsilon}_{ij} \overline{\nabla}^j \widetilde{\phi}\,. \tag{D.6}$$

---

[1]More correctly, G_Φ should be taken as the metric induced from the canonical path integral by integrating out canonical momenta. This gives G_Φ in terms of the path integral kinetic term.

The natural metric for Φ_i is the one given above, while that for ϕ and $\widetilde{\phi}$ is

$$\langle \delta\phi^{(1)}, \delta\phi^{(2)} \rangle_\phi = \int dt\, d^2\mathbf{x} \sqrt{\overline{g}}\, \delta\phi^{(1)} \delta\phi^{(2)}, \tag{D.7a}$$

$$\langle \delta\widetilde{\phi}^{(1)}, \delta\widetilde{\phi}^{(2)} \rangle_{\widetilde{\phi}} = \int dt\, d^2\mathbf{x} \sqrt{\overline{g}}\, \delta\widetilde{\phi}^{(1)} \delta\widetilde{\phi}^{(2)}. \tag{D.7b}$$

In the text we are primarily interested in the case where $\overline{g}$ is time-independent and whose spatial slice is a symmetric space. Then

$$\langle \delta\Phi, \delta\Phi \rangle_\Phi = \langle \delta\phi, -\overline{\Box}\delta\phi \rangle_\phi + \langle \delta\widetilde{\phi}, -\overline{\Box}\delta\widetilde{\phi} \rangle_{\widetilde{\phi}}. \tag{D.8}$$

Therefore,

$$\mathcal{O}_F = -\overline{\Box} \begin{pmatrix} 1 & 0 \\ 0 & 1 \end{pmatrix}, \tag{D.9}$$

and

$$\mathcal{J} = \sqrt{\det \mathcal{O}_F} = \det(-\overline{\Box}). \tag{D.10}$$

For another example, let us conside the Jacobian for the transformation defined in (C.2),

$$H_{ij} = \left(\overline{\varepsilon}_{jk} \overline{\nabla}_i \overline{\nabla}^k + \overline{\varepsilon}_{ik} \overline{\nabla}_j \overline{\nabla}^k \right) \eta + \left(\overline{\nabla}_i \overline{\nabla}_j - \frac{1}{2} \overline{g}_{ij} \overline{\Box} \right) \sigma. \tag{D.11}$$

Note that H_{ij} is traceless. A natural metric on the space of traceless tensors is

$$\langle \delta H^{(1)}, \delta H^{(2)} \rangle_H = \int dt\, d^2\mathbf{x} \sqrt{\overline{g}}\, \delta H^{(1)}_{ij} \overline{g}^{ik} \overline{g}^{j\ell} \delta H^{(2)}_{k\ell}. \tag{D.12}$$

For the scalar modes η and σ we define

$$\langle \delta\eta^{(1)}, \delta\eta^{(2)} \rangle_\eta = \int dt\, d^2\mathbf{x} \sqrt{\overline{g}}\, \delta\eta^{(1)} \delta\eta^{(2)}, \tag{D.13a}$$

$$\langle \delta\sigma^{(1)}, \delta\sigma^{(2)} \rangle_\sigma = \int dt\, d^2\mathbf{x} \sqrt{\overline{g}}\, \delta\sigma^{(1)} \delta\sigma^{(2)}. \tag{D.13b}$$

Then, applying Identity 8, we obtain

$$\langle \delta H, \delta H \rangle_H = \langle \delta\eta, 2\overline{\Box} \left(\overline{\Box} + \overline{R} \right) \delta\eta \rangle_\eta + \langle \delta\sigma, \tfrac{1}{2}\overline{\Box} \left(\overline{\Box} + \overline{R} \right) \delta\sigma \rangle_\sigma. \tag{D.14}$$

(In general there is an η-σ cross-term involving $\overline{\nabla}_i \overline{R}$, but this vanishes on the backgrounds used in Chapter 9.) Therefore, the associated Jacobian is

$$\mathcal{J}_H = \det\left[\overline{\Box} \left(\overline{\Box} + \overline{R} \right) \right]. \tag{D.15}$$

Bibliography

[1] Georges Aad et al. Observation of a new particle in the search for the Standard Model Higgs boson with the ATLAS detector at the LHC. *Phys. Lett.*, B716:1–29, 2012.

[2] Serguei Chatrchyan et al. Observation of a new boson at a mass of 125 GeV with the CMS experiment at the LHC. *Phys. Lett.*, B716:30–61, 2012.

[3] Joseph Polchinski. Effective field theory and the Fermi surface. In *Theoretical Advanced Study Institute (TASI 92): From Black Holes and Strings to Particles Boulder, Colorado, June 3-28, 1992*, pages 0235–276, 1992.

[4] Gerard 't Hooft. Naturalness, chiral symmetry, and spontaneous chiral symmetry breaking. *NATO ASI Series B*, 59:135, 1980.

[5] Petr Hořava. Membranes at quantum criticality. *JHEP*, 03:020, 2009.

[6] Petr Hořava. Quantum gravity at a Lifshitz point. *Phys. Rev.*, D79:084008, 2009.

[7] Shinji Mukohyama. Hořava-Lifshitz cosmology: a review. *Class.Quant.Grav.*, 27:223101, 2010.

[8] J. Ambjørn, A. Görlich, S. Jordan, J. Jurkiewicz, and R. Loll. CDT meets Hořava-Lifshitz gravity. *Phys.Lett.*, B690:413–419, 2010.

[9] Petr Hořava. General covariance in gravity at a Lifshitz point. *Class.Quant.Grav.*, 28:114012, 2011.

[10] Christian Anderson, Steven J. Carlip, Joshua H. Cooperman, Petr Hořava, Rajesh K. Kommu, et al. Quantizing Hořava-Lifshitz gravity via causal dynamical triangulations. *Phys.Rev.*, D85:044027, 2012.

[11] Stefan Janiszewski and Andreas Karch. String theory embeddings of nonrelativistic field theories and their holographic Hořava gravity duals. *Phys.Rev.Lett.*, 110(8):081601, 2013.

[12] Stefan Janiszewski and Andreas Karch. Non-relativistic holography from Hořava gravity. *JHEP*, 1302:123, 2013.

[13] Tom Griffin, Petr Hořava, and Charles M. Melby-Thompson. Lifshitz gravity for Lifshitz holography. *Phys. Rev. Lett.*, 110(8):081602, 2013.

[14] N.D. Mermin and H. Wagner. Absence of ferromagnetism or antiferromagnetism in one-dimensional or two-dimensional isotropic Heisenberg models. *Phys. Rev. Lett.*, 17:1133–1136, 1966.

[15] Shamit Kachru, Xiao Liu, and Michael Mulligan. Gravity duals of Lifshitz-like fixed points. *Phys.Rev.*, D78:106005, 2008.

[16] Roger Penrose. Structure of space-time, in *Battelle Rencontres*, eds: C. DeWitt and J. A. Wheeler. Benjamin, New York, 1968.

[17] Petr Hořava and Charles M. Melby-Thompson. General covariance in quantum gravity at a Lifshitz point. *Phys.Rev.*, D82:064027, 2010.

[18] Tom Griffin, Kevin T. Grosvenor, Petr Hořava, and Ziqi Yan. Multicritical symmetry breaking and naturalness of slow Nambu-Goldstone bosons. *Phys.Rev.*, D88:101701, 2013.

[19] Tom Griffin, Kevin T. Grosvenor, Petr Hořava, and Ziqi Yan. Scalar field theories with polynomial shift symmetries. *Commun. Math. Phys.*, 340(3):985–1048, 2015.

[20] Petr Hořava. Surprises with nonrelativistic naturalness. *International Journal of Modern Physics D*, page 1645007, 2016.

[21] Tom Griffin, Kevin T. Grosvenor, Petr Hořava, and Ziqi Yan. Multicritical phonons and electron-phonon interactions in metals. *to appear*.

[22] Tom Griffin, Kevin T. Grosvenor, Petr Hořava, and Ziqi Yan. Cascading multicriticality in nonrelativistic spontaneous symmetry breaking. *Phys. Rev. Lett.*, 115:241601, 2015.

[23] Kevin T. Grosvenor, Petr Hořava, Christopher J. Mogni, and Ziqi Yan. Nonrelativistic renormalization of scalar field theories with polynomial shift symmetries. *to appear*.

[24] Kevin T. Grosvenor, Petr Hořava, Christopher J. Mogni, and Ziqi Yan. Nonrelativistic short-distance completions of a naturally light Higgs. 2016.

[25] Tom Griffin, Kevin T. Grosvenor, Petr Hořava, Shinsei Ryu, Xueda Wen, and Ziqi Yan. Anisotropic nonlinear sigma model at a Lifshitz point. *to appear*.

[26] Tom Griffin, Kevin T. Grosvenor, Charles M. Melby-Thompson, and Ziqi Yan. Quantization of Hořava gravity in 2+1 dimensions. 2017.

[27] Yoichiro Nambu and G. Jona-Lasinio. Dynamical model of elementary particles based on an analogy with superconductivity. 1. *Phys. Rev.*, 122:345–358, 1961.

[28] Yoichiro Nambu. Quasiparticles and gauge invariance in the theory of superconductivity. *Phys. Rev.*, 117:648–663, 1960.

[29] J. Goldstone. Field theories with superconductor solutions. *Nuovo Cim.*, 19:154–164, 1961.

[30] Jeffrey Goldstone, Abdus Salam, and Steven Weinberg. Broken symmetries. *Phys. Rev.*, 127:965–970, 1962.

[31] Steven Weinberg. *The quantum theory of fields. Vol. 2: Modern applications.* Cambridge University Press, 1996.

[32] Adriaan M. Schakel. *Boulevard of broken symmetries: effective field theories of condensed matter.* World Scientific, 2008.

[33] C.P. Burgess. Goldstone and pseudo-Goldstone bosons in nuclear, particle and condensed matter physics. *Phys. Rept.*, 330:193–261, 2000.

[34] Tomáš Brauner. Spontaneous symmetry breaking and Nambu-Goldstone bosons in quantum many-body aystems. *Symmetry*, 2:609–657, 2010.

[35] G. E. Volovik and M. A. Zubkov. Higgs bosons in particle physics and in condensed matter. *J. Low Temp. Phys.175,486*, 175:486–497, 2014.

[36] Holger Bech Nielsen and S. Chadha. On how to count Goldstone bosons. *Nucl. Phys.*, B105:445, 1976.

[37] V.A. Miransky and I.A. Shovkovy. Spontaneous symmetry breaking with abnormal number of Nambu-Goldstone bosons and kaon condensate. *Phys. Rev. Lett.*, 88:111601, 2002.

[38] Yoichiro Nambu. Spontaneous breaking of Lie and current algebras. *J. Stat. Phys.*, 115(1/2):7–17, 2004.

[39] Haruki Watanabe and Hitoshi Murayama. Unified description of Nambu-Goldstone bosons without Lorentz invariance. *Phys. Rev. Lett.*, 108:251602, 2012.

[40] Haruki Watanabe and Hitoshi Murayama. Redundancies in Nambu-Goldstone bosons. *Phys. Rev. Lett.*, 110:181601, 2013.

[41] A. Michelson. Phase diagrams near the Lifshitz point I, II, III. *Phys. Rev.*, B16:577, 585, 5121, 1977.

[42] Roberto Iengo, Jorge G. Russo, and Marco Serone. Renormalization group in Lifshitz-type theories. *JHEP*, 0911:020, 2009.

[43] K. Anagnostopoulos, K. Farakos, P. Pasipoularides, and A. Tsapalis. Non-linear sigma model and asymptotic freedom at the Lifshitz point. 2010.

[44] Matt Visser. Lorentz symmetry breaking as a quantum field theory regulator. *Phys. Rev.*, D80:025011, 2009.

[45] Pedro R. S. Gomes, P.F. Bienzobaz, and M. Gomes. Competing interactions and the Lifshitz-type nonlinear sigma model. *Phys. Rev.*, D88:025050, 2013.

[46] Michael E. Peskin and Daniel V. Schroeder. *An introduction to quantum field theory.* Addison-Wesley, 1995.

[47] Jean Zinn-Justin. *Quantum field theory and critical phenomena, Ch. 30.6.* Oxford University Press, 2002.

[48] G. Grinstein. Spin-wave theory for the biaxial ($m = 2$) Lifshitz point problem in three dimensions. *J. Phys. A: Math. Gen.*, 13:L201, 1980.

[49] Alberto Nicolis, Riccardo Rattazzi, and Enrico Trincherini. The Galileon as a local modification of gravity. *Phys.Rev.*, D79:064036, 2009.

[50] Kurt Hinterbichler and Austin Joyce. Goldstones with extended shift symmetries. *Int.J.Mod.Phys.*, D23:1443001, 2014.

[51] Evgenii M. Lifshitz and Lev P. Pitaevskii. *Statistical physics: theory of the condensed state*, volume 9. Elsevier, 2013.

[52] Alekseĭ A. Abrikosov, Lev P. Gorkov, and Igor E. Dzyaloshinski. *Methods of quantum field theory in statistical physics.* Courier Corporation, 2012.

[53] Gerald D Mahan. *Many-particle physics.* Springer Science & Business Media, 2000.

[54] John M Ziman. *Electrons and phonons: the theory of transport phenomena in solids.* Oxford university press, 1960.

[55] Hermann Haken. Quantum field theory of solids, an introduction. 1976.

[56] Noëlle Pottier. *Nonequilibrium statistical physics: linear irreversible processes.* Oxford University Press, 2010.

[57] Kurt Hinterbichler and Austin Joyce. Goldstones with extended shift symmetries. *Int. J. Mod. Phys.*, D23(13):1443001, 2014.

[58] N.D. Mermin and H. Wagner. Absence of ferromagnetism or antiferromagnetism in one-dimensional or two-dimensional isotropic Heisenberg models. *Phys.Rev.Lett.*, 17:1133–1136, 1966.

[59] P.C. Hohenberg. Existence of long-range order in one and two dimensions. *Phys.Rev.*, 158:383–386, 1967.

[60] Sidney R. Coleman. There are no Goldstone bosons in two dimensions. *Commun.Math.Phys.*, 31:259–264, 1973.

[61] P. M. Chaikin and T. C. Lubensky. *Principles of Condensed Matter Physics*. Cambridge U.P., 1995.

[62] Anton Kapustin. Remarks on nonrelativistic Goldstone bosons. 2012.

[63] Clifford Cheung, Paolo Creminelli, A. Liam Fitzpatrick, Jared Kaplan, and Leonardo Senatore. The Effective Field Theory of Inflation. *JHEP*, 03:014, 2008.

[64] Steven Weinberg. Effective field theory for inflation. *Phys. Rev.*, D77:123541, 2008.

[65] Daniel Baumann and Liam McAllister. *Inflation and String Theory*. Cambridge University Press, 2015.

[66] Alberto Nicolis, Riccardo Rattazzi, and Enrico Trincherini. The Galileon as a Local Modification of Gravity. *Phys. Rev.*, D79:064036, 2009.

[67] Nima Arkani-Hamed, Hsin-Chia Cheng, Markus A. Luty, and Shinji Mukohyama. Ghost Condensation and a Consistent Infrared Modification of Gravity. *JHEP*, 05:074, 2004.

[68] Nima Arkani-Hamed, Paolo Creminelli, Shinji Mukohyama, and Matias Zaldarriaga. Ghost Inflation. *JCAP*, 0404:001, 2004.

[69] Shinji Mukohyama. Scale-invariant cosmological perturbations from Hořava-Lifshitz gravity without inflation. *JCAP*, 0906:001, 2009.

[70] Clifford Cheung, Karol Kampf, Jiri Novotný, and Jaroslav Trnka. Effective Field Theories from Soft Limits of Scattering Amplitudes. *Phys. Rev. Lett.*, 114:221602, 2015.

[71] Clifford Cheung, Karol Kampf, Jiri Novotný, Chia-Hsien Shen, and Jaroslav Trnka. On-Shell Recursion Relations for Effective Field Theories. *Phys. Rev. Lett.*, 116:041601, 2016.

[72] Sidney R. Coleman. The fate of the false vacuum. 1. semiclassical theory. *Phys. Rev.*, D15:2929–2936, 1977. [Erratum: Phys. Rev.D16,1248(1977)].

[73] Curtis G. Callan, Jr. and Sidney R. Coleman. The fate of the false vacuum. 2. first quantum corrections. *Phys. Rev.*, D16:1762–1768, 1977.

[74] Göran Grimvall. *The electron-phonon interaction in metals*, volume 8. North-Holland Amsterdam, 1981.

[75] Gia Dvali, Gian F. Giudice, Cesar Gomez, and Alex Kehagias. UV-Completion by Classicalization. *JHEP*, 08:108, 2011.

[76] Gia Dvali. Strong Coupling and Classicalization. In *Proceedings, LHCSki 2016 - A First Discussion of 13 TeV Results: Obergurgl, Austria, April 10-15, 2016*, 2016.

[77] I. R. Klebanov and A. M. Polyakov. AdS dual of the critical $O(N)$ vector model. *Phys. Lett.*, B550:213–219, 2002.

[78] Mikhail A. Vasiliev. Higher spin gauge theories in four-dimensions, three-dimensions, and two-dimensions. *Int. J. Mod. Phys.*, D5:763–797, 1996.

[79] Gian Francesco Giudice. Naturally Speaking: The Naturalness Criterion and Physics at the LHC. 2008.

[80] Gian F. Giudice. Naturalness after LHC8. *PoS*, EPS-HEP2013:163, 2013.

[81] Stefano Liberati. Tests of Lorentz invariance: a 2013 update. *Class. Quant. Grav.*, 30:133001, 2013.

[82] Laure Berthier, Kevin T. Grosvenor, and Ziqi Yan. Nonrelativistic Yang-Mills and a naturally light Higgs. *To appear*, 2017.

[83] Subir Sachdev. *Quantum phase transitions*. Cambridge University Press, 2001.

[84] M. Freedman, C. Nayak, and K. Shtengel. Line of critical points in 2+1 dimensions: quantum critical loop gases and non-Abelian gauge theory. *Physical Review Letters*, 94(14):147205, April 2005.

[85] Daniel S Rokhsar and Steven A Kivelson. Superconductivity and the quantum hard-core dimer gas. *Physical review letters*, 61(20):2376, 1988.

[86] Eddy Ardonne, Paul Fendley, and Eduardo Fradkin. Topological order and conformal quantum critical points. *Annals of Physics*, 310(2):493–551, 2004.

[87] Eduardo Fradkin. *Field theories of condensed matter physics*. Cambridge University Press, 2013.

[88] Jean Zinn-Justin. *Quantum field theory and critical phenomena*. International Series of Monographs on Physics, 4th edition, 2002.

[89] Walter Selke. The annni model — theoretical analysis and experimental application. *Physics Reports*, 170(4):213 – 264, 1988.

[90] Thomas Vojta. Quantum version of a spherical model: Crossover from quantum to classical critical behavior. *Physical Review B*, 53(2):710–714, 1996.

[91] Pedro R. S. Gomes, P. F. Bienzobaz, and M. Gomes. Competing interactions and the Lifshitz-type nonlinear sigma model. *Phys. Rev.*, D88:025050, 2013.

[92] Pedro R. S. Gomes and M. Gomes. Low-energy Lorentz invariance in Lifshitz nonlinear sigma models. *JHEP*, 06:173, 2016.

[93] Daniel Harry Friedan. Nonlinear models in two + epsilon dimensions. *Annals Phys.*, 163:318, 1985.

[94] A. Michelson". Phase diagrams near the lifshitz point. i. uniaxial magnetization. *Physical Review B*, 16(1):577–584, 1977.

[95] Petr Hořava. General covariance in gravity at a Lifshitz point. *Class. Quant. Grav.*, 28:114012, 2011.

[96] G. Ghika and M. Vişinescu. Renormalization group equations with multiple coupling constants. *Il Nuovo Cimento A (1965-1970)*, 31(2):294–304, 1976.

[97] Solomon Lefschetz. *Differential equations: Geometric theory*, volume 6. Interscience publishers New York, 1957.

[98] Jean Zinn-Justin. Renormalization and stochastic quantization. *Nucl. Phys.*, B275:135–159, 1986.

[99] Petr Hořava. On QCD string theory and AdS dynamics. *JHEP*, 01:016, 1999.

[100] A. G. Abanov and P. B. Wiegmann. Theta-terms in nonlinear sigma-models. *Nuclear Physics B*, 570:685–698, March 2000.

[101] A. Tanaka and X. Hu. Many-body spin berry phases emerging from the π-flux state: competition between antiferromagnetism and the valence-bond-solid state. *Physical Review Letters*, 95(3):036402, July 2005.

[102] T. Grover and T. Senthil. Topological spin Hall states, charged skyrmions, and superconductivity in two dimensions. *Physical Review Letters*, 100(15):156804, April 2008.

[103] S. Ryu, C. Mudry, C.-Y. Hou, and C. Chamon. Masses in graphenelike two-dimensional electronic systems: Topological defects in order parameters and their fractional exchange statistics. *Physical Review B*, 80(20):205319, November 2009.

[104] Edward Witten. Nonabelian bosonization in two dimensions. *Comm. Math. Phys.*, 92(4):455–472, 1984.

[105] E.-G. Moon. Skyrmions with quadratic band touching fermions: a way to achieve charge 4e superconductivity. *Physical Reivew B*, 85(24):245123, June 2012.

[106] Zhen Bi, Alex Rasmussen, Yoni BenTov, and Cenke Xu. Stable interacting $(2 + 1)$d conformal field theories at the boundary of a class of $(3 + 1)$d symmetry protected topological phases. 2016.

[107] Adriano Contillo, Stefan Rechenberger, and Frank Saueressig. Renormalization group flow of Hořava-Lifshitz gravity at low energies. *JHEP*, 12:017, 2013.

[108] Gaston Giribet, Diana Lopez Nacir, and Francisco D. Mazzitelli. Counterterms in semiclassical Hořava-Lifshitz gravity. *JHEP*, 09:009, 2010.

[109] Domenico Orlando and Susanne Reffert. On the perturbative expansion around a Lifshitz point. *Phys. Lett.*, B683:62–68, 2010.

[110] Domenico Orlando and Susanne Reffert. On the renormalizability of Hořava-Lifshitz-type gravities. *Class. Quant. Grav.*, 26:155021, 2009.

[111] Andrei O. Barvinsky, Diego Blas, Mario Herrero-Valea, Sergey M. Sibiryakov, and Christian F. Steinwachs. Renormalization of Hořava gravity. *Phys. Rev.*, D93(6):064022, 2016.

[112] J. Ambjorn, A. Gorlich, S. Jordan, J. Jurkiewicz, and R. Loll. CDT meets Hořava-Lifshitz gravity. *Phys. Lett.*, B690:413–419, 2010.

[113] Petr Hořava. General covariance in gravity at a Lifshitz point. *Class. Quant. Grav.*, 28:114012, 2011.

[114] Dario Benedetti and Filippo Guarnieri. One-loop renormalization in a toy model of Hořava-Lifshitz gravity. *JHEP*, 03:078, 2014.

[115] Petr Hořava. Quantum criticality and Yang-Mills gauge theory. *Phys. Lett.*, B694:172–176, 2011.

[116] G. A. Vilkovisky. The unique effective action in quantum field theory. *Nucl. Phys.*, B234:125–137, 1984.

[117] VP Gusynin. Seeley-Gilkey coefficients for fourth-order operators on a Riemannian manifold. *Nuclear Physics B*, 333(1):296–316, 1990.

[118] Bryce S. DeWitt. The spacetime approach to quantum field theory. In *Relativity, groups and topology: Proceedings, 40th Summer School of Theoretical Physics - Session 40: Les Houches, France, June 27 - August 4, 1983, vol. 2*, pages 381–738, 1984.

[119] Christos Charmousis, Gustavo Niz, Antonio Padilla, and Paul M. Saffin. Strong coupling in Hořava gravity. *JHEP*, 08:070, 2009.

[120] Anna Ceresole, P. Pizzochero, and P. van Nieuwenhuizen. The curved space trace, chiral and Einstein anomalies from path integrals, using flat space plane waves. *Phys. Rev.*, D39:1567, 1989.

[121] D. Blas, O. Pujolas, and S. Sibiryakov. Consistent extension of Hořava gravity. *Phys. Rev. Lett.*, 104:181302, 2010.

[122] Diego Blas, Oriol Pujolas, and Sergey Sibiryakov. Models of non-relativistic quantum gravity: The good, the bad and the healthy. *JHEP*, 04:018, 2011.

[123] I. A. Batalin and E. S. Fradkin. Operatorial quantization of dynamical systems subject to second class constraints. *Nucl. Phys.*, B279:514–528, 1987.

[124] E. S. Fradkin and Arkady A. Tseytlin. Conformal supergravity. *Phys. Rept.*, 119:233–362, 1985.